

*Marine and Terrestrial
Natural Products
Discovery*

Michael Timmers

Bsc. (Applied Science), Hons. (Chemistry)

A thesis submitted in fulfilment of the requirements for the degree of
Doctor of Philosophy

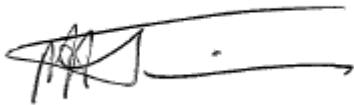
School of Applied Sciences (Discipline of Applied Chemistry)

RMIT University

February 2013

Declaration

I certify that except where due acknowledgement has been made, the work is that of the author alone; the work has not been submitted previously, in whole or in part, to qualify for any other academic award; the content of the thesis is the result of work which has been carried out since the official commencement date of the approved research program; and, any editorial work, paid or unpaid, carried out by a third party is acknowledged.

A handwritten signature in black ink, appearing to read 'M. Timmers', with a long horizontal line extending to the right.

Michael Anthony Timmers

20th February 2013

Dedication



To my family,
For your support and faith in me,
I dedicate my research to you.



"Bad times have a scientific value. These are occasions a good learner would not miss."

Ralph Waldo Emerson

(1803-1882)

Acknowledgements

I would like to thank my supervisor, Dr. Sylvia Urban for offering me this project, showing faith and for the effort she has put into editing my chapters. Dr Urban is an extremely hardworking and conscientious supervisor and I apologise for trying her patience on so many occasions. I do appreciate that she has gone beyond the call of duty and I would like to thank her for the great favours she has done me throughout the period of my candidature.

To my second supervisor, Dr Julie Niere, I am forever grateful for all that you have done for me over the years. From allowing me to reside in the NMR lab, to reading my chapters, your support during difficult times, listening to my rants and crazy times, taking on supervision of me for a year and always being there for me when I needed.

I would also like to acknowledge the Australian Postgraduate Award (APA), for granting me the scholarship to allow me to do this PhD.

To all past and present members of the MATNAP research group at RMIT University. I am especially grateful for the help provided by Dr Daniel Dias and Mrs Priyanka Reddy, particularly early in my PhD teaching me all I needed to know lab and instrument wise, and for giving up their time to assist me when needed.

I would like to thank, Dr Daniel Dias, Dr Gerald Kraft, Mrs Priyanka Reddy, Mr Allan Tinker, Dr Rick Tinker, and Dr Sylvia Urban for collections of organisms studied in this thesis. Also I would like to thank Dr Gerald Kraft for taxonomy of marine algae and to Mr Allan Tinker for the identification of two of the Australian plants.

I would like to acknowledge any previous studies and fractionation conducted within the MATNAP research group. I would like to thank Ngoc Han Nguyen for the preliminary studies and fractionation of the alga *Cystophora torulosa*, Dr Daniel Dias for help with the HPLC-NMR of the *Plocamium angustum* sample, as well as for his pre-fractionation and isolation of some compounds from the *Drosera* sample. I would also like to thank Dr Daniel Dias, Mr Claudio Silva and David Goble for their pre-fractionation of the initial collection of the *Haemodorum* sample, as well as providing spectra for comparison.

I would like to acknowledge Ms Gill Ellis from the University of Canterbury (Christchurch, New Zealand) for all of the biological activity work; Associate Professor Jonathan White from the University of Melbourne (Australia) for the X-ray crystallography work, including solving my crystal structure and attempts with other crystals, Miss Sally Duck from Monash University (Australia) for HR-ESI-MS analyses and Associate Professor Peter Cullis (RMIT University, Australia) for help with mass spectrometry. Thank you also to Professor Mark Rizzacassa from the University of Melbourne (Australia) for allowing me to use the polarimeter at the Bio21 Institute; to Mr Paul Morrison for his help with running HR-GC-MS for me. I also have to acknowledge and thank Dr Rachel Williamson from the Australia Synchrotron (Macromolecular crystallography beamline), for her attempts at obtaining a crystal structure on one of the new *Haemodorum* compounds isolated.

To the technical staff within the chemistry department at RMIT University, Mrs Shirley Cocks, Mr Sunly Prum for all of your support and help with everything that I needed, no matter how small or big the problem, you were both always willing to go out of your way to help me. To Mr Frank Antolasic for assistance with the GC-MS and ESI-MS and for maintaining the instruments. To Mr Karl Lang, without you the chemistry department at RMIT would never run. To Mr Peter Laming, Mrs Zahra Homan, Mrs Nadia Zakhartchouk, Mrs Ruth Cepriano-Hall and Mrs Dianne Mileo, thank you all for your assistance and technical support over the years.

To Dr Gemma Kirwan and Dr Krist Frost, your help with all manner of things along the way was invaluable and your friendship means a lot to me. To Dr Lisa Dias and Dr Konstantin Kouremenos and Mr Chris Ruehle, your support and lending an ear when needed was a wonderful when I needed it most. To Dr Zheng Liu, over the last few years you have become a very good friend and it was always a laugh having you around keeping my spirits up.

To my friends, firstly the Sefton family, you are always there for me through the rough times and were always willing to catch up for a coffee or a beer to chat about things that were going on. To the Martin family, your hospitality and also being there for when I needed you was wonderful. Thank you also, in no particular order, to Daniel Smith, Eleanor Dryley, Mel and Pyxee, among others, thank you all for your support and friendship over the past year, all the chats etc. over this time has kept me company and taking my mind off my thesis when needed.

A special thank you to Jacquelyn Evans for all of your support over the last year, I may have only met you about a year ago, but your friendship means so much to me. You are always there for a chat and a hug when they are needed, and your cooking always puts a smile on my face. From “I miss my cupcake”, “But I *need* tacos! I need them or I will explode” and my personal favourite, “WHY? WHY MY PIGGY? I LOVEDED YOU PIGGY! I LOVEDED YOUUUUU!”. I can’t thank you enough for all that you have done for me over the last year.

To Rowie’s family, your help, be it from realising how sane I am compared to all of you, your hospitality and help along the way have been great to me over the years. Being there for me when I needed, especially when things were not going well for me and allowing me to stay at your houses.

To my family, I would not be where I am today without all of your help and guidance. To my grandparents thank you for all you have done to assist me through the years. To my mum, you have always been there for me, supporting me always and allowing me to follow my dreams, you have sacrificed so much for me and for that I am eternally grateful. I know there have been some tough times, and I thank you for helping me get through them, and I am thankful that you were strong when the chips were down for you, it made things so much easier to cope with knowing you were positive through the whole thing.

Last but not least, to my fiancée Rowie, you mean the world to me. This period has been the most stressful and difficult part of my life so far, but you have always been there, through thick and thin and always there to support me through everything that has happened along the way. I cannot thank you enough for putting up with me, listening to my rants and whinging, putting up with the crazy, and everything especially during the writing of my thesis. My mood swings, tiredness and dealing with everything and being there for me through it all, I love you so much and I cannot wait to start the next part of our lives together.

Journal Publications

The following is a list of the journal publications that have arisen as a result of the studies conducted in this thesis:

1. Timmers, M.; Urban, S., On-line (HPLC-NMR) and Off-line Phytochemical Profiling of the Australian plant, *Lasiopetalum macrophyllum*. *Natural Product Communications*, **2011**, 6, 1605-1616.

This paper was awarded the "Gerald Blunden Award" for the best paper in *Natural Products Communications* for 2011 and was republished as detailed below.

2. Timmers, M.; Urban, S., On-line (HPLC-NMR) and Off-line Phytochemical Profiling of the Australian plant, *Lasiopetalum macrophyllum*. *Natural Product Communications*, **2012**, 7, 551-560.
3. Timmers, M. A.; Dias, D. A.; Urban, S., Application of HPLC-NMR in the Identification of Plocamenone and Isoplocamenone from the Marine Red Alga *Plocamium angustum*. *Marine Drugs* **2012**, 10, 2089-2102.
4. Timmers, M. A.; Dias, D. A.; Urban, S., HPLC-NMR Chemical Profiling of the Australian Carnivorous plant, *Drosera erythrorhiza* subspecies *magna*. *The Natural Products Journal*, **2013**, 3, (1), 35-41.
5. Urban, S.; Timmers, M. A., HPLC-NMR Chemical Profiling and Dereplication Studies of the Marine Brown Alga, *Cystophora torulosa*. *Natural Product Communications*, **2013**, 8 (6) 715-719.
6. Timmers, M. A.; Brkljača, R.; White, J. M.; Urban, S., Phenylphenalenones and Oxabenzochrysenones from the Australian Plant *Haemodorum simulans*. *Phytochemistry*, (submitted).

Conference Presentations (Posters)

The following is a list of the conference presentations (posters) that have been presented as a result of the studies conducted in this thesis:

1. Dias, D.; Timmers, M.; Urban, S. "Application of On-flow LC-NMR Analysis to Profile Natural Products from Marine Extracts" 12th International Conference on Marine Natural Products (Manapro XII), Queenstown, New Zealand, 4th – 9th February, 2007.
2. Dias, D.; Reddy, P.; Timmers, M.; and Urban, S. "Bioprospecting for Drugs from the Marine Environment", 12th International Symposium on Marine Natural Products (MANAPRO XII), Queenstown, New Zealand, 4th-9th February, 2007.
3. Dias, D.; Timmers, M.; and Urban, S. "Application of On-flow LC-NMR to Profile Natural Products from Marine Extracts", RACI Natural Products Chemistry Group One-Day Symposium, University of New South Wales, Sydney, Australia, 28th September, 2007.
4. Dias, D, Reddy, P, Timmers, M, and Urban, S, "Bioprospecting for Drugs from the Marine Environment", RACI Natural Products Chemistry Group One-Day Symposium, University of New South Wales, Sydney, Australia, 28th September, 2007.
5. Timmers, M.; Niere, J.; Urban, S. "Application of HPLC-NMR to Identify Secondary Metabolites from the Plant *Drosera* sp." RMIT College of Science, Engineering and Health Higher Degree by Research Student Conference, 23rd October, 2009.
6. Timmers, M.; Urban, S. "Chemical Profiling of Flavonoid Glycosides from *Lasiopetalum macrophyllum*" 27th International Symposium on the Chemistry of Natural Products (ISCNP27), Brisbane, Australia, 10th – 15th July, 2011.
7. Brkljača, B, Timmers, M, and Urban, S., "Recent Advancements in HPLC-NMR and its Application to Rapidly Profile Marine Natural Products", 27th International Symposium on the Chemistry of Natural Products (ISCNP27), Brisbane, Australia, 10th-15th July, 2011.

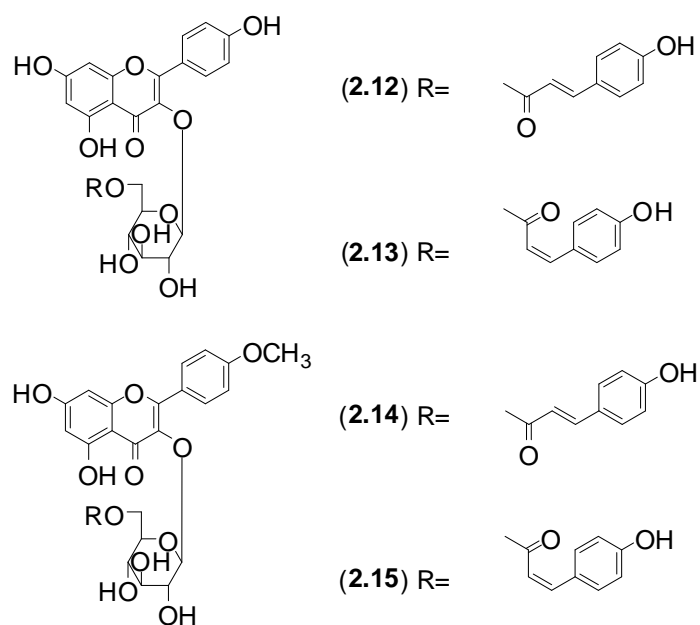
Abstract

This thesis describes the study of three Australian plants and two marine algae. The application of the hyphenated spectroscopic technique, HPLC-NMR, was successfully implemented in the partial identification or as a dereplication of the secondary metabolites present in each of the studied organisms. HPLC-NMR was particularly suited to the identification of an unstable new secondary metabolite identified from one of the marine organisms. In total this thesis has resulted in the isolation and structural elucidation of five new secondary metabolites, one new X-ray crystal structure of a previously reported compound and twenty-two known secondary metabolites, of which five structural and/or chemical shift re-assignments were deduced. The five new natural products were isolated from two of the Australian plants and one marine alga, and were elucidated using detailed spectroscopic and chemical techniques. Also presented are the biological activities of all crude extracts studied and a selection of the isolated secondary metabolites.

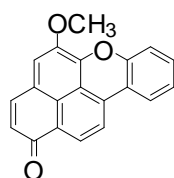
Chapter 1: A general introduction of marine and terrestrial natural products, covering both the history of natural products isolation and advancements in technology is detailed. Following this a review of the biological activity (anti-cancer and anti-parasitic activity) of the flavonoid and naphthoquinone structure classes covering the period 2008-2012 is presented. The selection of the flavonoids and naphthoquinones was made on the basis that these represented two of the structure classes that were isolated during the course of these studies that either displayed bioactivity or are known to possess biological activity.

Chapter 2: Describes the on-line (HPLC-NMR) and off-line (HPLC, NMR and MS) methodologies utilised to profile the constituents present in the crude methanolic extract of the Australian plant, *Lasiopetalum macrophyllum*. On-flow and stop-flow HPLC-NMR supported the presence of *trans*-tiliroside (**2.12**) and permitted partial identification of *cis*-

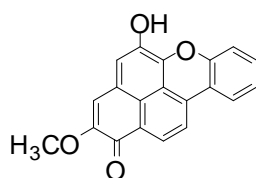
tiliroside (**2.13**) and 4'-methoxy-*trans*-tiliroside (**2.14**), while a fourth related secondary metabolite, observed in the analytical HPLC chromatogram, was not observed in the on-flow or stop-flow analyses due to its low concentration in the crude extract. Subsequent off-line isolation led to the unequivocal identification of four flavonoid glycosides including a new structural derivative, 4'-methoxy-*cis*-tiliroside (**2.15**). This is the first report of flavonoid glycosides occurring in this plant genus. In addition, a number of structure revisions have been proposed for previously reported flavonoid glycosides that were incorrectly assigned. The stability of flavonoid glycosides was also determined, with a conversion of pure *trans* or *cis* isomers into a mixture of the two isomers over time. It was observed that the *cis* isomers converted into a mixture at a much quicker rate than that of the *trans* isomers. With this conversion, it was found that *trans*-tiliroside (**2.12**) converted to an equilibrium mixture of *trans*- (**2.12**) and *cis*-tiliroside (**2.13**) in a ratio of ~4:1, which corresponded to the approximate ratio observed in the initial extract. The methoxy derivatives of *trans*-tiliroside (**2.12**) and *cis*-tiliroside (**2.13**) were established to be natural products and not artefacts of the isolation procedure.



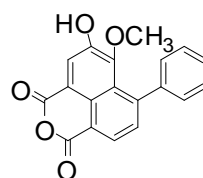
Chapter 3: The investigation of the Australian plant *Haemodorum simulans* (Haemodoraceae) was carried out using a combination of on-line HPLC-NMR chemical profiling of enriched fractions as well as off-line isolation and purification methodologies. This resulted in the isolation and identification of two new phenylphenalenones, haemoxiphidone (**3.42**) and haemodordioxolane (**3.45**), from the bulbs together with the first report of an oxabenzochrysenone glycoside, haemodoroxychrysenose (**3.46**), from the aerial parts of the plant. Also isolated were two previously described phenylphenalenones 5,6-dimethoxy-7-phenyl-1*H*,3*H*-naphtho[1,8-*cd*]pyran-1,3-dione (**3.44**) and haemodorone (**3.41**) and two oxabenzochrysenones 5-hydroxy-2-methoxy-1*H*-naphtho[2,1,8-*mna*]xanthen-1-one (**3.4**) and 5-methoxy-1*H*-naphtho[2,1,8-*mna*]xanthen-1-one (**3.2**). The X-ray structure of the phenylphenalenone 5,6-dimethoxy-7-phenyl-1*H*,3*H*-naphtho[1,8-*cd*]pyran-1,3-dione (**3.44**) was secured for the first time. HPLC-NMR chemical profiling of an enriched fraction containing a mixture of haemodordioxolane (**3.45**) and 5,6-dimethoxy-7-phenyl-1*H*,3*H*-naphtho[1,8-*cd*]pyran-1,3-dione (**3.44**) as well as a separate HPLC-NMR analysis of an enriched fraction containing haemodorone (**3.41**) and haemoxiphidone (**3.42**), facilitated the partial identification of these secondary metabolites. All structural elucidations were unequivocally established via detailed spectroscopic analyses.



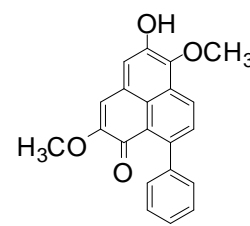
(3.2)



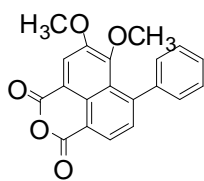
(3.4)



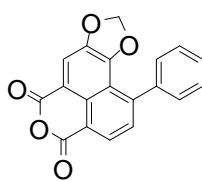
(3.41)



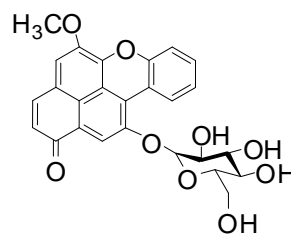
(3.42)



(3.44)

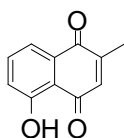


(3.45)

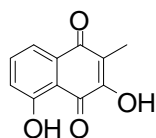


(3.46)

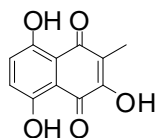
Chapter 4: Describes the on-line HPLC-NMR chemical profiling of crude extracts derived from the bulbs of the Australian carnivorous plant *Drosera erythrohiza* subspecies *magna*. A combination of on-flow and stop-flow HPLC-NMR methodologies enabled partial identification of two structurally related naphthoquinones, droserone (**4.7**) and hydroxydroserone (**4.8**), as well as a mixture of their corresponding glycosides (**4.9** and **4.10**). Subsequent semi-preparative HPLC off-line isolation followed by NMR spectroscopic and mass spectrometric analysis of the crude extracts of the bulbs of the plant permitted the unequivocal identification of droserone (**4.7**), hydroxydroserone (**4.8**), droserone-5-O- β -glycoside (**4.9**) and hydroxydroserone-5-O- β -glycoside (**4.10**). In addition off-line separation methodologies of the aerial parts of the plant led to the identification of plumbagin (**1.267**). Of the isolated compounds, plumbagin (**1.267**), was found to be the most active, with potent P388 anti-tumour activity, potent anti-microbial activity against *Candida albicans*, *Bacillus subtilis* and *Trichophyton mentagrophytes*, while possessing selective mild anti-fungal activity against *Cladosporium resinae*.



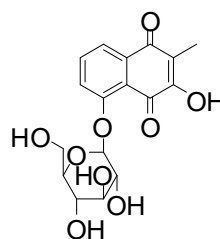
(1.267)



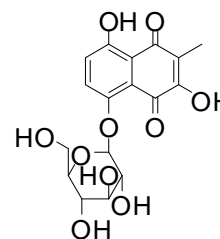
(4.7)



(4.8)

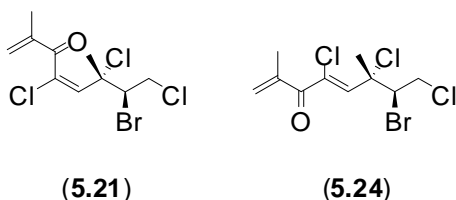


(4.9)



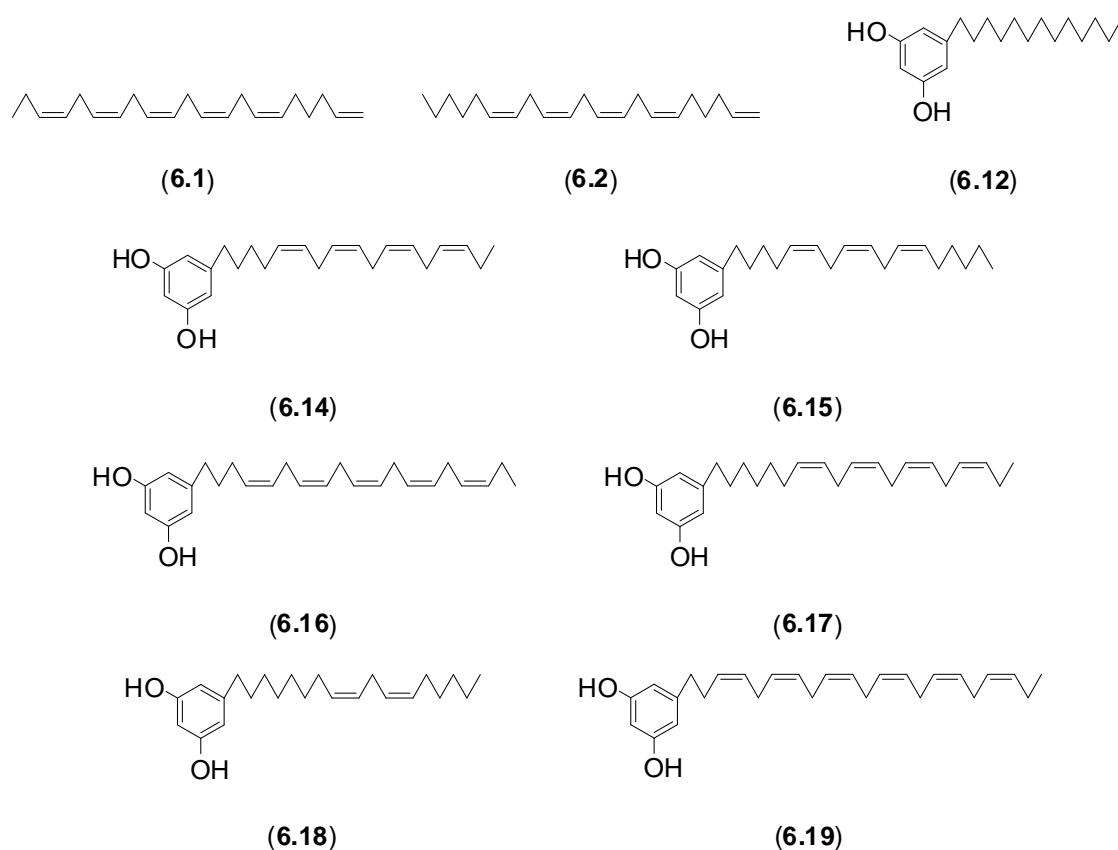
(4.10)

Chapter 5: Describes the use of a combination of on-line HPLC-NMR and off-line chemical investigations of the crude extract of the southern Australian red alga *Plocamium angustum* that resulted in the identification of the previously reported polyhalogenated monoterpene plocamenone (5.21), together with the new structural analogue isoplocamenone (5.24). On-flow and stop-flow HPLC-NMR analyses (including the acquisition of WET 2D NMR spectra) rapidly assisted in the identification of the major component plocamenone (5.21) and in the partial identification of its unstable double bond isomer isoplocamenone (5.24). Conventional off-line isolation and structural characterisation techniques were employed to unequivocally confirm both structures, leading to a structural revision for plocamenone (5.21), as well as obtaining sufficient quantities for biological testing. The unstable isoplocamenone (5.24) was isolated as a mixture with plocamenone (5.21) in order to allow for the unequivocal assignment of isoplocamenone (5.24).



Chapter 6: Describes the on-line HPLC-NMR chemical profiling/dereplication study of the southern Australian brown alga, *Cystophora torulosa*. On-flow HPLC-NMR analyses of the crude extract in combination with the use of the MarinLit database ultimately allowed for the identification of two classes of secondary metabolites, resorcinol derivatives and polyenes. In total seven secondary metabolites were identified by on-flow HPLC-NMR analysis, including five resorcinol derivatives (6.14 and 6.16-6.18) and two polyenes (6.1 and 6.2). Off-line small-scale analytical HPLC collection and subsequent ESI-MS analysis of the crude extract allowed for the identification of seven resorcinol derivatives, with two additional resorcinol derivatives (6.12 and 6.19) identified from the analytical HPLC

collection, subsequent ESI-MS analysis and the use of the MarinLit database. The two polyenes (**6.1** and **6.2**) were also isolated by analytical HPLC collection and subjected to GC-MS analysis, thereby allowing these secondary metabolites to be identified. Validation of this on-line dereplication strategy was supported by the isolation and complete 2D NMR assignment of the major secondary metabolite (**6.14**). The data was in full accordance with that reported for the major secondary metabolite (**6.14**) in the literature, while the off-line ^1H NMR spectrum was very similar in appearance to that of the WET-1D ^1H NMR spectrum obtained from the HPLC-NMR chemical profiling exercise. This indicated that this methodology is suitable for the rapid on-line identification of the resorcinol and polyene structure classes which are often observed in the genus *Cystophora*.



Abbreviations

1D	one dimensional
2D	two dimensional
3D	three dimensional
Å	angstrom (unit of length = 10^{-10} m used for bond length)
bs	broad singlet (NMR)
BSC-1	African Green Monkey kidney cell line
°C	degrees Celsius
C ₁₈	octadecyl stationary phase (chromatography)
CAS	Chemical Abstracts Service registry number
CH	methine (NMR)
CH ₂	methylene (NMR)
CH ₃	methyl (NMR)
CH ₃ CN	acetonitrile
¹³ C NMR	carbon NMR
CDCl ₃	deuterated chloroform
CD ₃ OD	deuterated methanol
CHCl ₃	chloroform
CIGAR	Constant time Inverse Detection Gradient Accordion Rescaled
cm ⁻¹	reciprocal centimeters (FT-IR spectroscopy)
δ	chemical shift in parts per million
d	doublet (NMR)
D ₂ O	deuterated water
d ₆ -acetone	deuterated acetone
d ₆ -DMSO	deuterated dimethyl sulfoxide
DCM	dichloromethane
DEPT	Distortionless Enhanced by Polarisation Transfer
d _f	film thickness
DMSO	dimethyl sulfoxide
ε	molar absorptivity
EI	electron impact
EtOH	ethanol
EtOAc	ethyl acetate
ESI-MS	Electrospray Ionisation-Mass Spectrometry

FT-IR	Fourier Transform-Infrared Spectroscopy
g	grams
GC-MS	Gas Chromatography-Mass Spectrometry
gCOSY	gradient Correlation Spectroscopy
gHMBC	gradient Heteronuclear Multiple Bond Correlation
gHSQCAD	gradient Heteronuclear Single Bond Coherence Adiabatic
GI ₅₀	concentration required to inhibit the proliferation of cells by 50%
¹ H NMR	proton NMR
H ₂ BC	Heteronuclear two Bond Correlation
H ₂ O	water
HCl	hydrochloric acid
HDO	residual water in D ₂ O
HOAc	acetic acid
HPLC	High Pressure Liquid Chromatography
HPLC-ESI-MS	High Pressure Liquid Chromatography-Electrospray Ionisation-Mass Spectrometry
HPLC-MS	High Pressure Liquid Chromatography-Mass Spectrometry
HPLC-NMR	High Pressure Liquid Chromatography-Nuclear Magnetic Resonance Spectroscopy
HPLC-NMR-MS	High Pressure Liquid Chromatography-Nuclear Magnetic Resonance Spectroscopy-Mass Spectrometry
HR-ESI-MS	high resolution-Electrospray Ionisation-Mass Spectrometry
HR-GC-MS	high resolution-Gas Chromatography-Mass Spectrometry
H ₂ SO ₄	sulphuric acid
HSV	<i>Herpes simplex</i> virus
HTS	High Throughput Screening
Hz	hertz
IC ₅₀	concentration of sample required to inhibit the P388 cell growth by 50%
ID	internal diameter
IR	Infrared
IU	International Unit (measuring amount of a substance, based on biological activity)
<i>J</i>	coupling constant (Hz)
K	Kelvin
km	kilometre
L	litre

LC	Liquid Chromatography
λ_{\max}	wavelength of maximum absorbance
m	metre
m.p.	melting point
<i>m/z</i>	mass-to-charge-ratio (mass spectrometry)
MATNAP	Marine and Terrestrial Natural Products research group
mg	milligram
MHz	megahertz
min	minute
mL	millilitre
mm	millimetre
MeOH	methanol
MS	Mass Spectrometry
μ	micro
<i>n</i> -BuOH	butanol
NaCl	sodium chloride
NCI	National Cancer Institute (US)
ng	nanogram
nm	nanometre
NMR	Nuclear Magnetic Resonance spectroscopy
NOE	Nuclear Overhauser Enhancement
NOESY	two dimensional Nuclear Overhauser Enhancement Spectroscopy
ODS	octadecylsilane
ORTEP	Oak Ridge Thermal-Ellipsoid Plot Program
PDA	Photo Diode Array detector
ppm	parts per million
PTFE	Poly Tetra Fluoro Ethylene (Teflon)
q	quartet (NMR)
ROESY	Rotating Frame Overhauser Enhancement Spectroscopy
R_f	Retention factor (in TLC)
RP	Reversed Phase
s	singlet (NMR)
S/N	signal-to-noise
SCUBA	Self-Contained Underwater Breathing Apparatus
sp.	species
t	triplet (NMR)
TCM	Traditional Chinese Medicine

TLC	Thin Layer Chromatography
TOCSY	Total Correlation Spectroscopy
TOF	Time of Flight (mass spectrometry)
UV-Vis	Ultraviolet Spectroscopy
ν_{\max}	maximum wavenumber
VLC	Vacuum Liquid Chromatography
WET-1D	one dimensional Water Enhanced through Transverse gradients
WET-2D	two dimensional Water Enhanced through Transverse gradients
WHO	World Health Organisation
$[\alpha]_D$	specific optical rotation

List of figures

Figure 1.1. All approved drugs from 1981-2010 (sourced from Newman and Cragg [5])... 2	2
Figure 1.2. All approved cancer drugs from 1981-2010 (sourced from Newman and Cragg [5]).	3
Figure 1.3. Structure classes described as flavonoids.....	10
Figure 2.1. [A] 2D HPLC-NMR contour plot showing the major compound (2.12) (on-flow HPLC-NMR) and [B] Extracted WET-1D ¹ H NMR spectra of compounds (2.12-2.14) (stop-flow HPLC-NMR).	73
Figure 2.2. HPLC chromatogram and 2D PDA plot of on-flow HPLC-NMR analysis of <i>L. macrophyllum</i> .	74
Figure 2.3. ¹ H NMR (500 MHz, <i>d</i> ₆ -DMSO) spectrum of <i>trans</i> -tiliroside (2.12).	77
Figure 2.4. Key HMBC correlations for <i>trans</i> -tiliroside (2.12).	78
Figure 2.5. Fragments linked to the sugar for the major component (2.12).	78
Figure 2.6. Fragments linked to the sugar for the major component (2.13).	83
Figure 2.7. 2D gHMBC NMR spectrum of 4'-methoxy- <i>trans</i> -tiliroside (2.14), showing key correlations.	86
Figure 2.8. HMBC NMR correlation of compound (2.17).	87
Figure 2.9. Comparison of NMR data for structurally related flavonoids.	89
Figure 2.10. Comparison of NMR data for structurally related flavonoids.	91
Figure 2.11. 2D gHSQCAD NMR spectrum of kaempferol-4'-methyl ether-3-O-β-D-(6-O- <i>cis-p</i> -coumaroyl)-glucopyranoside (2.15).	94
Figure 2.12. Analytical HPLC chromatogram of the UV exposed mixture of 2.12 and 2.13.	95
Figure 3.1. General structures and numbering of phenylphenalenones and oxabenzochrysenones.	98
Figure 3.2. Positions corresponding to the acetate incorporation in the biosynthesis of phenylphenalenones.	101
Figure 3.3. Example of the interconversion of a phenylpropanoid into a dihydrophenylpropanoid.	101
Figure 3.4. [A] 2D HPLC-NMR contour plot showing compounds (3.44 and 3.45) (on-flow HPLC-NMR) and [B] Extracted WET-1D ¹ H NMR spectra of compounds (3.44 and 3.45) (stop-flow HPLC-NMR).	112
Figure 3.5. UV profiles of 3.44 and 3.45 extracted from HPLC-NMR analysis.	113
Figure 3.6. [A] 2D HPLC-NMR contour plot (on-flow HPLC-NMR) and [B] Extracted WET-1D ¹ H NMR spectra of compounds (3.41 and 3.42) (stop-flow HPLC-NMR).	115

Figure 3.7. ^1H NMR (500 MHz, d_6 -DMSO) spectrum of haemoxiphidone (3.42).....	118
Figure 3.8. 2D gHMBC NMR spectrum showing key correlations of haemoxiphidone (3.42).....	121
Figure 3.9. HR-ESI-MS (positive mode) spectrum of haemodordioxolane (3.45).	122
Figure 3.10. ^1H NMR (500 MHz, CDCl_3) spectrum of haemodordioxolane (3.45).	123
Figure 3.11. 2D gHSQCAD NMR spectrum of haemodordioxolane (3.45).	126
Figure 3.12. ^1H NMR (500 MHz, CDCl_3) spectrum of haemodoroxychrysenose (3.46)...	129
Figure 3.13. 2D gHSQCAD NMR spectrum of haemodoroxychrysenose (3.46).....	130
Figure 3.14. [A] Key HMBC correlations and [B] key NOESY and ROESY enhancements observed for haemochrysenone (3.46).	131
Figure 3.15. Single crystal X-ray structure (ORTEP) of 3.44.	132
Figure 4.1. HPLC chromatogram obtained from the on-flow HPLC-NMR analysis of the crude extract of <i>D. erythrorhiza</i> subspecies <i>magna</i>	140
Figure 4.2. On-flow 2D HPLC-NMR contour plot showing the presence of the major compound (4.7) and one of the minor compounds (4.8).....	141
Figure 4.3. WET-1D ^1H NMR spectra of the peaks observed in the stop-flow HPLC-NMR analysis.....	142
Figure 4.4. Extracted UV profile of the major component observed in the HPLC-NMR analyses.	143
Figure 4.5. ^1H NMR (500 MHz, d_6 -DMSO) spectrum of droserone (4.7).....	145
Figure 4.6. Literature ^{13}C NMR assignments and re-assignments of positions C-6 and C-8 for droserone (4.7).....	146
Figure 4.7. Expansion of 2D gHMBC NMR spectrum, displaying the direct $^1J_{\text{C-H}}$ correlations for the assignment of droserone (4.7).	147
Figure 4.8. Literature ^{13}C NMR assignments and re-assignments of positions C-6 and C-8 for droserone-5-O- β -glycoside (4.9).....	148
Figure 4.9. 2D gHSQCAD NMR spectrum of droserone-5-O- β -glycoside (4.9).	149
Figure 4.10. ^1H NMR (500 MHz, d_6 -DMSO) spectrum of hydroxydroserone-5-O- β -glycoside (4.10).	150
Figure 4.11. Key ^{13}C NMR assignments allowing the sugar moiety for hydroxydroserone-5-O- β -glycoside (4.10) to be positioned.	151
Figure 4.12. Key HMBC correlations and single irradiation NOE NMR enhancement observed in the unequivocal assignment of hydroxydroserone-5-O- β -glycoside (4.10). .	153
Figure 5.1. Analytical HPLC method development for the DCM extract of <i>P. angustum</i> . 162	
Figure 5.2. [A] HPLC chromatogram of the HPLC-NMR analysis (UV detection at λ_{max} 250 nm), [B] HPLC 2D contour plot of the HPLC-NMR analysis (200-400 nm), [C] On-flow	

HPLC-NMR contour plot of the DCM extract of <i>P. angustum</i> and [D] Stop-flow HPLC-NMR WET-1D ¹ H NMR spectra of compounds (5.21 and 5.24).	164
Figure 5.3. Stop-flow HPLC-NMR WET-2D gCOSY NMR spectrum of plocamenone (5.21).	166
Figure 5.4. Stop-flow HPLC-NMR WET-2D gHSQCAD NMR spectrum of plocamenone (5.21).	167
Figure 5.5. Semi-preparative HPLC chromatogram with 2D contour plot showing the isolation of plocamenone (5.21) and isoplocamenone (5.24), as well as the extracted UV profile of the major compound, plocamenone (5.21).	168
Figure 5.6. ¹ H NMR (500 MHz, CDCl ₃) spectrum of plocamenone (5.21).	170
Figure 5.7. ¹ H NMR (500 MHz, CD ₃ OD) spectrum of isoplocamenone (5.24) in a mixture with plocamenone (5.21).	172
Figure 5.8. ¹ H and ¹³ C NMR chemical shift comparisons of configurational isomers.	175
Figure 5.9. ¹ H NMR comparison of configurational and double bond isomers.	176
Figure 6.1. Analytical HPLC chromatogram of the crude DCM extract of <i>C. torulosa</i> showing the presence of two distinct classes of compounds.	189
Figure 6.2. Extracted UV profiles of the two classes of compounds observed in the analytical HPLC analysis of the crude extract.	191
Figure 6.3. [A] On-flow 2D HPLC-NMR contour plot showing the presence of five structurally related compounds (6.14-6.18) and [B] Extracted WET-1D ¹ H NMR spectra of compounds (6.14-6.18) from the on-flow HPLC-NMR analysis.	192
Figure 6.4. [A] Search parameters input into the MarinLit database for the class of compounds observed from the HPLC-NMR analysis [B] Compounds in the MarinLit database that conform to the search parameters in [A].	194
Figure 6.5. Resorcinol and phloroglucinol derivatives	195
Figure 6.6. [A] Search parameters from the MarinLit database for the major compound observed in the HPLC-NMR analysis including ESI-MS mass [B] Single compound from MarinLit that conformed to the search parameters entered for the major compound.	196
Figure 6.7. HPLC chromatogram showing the seven compounds (see Table 6.1) collected from the analytical HPLC, resulting in the identification of the resorcinols (6.12, 6.14-6.19).	197
Figure 6.8. [A] WET-1D ¹ H NMR spectrum of the major compound (6.14) [B] Off-line ¹ H NMR (500 MHz, <i>d</i> ₆ -DMSO) spectrum of compound (6.14) and [C] ESI-MS (negative mode) of compound (6.14).	200
Figure 6.9. Analytical HPLC chromatogram (100% CH ₃ CN) of the later eluting compounds (6.1 and 6.2) in the crude extract of <i>C. torulosa</i>	201

Figure 6.10. [A] On-flow 2D HPLC-NMR contour plot showing the two structurally related compounds (6.1 and 6.2) and [B] Extracted WET-1D ¹ H NMR spectra of compounds (6.1 and 6.2) from the on-flow HPLC-NMR analysis.....	202
Figure 6.11. Mass Spectrum obtained from the GC-MS of the polyene (6.1)	204
Figure 6.12. [A] Search parameters from the MarinLit database entered for the first polyene (6.1) observed in the HPLC-NMR analysis [B] Compounds in the MarinLit database that conform to the search parameters entered [C] Reference details of the polyene (6.1) matching search criteria and [D] The two polyenes (6.1 and 6.2) identified from matching reference.	205
Figure 7.1. Analytical HPLC gradient used for all initial analytical HPLC analyses.	211
Figure 7.2. Micro-titre (96 well) plate with control and test dilutions showing the colour change due to inhibition.	212
Figure 7.3. Zones of inhibition of anti-microbial assays.	214

List of Schemes

Scheme 1.1. The biosynthetic pathway for the major subclasses of flavonoids (sourced from Tsao and McCallum [21])	11
Scheme 3.1. The biosynthetic pathway for phenylphenalenones (sourced from Schmitt and Schneider [175], Hölscher and Schneider [177], Munde and Maddula <i>et al</i> [178], Schmitt and Hölscher <i>et al</i> [179] and Brand and Hölscher <i>et al</i> [180]).....	102
Scheme 3.2. Isolation and purification scheme for the partial identification of secondary metabolites by HPLC-NMR analysis.	108
Scheme 6.1. Methodologies used for the chemical profiling of <i>C. torulosa</i>	190

List of Tables

Table 1.1. Anti-leishmanial activity of synthetic flavonoid dimers 1.48-1.61 given as an IC ₅₀ (μM).....	39
Table 1.2. Anti-cancer activity of the synthetic naphthoquinones 1.169-1.185 shown as an GI ₅₀ (μM).....	44
Table 1.3. Anti-tumour activity of naphthoquinones (1.286-1.299) given as an IC ₅₀ (μM). 56	
Table 2.1. ¹ H (500 MHz) and ¹³ C (125 MHz) NMR spectroscopic data of <i>trans</i> -tiliroside (2.12) in <i>d</i> ₆ -DMSO.	80
Table 2.2. ¹ H (500 MHz) and ¹³ C (125 MHz) NMR spectroscopic data of <i>cis</i> -tiliroside (2.13) in <i>d</i> ₆ -DMSO.	82
Table 2.3. ¹ H (500 MHz) and ¹³ C (125 MHz) NMR spectroscopic data of 4'-methoxy- <i>trans</i> -tiliroside (2.14) in <i>d</i> ₆ -DMSO.	85
Table 2.4. Chemical shift comparison of 2.14 and literature reports of 2.17 and 2.14 in CD ₃ OD.....	88
Table 3.1. ¹ H (500 MHz) and ¹³ C (125 MHz) NMR data for haemoxiphidone (3.42) in <i>d</i> ₆ -DMSO.....	117
Table 3.2. ¹ H NMR (500 MHz) comparison of haemoxiphidone (3.42) and the literature data for xiphidone (3.43) in <i>d</i> ₆ -acetone.	119
Table 3.3. ¹ H (500 MHz) and ¹³ C (125 MHz) NMR data for haemodordioxolane (3.45). .125	
Table 3.4. ¹ H (500 MHz) and ¹³ C (125 MHz) NMR data for haemodoroxychrysenose (3.46) in <i>d</i> ₆ -DMSO.....	127
Table 4.1. Biological evaluation of <i>D. erythrohiza</i> subspecies <i>magna</i> compounds isolated.	137
Table 4.2. ¹ H (500 MHz) and ¹³ C NMR (125 MHz) chemical shift comparison of isolated and authentic plumbagin (1.267) in <i>d</i> ₆ -DMSO.	144
Table 4.3. ¹ H (500 MHz) and ¹³ C (125 MHz) NMR spectroscopic data of hydroxydroserone-5-O-β-glycoside (4.10) in <i>d</i> ₆ -DMSO.....	152
Table 5.1. Summary of the P388 cytotoxicity of plocamenone (5.21) and isoplocamenone (5.24) isolated from three separate specimens of <i>P. angustum</i>	160
Table 5.2. ¹ H (500 MHz) and ¹³ C (125 MHz) NMR data for plocamenone (5.21) in CDCl ₃	169
Table 5.3. ¹ H (500 MHz) and ¹³ C (125 MHz) NMR data for isoplocamenone (5.24) in CD ₃ OD.....	173
Table 5.4. ¹ H and ¹³ C NMR chemical shift differences for plocamenone (5.21) and isoplocamenone (5.24) (500 MHz, CD ₃ OD).	174

Table 6.1. Resorcinol derivatives as isolated from the crude extract of <i>C. torulosa</i> with the seven compounds collected (see Figure 6.7), their mass from ESI-MS and their identified structure based on MarinLit database searching.....	198
Table 6.2. ¹ H (500 MHz) and ¹³ C (125 MHz) NMR spectroscopic data of the major resorcinol derivative (6.14) in CDCl ₃	199
Table 6.3. Polyenes isolated and identified from <i>C. torulosa</i>	203

Table of contents

Statement of Authenticity	ii
Dedication	iii
Acknowledgements	v
Journal Publications	ix
Conference Presentations (Posters)	x
Abstract	xi
Abbreviations	xvii
List of Figures	xxi
List of Schemes	xxv
List of Tables	xxvi
Table of Contents	xxviii
Chapter 1. Introduction	1
1.1 General Introduction	1
1.1.1 History of Natural Products	1
1.1.2 Approaches to Natural Products Isolation	4
1.1.3 Hyphenated Spectroscopic Techniques	5
1.1.4 Marine Natural Products	7
1.1.5 Plant Natural Products	9
1.1.6 Natural Product Studies Conducted	9
1.2 Flavonoids	10
1.2.1 General Introduction	10
1.2.2 Biological Activity	12
1.2.2.1 Anti-cancer flavonoids	12
1.2.2.2 Anti-parasitic flavonoids	26
1.2.3 Summary	41
1.3 Naphthoquinones	42
1.3.1 General Introduction	42
1.3.2 Biological Activity	42
1.3.2.1 Anti-cancer naphthoquinones	42
1.3.2.2 Anti-parasitic naphthoquinones	59
1.3.3 Summary	66
Chapter 2. On-line (HPLC-NMR) and Off-line Phytochemical Profiling of the Australian Plant, <i>Lasiopetalum macrophyllum</i>	67
2.1 Introduction	67

2.2	Experimental	69
2.2.1	General Experimental	69
2.2.2	Plant material	69
2.2.3	Extraction and Isolation	70
2.2.3.1	Preparation of the extract of <i>L. macrophyllum</i> for on-flow and stop-flow HPLC-NMR analysis	70
2.2.3.2	Preparation of the extract for off-line isolation of secondary metabolites from <i>L. macrophyllum</i>	71
2.3	Results and Discussion	72
2.4	Concluding Remarks	96
Chapter 3. Phenylphenalenones and Oxabenzochrysenones from the Australian plant <i>Haemodorum simulans</i>		97
3.1	Introduction	97
3.1.1	Biosynthesis of phenylphenalenones.....	99
3.1.2	Biological activity of phenylphenalenones.....	103
3.2	Experimental	104
3.2.1	General Experimental.....	104
3.2.2	Plant material	105
3.2.3	Extraction and Isolation	107
3.2.3.1	Preparation of the extract of <i>H. simulans</i> for on-flow and stop-flow HPLC-NMR analysis.....	107
3.2.3.2	Preparation of the extract for off-line isolation of secondary metabolites from the bulbs of <i>H. simulans</i>	108
3.2.3.3	Preparation of the extract for off-line isolation of secondary metabolites from the aerial parts of <i>H. simulans</i>	109
3.2.4	Acid hydrolysis.....	110
3.2.5	Crystallography.....	110
3.3	Results and Discussion	111
3.4	Conclusion	132
Chapter 4. On-line and off-line chemical profiling of the Australian plant, <i>Drosera erythrorhiza</i> subspecies <i>magna</i>		133
4.1	Introduction	133
4.2	Experimental	135
4.2.1	General Experimental.....	135
4.2.2	Plant material	135
4.2.3	Extraction and Isolation	138

4.2.3.1	Preparation of the extract of <i>D. erythrorhiza</i> subspecies <i>magna</i> for on-flow and stop-flow HPLC-NMR analysis	138
4.2.3.2	Preparation of the extract for off-line isolation of secondary metabolites from <i>D. erythrorhiza</i> subspecies <i>magna</i>	138
4.3	Results and Discussion	139
4.4	Concluding Remarks	153
Chapter 5. On-line and Off-line Methodologies for the Identification of Secondary Metabolites from the Marine Red Alga <i>Plocamium angustum</i>		155
5.1	Introduction	155
5.2	Experimental	158
5.2.1	General Experimental.....	158
5.2.2	Algal material.....	158
5.2.3	Extraction and Isolation	161
5.2.3.1	Preparation of the extract of <i>P. angustum</i> for on-flow and stop-flow HPLC-NMR analysis	161
5.2.3.2	Preparation of the extract for off-line isolation of secondary metabolites from <i>P. angustum</i>	161
5.3	Results and Discussion	162
5.4	Concluding Remarks	179
Chapter 6. HPLC-NMR Chemical Profiling and Dereplication Studies of the Marine Brown Alga, <i>Cystophora torulosa</i>		180
6.1	Introduction	180
6.2	Experimental	185
6.2.1	General Experimental.....	185
6.2.2	Algal material.....	186
6.2.3	Extraction and Isolation	188
6.2.3.1	Preparation of the crude extract of <i>C. torulosa</i> for on-flow HPLC-NMR analysis	188
6.2.3.2	Preparation of the crude extract of <i>C. torulosa</i> for off-line isolation of secondary metabolites from <i>C. torulosa</i>	188
6.3	Results and Discussion	189
6.4	Concluding remarks.....	206
Chapter 7. Experimental		208
7.1	General Experimental.....	208
7.1.1	Spectroscopic Analyses.....	208
7.1.2	Analytical and semi-preparative HPLC	210
7.1.3	HPLC-NMR	211

7.1.4	Biological Activity Assays	212
7.1.4.1	Anti-tumour (P388 Murine Leukaemia Cell Line) Assay	212
7.1.4.2	Anti-microbial Activity Assays	213
7.1.4.3	Anti-viral (<i>Herpes simplex</i> virus and <i>Polio</i> virus) Assays	214
7.1.5	Miscellaneous.....	214
7.1.5.1	Photography	214
7.1.5.2	Chemical Structures.....	214
7.1.5.3	Crystal structure data analysis	215
7.2	Chapter 2 Experimental.....	215
7.2.1	Chapter 2 HPLC-NMR Characterisation (from stop-flow HPLC-NMR)	215
7.2.2	Chapter 2 Off-line Characterisation.....	216
7.3	Chapter 3 Experimental.....	221
7.3.1	Chapter 3 HPLC-NMR Characterisation (from on-flow and stop-flow HPLC-NMR)	221
7.3.2	Chapter 3 Off-line Characterisation.....	222
7.4	Chapter 4 Experimental.....	226
7.4.1	Chapter 4 HPLC-NMR Characterisation (from stop-flow HPLC-NMR)	226
7.4.2	Chapter 4 Off-line Characterisation.....	227
7.5	Chapter 5 Experimental.....	230
7.5.1	Chapter 5 HPLC-NMR Characterisation (from stop-flow HPLC-NMR)	230
7.5.2	Chapter 5 Off-line Characterisation.....	230
7.6	Chapter 6 Experimental.....	232
7.6.1	Chapter 6 HPLC-NMR Characterisation (from on-flow HPLC-NMR)	232
7.6.2	Chapter 6 Off-line Characterisation.....	235
	References.	236

Chapter 1

Introduction

1.1 General Introduction

1.1.1 History of Natural Products

The term “natural product” or “secondary metabolite” refers to a compound that is produced by an organism that is not directly associated with the growth and survival of the organism [1]. The use of natural extracts for the treatment of illnesses and disease dates back thousands of years to ancient China with the Traditional Chinese Medicines (TCM) (~3,000 BC), India with Ayurvedic medicine (~1,000-3,000 BC) and Egypt with the ancient Ebers papyrus and Kahun papyrus describing early Egyptian medicinal knowledge (~3,000 BC) [2, 3]. The use of specific compounds as medicines began in the 18th and 19th centuries, with compounds such as digoxin (**1.1**) (from the plant genus *Digitalis*), aspirin (**1.2**) (a derivative of salicylic acid obtained from the bark of the willow tree) and morphine (**1.3**) (from the plant *Papaver somniferum*) [2]. In the 20th century, the focus continued to transfer from natural/herbal medicines to pharmaceuticals for the treatment of illnesses and diseases, with the discovery of penicillin (**1.4**) a major influence on the pharmaceutical industry. Following this, in the 1930’s and later, drug discovery moved to the screening of natural products and the isolation of active compounds from well-established biologically active plant extracts [3]. Despite the increasing prominence of the pharmaceutical industry during the 20th century to

the present day, it is estimated by the World Health Organisation (WHO) that 75% of the world's population still relies on traditional medicines for primary health care [1].

After 1980, the focus moved away from looking at natural products as a means of providing new pharmacophores or new drugs, instead progressing to other methods as a means to discover new drugs and drug leads [3]. This was mainly due to advancements in high-throughput screening (HTS) and combinatorial chemistry methodologies, where micro-scale syntheses produced a vast array of compounds which could be tested for biological activity and therapeutic potential. However these HTS techniques were not as successful as anticipated, with only one compound derived from combinatorial chemistry resulting in an approved drug, namely the anti-tumour drug sorafenib (**1.5**). This lack of success prompted the re-instatement of natural products as a means for providing potential drug leads [3, 4]. In the period from 1981-2010, a total of 1,355 drugs were approved, with fifty-nine (4%) being natural products and two hundred and ninety-nine (22%) derived from natural products as shown in **Figure 1.1** [5].

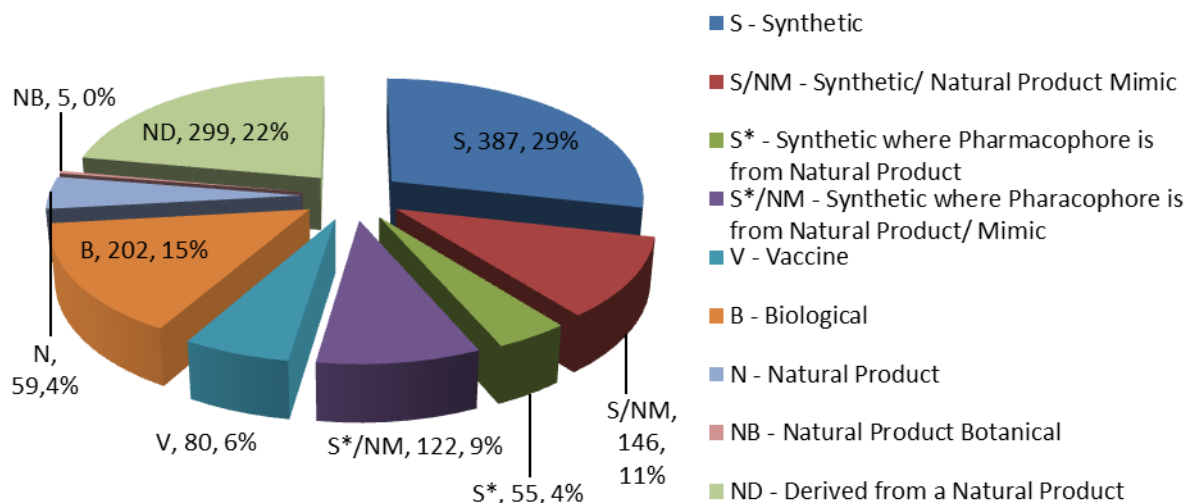


Figure 1.1. All approved drugs from 1981-2010 (sourced from Newman and Cragg [5]).

Also in this period the total number of approved anti-cancer drugs was one hundred and twenty-eight, with eleven (9%) being of natural product origin. The most well-known of these is paclitaxel (also known as Taxol) (1.6) from the Pacific yew tree, *Taxus brevifolia*. Another thirty-two (25%) approved anti-cancer drugs were derived from natural products (Figure 1.2) [5].

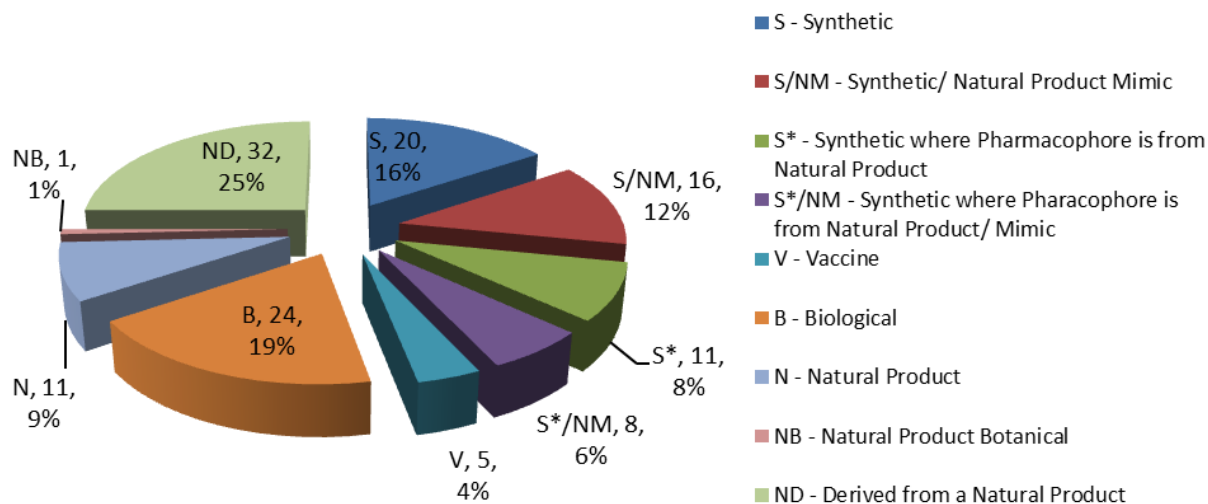
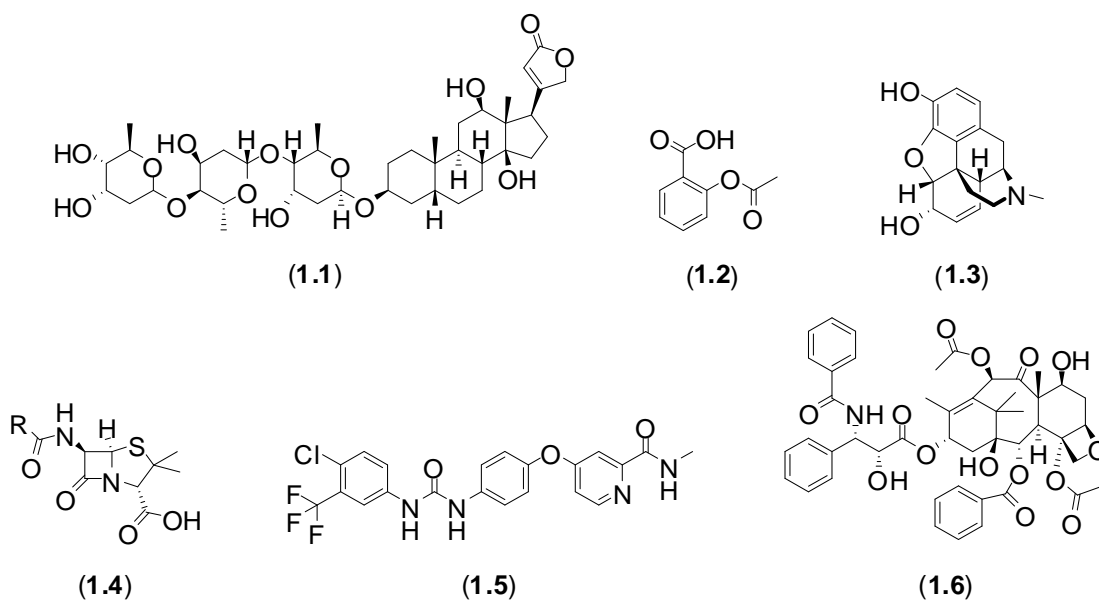


Figure 1.2. All approved cancer drugs from 1981-2010 (sourced from Newman and Cragg [5]).



1.1.2 Approaches to Natural Products Isolation

Classical approaches used in the isolation, characterisation and biological evaluation of secondary metabolites from natural product extracts can still result in the discovery of biologically active new compounds. Often these studies are motivated by the ethnobotanical and/or ethnopharmacological properties that the extract is known to possess. The limitation of this approach is that there is no way of predicting if the isolated compounds will possess biological activity [1]. There is also the problem that isolated compounds are generally only tested for biological activity in a limited number of bioassays, which decreases the chances of observing significant biological activity.

Modern strategies for the isolation of natural product drug leads involve the use of bioassay-guided fractionation, whereby the biological activity of the crude extract and subsequent fractions are assessed throughout the isolation procedure. This approach guides the fractionation/isolation process so as to assist in the isolation of bioactive compounds and can therefore remove the uncertainty as to whether compounds may or may not possess the activity displayed by the crude extract. Limitations arise when activity of the crude extract diminishes as fractionation/isolation steps are conducted or when active fractions are obtained in such low quantities that identification of individual compounds is impossible with current techniques. Further technological advancements in the area of natural products isolation/identification include chemical fingerprinting/profiling, metabolomics and dereplication [1].

Dereplication is the methodology by which bioactive natural product extracts can be excluded from in-depth chemical investigation studies so as to avoid re-discovery of either previously well-established biologically active natural products or isolation of nuisance compounds (eg. chlorophylls, fatty acids etc.). The process involves the analysis of natural product extracts or enriched fractions in order to quickly ascertain information regarding the possibility of novel compounds being present [1]. Together with the spectroscopic information obtained from a dereplication exercise (eg. NMR, MS and UV-Vis), the use of specific databases can be an

invaluable tool in this process. The ability to search the chemical literature based on taxonomy, structural information, as well as other spectroscopic information such as molecular mass, is particularly important to circumvent lengthy isolation procedures that would otherwise lead to the re-isolation of previously reported compounds. These databases can be very broad in their scope, for example Chemical Abstracts [6] and the Dictionary of Natural Products [7], or they can be more specific such as databases like MarinLit [8] which contains only information pertaining to the marine natural product literature.

1.1.3 Hyphenated Spectroscopic Techniques

The use of hyphenated spectroscopic techniques is also a key advancement in the dereplication process as structural information can be obtained much more quickly than from conventional isolation methods. The combination of a separation technique followed by spectroscopic analysis without intervening handling, allows for the collection of information that can be entered into databases to determine whether the extract should be subjected to off-line isolation procedures. The major hyphenated techniques used in the dereplication process include HPLC-NMR, HPLC-MS, GC-MS, as well as HPLC-NMR-MS. Each hyphenated technique has advantages and limitations, for example GC-MS analysis is very sensitive and only requires small quantities of material in order to obtain the mass spectra of compounds that are present in the sample as well as often providing fragmentation to give further structural insights. GC-MS however is a destructive technique and is only suited to the analysis of volatile compounds. This often means that there is a requirement to derivatise compounds to increase their volatility and this is not suited to an isolation in which the compound's integrity needs to be maintained for bioassay. HPLC-MS has the advantage of being a less destructive technique than GC-MS, with only the small portion of the sample that is diverted through to the mass spectrometer being destroyed. Overall this is a non-destructive technique which offers separation and mass spectral information. One limitation with HPLC-MS, specifically HPLC-ESI-MS, is that not all compounds in an extract will ionise readily in both or either ionisation modes, meaning multiple injections are required in an

attempt to get all of the compounds present to ionise. In addition, solubility issues can often arise for non-polar constituents.

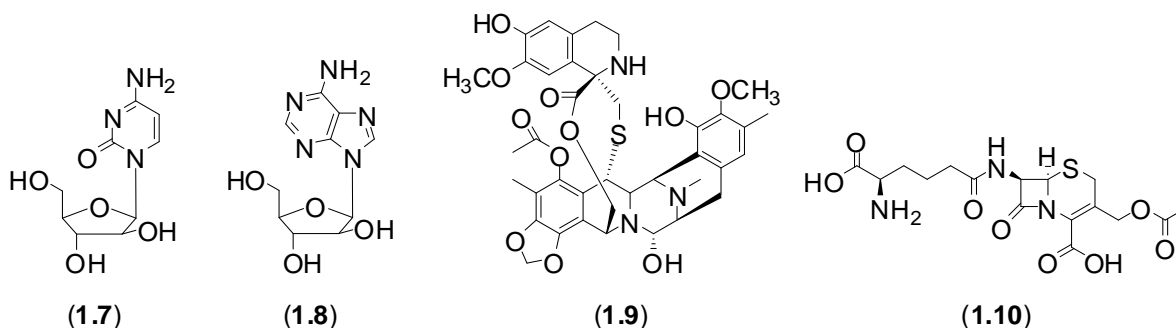
HPLC-NMR is a hyphenated spectroscopic technique that is not as popular as HPLC-MS (owing to the marked difference in sensitivity) in the dereplication process. However, it can offer great insights into the structures of the compounds that are present. HPLC-NMR is a non-destructive technique that allows for the fraction/extract injected to be analysed *in situ* and then collected intact. This provides the ability for the fraction/extract to be evaporated and then re-used for the isolation of the secondary metabolites present. The three modes of operation in HPLC-NMR are the on-flow, stop-flow and time-sliced modes. On-flow HPLC-NMR analysis allows for direct on-line analysis of the compounds present in an extract or fraction, whereby a series of continuous WET-1D ^1H NMR spectra as separated out by HPLC can be obtained for the sample. Stop-flow analysis allows for the trapping of single compounds in the NMR flow cell for an indefinite period, allowing for longer acquisition times and for 2D NMR analysis of individual components. Once one component is analysed, the HPLC pumps can be re-started so as to continue the elution, allowing for the next peak to be trapped for similar analysis. Time-slicing is a method where the pump is stopped automatically at intervals during the HPLC run and longer WET-1D spectra are acquired. Once these are complete, the pump then restarts and is then stopped after the next interval [9]. Time-slicing is a good method for the detection of peaks with poor separation and for automated stop-flow analysis of compounds that do not possess a UV chromophore. As noted earlier, the limitations with HPLC-NMR are those associated with sensitivity. With the NMR as the detector, higher concentrations of compounds than is suitable for analytical HPLC are required. This translates to the need to overload the analytical HPLC separation method to accommodate the need for greater quantities of compounds that are necessary for the NMR analysis, often at a cost to the quality of the chromatography. This need for overloading of the sample is diminishing with the advancements in technology, with high-field magnets, cryogenic probes and software improvements allowing for smaller quantities of material to be analysed. Another major problem associated with HPLC-NMR usage is the

need for at least one deuterated solvent for the analysis (generally D₂O is used) which is costly given the constant flow during analysis. An extension of HPLC-NMR is the addition of a further spectroscopic technique, as in the case of HPLC-NMR-MS, whereby the sample, once separated by HPLC, is diverted for analysis by NMR and MS simultaneously. Alternatively, after analysis by NMR, the sample is split between the MS and waste to allow for the MS analysis. The greater amount of information that can be acquired by a single analysis, complemented by the use of databases, can dramatically reduce the need for an off-line isolation and therefore also reduce the total number of previously reported compounds being re-isolated. These hyphenated spectroscopic approaches allow for a greater insight into the probable secondary metabolites present in any given organism.

1.1.4 Marine Natural Products

While the terrestrial environment has been studied extensively for biologically active natural products, especially those derived from traditional medicines, the marine environment has not been studied as thoroughly. The focus for the study of marine organisms as a means of providing potentially biologically active compounds was prompted by the fact that 70% of the world's surface is oceans [10] and should therefore provide rich biodiversity. Marine natural products research was initially limited to the study of organisms from shallow waters until the advancements in the areas of SCUBA diving and trawling [10]. The world's oceans provide tremendous biodiversity with many areas (e.g. hydrothermal vents and sea mounts) not having been extensively studied owing to the difficulty in collection. Because there is very little traditional medicinal knowledge associated with marine organisms (as opposed to the rich lore regarding terrestrial organisms such as plants), the search for biologically active compounds from marine sources has occurred via a more random selection of organisms. The first drug candidates that were isolated from marine sources were Ara-C (**1.7**), an anti-leukemic drug, and the similar Ara-A (**1.8**) an anti-viral drug, both derived from the marine sponge *Tethya crypta* [11, 12]. The field of marine natural products has grown extensively over the last fifty years, as shown by an increase in the total number of isolated compounds

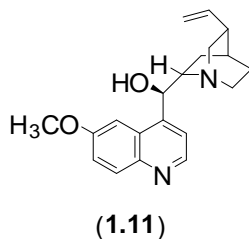
per year. In 2003, six hundred and fifty-six compounds were reported [13] while in 2009, 1,011 compounds were documented [14]. While there has been a steady increase in the number of marine natural products isolated or reported, the number of potential pharmaceuticals that have been discovered from marine sources is limited. The most notable marine natural product pharmaceuticals include the anti-tumour drug ET-743 (**1.9**), from the tunicate *Ecteinascidia turbinata* [12], the analgesic conotoxin peptide Ziconotide, from the cone snail *Conus magus* [11] and cephalosporins such as cephalosporin C (**1.10**) from marine fungi [15].



The discovery of marine natural products as potential drug candidates comes with some problems. Firstly, these biologically active constituents are generally present in very small quantities within the sample. This poses difficulties in terms of re-isolation or scale-up for further biological testing and has implications in terms of harvesting (the actual mass of organism required for large-scale isolation as well as issues associated with ecological considerations). Consequently, synthesis of the active compound(s) is often required to provide sufficient material for further biological activity studies [12]. These problems are compounded by the inherent complex nature of many of the marine natural product scaffolds. One of the strategies to overcome the problems associated with obtaining sufficient quantities of these compounds is to adopt a semi-synthetic approach in the synthesis of biologically active marine natural products (which also results in the synthesis of structural analogues). Technological advances such as HTS, computational biology and bioinformatics are also being increasingly employed [12].

1.1.5 Plant Natural Products

Plants have been studied for centuries for their biologically active components, primarily on the basis of the traditional uses of the plants. For example, in 1630 it was discovered that the bark of the *Cinchona* tree in Peru could overcome fevers. When it was introduced to Europe, it was found to have specific anti-malarial activity [16]. This activity was later shown to be due to the primary component, quinine (1.11) [16]. For nearly three hundred years, the only recorded treatments of malaria were quinine (1.11) or its natural source, the powdered bark of the *Cinchona* tree [16]. Other examples of plant natural product derived drugs are listed in the general introduction in **Section 1.1.1**.



1.1.6 Natural Product Studies Conducted

During the course of this research, a total of two marine and three terrestrial plants were investigated. A combination of on-line profiling and traditional natural product isolation methodologies resulted in a total of seven structure classes being identified. Two of the structure classes that were identified during this research were of the flavonoid and naphthoquinone structure classes. These classes of compounds are well-known to possess a broad range of biological activity, as well as being found throughout the plant kingdom. A range of natural and synthetic derivatives of these two structure classes are provided as a review in the sections that follow (**Section 1.2** and **Section 1.3**)

1.2 Flavonoids

1.2.1 General Introduction

Flavonoids is the general name given to the group of polyphenolics such as the flavanones, flavones, flavonols, flavanol, isoflavones and anthocyanidins, the structures of which are given in **Figure 1.3** [17]. Flavonoids can be present in nature as the free aglycones or as glycosides [18], with the main variations in structure being the degree of oxygenation as well as type, degree and pattern of alkyl substitution throughout the core flavonoid structure [19]. Flavonoids are one of the most widely spread classes of natural products found within the plant kingdom [18, 20], with more than 6,500 different flavonoids known to exist [19]. The biological activities of flavonoids, especially those found in food, have been studied extensively, with the use of flavonoid-containing extracts (e.g. from *Ginkgo biloba*, *Tilia* spp., *Equisetum* spp., *Moringa oleifera* and *Sophora japonica*), being used for the treatment of many types of illnesses [20]. Flavonoids have been found to possess anti-oxidant, anti-osteoporotic, anti-diabetic, anti-inflammatory, anti-microbial, anti-cancer, cardio-protective, neuro-protective, estrogenic/anti-estrogenic, anxiolytic, analgesic and anti-allergic activities [20].

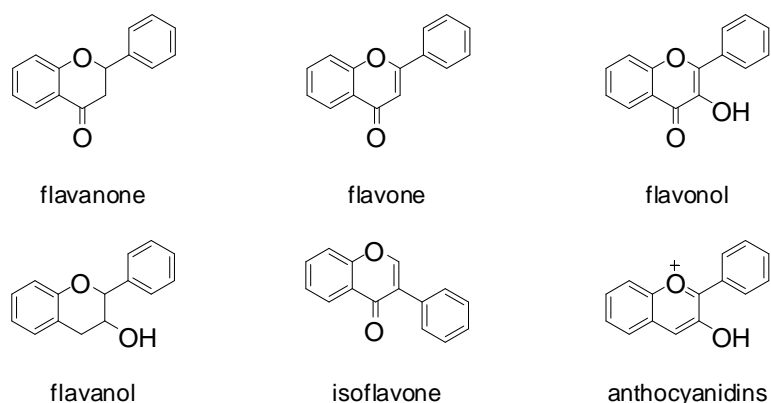
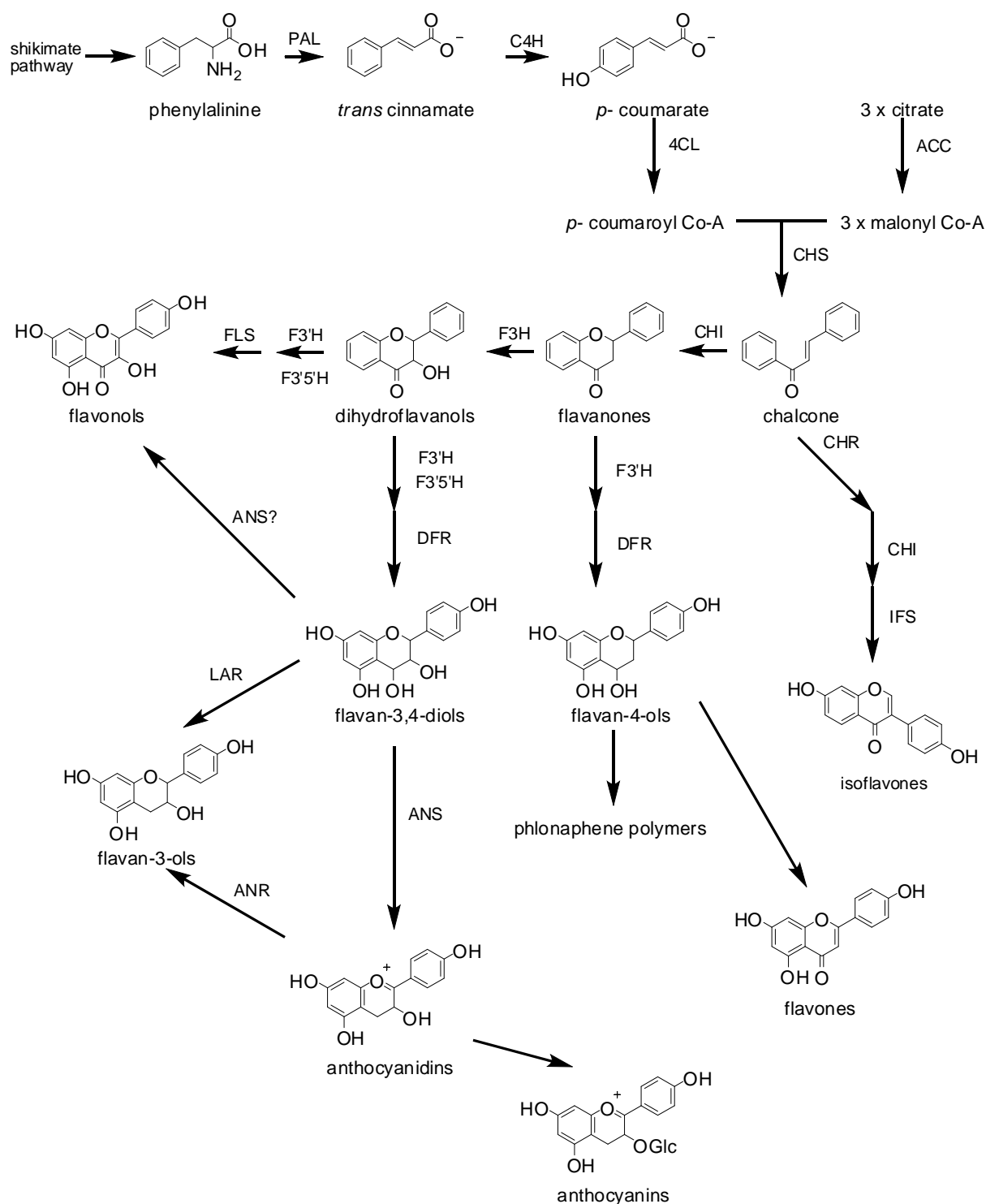


Figure 1.3. Structure classes described as flavonoids



4CL - 4-coumarate:CoA ligase; **ANR** - anthocyanidin reductase; **ANS** - anthocyanidin synthase; **C4H** - cinnamate 4-hydroxylase; **CHI** - chalcone isomerase; **CHR** - chalcone reductase; **CHS** - chalcone synthase; **DFR** - dihydroflavonol 4-reductase; **F3H** - flavonone 3-hydroxylase; **F3'H** - flavonoid 3'-hydroxylase; **F3'5'H** - flavonoid 3'5'-hydroxylase; **FLS** - flavonol synthase; **FNSI/II** - flavone synthase; **Glc** – glucose; **IFS** - isoflavone synthase; **LAR** - leucoanthocyanidin reductase; **PAL** - phenylalanine ammonia lyase; **UFGT** - UDP-glucose: flavonoid 3-O-glucosyltransferase

Scheme 1.1. The biosynthetic pathway for the major subclasses of flavonoids (sourced from Tsao and McCallum [21])

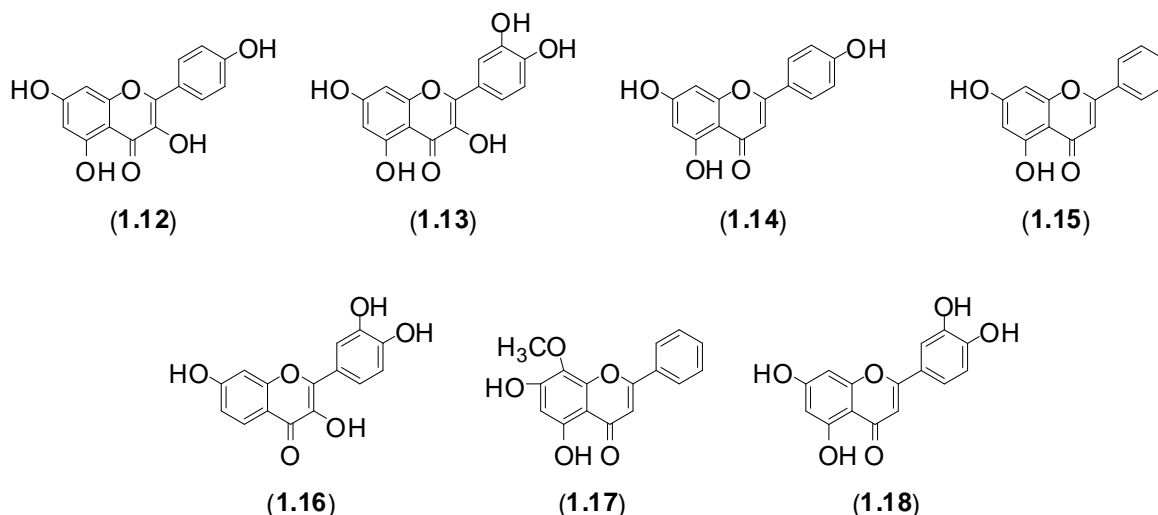
1.2.2 Biological Activity

1.2.2.1 Anti-cancer flavonoids

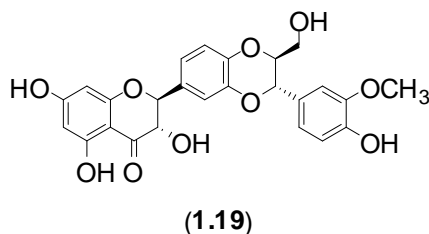
The anti-cancer activity of flavonoids has been well documented since 2008, with over six hundred references citing the cytotoxicity and anti-cancer activity of flavonoids [22]. Selected references from the period 2008-2012 are reviewed below.

Many studies into the anti-cancer activity of flavonoids and flavonoid glycosides have shown that flavonoids such as kaempferol (**1.12**) have a preventative effect against many forms of cancer [20, 23]. It has been shown that dietary flavonoids inhibit cytochrome P450 CYP1 enzymes, which is important for their cancer preventative characteristics [24, 25]. The direct mode of action of flavonoids and flavonoid glycosides against different forms of cancer is starting to become understood, together with the mechanism of the synergistic effect of flavonoids such as kaempferol (**1.12**) that are administered with other anti-cancer drugs. These reports are accompanied by suggestions that flavonoids may have adjuvant therapy applications [20, 25]. The actual mechanism for the anti-cancer activity of some flavonoids has been suggested to be associated with their antimitotic activity [25]. The flavonoids kaempferol (**1.12**), quercetin (**1.13**), apigenin (**1.14**), chrysin (**1.15**), fisetin (**1.16**), wogonin (**1.17**) and lutelin (**1.18**), are all known to exhibit anti-cancer activity [26]. It was thought that the anti-cancer activity of these flavonoids (**1.12-1.18**) may be due to the anti-angiogenic activity shown [26].

The flavonoid wogonin (**1.17**), isolated from *Scutellaria baicalensis* Georgi has been shown to possess cytotoxic and cytostatic activity towards several anti-cancer cell lines, while also having low toxicity towards normal cells, as well as possessing synergistic effects when administered with other drugs [27].

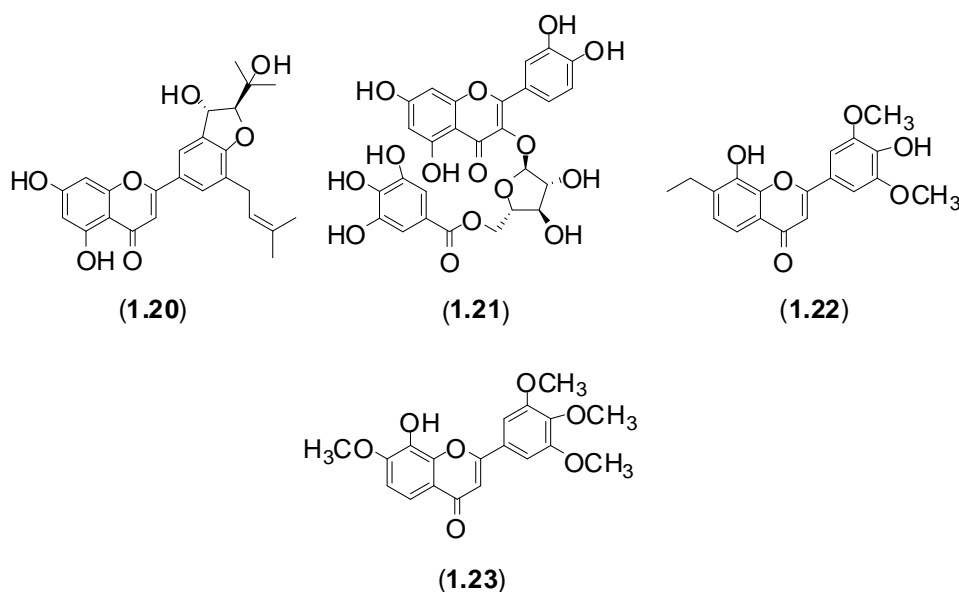


Silibinin (**1.19**), isolated from *Silybum marianum*, is known to possess anti-cancer activity towards prostate, colon, bladder and lung cancers, with the compound found to be active against the migration, invasion and metastasis of cancer cells [27]. Silibinin (**1.19**) has also been found to protect against angiogenesis and late-stage metastasis, suggesting it has the potential to improve the survival and reduce the morbidity in prostate cancer patients [27].



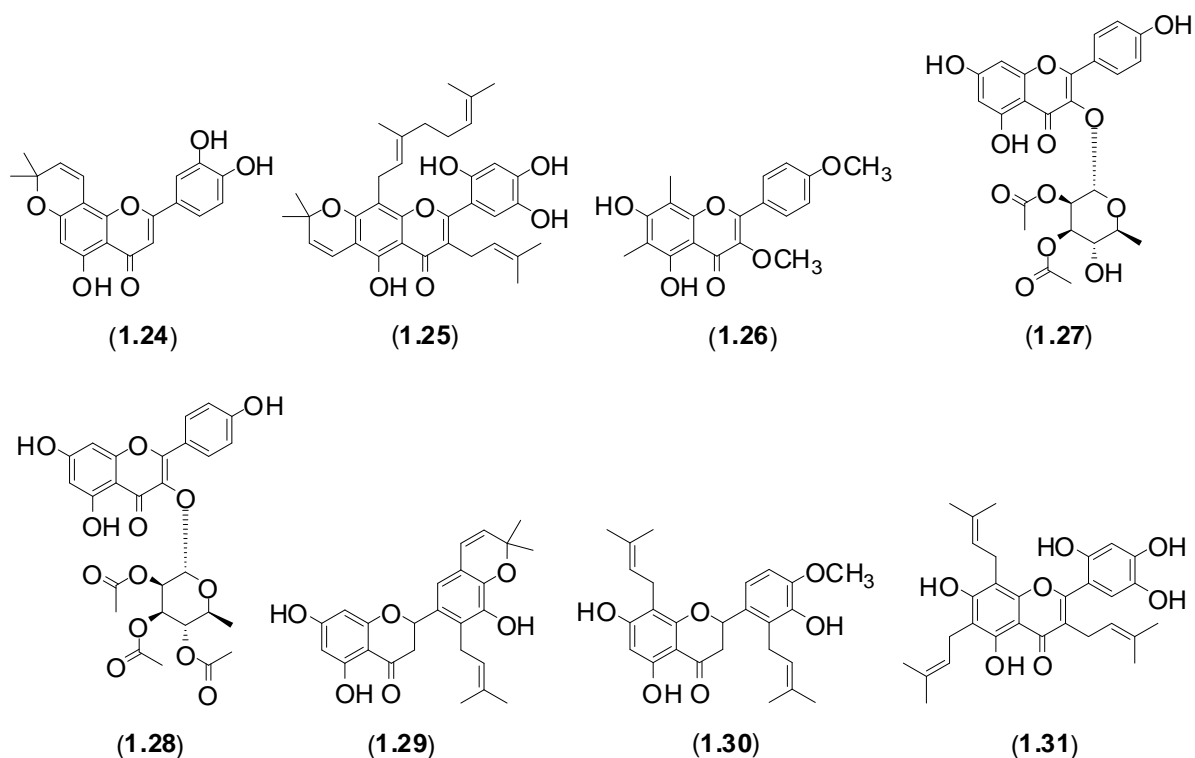
Luteolin (**1.18**), a dietary flavonoid that can be found in many green vegetables, has been found to possess anti-tumour activity for various types of cancer *in vitro*, with IC₅₀ values ranging from 3 μM to 50 μM [27]. Apigenin (**1.14**), another dietary flavonoid, has been shown to provide cancer preventative benefits, displaying anti-cancer activity against many forms of cancer, while also possessing low toxicity levels to normal cells [23, 28]. Apigenin (**1.14**) has also been shown to inhibit regulation of the p14ARF-Mdm2-p53 pathway in breast cancer cell growth as well as increasing the expression of UDP-glucuronosyltransferase in colon cancer and increasing the down-regulation of NF- κ B activity with the suppression of Akt in pancreatic

cancer [23]. Quercetin (**1.13**) increases the efficacy of cisplatin both *in vivo* and *in vitro*, while also providing protection from cisplatin toxicity in normal cells [29]. *In vitro* studies have also revealed that quercetin (**1.13**) possesses synergistic effects when combined with anti-cancer compounds such as busulfan and cyclophosphamide, while also decreasing resistance of multidrug-resistant cell lines to chemotherapy [29]. Quercetin (**1.13**) is known to inhibit the MCF-7 breast adenocarcinoma, HT-29 human colon adenocarcinoma and K562 human chronic myelogenous leukaemia cell lines [30]. The flavonoid breviflavone B (**1.20**), isolated from *Epimedium brevicornum*, was found to possess activity against breast cancer cell proliferation [31]. Compound **1.21**, from *Triplaris cumingiana*, showed cytotoxicity to the H-460 lung cancer cell line [31], while a study of *Muntingia calabura* afforded compounds **1.22** and **1.23** which showed cytotoxicity towards the P388 cell line [31].



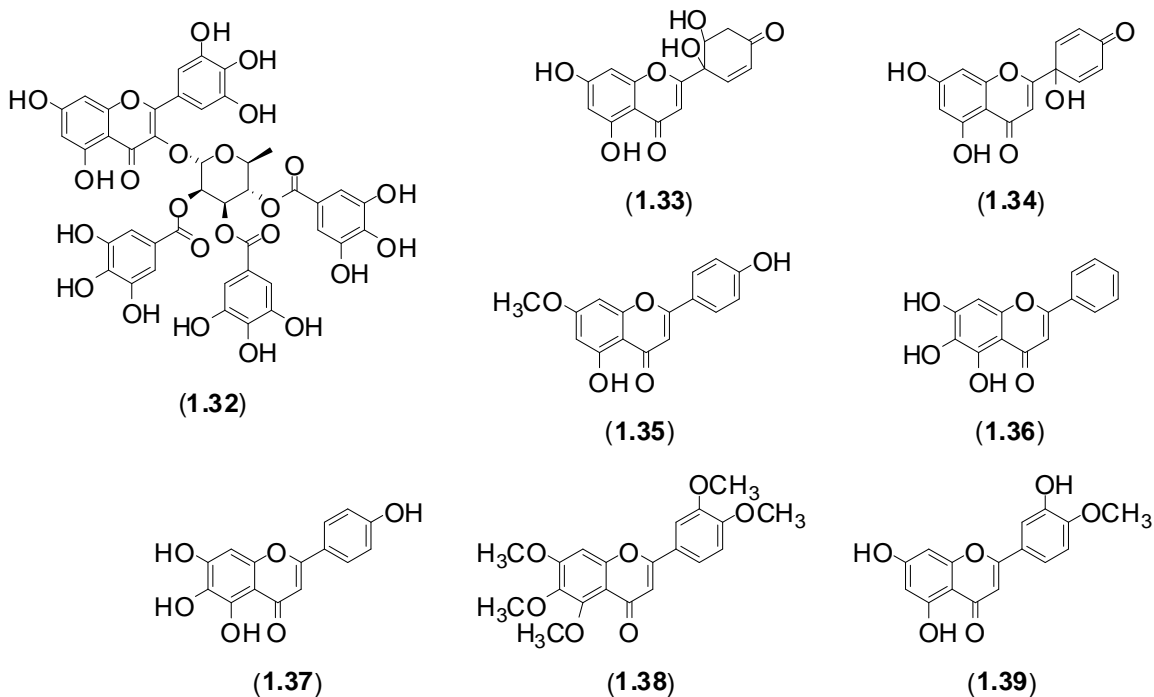
In a study of the prenylated flavonoid, arochamin C (**1.24**), this compound showed activity against a number of human tumour cell lines, while artoindonesianin U (**1.25**) was found to possess P388 anti-tumour activity [31]. In a study on the aerial parts of *Eucalyptus occidentalis*, compound **1.26** was found to induce apoptosis in human myeloid leukemia cells [31]. The flavonoids **1.27** and **1.28**, isolated from *Zingiber aromaticum*, have been shown to

have activity against the CYP3A4 and CYP2D6 cytochromes, with the tri-acetyl derivative **1.28** being the more active (IC_{50} values of 14.4 μ M and 43.3 μ M against the two isoforms respectively) [31]. The flavonoids **1.29** and **1.30**, isolated from *Dendrolobium lanceolatum*, were found to possess moderate activity in cytotoxicity assays [31]. The flavonoid styracifolin B (**1.31**) was shown to be active against the KB mouth epidermoid carcinoma cell line and MRC-5 human diploid embryonic lung cells, with IC_{50} values of 5.6 μ M and 4.7 μ M respectively [32]. The use of fisetin (**1.16**) in combination with the anti-cancer compound cisplatin established that these two compounds activate the cell death receptor pathway and could be a useful combined therapy for the elimination of embryonic carcinoma cells [33].

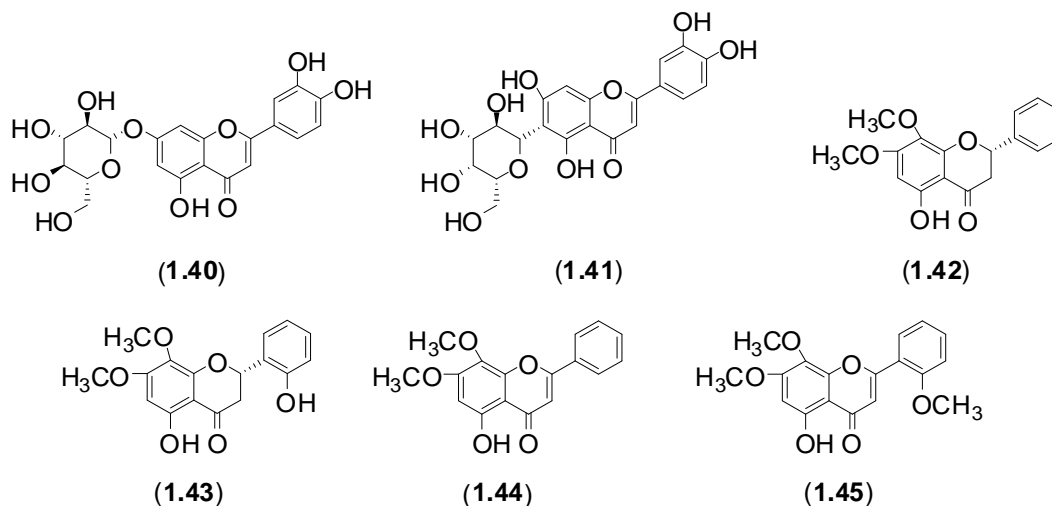


From a study of *Leucenia leucocephala* myricetin 3-O-(2',3',4'-tri-O-galloyl)- α -L-rhamnopyranoside (**1.32**) was found to possess Hep-G2 hepatocellular carcinoma cell line activity, with an IC_{50} value of 2.14 μ g/mL [34]. In a study, the flavonoid **1.33** isolated from *Macrothelypteris torresiana*, a structural derivative of protoapigenone (**1.34**), was found to have activity towards the human Hep-G2 cell line, while being inactive towards normal cells

[35]. A further study of protoapigenone (**1.34**) from the same source showed that this compound was active against Hep-G2 (2.3 $\mu\text{g/mL}$), Tca-8113 oral squamous cell carcinoma (0.6 $\mu\text{g/mL}$), MCF-7 (0.8 $\mu\text{g/mL}$) and K562 human erythroleukemic (0.9 $\mu\text{g/mL}$) cell lines [36]. Chrysin (**1.15**) has been found to possess activity against many varieties of cancer, such as the cervical cancer cell line HeLa (IC_{50} values of between 14.2 μM and 30 μM), U937 leukaemia cell line (16 μM), possessing activity against other cell lines of leukaemia, cytotoxicity towards KYSE-510 oesophageal squamous carcinoma (63 μM), as well as showing activity against malignant glioma, breast carcinoma and prostate cancer [37]. From a study into the MDA-MB-468 human breast cancer cell line, activities of the flavonoids chrysin (**1.15**) (IC_{50} 20.5 μM), genkwanin (**1.35**) (IC_{50} 1.6 μM), baicalein (**1.36**) (IC_{50} 6.3 μM), scutellarein (**1.37**) (IC_{50} 12.8 μM) and sinensetin (**1.38**) (IC_{50} 0.2 μM) were established [38]. The flavonoids luteolin (**1.18**) and diosmetin (**1.39**) from the flowers of the plant species *Chrysanthemum morifolium* were found to possess anti-cancer activity against the Colon205 cell line, with IC_{50} values of 96.9 μM and 82.9 μM respectively for the two compounds [39].



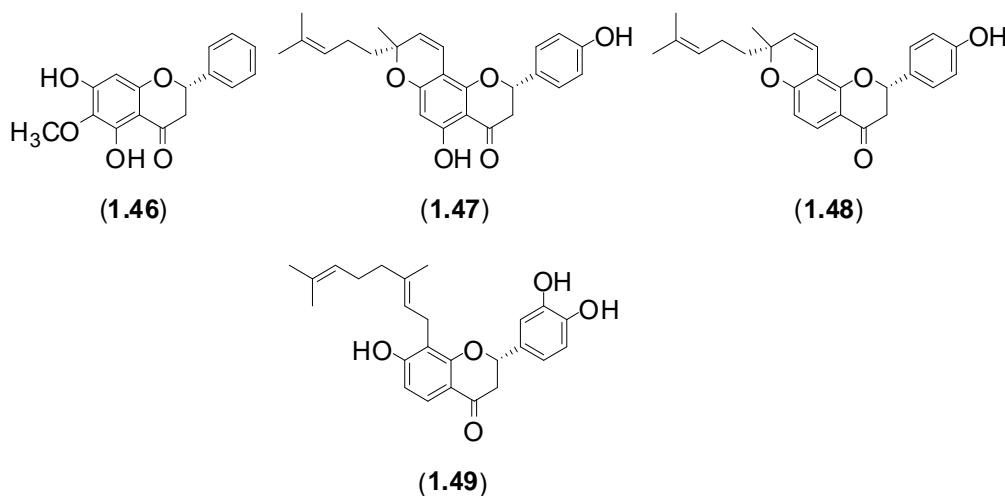
In a report of the cytotoxicity of the flavonoid and flavonoid glycosides isolated from *Horwoodia dicksoniae* against the Hep-G2 hepatocellular carcinoma cell line, MCF-7 breast adenocarcinoma and HCT-116 colon cell line, the activity for the flavonoids luteolin (**1.18**) (**pg 12**) (IC_{50} values for HEP-G2 12.3 μ M, HCT-166 9.5 μ M and MCF-7 12.7 μ M), luteolin 7-*O*- β -D-glucopyranside (**1.40**) (10.7 μ M, 9.3 μ M and 9.9 μ M) and luteolin 6-C- β -D-galactopyranoside (**1.41**) (15.8 μ M, 11.2 μ M and 19.5 μ M) showed that each compound displayed activity in the same order of magnitude to that of doxorubicin (~4.5 μ M against each cell line) [40]. From a study of the constituents present in *Andrographis paniculata* four flavonoids (**1.42-1.45**) were evaluated for biological activity against the Jurkat human lymphocytic cancer cell line, the PC-3 human prostate cancer cell line and the Colon205 human colonic cancer cell line, with **1.42-1.45** displaying activity towards the Jurkat cell line with IC_{50} values between 50-150 μ M, while displaying no cytotoxicity towards any of the other cell lines up to the highest concentration tested of 20 μ M [41].



Of the twenty-two flavonoids isolated from a Brazilian propolis, a natural resinous product collected by honey bees from various plants, (2*S*)-7-hydroxy-6-methoxyflavanone (**1.46**) was found to be the most active compound against all strains of cancer, with activity against Colon 26-L5 colon carcinoma (IC_{50} 5.9 μ M), B16-BL6 melanoma (IC_{50} 6.7 μ M), LLC lewis lung carcinoma (IC_{50} 9.3 μ M), A549 lung adenocarcinoma (IC_{50} 8.6 μ M), HeLa cervical

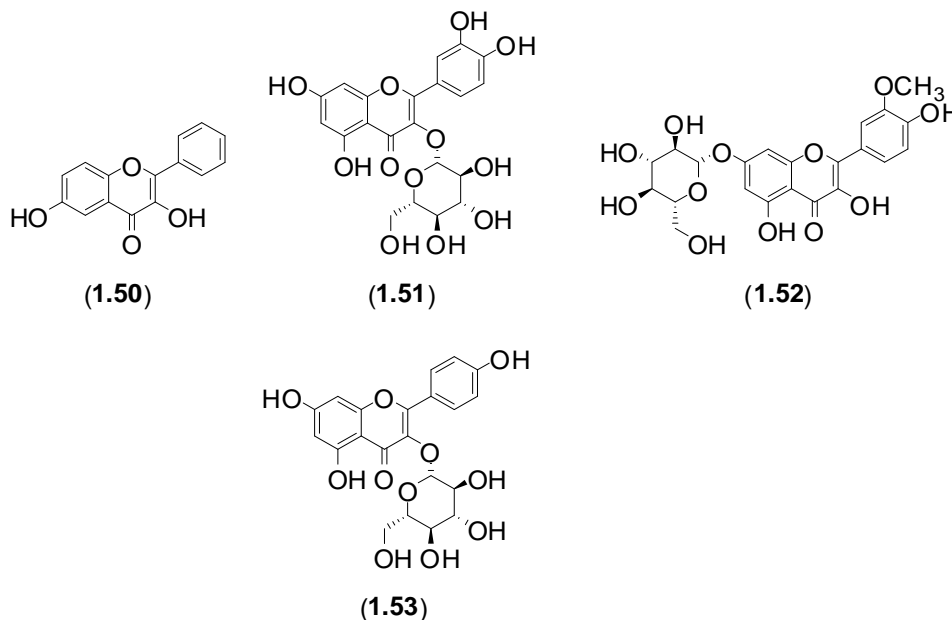
adenocarcinoma (IC_{50} 5.6 μ M) and HT-1080 fibrosarcoma (IC_{50} 7.9 μ M) having been observed [42].

Isolated from the plant species *Artocarpus communis*, the flavonoids arcommunol A (**1.47**), arcommunol B (**1.48**) and 8-geranyl-3',4',7'-trihydroxyflavone (**1.49**) were shown to possess activity against the Hep-G2 hepatocellular carcinoma cell line, Hep-3B hepatoma, PLC-5 hepatocellular carcinoma and SK-Hep-1 hepatocellular carcinoma cell lines [43]. The activity of each compound was assessed and the following IC_{50} values were reported: arcommunol A (**1.47**) (IC_{50} values Hep-G2 9.19 μ M, Hep-3B 20.4 μ M, PLC-5 30.3 μ M and SK-Hep-1 2.05 μ M); arcommunol B (**1.48**) (IC_{50} values of 5.55 μ M, 23.9 μ M, 13.1 μ M and 7.82 μ M) and 8-geranyl-3',4',7'-trihydroxyflavone (**1.49**) (IC_{50} values of 4.42 μ M, 9.95 μ M, 9.24 μ M and 6.65 μ M) [43].



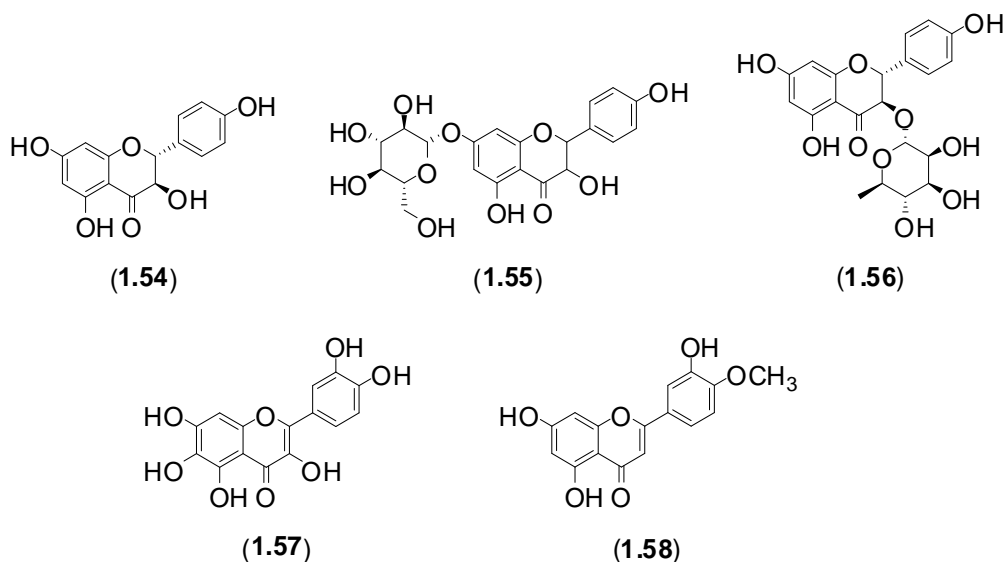
The study by Lee *et al* [44] of four hundred and fifty flavonoids for anti-cancer activity against human cervical and prostate cancer cells, revealed that 3,6-dihydroxyflavone (**1.50**) is a potent agonist of hPPAR with cytotoxicity towards both cervical and prostate cancer cells [44]. Flavonoids isolated from *Diplotaxis harra* (Forssk.) Boiss. were assessed for cytotoxicity against the HCT-116 human colonic carcinoma cell line, with quercetin (**1.13**) (page 12) (IC_{50} 20.1 μ g/mL), quercetin-3-*O*- β -glycoside (**1.51**) (IC_{50} 24.3 μ g/mL), isorhamnetin-7-*O*- β -

glycoside (**1.52**) (IC_{50} 22.8 $\mu\text{g/mL}$) and kaempferol-3-*O*- β -glycoside (**1.53**) (IC_{50} 41.9 $\mu\text{g/mL}$) displaying moderate cytotoxicity [45].

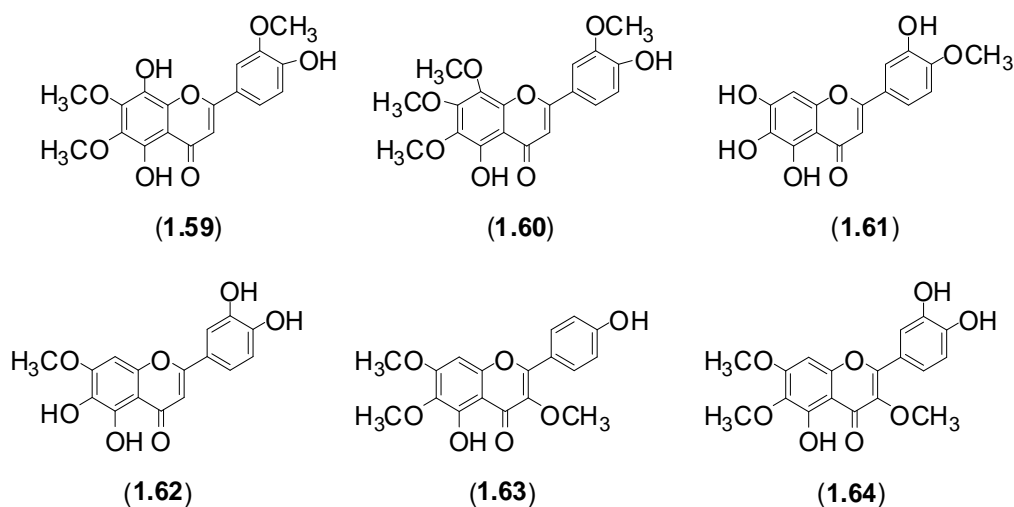


The three flavonoids isolated from the shrub *Smilax china* L. were found to possess anti-cancer activity towards the MCF-7 breast adenocarcinoma and MDA-MB-231 human breast carcinoma cell lines, namely dihydrokaempferol (**1.54**) (IC_{50} values of MCF-7 15.1 $\mu\text{g/mL}$, MDA-MB-231 33.1 $\mu\text{g/mL}$), kaempferol-7-*O*- β -glycoside (**1.55**) (IC_{50} values of 8.4 $\mu\text{g/mL}$, 23.1 $\mu\text{g/mL}$) and dihydrokaempferol-3-*O*- β -L-rhamnoside (**1.56**) (IC_{50} values of 18.0 $\mu\text{g/mL}$, 20.8 $\mu\text{g/mL}$) [46].

From a study into the flavonoids found in citrus fruits, it was determined that apigenin (**1.14**) (pg 12) and quercetagenin (**1.57**) exhibit potent anti-cancer activity against SW480 human colon cancer cells by inducing apoptosis [47]. A separate study of hesperetin (**1.58**), found in citrus fruits such as oranges and grapefruit, showed that **1.58** possessed activity towards the Notch1 signalling pathway, which was shown to be essential in the suppression of carcinoid tumours proliferation, suggesting that **1.58** could be a potential treatment for carcinoid cancers such as colon, renal and small cell lung cancers [48].



The flavonoids (1.13, 1.18 and 1.59-1.64) isolated from the Chinese herb, *Rabdosia rubescens*, were assessed against the HL-60 human promyelocytic leukemia cell line and while 5,8,4'-trihydroxy-6,7,3'-trimethoxyflavone (1.59) showed no activity at the highest concentration tested (100 μM), quercetin (1.13) (pg 12) (IC_{50} 69.68 μM), luteolin (1.18) (IC_{50} 46.64 μM), nodifloretin (1.61) (IC_{50} 69.34 μM), pedalin (1.62) (IC_{50} 61.98 μM) and penduletin (1.63) (IC_{50} 52.00 μM) showed moderate activity, with 5,4'-dihydroxy-6,7,8,3'-tetramethoxyflavone (1.60) being the most active with an IC_{50} of 7.55 μM , comparable to the known anti-cancer drug doxorubicin (IC_{50} 4.64 μM) [49].



Rosa canina L. was also found to contain the flavonoid quercetin (**1.13**) (pg 12) and it was once again found to be a potent inhibitor of the HeLa cervical adenocarcinoma (IC₅₀ 10.3 µg/mL), HT-29 colon adenocarcinoma (IC₅₀ 12.7 µg/mL) and MCF-7 breast adenocarcinoma (IC₅₀ 25.3 µg/mL) cell lines [50].

Of the ten flavonoids isolated from *Rosmarinus officinalis* it was found that kaempferol (**1.12**) possessed weak activity against the HL-60 human promyelocytic leukemia cell line (IC₅₀ 82 µM) and that luteolin (**1.18**) possessed moderate activity against the same cell line (IC₅₀ 39.6 µM) [51].

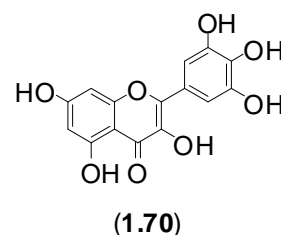
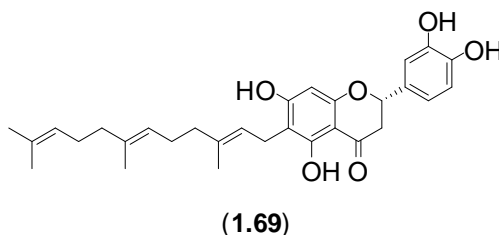
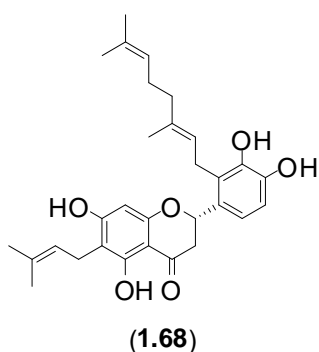
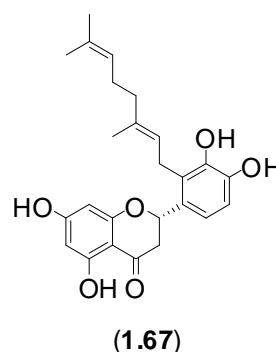
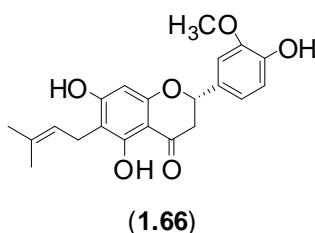
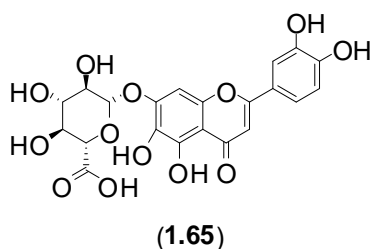
In a report of the flavonoids from the two species of the perennial herb *Scutellaria* (*S. immaculata* and *S. ramosissima*), a total of thirty-one flavonoids were identified and evaluated for biological activity towards the HeLa cervical adenocarcinoma, Hep-G2 hepatocellular carcinoma and MCF-7 breast adenocarcinoma cell lines [52]. It was found that of the six flavonoids subjected to biological evaluation against these cancer cell lines, only apigenin (**1.14**) (IC₅₀ 33.3 µg/mL) and chrysin (**1.15**) (IC₅₀ 22.8 µg/mL) showed moderate activity towards the HeLa cell line, while apigenin (**1.14**) (IC₅₀ 64.6 µg/mL), chrysin (**1.15**) (IC₅₀ 14.0 µg/mL) and scutellarin (**1.65**) (IC₅₀ 94.6 µg/mL) displayed moderate activity towards the Hep-G2 cell line. The same three compounds displayed moderate activity towards the Hep-G2 cell line (apigenin (**1.14**) (IC₅₀ 17.3 µg/mL), chrysin (**1.15**) (IC₅₀ 22.7 µg/mL) and scutellarin (**1.65**) (IC₅₀ 31.8 µg/mL)) [52].

A study into the activity of the dietary flavonoid luteolin (**1.18**) on oral squamous cell carcinoma concluded that continuous administration of luteolin (**1.18**) was effective in the suppression of xenograft tumours in mice, while used in conjunction with taxol, it enhanced the cytotoxic effect of taxol [53].

Four of the flavonoids (**1.66-1.69**) that were isolated from the tropical tree, *Macaranga triloba*, were evaluated against the HL-60, MCF-7 and HeLa cell lines, with 6-prenyl-3'-methoxyeriodictyol (**1.66**) (HL-60 IC₅₀ 15.1 µg/mL, MCF-7 IC₅₀ 22.8 µg/mL and HeLa IC₅₀ 12.2 µg/mL), nymphaeol B (**1.67**) (IC₅₀ 21.3 µg/mL, IC₅₀ 23.5 µg/mL, IC₅₀ 17.0 µg/mL) and

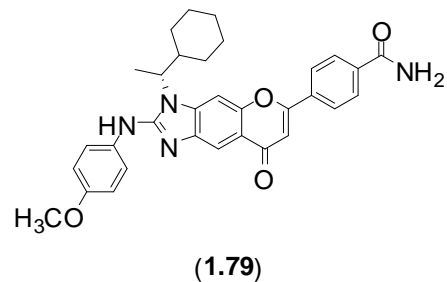
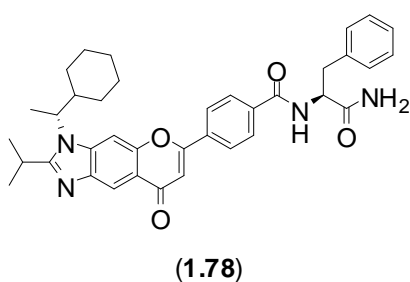
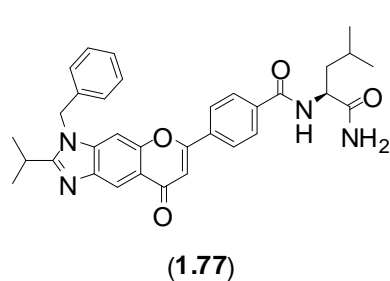
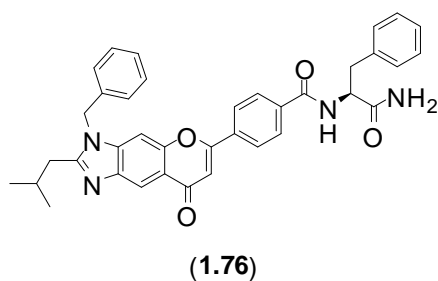
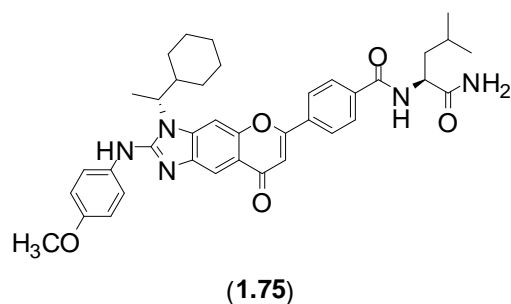
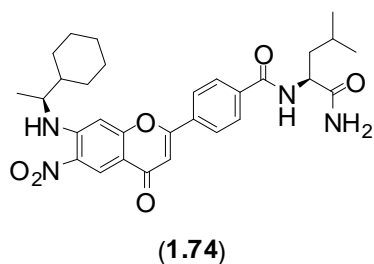
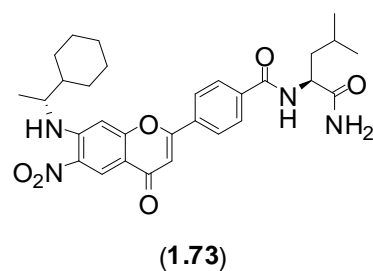
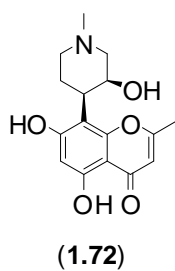
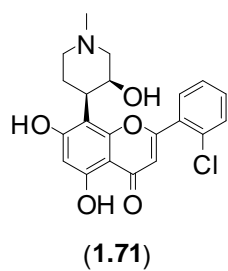
nymphaeol C (**1.68**) (IC_{50} 11.6 $\mu\text{g/mL}$, IC_{50} 23.0 $\mu\text{g/mL}$, IC_{50} 18.2 $\mu\text{g/mL}$) showing moderate to weak activity against the cell lines, while 6-farnesyl-3',4',5,7-tetrahydroxyflavanone (**1.69**) (IC_{50} 3.3 $\mu\text{g/mL}$, IC_{50} 5.6 $\mu\text{g/mL}$, IC_{50} 1.3 $\mu\text{g/mL}$) was found to have potent activity against each of these cell lines [54].

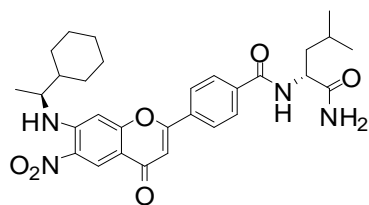
Research into the effect of commercial myricetin (**1.70**) on pancreatic cancer showed that, *in vitro*, myricetin (**1.70**) induced pancreatic cancer cell death via apoptosis, while *in vivo* treatment resulted in the regression of tumours and decreased the level of metastatic spread. These observations together with the fact that, *in vitro* and *in vivo*, myricetin (**1.70**) was non-toxic to normal cells, suggest that **1.70** is a potential therapeutic agent against pancreatic cancer [55].



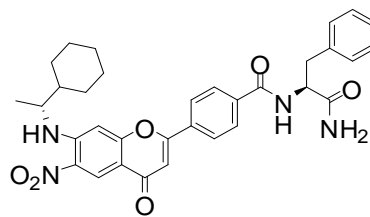
The synthetic flavonoid flavopiridol (**1.71**), a derivative of the natural product, rohutikine (**1.72**), isolated from *Dysoxylum binectariferum* Hook., is currently undergoing Phase I/II clinical trials against various forms of cancer, with fifty-one active or completed trials [9, 56]. From a series of forty-nine synthetically prepared flavonoid derivatives that were screened

for breast cancer activity, compound (**1.73**) was found to be the most active with an IC_{50} of 1 μ M, while compounds **1.74** (IC_{50} 2 μ M), **1.75** (IC_{50} 5 μ M), **1.76** (IC_{50} 5 μ M), **1.77** (IC_{50} 7 μ M), **1.78** (IC_{50} 5 μ M), **1.79** (IC_{50} 5 μ M), **1.80** (IC_{50} 5 μ M) and **1.81** (IC_{50} 7 μ M) also displayed potent activity [57].



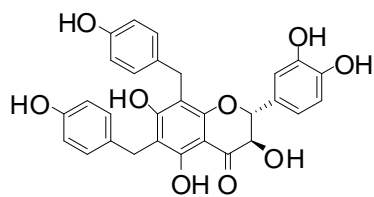


(1.80)

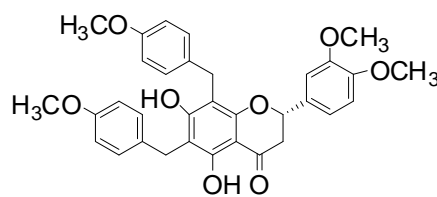


(1.81)

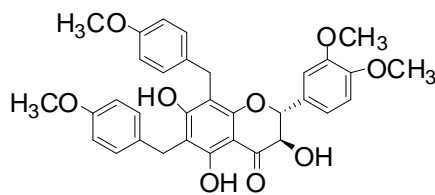
Two synthetic analogues (**1.83** and **1.84**) based on the natural flavonoid gericudranin A (**1.82**) were tested for anti-cancer activity towards sixteen human cancer cell lines and were found to possess potent activity. Compound **1.83** was active against CAKi-1 kidney clear cell carcinoma (IC_{50} 1.9 μ M), SNB-75 glioblastoma (IC_{50} 2.7 μ M) and NCI-H522 lung Cancer (IC_{50} 2.3 μ M), while **1.84** was most active against LOX-IMVI melanoma (IC_{50} 2.1 μ M), HCT-15 colon carcinoma (IC_{50} 2.8 μ M) NCI-H522 (IC_{50} 3.0 μ M) and SNB-19 glioblastoma (IC_{50} 0.7 μ M), the last of which was comparable to doxorubicin (IC_{50} 0.6 μ M) [58].



(1.82)



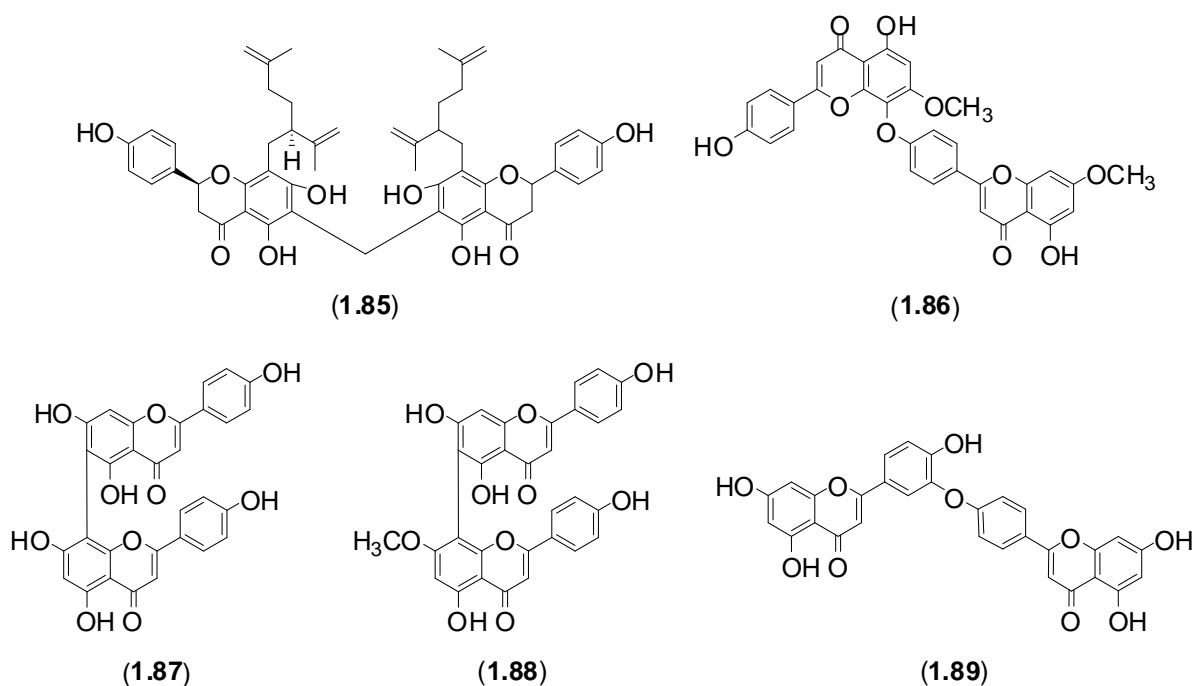
(1.83)



(1.84)

The flavonoid dimer remangiflavone C (**1.85**) from *Physena madagascariensis* was shown to exhibit activity in the A2780 ovarian cancer cell line cytotoxicity assay, with an IC_{50} of 2.5 μ g/mL [31]. The flavonoid dimers 7,7''-dimethyl lanarafflavone (**1.86**), agathisflavone (**1.87**) and 7''-methyl agathisflavone (**1.88**), isolated from *Lonicera japonica* (Japanese

Honeysuckle) and *Benincasa hispida* (Chinese Winter Melon) were evaluated for their activities against HT-29 human colon adenocarcinoma, NCI-H460 human non-small cell lung carcinoma, RXF-393 human renal cell carcinoma, MCF-7 breast adenocarcinoma and OVCAR-3 human ovarian adenocarcinoma cell lines [59]. The study established that 7,7''-dimethyl lanaraflavone (**1.86**) possessed activity against the NCI-H460 (IC_{50} value of 1.77 μ M), RXF-393 (IC_{50} 41.6 μ g/mL), MCF-7 (IC_{50} 3.42 μ g/mL) and OVCAR-3 (IC_{50} 3.59 μ g/mL) cell lines but no activity against HT-29. Compound **1.88** was found to be active against HT-29 (IC_{50} 4.38 μ g/mL), NCI-H460 (IC_{50} 5.36 μ g/mL), RXF-393 (IC_{50} 4.86 μ g/mL), MCF-7 (IC_{50} 5.58 μ g/mL) and OVCAR-3 (IC_{50} 5.18 μ g/mL) but agathisflavone (**1.87**) was only slightly active against RXF-393 (IC_{50} 45.9 μ g/mL), and showed no activity against the other cell lines used in this study [59]. Investigations into the biological activity of the flavonoid dimer ochnaflavone (**1.89**), also found in *Lonicera japonica*, showed anti-cancer activity towards the HCT-15 colon cancer cell line, with an IC_{50} value of 4.1 μ M. The authors suggested that cell cycle arrest and induction of apoptosis could be the mechanism by which these compounds target cancer cells [60].



1.2.2.2 Anti-parasitic flavonoids

Parasitic diseases are a major cause of death in tropical and sub-tropical regions and many of the most deadly parasitic infections affect some of the poorest regions of the world [61, 62]. Prevention and treatment of parasitic infections is very important, with the need for cheap treatment methods being imperative, due to the poor economic regions mainly affected by these parasites. The use of traditional remedies for the treatment of these diseases has led to the isolation of novel compounds with anti-parasitic properties, and synthetic chemists have developed new compounds based on known pharmacophores in order to find more effective treatments for these diseases. The three major parasitic diseases that affect some of the poorest regions of the world are malaria, leishmaniasis and trypanosomiasis.

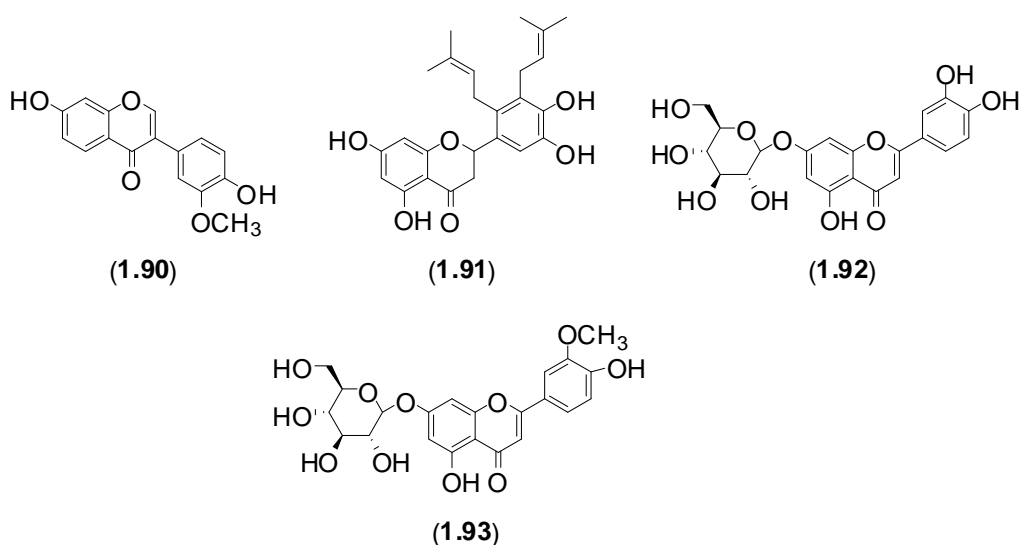
1.2.2.2.1 Anti-malarial flavonoids

Malaria is a parasitic disease caused by five species of *Plasmodium* parasites and spread by the *Anopheles* mosquito [61]. Malaria is largely prominent in equatorial countries, with sub-Saharan Africa being the major area for cases of malaria, although Asia, Latin America and, to a lesser extent, the Middle East and parts of Europe are also areas of risk [62]. WHO reports that ninety-nine countries or territories have ongoing transmission of malaria and estimates that 216 million cases of malaria occurred in 2010 and that 655,000 people died of which 86% were children under five years of age [62]. The WHO has noted that growth in global funding for malaria prevention slowed between 2010 and 2012 and has suggested that this could threaten the recent gains in the fight against malaria [62]. The WHO has a target for a 75% reduction in cases of malaria by 2015, with fifty of the ninety-nine countries expected to reduce new cases of malaria by this amount. However, these fifty countries only represent ~3% of worldwide malaria cases [62]. With the large number of cases and deaths caused by malaria each year, and the ongoing issues with the treatment of people with

malaria, development of compounds for prevention and treatment of malaria are two major areas of interest for both natural product and synthetic chemists.

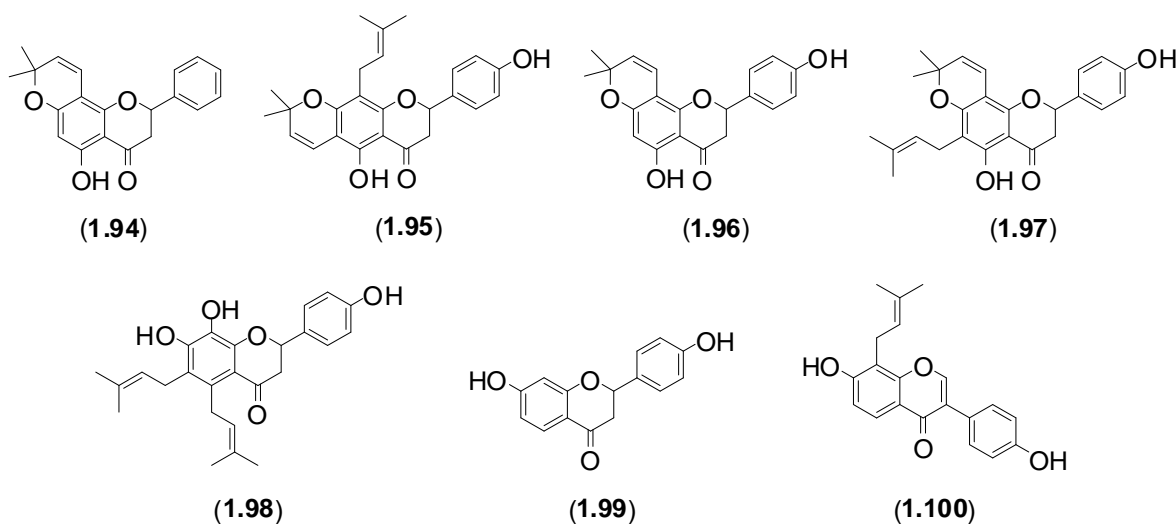
The extract of the Madagascan legume, *Dalbergia louvelii*, which is a traditional anti-malarial treatment, was found to contain the flavonoid 7,4'-dihydroxy-3'-methoxyflavone (**1.90**). This compound possesses moderate anti-parasitic activity towards the chloroquine-resistant strain FcB1 of *P. falciparum*, with an IC_{50} of 8.7 μ M [9].

In Kenya, the use of the bark of *Erythrina abyssinica* is the most prominent malaria treatment. Flavonoids isolated from the bark displayed activity against the D6 and W2 strains of *P. falciparum*, with the prenylated flavonoid abyssinin III (**1.91**) displaying the greatest activity towards *P. falciparum*, with an IC_{50} of 4.9 μ M against the W2 strain [9]. The flavonoid glycosides luteolin-7-O- β -D-glucopyranoside (**1.92**) and chrysoeriol-7-O- β -D-glucopyranoside (**1.93**), isolated from the perennial herb, *Phlomis brunneogaleata*, were shown to possess IC_{50} values of 5.4 μ M and 12.8 μ M respectively against the chloroquine-resistant strain K1 of *P. falciparum* [9]. Compound **1.92** also showed further activity with enzyme-inhibitory potential towards enoyl-ACP reductase (FAB I) of *P. falciparum* with an IC_{50} of 22.3 μ M [10]. This is the first natural product to target the FAB I enzyme, the key regulator of type II fatty synthase (FAS-II) in *P. falciparum* [9].

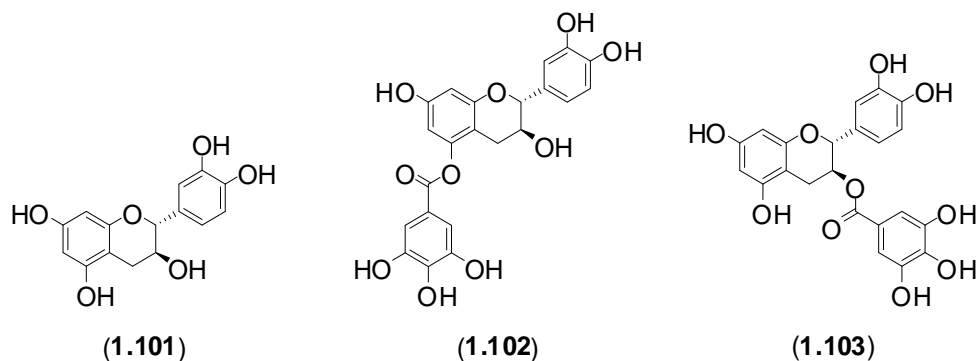


The flavonoid obovatin (**1.94**), isolated from seedpods of the bushy perennial, *Tephrosia elata*, was found to possess an IC_{50} of less than 27.6 μ M against both D6 and W2 strains of *P. falciparum* [63].

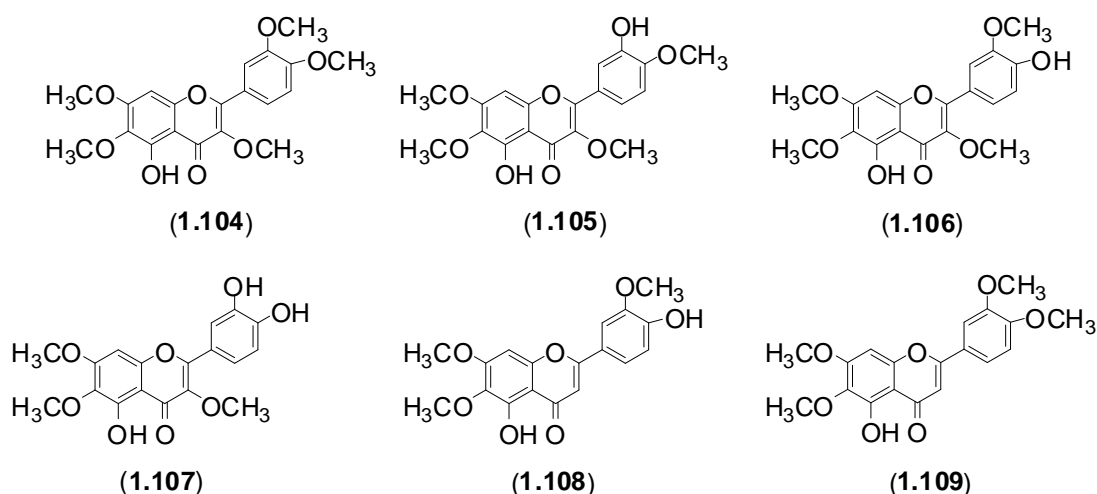
The anti-malarial activity of the natural flavonoids lupinifolin (**1.95**), citflavone (**1.96**), erythrisenegalone (**1.97**), lonchocarpol A (**1.98**), liquiritigenin (**1.99**) and 8-prenyldaidzein (**1.100**), isolated from *Erythrina fusca* Lour., towards the K1 strain of *P. falciparum* was assessed. Compounds **1.96**, **1.98** and **1.100** all displayed an IC_{50} of less than 12.5 μ M, with **1.98** being the most active with an IC_{50} of 3.9 μ M [63].



Tests on (+)-catechin (**1.101**) and its 5-gallate (**1.102**) and 3-gallate (**1.103**) derivatives, isolated from *Piptadenia pervillei* Vatke revealed that, while (+)-catechin (**1.101**) showed no activity towards the chloroquine-resistant FcB1 strain *P. falciparum*, the 5-gallate (**1.102**) and 3-gallate (**1.103**) derivatives possessed anti-malarial activity with IC_{50} values of 1.2 μ M and 1.0 μ M respectively [63].



Anti-malarial activity was also found for the flavonoids artemetin (**1.104**) (IC_{50} 26 μ M), casticin (**1.105**) (IC_{50} 24 μ M), chrysoplenetin (**1.106**) (IC_{50} 23 μ M), chrysosplenol-D (**1.107**) (IC_{50} 32 μ M), cirsilineol (**1.108**) (IC_{50} 36 μ M) and eupatorin (**1.09**) (IC_{50} 65 μ M), isolated from *Artemisia annua* [64].

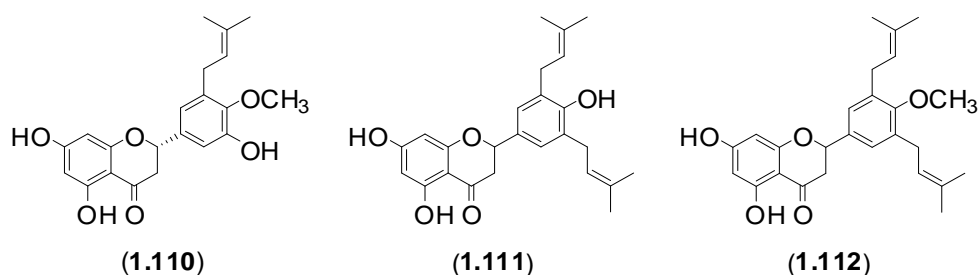


The dietary flavonoid luteolin (**1.18**) (pg 12), as well as displaying anti-cancer activity, was found to possess anti-malarial activity towards the 3D7 and 7G8 strains of *P. falciparum* with an IC_{50} of 11 μ M and 12 μ M respectively [63]. Luteolin (**1.18**) prevents the progression of parasite growth, but does not affect susceptibility to the anti-malarial drugs chloroquine or artemisinin [63].

As well as the anti-cancer activity mentioned earlier in this review (pg 21), anti-malarial activity towards the 3D7 strain of *P. falciparum* was also found for nymphaeol B (**1.66**) (IC_{50}

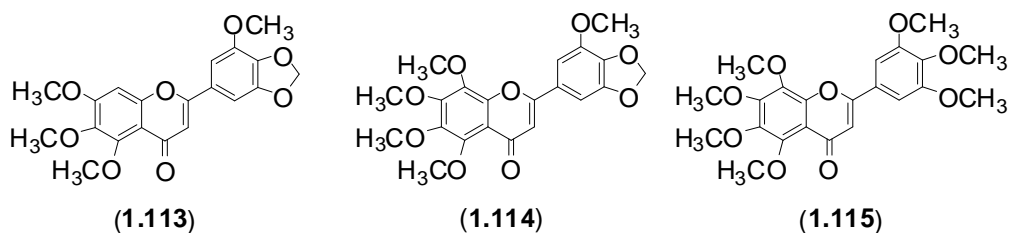
4.02 μM), nymphaeol C (**1.67**) (IC_{50} 2.04 μM) and 6-farnesyl-3',4',5,7-tetrahydroxyflavanone (**1.68**) (IC_{50} 0.06 μM), isolated from *Macaranga triloba*. [54].

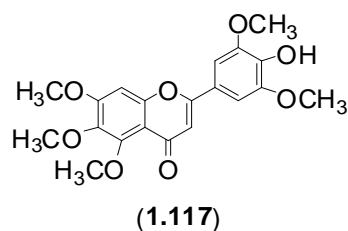
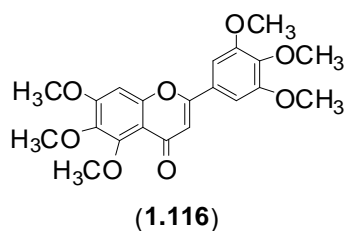
The Coral or Lucky Bean Tree, *Erythrina burttii*, contains many compounds that possess anti-malarial activity towards the D6 and W2 strains of *P. falciparum*, namely the flavonoids 4'-O-methylsigmoidin B (**1.110**) (IC_{50} values of 12.4 μM , 12.7 μM respectively), abyssinone V (**1.111**) (IC_{50} values of 5.7 μM , 6.6 μM) and abyssinone V methyl ether (**1.112**) (IC_{50} values of 10.7 μM , 11.9 μM) [65].



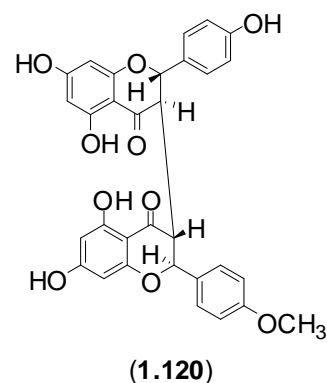
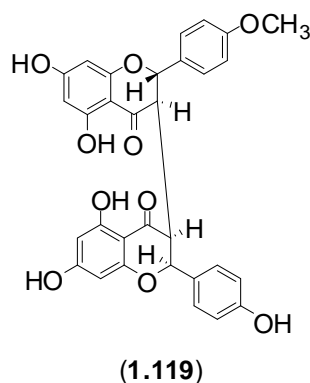
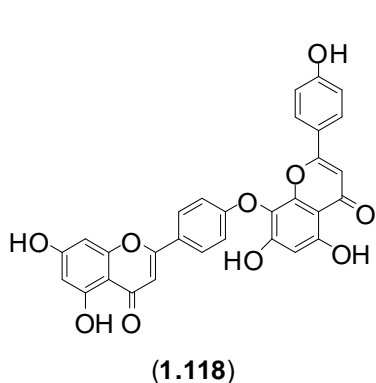
The anti-malarial activity towards the K1 strain of *P. falciparum* of compounds **1.113** to **1.117**, isolated from Goat Weed (*Ageratum conyzoides* L.), has been measured [66]. Compounds **1.113** (IC_{50} 11 μM), **1.114** (IC_{50} 11 μM), **1.116** (IC_{50} 7 μM) and **1.117** (IC_{50} 9 μM) displayed moderate activity, while compound **1.115** was found to be inactive [66].

The flavonoid styracifolin B (**1.31**) (**pg 14**) isolated from *Artocarpus styracifolium* was found to possess activity towards the FcB1 strain of *P. falciparum*, with an IC_{50} value of 1.12 μM [32].

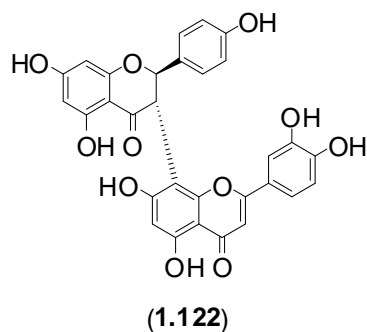
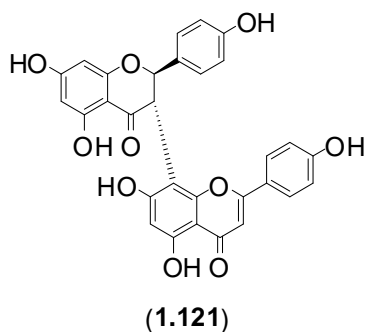




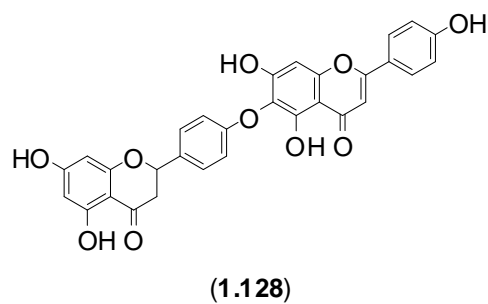
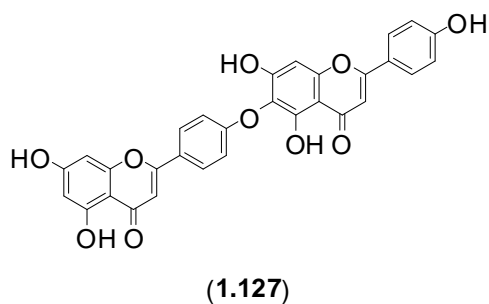
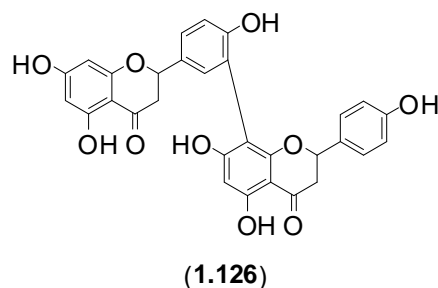
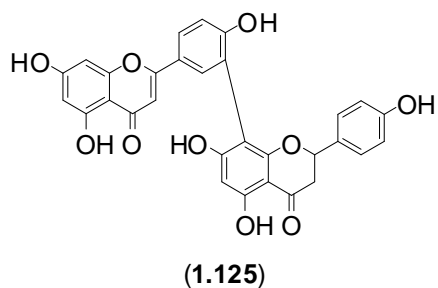
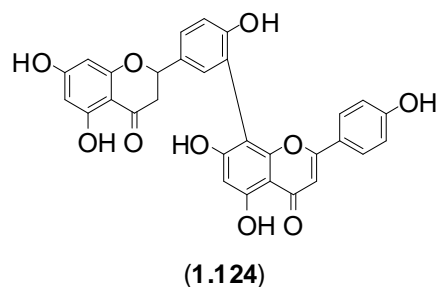
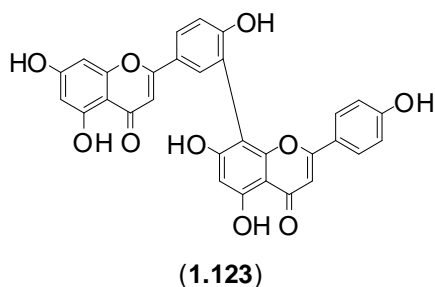
Dimeric flavonoids have also been isolated and tested for their anti-malarial properties. The flavonoid dimer lanaroflavone (**1.118**), isolated from *Camptosperma panamense*, possesses an IC_{50} of $0.37 \mu\text{M}$ against the chloroquine-resistant K1 strain of *P. falciparum*, and also exhibits anti-leishmanial activity [9]. The anti-malarial activity of the dimeric flavonoids isolated from the *Wikstroemia indica*, sikokianin B (**1.119**) and sikokianin C (**1.120**), was determined for the chloroquine-sensitive strain FcR3 (IC_{50} values of $\sim 0.9 \mu\text{M}$ and $1 \mu\text{M}$ respectively) and a chloroquine-resistant K1 strain (IC_{50} values of $\sim 0.9 \mu\text{M}$ and $0.61 \mu\text{M}$ respectively) [9].

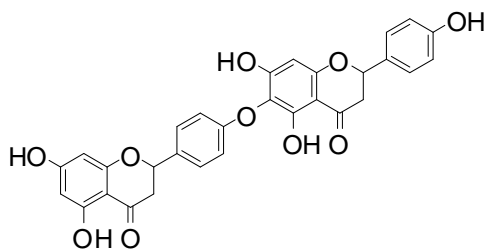


The flavonoid dimers morelloflavone (**1.121**) and volkensiflavone (**1.122**) were found to possess anti-malarial activity with an IC_{50} of $< 23.6 \mu\text{M}$ [63].

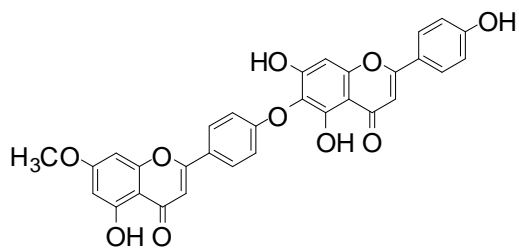


In an investigation of the Indian medicinal herb *Selaginella bryopteris*, of the eleven flavonoid dimers (1.123-1.133) tested for their activity towards the K1 strain of *P. falciparum* compounds 1.131 and 1.133 exhibited potent activity with IC_{50} values of 0.30 μ M and 0.26 μ M respectively [67].

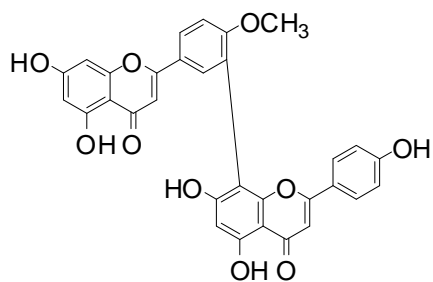




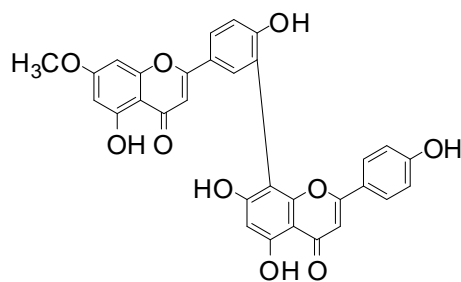
(1.129)



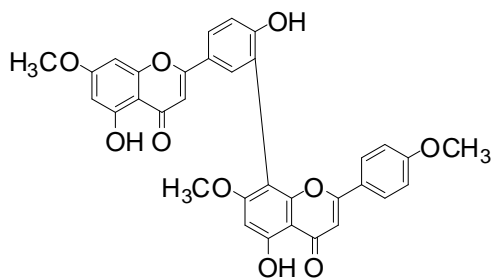
(1.130)



(1.131)

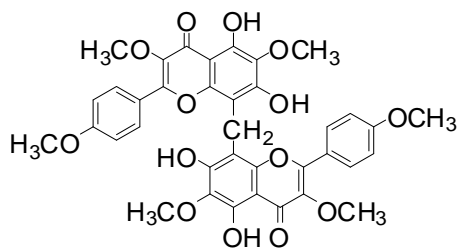


(1.132)



(1.133)

The dimeric flavonoid methylenebissantin (**1.134**), isolated from *Dodonaea viscosa*, was found to have moderate enzyme inhibitory activity against *P. falciparum* enoyl-ACP reductase with an IC₅₀ value of 91 μM [68].

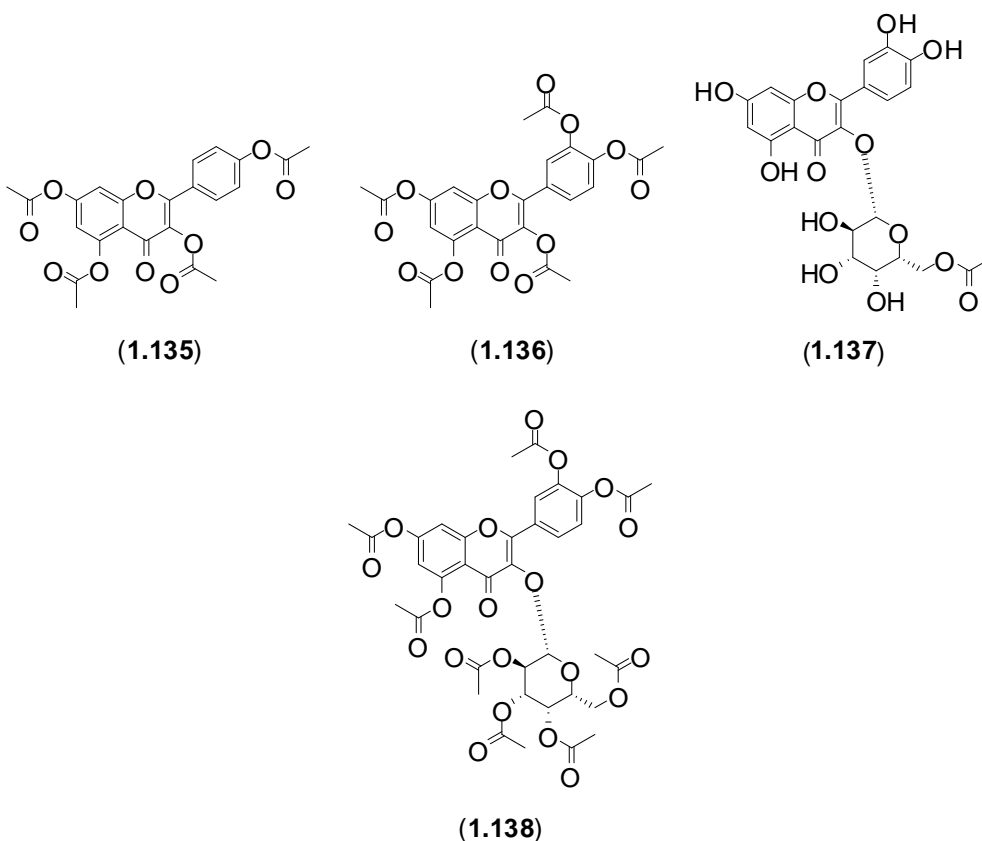


(1.134)

1.2.2.2.2 Anti-leishmanial flavonoids

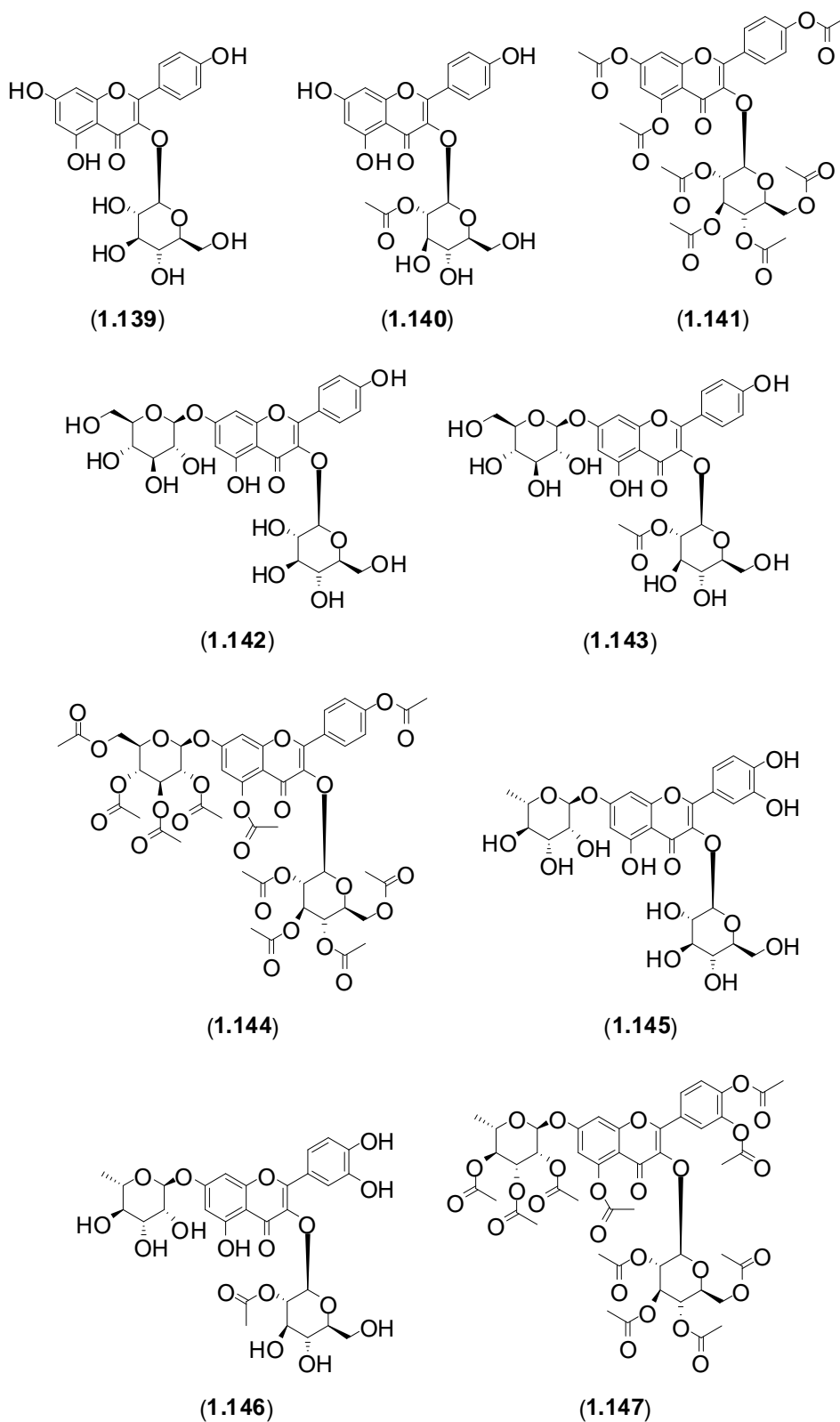
Leishmaniasis is one of the most neglected parasitic diseases. It is caused by protozoa of the genus *Leishmania* and is transmitted by phlebotomine sand flies [62, 69]. It has been suggested that 350 million people are considered at risk of leishmaniasis in eighty-eight countries, with approximately two million new cases of leishmaniasis occurring annually [69]. There are four main types of leishmaniasis, with cutaneous forms (heals within a few months leaving scars), diffuse cutaneous form (leaves chronic disseminated skin lesions similar to lepromatous leprosy and is very difficult to treat), mucocutaneous forms (lesions can partially or fully destroy mucous membranes of the nose, mouth, throat and surrounding tissues) and visceral forms (cause high fever, weight loss, swelling to spleen and liver, as well as anaemia, and when left untreated can cause death) [62]. For cutaneous leishmaniasis, it is thought that there are up to 1.5 million new cases per year, while for visceral leishmaniasis, it is estimated that there are about 500,000 new cases each year [61]. Visceral leishmaniasis affects poor areas of India, Bangladesh and Nepal, which have a great need for cost effective, viable treatments [62].

The flavonoids **1.92** and **1.93** (pg 26) possess anti-leishmanial activity against *Leishmania donovani*, with IC₅₀ values of 2.5 μM and 8.9 μM respectively [9]. Flavonoids isolated from *Consolida oliveriana* were tested for activity towards *Leishmania (V) peruviana* and *Leishmania (V) braziliensis* [70]. It was found that the activity towards *L.(V) peruviana* and *L.(V) braziliensis* was observed for kaempferol (**1.12**) (pg 12) (IC₅₀ 71 μM and 54 μM respectively), acetylated kaempferol (**1.135**) (IC₅₀ 53 μM and 69 μM respectively), quercetin (**1.13**) (IC₅₀ 60 μM and 30.5 μM respectively), acetylated quercetin (**1.136**) (IC₅₀ 11 μM and 47 μM respectively), 6''-O-acetylhyperoside (**1.137**) (IC₅₀ 87 μM and 52 μM respectively) and octa-O-acetylhyperoside (**1.138**) (IC₅₀ 7 μM and 6 μM respectively) [70].



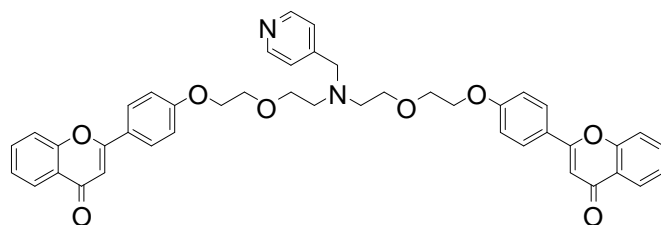
While all nine flavonoid and flavonoid glycosides (**1.139-1.147**) isolated from *Delphinium staphisagria* were active against the two strains *Leishmania infantum* and *Leishmania braziliensis*, compound **1.146** was found to be the most active [69].

The anti-leishmanial activity (*Leishmania donovani* axenic amastigotes assay) of the biflavonoids (**1.123-1.133**) (pg 31), isolated from *Selaginella bryopteris* was determined, with hinokiflavone (**1.127**) (IC_{50} 2.9 μ M), 2,3-dihydrohinokiflavone (**1.128**) (IC_{50} 1.6 μ M), 2,3,2'',3''-tetrahydrohinokiflavone (**1.129**) (IC_{50} 4.2 μ M) and 7-O-methylhinokiflavone (**1.130**) (IC_{50} 1.7 μ M) found to be active [67]. The anti-leishmanial activity towards *Leishmania donovani* was determined for the flavonoids **1.115** (pg 30) (IC_{50} 12 μ M), **1.116** (IC_{50} 21 μ M), **1.117** (IC_{50} 9 μ M), isolated from *Ageratum conyzoides* L. [66].

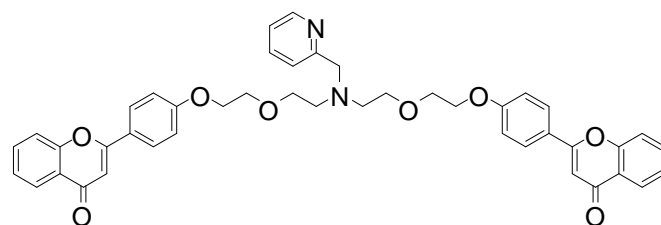


A group of seventy-three synthetic flavonoid dimers with polyethylene glycol or aminoethyleneglycol linkers were assessed for anti-leishmanial activity towards three strains of *Leishmania donovani* (LdAG83, Ld39 and LdAG83PentR50). Of the seventy-three

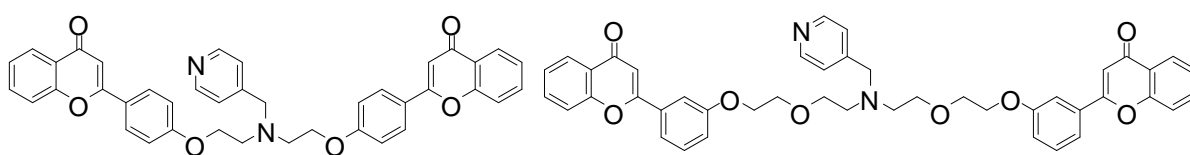
synthetic flavonoid dimers, fourteen (1.148-1.161) were found to possess potent activity towards one or more of the three strains, with values for each of these fourteen compounds given in **Table 1.1**.



(1.148)

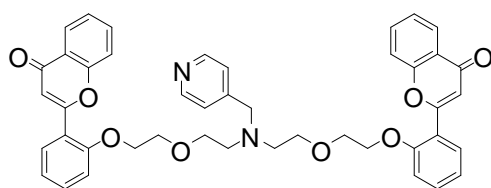


(1.149)

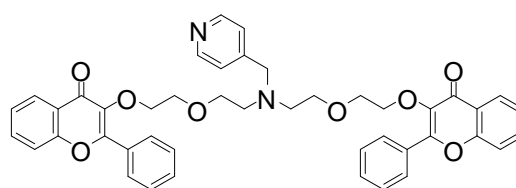


(1.150)

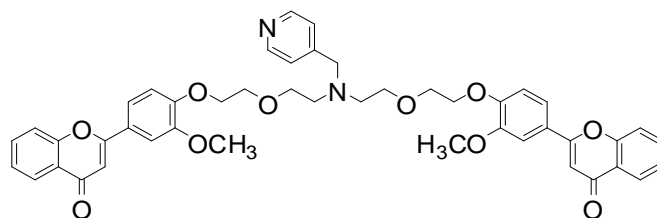
(1.151)



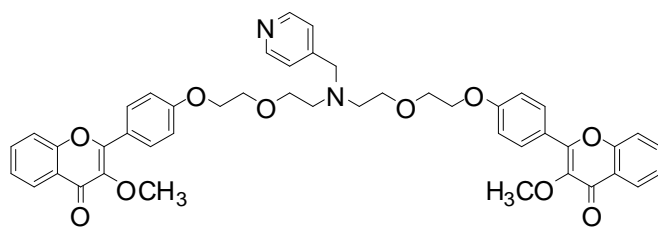
(1.152)



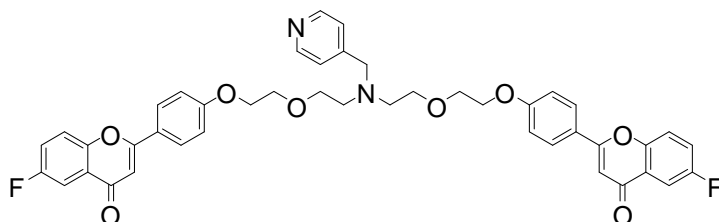
(1.153)



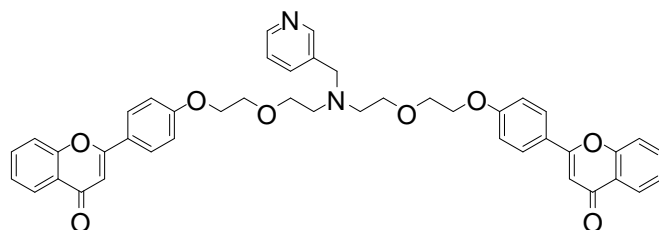
(1.154)



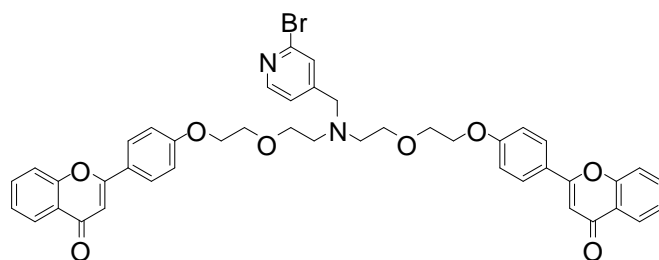
(1.155)



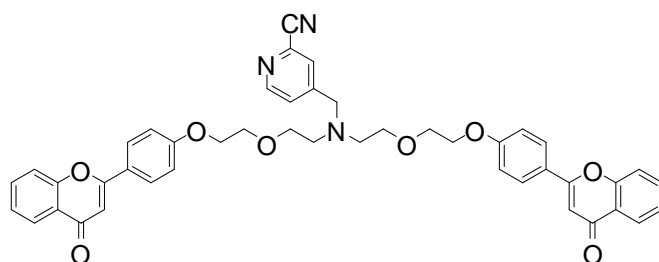
(1.156)



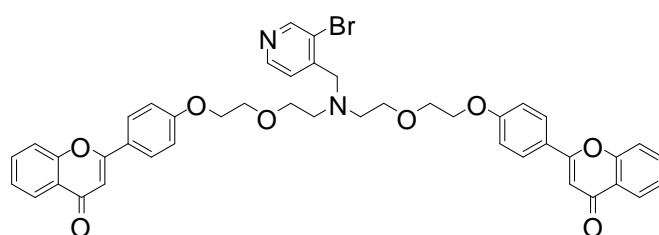
(1.157)



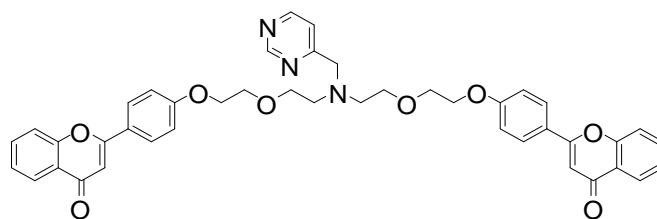
(1.158)



(1.159)



(1.160)



(1.161)

Table 1.1. Anti-leishmanial activity of synthetic flavonoid dimers **1.48-1.61** given as an IC_{50} (μM).

Compound	LdAG83	Ld39	LdAG83PentR50
1.148	0.20	0.21	0.13
1.149	5.0	4.2	ND
1.150	1.4	>50	ND
1.151	0.19	0.44	ND
1.152	2.3	4.0	ND
1.153	2.5	3.1	ND
1.154	0.63	0.69	ND
1.155	0.98	0.98	ND
1.156	0.31	0.36	ND
1.157	0.56	0.98	ND
1.158	1.8	>50	ND
1.159	1.1	>50	ND
1.160	0.65	>50	ND
1.161	0.44	0.58	ND

ND indicates no activity was detected

1.2.2.2.3 Anti-trypanosomal flavonoids

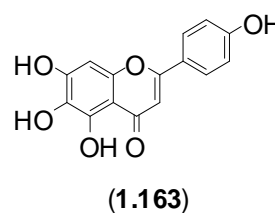
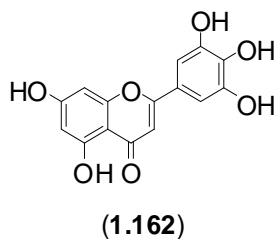
Trypanosomiasis is a parasitic disease caused by protozoa of the genus *Trypanosoma* [62].

Trypanosomiasis has two major forms, Chagas disease and African sleeping sickness [62].

Chagas disease is found mostly in twenty-one Latin American countries, is caused by the species *Trypanosoma cruzi* and is spread by infected insects called triatomine bugs, with 10 million people suspected of being infected each year [61, 62]. Chagas disease in the acute stage lasts from four to eight weeks and can show very little to no symptoms. It can cause swelling at the site of infection during the acute stage, while the chronic phase can last for decades and can cause death. This occurs in ~20-30% of Chagas disease patients [61]. African sleeping sickness is caused by the parasites *Trypanosoma brucei gambiense* and *Trypanosoma brucei rhodesiense* and is transmitted mostly by the tsetse fly that is endemic to sub-Saharan Africa. A suspected seven thousand new cases were reported in 2010 [61, 62]. African sleeping sickness occurs in thirty-six sub-Saharan African countries and 95% of cases are due to *T. brucei gambiense*. [62]. Only two treatments are available for the first stage of African sleeping sickness, while the four treatments available for second stage can be quite dangerous as they need to cross the blood-brain barrier [62].

Styracifolin B (**1.31**) (**pg 14**), isolated from *Atrocarpus styracifolius* was found to exhibit activity towards *Trypanosoma brucei brucei*, with an IC_{50} value of 6.9 μ M [32]. The anti-trypanosomal activity towards *Trypanosoma brucei rhodesiense* and *Trypanosoma cruzi* was determined for the flavonoids (**1.113-1.117**) (**pg 30**) isolated from *Ageratum conyzoides* L. Activity towards *T. brucei rhodesiense* was observed for **1.113** (IC_{50} 16 μ M), **1.114** (IC_{50} 19 μ M), **1.115** (IC_{50} 11 μ M), **1.116** (IC_{50} 21 μ M) and **1.117** (IC_{50} 8 μ M), while for *T. cruzi* only slight activity was observed for **1.114** (IC_{50} 51 μ M) and **1.115** (IC_{50} 61 μ M) [66]. Further studies on the series of compounds (**1.139-1.147**) (**pg 35**) isolated by Marin and colleagues from *Delphinium staphisagria* for activity against *T. cruzi* revealed that astragalin (**1.139**) (IC_{50} 16 μ M), 2''-acetylastragalin (**1.140**) (IC_{50} 6.5 μ M), astragalin heptaacetate (**1.141**) (IC_{50} 0.8 μ M), paeonoside (**1.142**) (IC_{50} 21 μ M), 2''-acetylpaeonoside (**1.143**) (IC_{50} 22 μ M), paeonoside decaacetate (**1.144**) (IC_{50} 17 μ M), petiolaroside (**1.145**) (IC_{50} 30 μ M), 2''-acetylpetiolaroside (**1.146**) (IC_{50} 27 μ M) and petiolaroside decaacetate (**1.147**) (IC_{50} 27 μ M) possessed moderate activity. The selectivity index (calculated as IC_{50} of toxicity/*T. cruzi* IC_{50}) of astragalin

heptaacetate (**1.141**) was found to be 205 [71]. Of the nineteen flavonoids tested for anti-trypanosomal activity towards *T. cruzi* trans-sialidase [72], myricetin (**1.70**) (pg 21) (IC_{50} 17 μ M), quercetin (**1.13**) (pg 12) (IC_{50} 58 μ M), tricetin (**1.162**) (IC_{50} 39 μ M), luteolin (**1.18**) (IC_{50} 22 μ M), apigenin (**1.14**) (IC_{50} 78 μ M), and 6-hydroxy-apigenin (**1.163**) (IC_{50} 50 μ M) were found to possess moderate activity [72].



1.2.3 Summary

Flavonoids represent a class of compounds that is widely distributed throughout the plant kingdom [73]. Many fruits and edible plants contain flavonoids, with some being used as traditional remedies for illnesses and diseases. The anti-cancer and anti-parasitic properties of flavonoids and their glycosides are not yet fully understood. It has been established that the synergistic effects of flavonoids with other known drugs can increase the efficacy of the drug(s) *in vivo*. While the use of flavonoids as independent drugs is not well established (none have made it to market as a drug to date), the usefulness of flavonoids is well established against some diseases and these compounds are still being studied in other areas such as in the prevention of cancer.

During the course of the research described in this thesis, four flavonoid glycosides were isolated, as detailed in **Chapter 2**. Of these four flavonoid glycosides, one represents a new structural analogue.

1.3 Naphthoquinones

1.3.1 General Introduction

Naphthoquinones represent one of the most widespread classes of compounds that occur in plants [74, 75]. They can appear in nature as either free aglycones or glycosides, or as dimers or trimers [75]. The use of naphthoquinone-containing extracts for medicinal purposes and in cosmetics is fairly well known: Henna from the plant *Lawsonia alba* is used for skin and hair colouring [76], while in Brazil, the naphthoquinone-containing inner bark of *Tabebuia avellanedae* is used for its anti-inflammatory, anti-neoplastic, diuretic and analgesic properties, as well as being used as a treatment against cancer [74, 77]. Naphthoquinones have been found to possess a wide variety of biological activities, with anti-bacterial, anti-fungal, anti-inflammatory, anti-parasitic, anti-insecticidal and anti-cancer activity having been reported [75, 77].

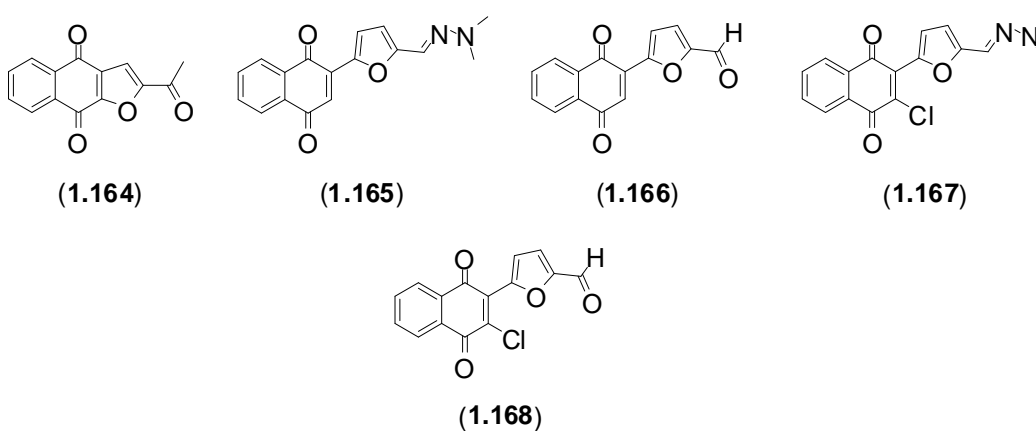
1.3.2 Biological Activity

1.3.2.1 Anti-cancer naphthoquinones

The anti-cancer activity of the naphthoquinones has been thoroughly documented between 2008 and 2012, with over one hundred and seventy articles published within this period [22]. In this review a selection of these references are discussed.

The natural naphthoquinone, 2-acetylfuro-1,4-naphthoquinone (**1.164**), previously isolated from the Cameroonian medicinal plant *Newbouldia laevis*, was subjected to screening against fourteen cancer cell lines, with activity observed towards the CCRF-CEM leukaemia cell line (IC₅₀ 35.9 μM), CEM/ADR5000 multidrug-resistant leukaemia (IC₅₀ 69.2 μM), PF-382 leukaemia T-cells (IC₅₀ 2.36 μM), HL-60 promyelocytic leukemia cells (IC₅₀ 19.9 μM), MiaPaCa-2 pancreatic carcinoma (IC₅₀ 7.48 μM), Capan-1 pancreatic adenocarcinoma (IC₅₀ 15.7 μM), MCF-7 breast adenocarcinoma (IC₅₀ 6.86 μM), SW-680 colon carcinoma (IC₅₀ 14.7

μM), 786-O renal carcinoma (IC_{50} 28.1 μM), U87MG glioblastoma-astrocytoma (IC_{50} 8.02 μM), A549 lung adenocarcinoma epithelial (IC_{50} 22.7 μM), Colo-38 skin melanoma (IC_{50} 2.77 μM), HeLa cervical carcinoma (IC_{50} 1.65 μM) and Caski cervical carcinoma (IC_{50} 0.70 μM) cell lines, with 2-acetylfuro-1,4-naphthoquinone (**1.164**) being more potent than doxorubicin against PF-382 and Caski cells but possessing similar activity to doxorubicin in the Colo-38 and HeLa cell lines [78]. A study of the naphthoquinones **1.165-1.168** and their *in vitro* anti-cancer activity against the TLT murine hepatocarcinoma cell line, indicated that at 10 $\mu\text{g}/\text{mL}$ compounds **1.165** and **1.168** showed an increase in cell death in TLT cells [79]. It was also observed that at a higher concentration (25 $\mu\text{g}/\text{mL}$), **1.167** was also found to be active, while **1.166** was inactive against TLT cells [79]. The anti-tumour activity of compounds **1.165** and **1.167** had previously been established against MCF-7, NCI-H460, and SF-268 glioblastoma cell lines with IC_{50} values of ~ 10 μM [79].

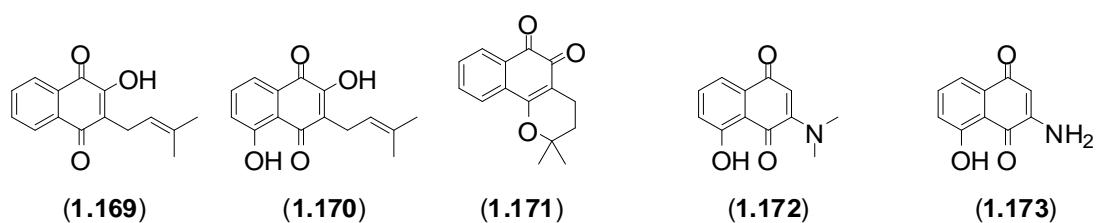


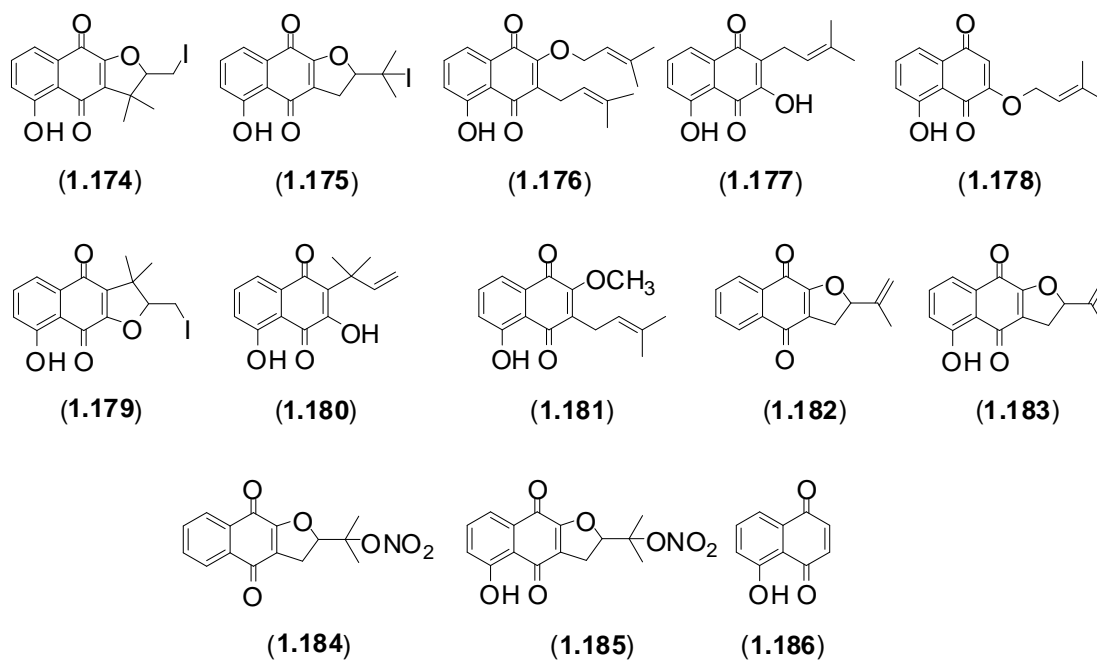
As a result of a study into the anti-cancer activity of the synthetic naphthoquinones **1.169-1.185** synthesised from the natural naphthoquinone juglone (**1.186**), it was found that many of these synthetic naphthoquinones were active in one or more of the anti-cancer assays as given in **Table 1.2**, with **1.170**, **1.171** and **1.184** being the most active [80].

Table 1.2. Anti-cancer activity of the synthetic naphthoquinones **1.169-1.185** shown as an GI_{50} (μM).

Compound	A2780	HBL-100	HeLa	SW1573	T-47D	WiDr
1.169	1.9	7.8	2.3	34	76	36
1.170	0.57	0.60	0.42	0.70	8.1	6.3
1.171	1.1	0.69	0.81	0.76	2.3	2.0
1.172	2.4	5.7	7.1	5.3	34	17
1.173	3.1	2.9	5.7	2.0	4.0	3.5
1.174	1.7	1.9	1.7	1.3	1.8	2.0
1.175	2.1	2.0	2.4	2.3	2.3	1.9
1.176	1.0	1.6	1.9	4.3	21	11
1.177	3.9	21	2.6	18	30	19
1.178	2.0	19	4.5	7.7	23	7.3
1.179	1.6	0.41	1.3	0.40	2.5	2.0
1.180	21	16	24	3.8	30	23
1.181	1.8	20	3.5	4.8	22	20
1.182	2.6	2.3	2.1	1.9	21	2.7
1.183	2.1	2.1	1.8	2.5	20	4.8
1.184	0.82	0.94	0.80	0.83	2.2	2.0
1.185	2.2	2.8	2.2	2.7	23	18

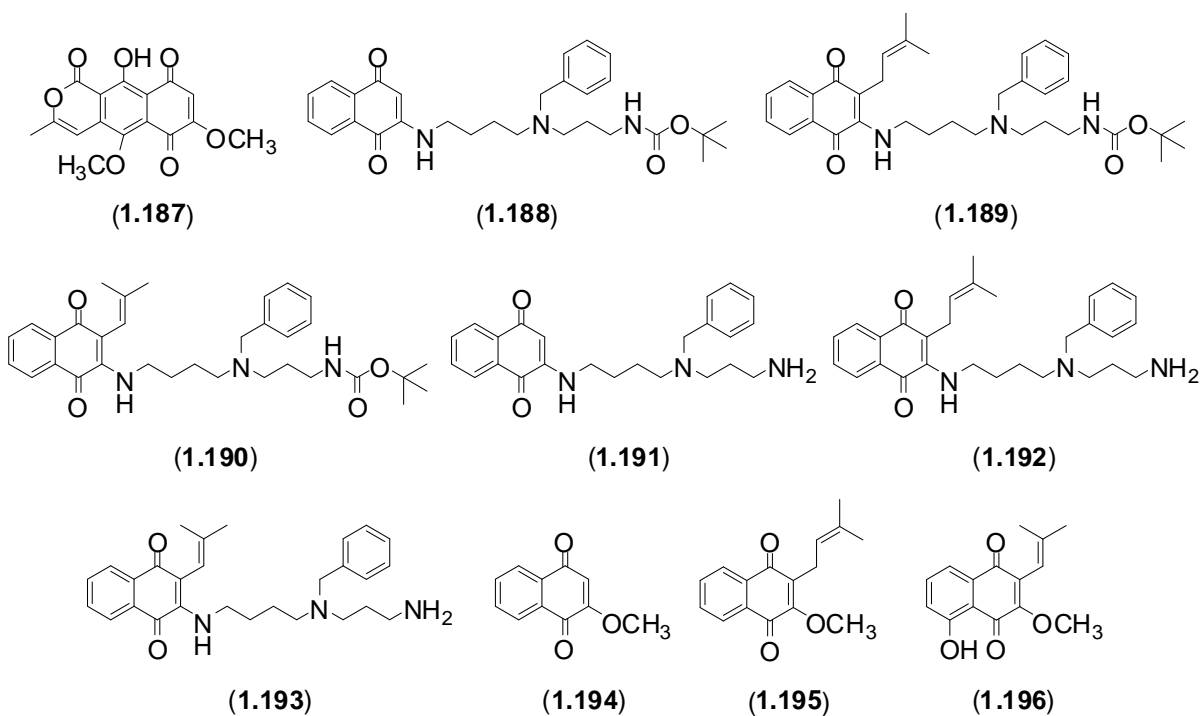
GI_{50} indicates the concentration required to inhibit the proliferation of cells by 50%



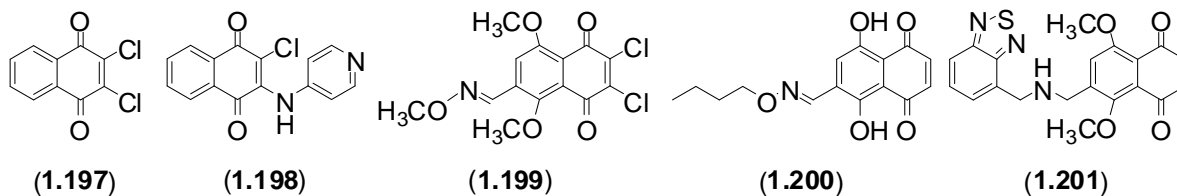


The naphthoquinone 5-methoxy-3,4-dehydroxanthomegnin (**1.187**), isolated from *Paepalanthus latipes* displayed activity towards LM2 murine mammary tumour cells (CI_{50} [Cytotoxicity index*] 74.6 μ M) and LPO7 lung adenocarcinoma tumour cells (CI_{50} 6.2 μ M) and was found to be of a similar potency or more potent than cisplatin (CI_{50} 168.4 μ M and CI_{50} 4.34 μ M respectively) [81]. The synthetic polyamine naphthoquinones (**1.188-1.193**), which are derivatives of the natural naphthoquinones 2-methoxy-lawsone (**1.194**), 2-methoxy-lapachol (**1.195**) and 2-methoxy-*nor*-lapachol (**1.196**), displayed moderate activity towards the Ehrlich murine breast tumour cell line, with IC_{50} values between 25 and 50 μ M, while against the HL-60 cell line, compounds **1.188-1.193** displayed IC_{50} values from 10 to 22 μ M [82]. In addition compounds (**1.191-1.193**) were found to be active against the MV-3 cell line (IC_{50} 39 to 45 μ M). All compounds (**1.188-1.193**), were active against the GLC-4 small cell lung carcinoma cell line (IC_{50} 14-29 μ M), while activity against Daudi Burkitt lymphoma cells was also displayed by all compounds (IC_{50} 17-30 μ M), with these amine derivatives being more active than the natural products in all of the assays [82].

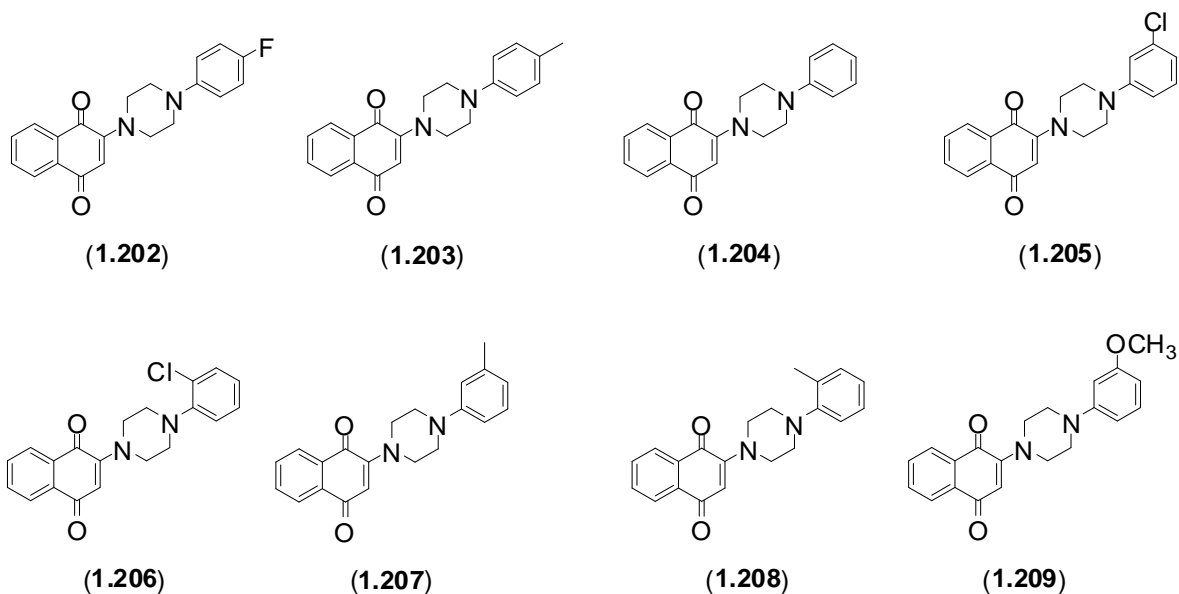
* In this reference the authors used a CI_{50} terminology to describe the cytotoxic index (CI) when referring to the anti-tumour activity. For comparative purposes the IC_{50} notation should have been adopted.

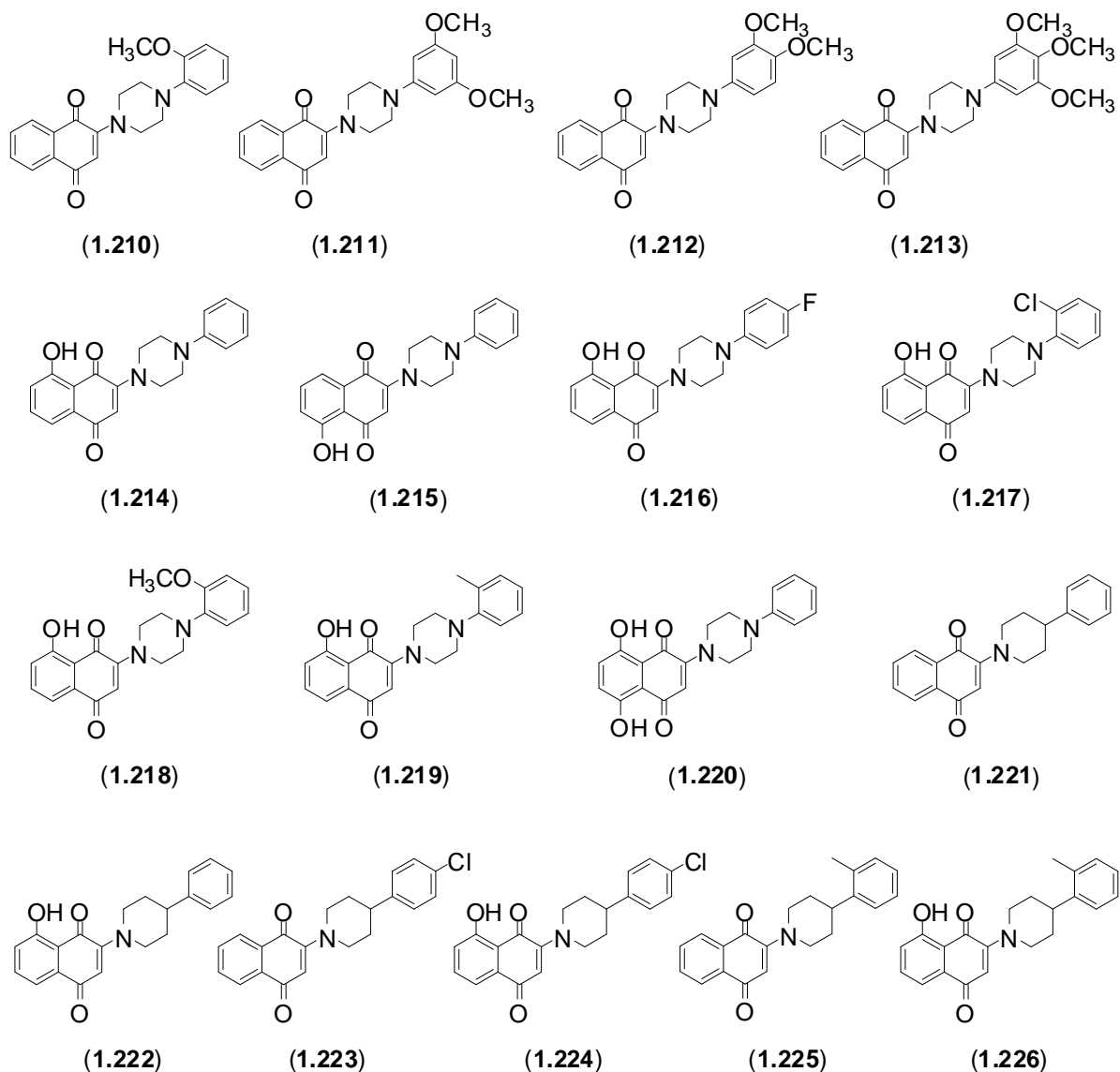


Both 2',3-dichloro-1,4-naphthoquinone (**1.197**) and the synthetically derived compound 2-chloro-3-(4-pyridyl-amino)naphthoquinone (**1.198**) were analysed for anti-cancer activity towards the MCF-7 cell line, with 2',3-dichloro-1,4-naphthoquinone (**1.197**) (IC_{50} 30 μ M) showing less activity than the synthetic 2-chloro-3-(4-pyridyl-amino)-naphthoquinone (**1.198**) (10 μ M) [83]. It was observed that the synthetic naphthoquinones, **1.199-1.201**, were active against HCT-116 colon cancer cells and it was postulated that the production of reactive oxygen species (ROS) by naphthoquinones played a critical role in the induction of apoptosis [84].

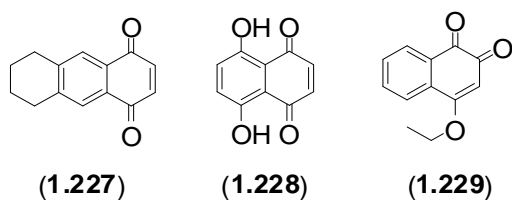


Synthetic 2-piperazinyl naphthoquinones such as compound **(1.202)** and 2-piperidinyl naphthoquinone derivatives such as compound **(1.221)** were evaluated for biological activity towards the DU-145 prostate carcinoma cell line [85]. Compounds **(1.202-1.226)** displayed activity with IC_{50} values less than 18 μM , with **1.220** (IC_{50} 1.3 μM) being the most active [85]. Again it was suggested that this activity was due to the induction of apoptosis caused by these compounds [85] 20 μM , with **1.218** (IC_{50} 1.8 μM). As part of the same study, selected compounds were evaluated against thirteen human cancer cell lines, with the most active against most cell lines being **1.220**. Compound **(1.220)** also displayed the most potent activity against the A549 lung adenocarcinoma cell line (IC_{50} 1.7 μM) and L-78 (IC_{50} 1.9 μM) cell lines and was found to be more active than the anti-cancer drug doxorubicin (IC_{50} 1.9 μM and 2.4 μM respectively). The most active compounds against each cell line were: **1.217** against HT-29 cell line (IC_{50} 1.4 μM); **1.218** against the HepG2 (IC_{50} 3.9 μM) and U251 cell lines (IC_{50} 4.4 μM); **1.220** against the HeLa (IC_{50} 2.1 μM), HT-1080 (IC_{50} 2.8 μM), KB (IC_{50} 1.4 μM), MCF-7 (IC_{50} 3.0 μM), MOLT-4 acute lymphoblastic leukaemia (IC_{50} 2.7 μM) and SGC-7901 (IC_{50} 2.5 μM) cell lines [85]. Within this study, compounds **(1.214, 1.217-1.220, 1.222, 1.224 and 1.226)** were found to be more potent than doxorubicin against the OS-RC-2 renal carcinoma cell line [85].

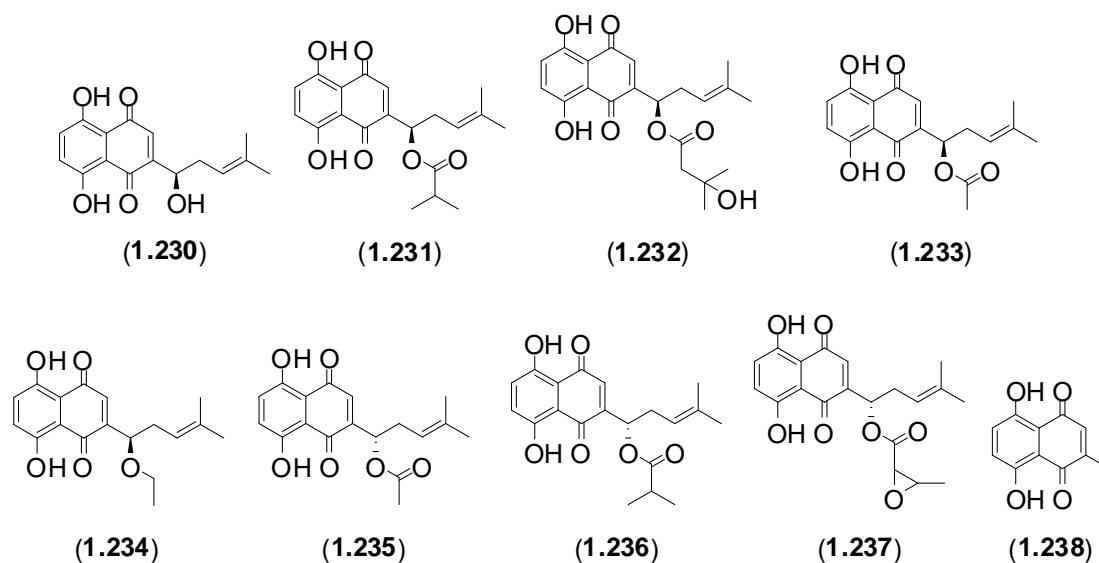




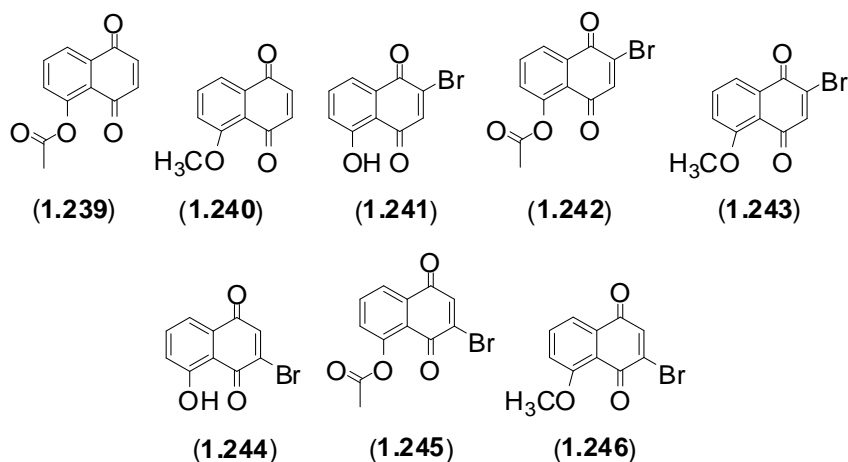
The synthetically prepared naphthoquinones **1.227**, **1.228** and **1.229** displayed similar activity against the A2780 cell line, with IC_{50} values of 0.75 μ M, 0.08 μ M and 0.37 μ M respectively [86].



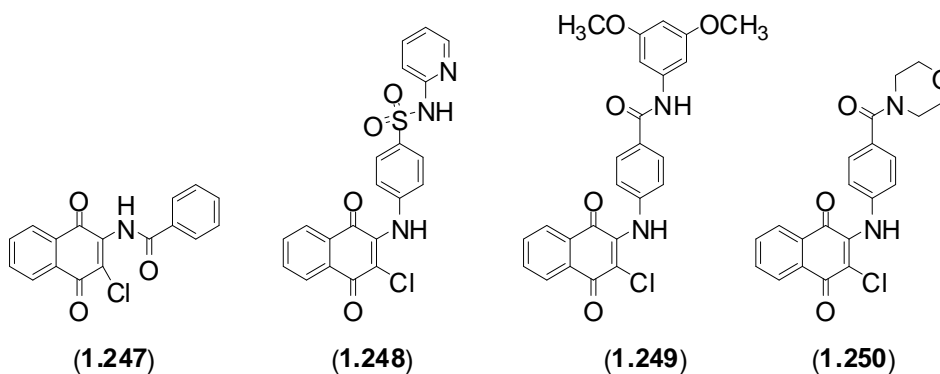
Of the natural naphthoquinones isolated from *Lithospermum erythrorhizon* Sieb. et Zucc. and *Macrotomia euchroma* (Royale) Pauls. it was found that the naphthoquinones **1.230-1.237** displayed activity against the HCT-116 cell line (IC_{50} values of 0.23-0.45 μM), and against the Hep-G2 cell line (IC_{50} values of 0.22-0.59 μM), while vitamin K (**2.238**) was less active against both cell lines with IC_{50} values of 1.19 μM and 2.34 μM respectively [87].

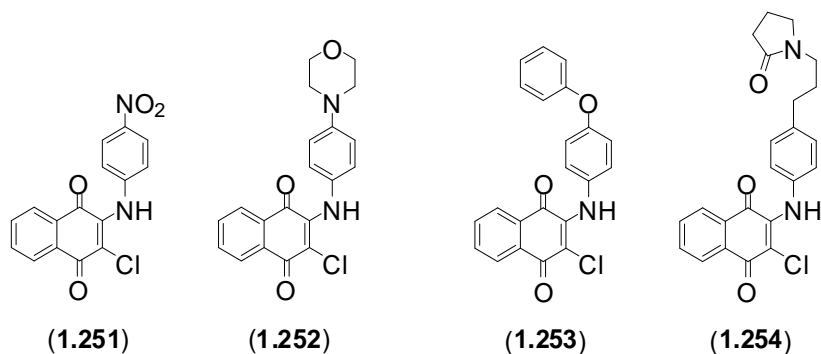


On this basis of these results, it was suggested that the enhancement of the activity from vitamin K to the hydroxyl-naphthoquinones was due to the hydroxyl moieties present in these compounds [87]. The eight naphthoquinone derivatives (**1.239-1.246**) that were synthesised from juglone (**1.186**) (pg 44) were assessed for anti-cancer activity towards four cell lines, HL-60, MDA-MB-435, HCT-8 and SF-295, with IC_{50} values ranging from 1.7 μM to 4.7 μM being observed. For juglone (**1.186**) the range of IC_{50} values against these cell lines ranged from 7.6 μM to 28.7 μM [88]. On the basis of this work, it was established that the introduction of a methoxy group at the 5 position increased the toxicity of juglone (**1.186**), and it was demonstrated that 5-methoxy-1,4-naphthoquinone induces apoptosis by an extrinsic pathway, indicating that the event was independent of mitochondrial depolarisation [88].

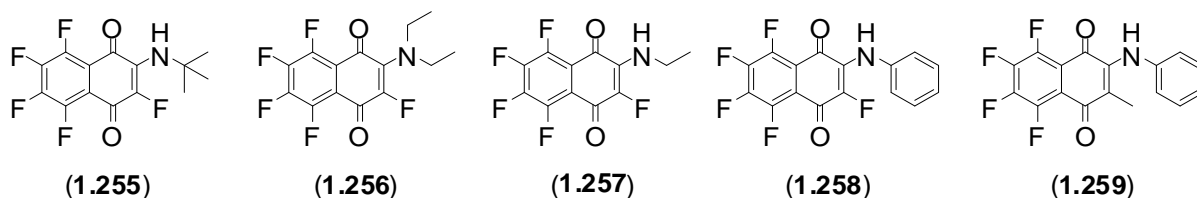


A study of the synthetic naphthoquinone derivative, *N*-(3-chloro-1,4-dioxo-1,4-dihydro-naphthalen-2-yl)-benzamide (**1.247**), revealed anti-cancer properties against CWR-22 prostate carcinoma (IC_{50} 2.5 μ M) and the PC-3 (IC_{50} 2.5 μ M), DU-145 (IC_{50} 6.5 μ M) and HS-5 bone marrow stromal (IC_{50} 25 μ M) cell lines [89]. Compound (**1.247**) arrested the G_1 -phase cell cycles of the CWR-22, PC-3 and DU-145 cell lines, while no effect was observed for the cell cycle progression of the HS-5 cells, indicating that this compound may be investigated as a possible treatment for prostate cancer, while protecting the bone marrow [89]. Of the fourteen synthetic derivatives of putative proteasome inhibitor PI-083 (**1.248**), six of these derivatives (**1.249-1.254**) were found to possess anti-proliferation activity towards the A-549, DU-145, KB and KBvin cell lines, with IC_{50} results ranging from 1.3 μ M to 23 μ M for these compounds [90].

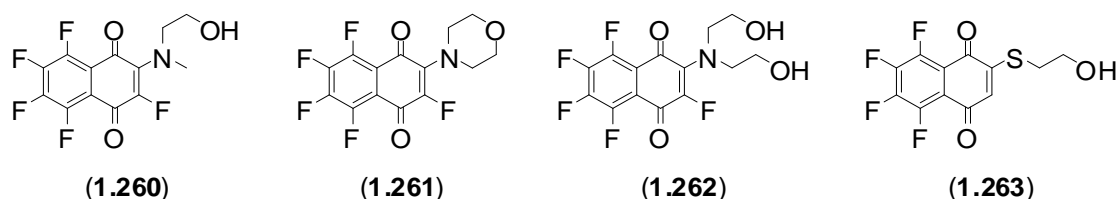




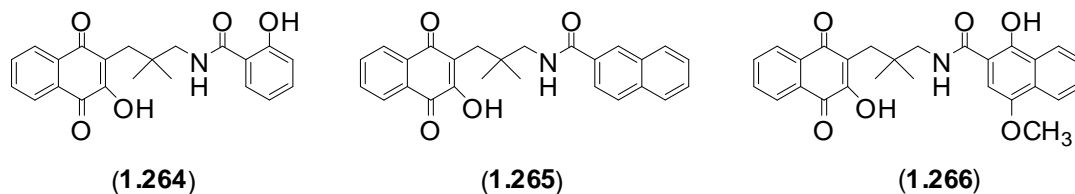
From a study of five fluorinated 1,4-naphthoquinones (**1.255-1.259**) against the RPMI-8226 human mammary adenocarcinoma and MCF-7 cell lines, compounds (**1.255-1.258**) exhibited activity with IC_{50} 's between 0.7 μ M and 2.5 μ M against the two cell lines, while **1.259** was less active with IC_{50} values of 7.5 μ M and 4.5 μ M against RPMI-8226 and MCF-7 respectively [91]. The same study also determined that the fluorinated naphthoquinones were less active against normal cells, with **1.257** and **1.258** showing the greatest difference in activity against cancer cells compared to normal cells [91].



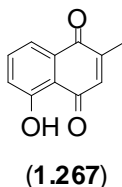
A study of another group of nine synthetic fluorinated naphthoquinones showed that four of these naphthoquinones (**1.260-1.263**) possessed potent anti-cancer activity towards the RPMI-8226 and MCF-7 cell lines, with IC_{50} values in the range of 2.4 to 12.8 μ M, while also being comparatively non-toxic to normal cells [92].



Three naphthoquinones (**1.264-1.266**) from a group of sixteen synthetic naphthoquinones were found to possess potent activity, with **1.264** possessing activity towards the NCI-H187 cell line (IC_{50} 8.83 μ M), while **1.265** and **1.266** were the most active towards the KB cell line with IC_{50} values of 9.00 μ M and 8.62 μ M respectively [93].

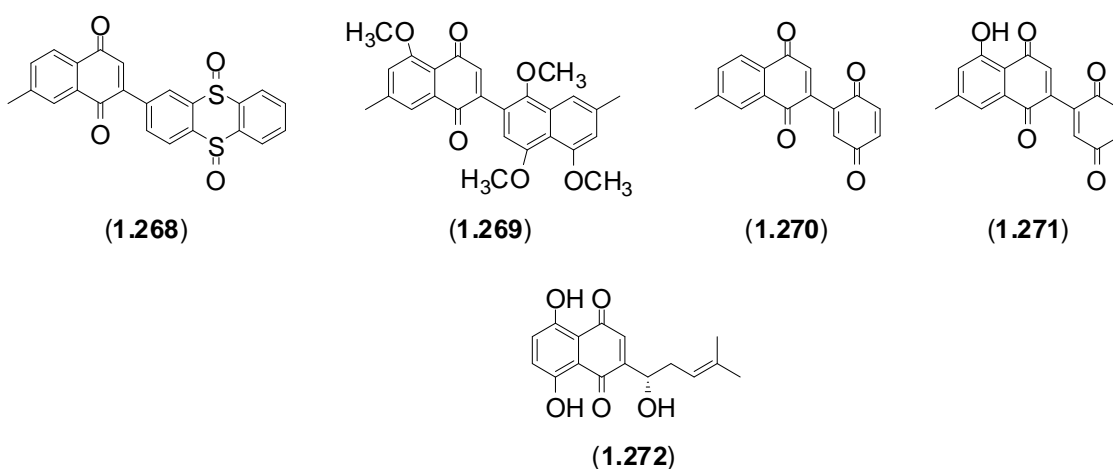


The naphthoquinone of 2-methoxy-1,4-naphthoquinone (2-methoxy-lawsone) (**1.194**) (pg 45) from *Impatiens balsamina*, used in traditional Chinese medicine for the treatment of pain and infection, was analysed for *in vitro* anti-tumour activity against the HepG2 cell line and showed an IC_{50} of 6.08 μ g/mL [94]. The natural naphthoquinone, plumbagin (**1.267**), was subjected to an *in vivo* study for the inhibition of transgenic adenocarcinoma of mouse prostate, where it was discovered that it could be used as a chemopreventative against prostate cancer [95]. Another study subjected plumbagin (**1.267**) to screening against the A-549 cell line, with moderate activity being observed (IC_{50} 14.6 μ M).



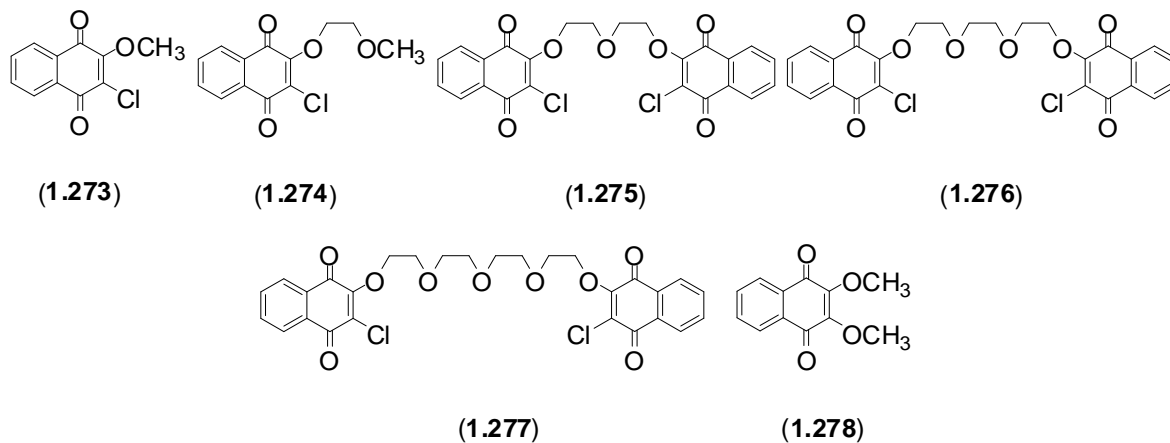
The four synthetic naphthoquinones, **1.268-1.271**, were analysed for activity towards HeLa cancer cells and, at a concentration of 10 μ M, compound (**1.271**) showed ~99% cell death of HeLa cells *in vitro* after 72 h [96]. The natural naphthoquinone, shikonin (**1.272**), the main

component of the traditional Chinese medicinal herb *Zi Cao* (*gromwell*), when tested against the H22 murine hepatoma and PC-3 cell lines, showed inhibition of cell growth associated with suppression of proteasomal activity and induction of cell death *in vivo* [97]. It was also observed that mice with P388 leukaemia, when treated with shikonin (**1.272**) had significantly increased survival times [97]. A further study of shikonin (**1.272**) found that this compound induces apoptosis in hepatocellular carcinoma cells both *in vitro* and *in vivo*, with activity towards the Huh-7 and BEL-7402 cell lines, but is non-toxic to regular cells [98].



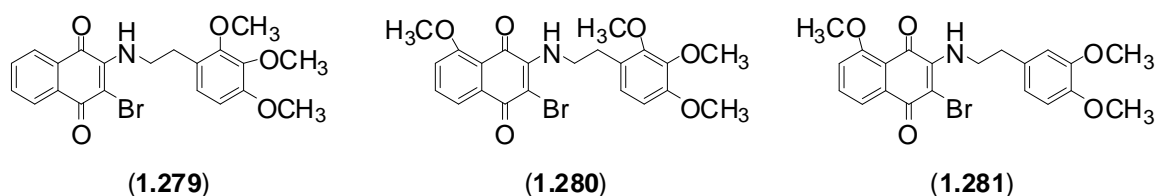
A series of 2,3-disubstituted naphthoquinones (**2.273-2.278**), synthetically prepared from 2,3-dichloro-1,4-naphthoquinone (**1.197**) (pg 45), were analysed for anti-cancer activity towards HL-60, AGS gastric adenocarcinoma, SK-MES-1 lung carcinoma and J-82 malignant human urothelial cell lines [99]. It was established that **1.277** displayed moderate activity against the SK-MES-1 cell line with an IC_{50} of 12.2 μ M, while exhibiting very weak activity against the other cell lines [99]. The other compounds from this study (**1.273-1.276** and **1.278**) were more active, with **1.273** displaying potent HL-60 activity with an IC_{50} of 1.8 μ M as well as displaying activity between 9 μ M and 12 μ M against the other cell lines [99]. Compounds (**1.274**, **1.275** and **1.278**) displayed activity against HL-60 with an IC_{50} of 1.7 μ M, 1.9 μ M and 8.9 μ M respectively. These three compounds displayed activities of between 5 μ M and 27 μ M against the other cell lines [99]. Compound **1.276** was the most consistently active of this

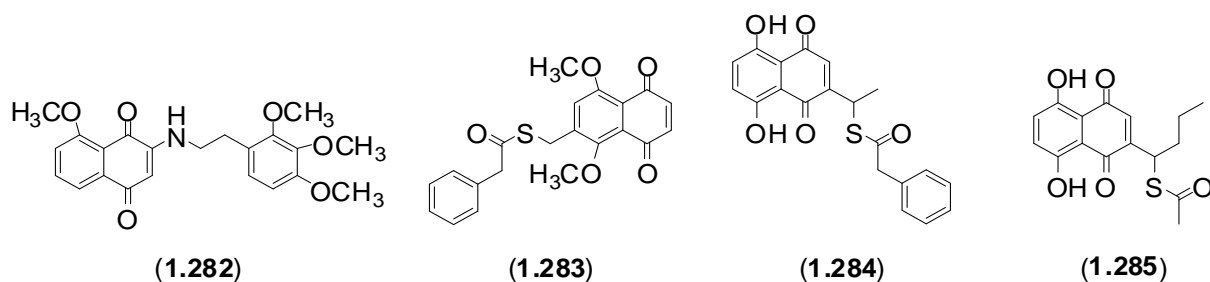
group of synthetic naphthoquinones, with activity observed against each cell line of HL-60 (IC_{50} 1.3 μ M), AGS (IC_{50} 5.2 μ M), SK-MES-1 (IC_{50} 7.1 μ M) and J-82 (IC_{50} 8.6 μ M) [99].



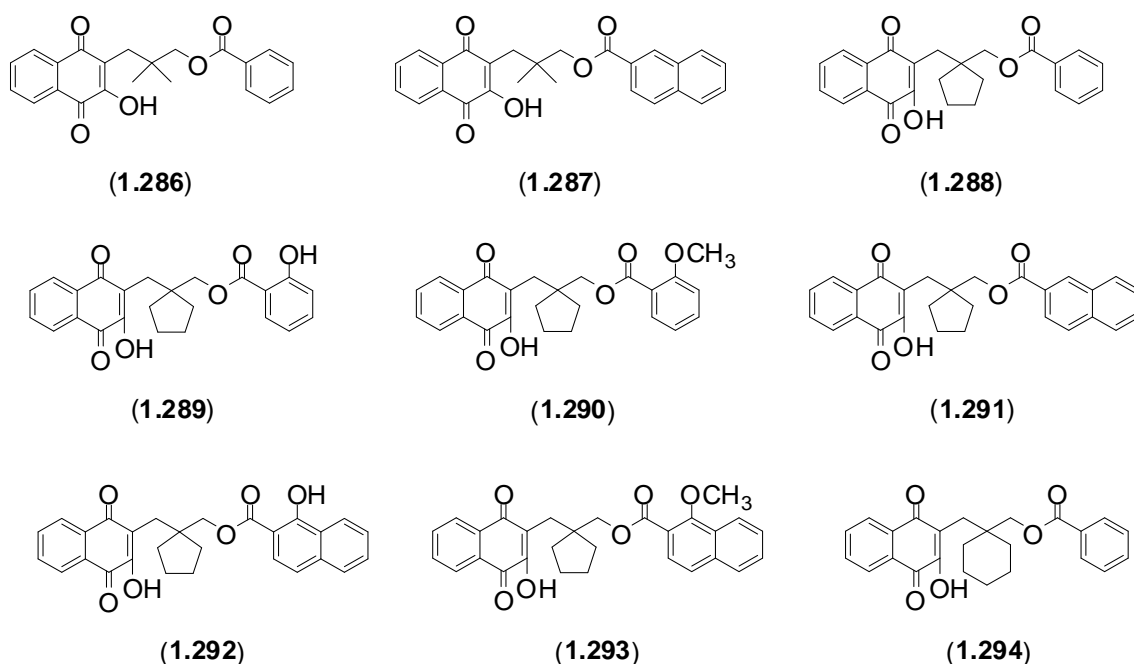
Of fifteen synthetic naphthoquinones, four (**1.279-1.282**) were found to possess activity, with **1.279** displaying moderate activity towards the HaCaT human keratinocyte cell line (IC_{50} 21.0 μ g/mL) [100]. Compounds **1.280** and **1.282** were both active towards the MCF-7 cell line (IC_{50} 22.0 μ g/mL and 26.0 μ g/mL respectively) as well as towards the Hep-G2 cell line (IC_{50} 24.0 μ g/mL and 25.0 μ g/mL respectively), while the most active compound was **1.281** with an IC_{50} towards Hep-G2 of 5.8 μ g/mL [100].

Three synthetic naphthoquinones (**1.283-1.285**) of a group of sixteen were found to possess potent anti-cancer activity towards the HT-29 cell line, with IC_{50} values of 4.24 μ g/mL, 7.45 μ g/mL and 2.40 μ g/mL respectively [101].





The fourteen synthetically prepared naphthoquinones (**1.286-1.299**), twelve of which contained side chains of 2'-cyclopentyl or 2'-cyclohexyl esters, were tested for anti-tumour activity towards the KB, HeLa and Hep-G2 cell lines, with results given in **Table 1.3** [102]. It was concluded that the 2',2'-dimethyl naphthoquinone esters were the most active, followed by the 2'-cyclopentyl derivatives. The least active were the 2'-cyclohexyl derivatives [102]. Among the cyclopentyl derivatives **1.288** to **1.293**, **1.288** and **1.292** were found to be most active against the KB and HeLa cell lines, with IC_{50} values of $<10 \mu\text{M}$, while **1.289-1.291** showed selective potent activity towards the KB cell line with IC_{50} values of $<10 \mu\text{M}$ and **1.293** showed selective potent activity towards the HeLa cell line with an IC_{50} of $5.84 \mu\text{M}$ [102].



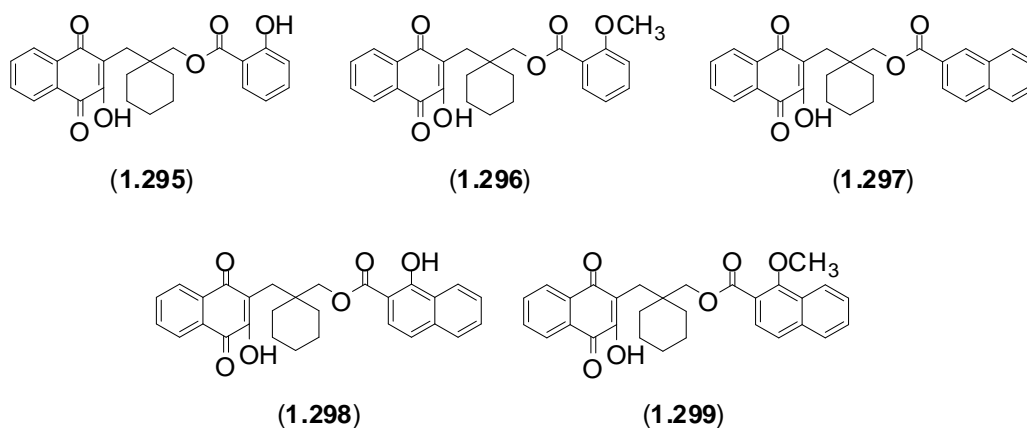
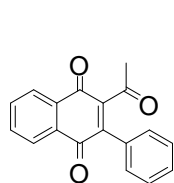


Table 1.3. Anti-tumour activity of naphthoquinones (1.286-1.299) given as an IC₅₀ (μM).

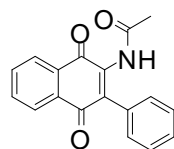
Compound	KB	HeLa	Hep-G2
1.286	1.53	3.02	4.85
1.287	1.59	1.17	1.30
1.288	3.53	7.04	16.90
1.289	5.41	15.99	83.66
1.290	4.23	57.80	18.31
1.291	5.63	16.35	83.09
1.292	3.68	6.40	21.47
1.293	65.48	5.48	63.76
1.294	11.45	17.93	23.24
1.295	9.56	11.42	14.75
1.296	11.76	14.91	72.27
1.297	9.42	15.58	50.16
1.298	13.81	10.63	50.58
1.299	11.35	10.22	62.73

Twenty-nine synthetic naphthoquinones (1.300-1.328) were evaluated for activity towards the MCF-7 and SK-Br-3 human breast adenocarcinoma cell lines and all were found to be active [102]. The most active of these compounds was **1.300** with IC₅₀ values against MCF-7 (0.21

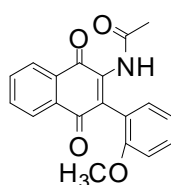
μM) and SK-Br-3 (0.82 μM), while **1.318** was the most active towards SK-Br-3 (0.6 μM), with the remaining compounds being active in one or both assays with IC_{50} values of $<10 \mu\text{M}$ [102].



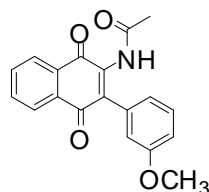
(1.300)



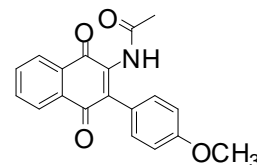
(1.301)



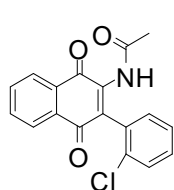
(1.302)



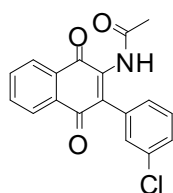
(1.303)



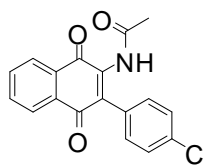
(1.304)



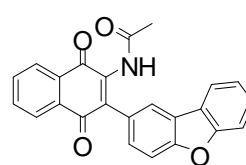
(1.305)



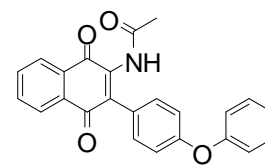
(1.306)



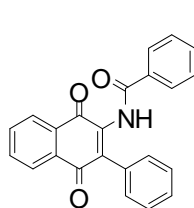
(1.307)



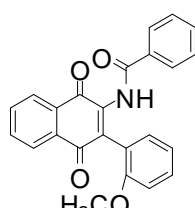
(1.308)



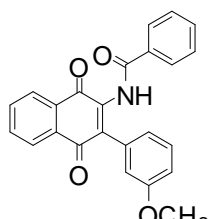
(1.309)



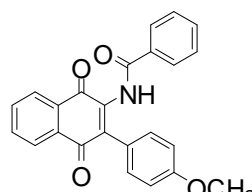
(1.310)



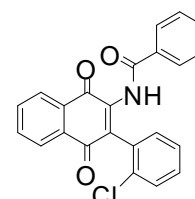
(1.311)



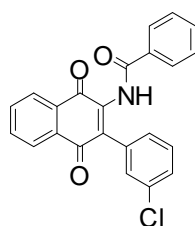
(1.312)



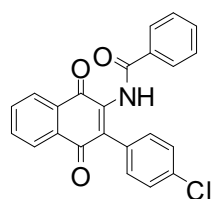
(1.313)



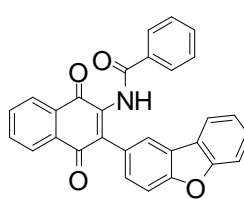
(1.314)



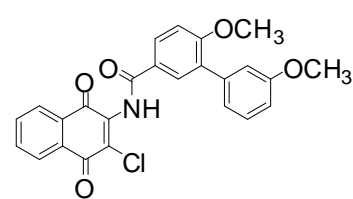
(1.315)



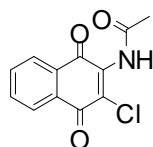
(1.316)



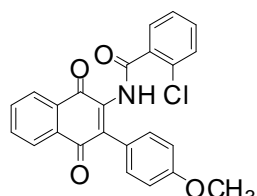
(1.317)



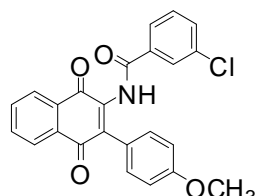
(1.318)



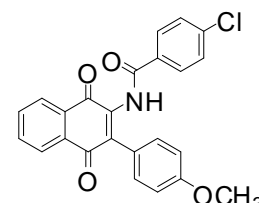
(1.319)



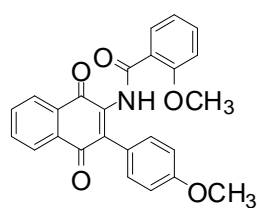
(1.320)



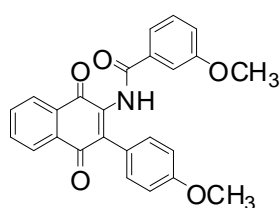
(1.321)



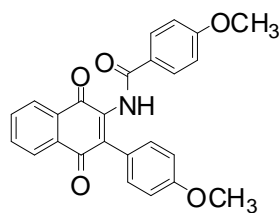
(1.322)



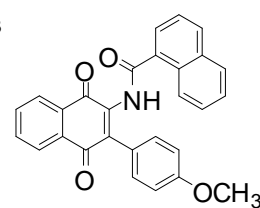
(1.323)



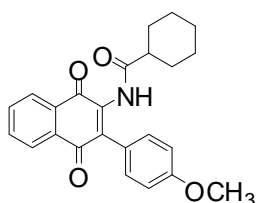
(1.324)



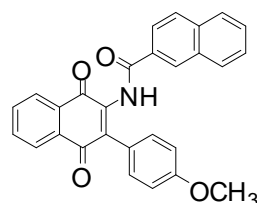
(1.325)



(1.326)

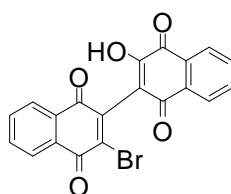


(1.328)

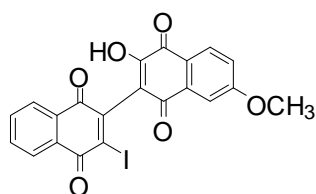


(1.327)

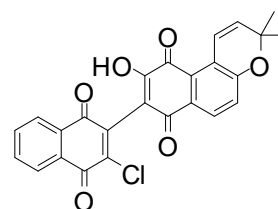
The naphthoquinone dimers, **1.329-1.333**, were shown to possess cytotoxicity towards prostate cancer cell lines. This activity was suggested to be due to the accumulation of reactive oxygen species and mitochondrial dysfunction [103].



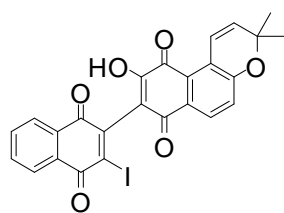
(1.329)



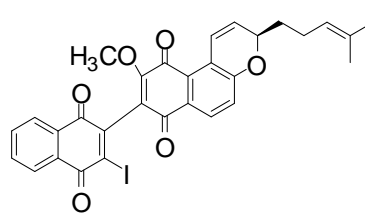
(1.330)



(1.331)



(1.332)



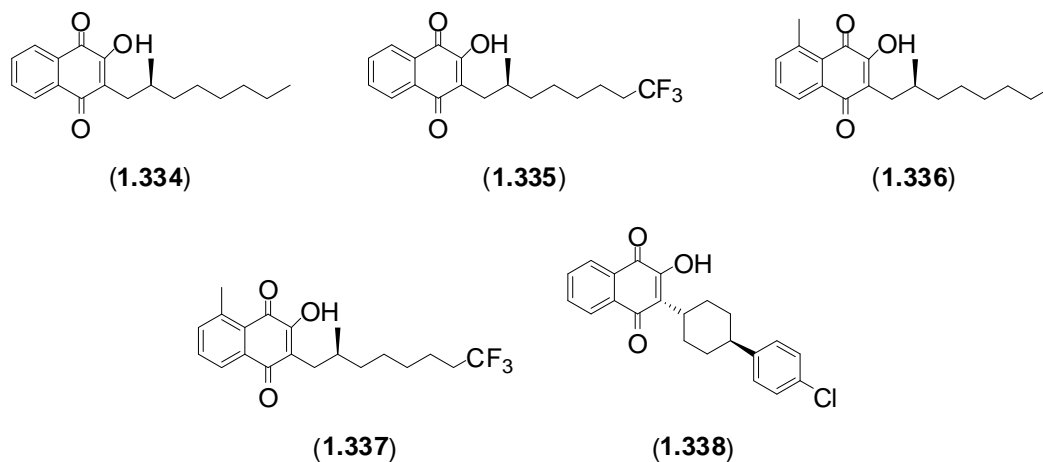
(1.333)

1.3.2.2 Anti-parasitic naphthoquinones

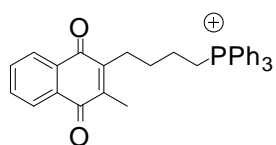
For a general introduction to parasitic diseases see **Section 1.2.2.2**. The anti-parasitic activities of naphthoquinones against malaria, leishmaniasis and trypanosomiasis are discussed below.

1.3.2.2.1 Anti-malarial naphthoquinones

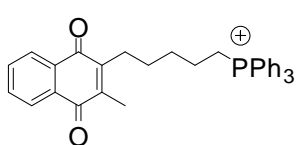
The synthetic naphthoquinones, **1.334-1.337**, were tested for their activity against *Plasmodium falciparum* and compared to the known anti-malarial naphthoquinone atovaquone (**1.338**). Compound (**1.335**) displayed the most potent activity with an IC_{50} of 17.07 nM, being more potent than atovaquone (**1.338**) with an IC_{50} of 19.7 nM, while the remaining naphthoquinones also displayed potent activity: **1.334** (IC_{50} 96.2 nM), **1.336** (IC_{50} 246.5 nM) and **1.337** (IC_{50} 4,452 nM) [104].



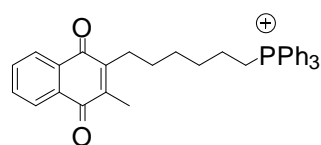
The synthetic cationic naphthoquinones, **1.339-1.355**, were found to possess potent anti-malarial activity towards *P. falciparum*, with **1.339** and **1.353** exhibiting the greatest activity with IC_{50} values of 18.7 nM and 17.4 nM respectively, while the activity for **1.340-1.355** ranged from 28.5 nM to 167.0 nM [105].



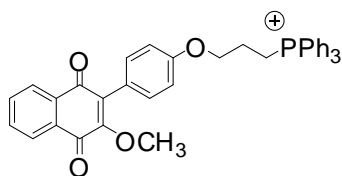
(1.339)



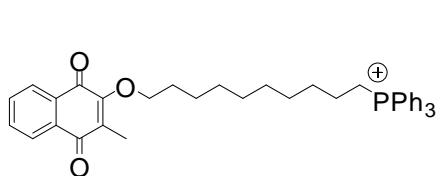
(1.340)



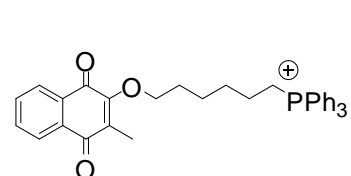
(1.341)



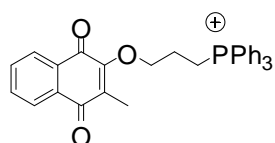
(1.342)



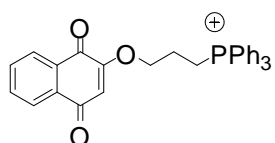
(1.343)



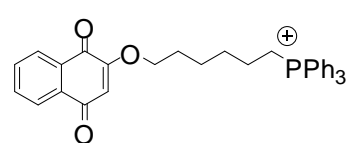
(1.344)



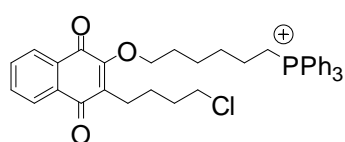
(1.345)



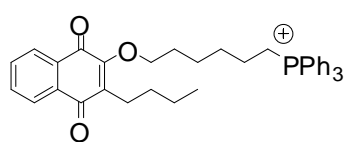
(1.346)



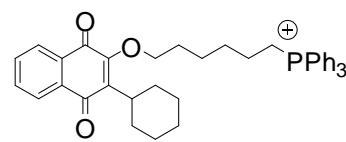
(1.347)



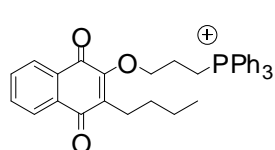
(1.348)



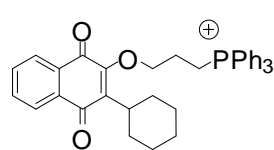
(1.349)



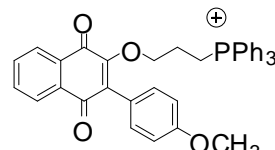
(1.350)



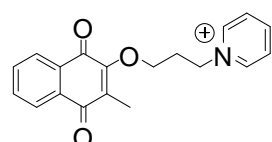
(1.351)



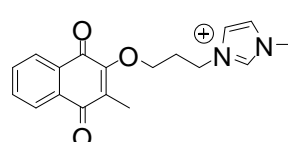
(1.352)



(1.353)

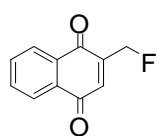


(1.354)

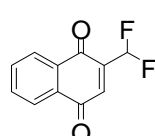


(1.355)

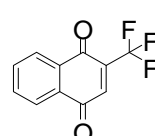
The fluorinated methyl-1,4-naphthoquinones, **1.356-1.358**, were found to possess activity against *P. falciparum* with IC_{50} values of 27.5 μ M, 22.8 μ M and 7.0 μ M respectively [106].



(1.356)

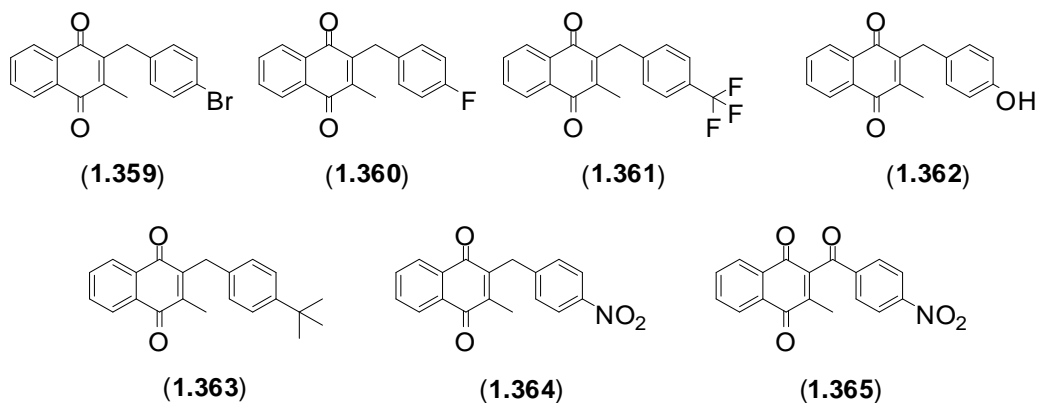


(1.357)

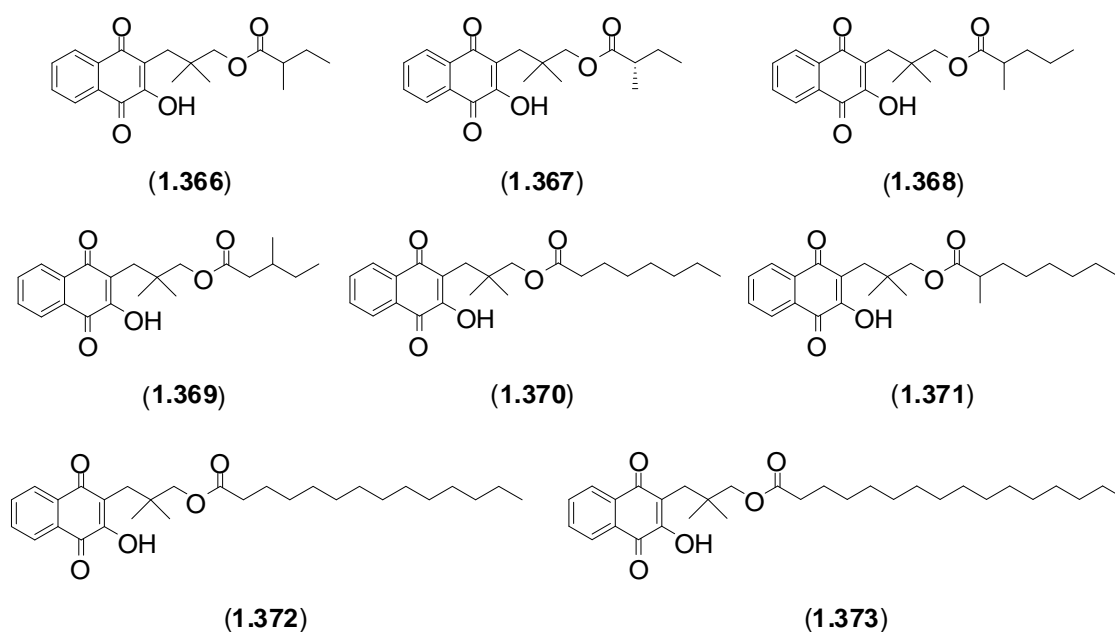


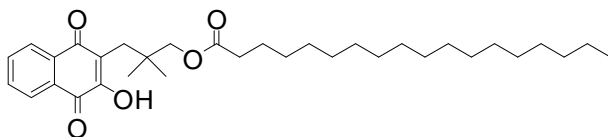
(1.358)

From a series of synthetic naphthoquinones, it was found that seven of these compounds (1.359-1.365) possessed anti-malarial activity towards the multidrug-resistant *P. falciparum* Dd2 strain, with IC_{50} values of 46 nM, 79 nM, 29 nM, 55 nM, 54 nM, 46 nM and 103 nM respectively, where all compounds were more potent than the anti-malarial drug chloroquine (IC_{50} 110 nM) [107].



Of a group of twenty six naphthoquinone aliphatic esters, nine (1.366-1.374) were found to possess potent activity towards *P. falciparum*, with activity ranging from IC_{50} 0.03 μ M to 0.22 μ M [108].

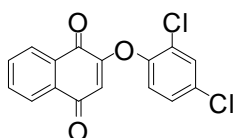




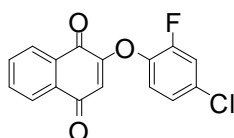
(1.374)

1.3.2.2.2 Anti-leishmanial naphthoquinones

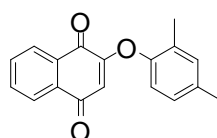
The synthetic naphthoquinones, **1.375-1.382**, were evaluated for activity against *Leishmania donovani*. It was found that all were potent inhibitors, with IC_{50} values ranging between 0.51 μ M and 2.37 μ M, with the most potent being **1.377** [109].



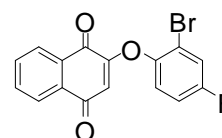
(1.375)



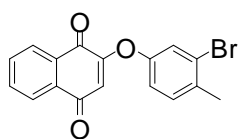
(1.376)



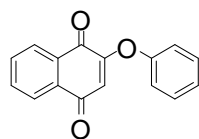
(1.377)



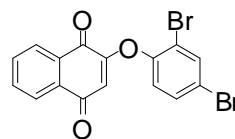
(1.378)



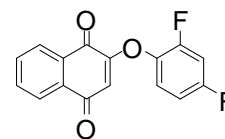
(1.379)



(1.380)

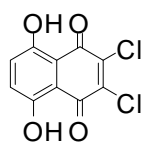


(1.381)

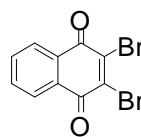


(1.382)

The anti-leishmanial activity of the two naphthoquinones, **1.383** and **1.384**, was evaluated, with activity towards both promastigotes and amastigotes of *L. donovani* being observed [110]. It was established that compounds (**1.383** and **1.384**) displayed promastigote activity at IC_{50} values of 5.4 μ M and 7.04 μ M respectively, while **1.383** and **1.384** showed amastigote activity at IC_{50} values of 0.069 μ M and 0.26 μ M respectively [110]. It was also found that IC_{50} values for these two compounds towards regular cells were quite high (46.5 μ M and 49.2 μ M respectively), compared to their IC_{50} values towards *L. donovani* cells. The differences in cytotoxicity suggested that these compounds could be considered for further analysis for the possible treatment of visceral leishmaniasis [110].



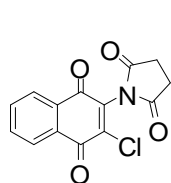
(1.383)



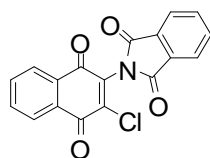
(1.384)

1.3.2.2.3 Anti-trypanosomal naphthoquinones

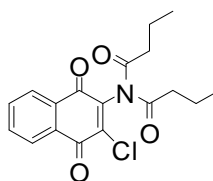
The activity of the synthetic naphthoquinones, **1.375-1.382**, against *Trypanosoma cruzi* and *Trypanosoma brucei rhodesiense* was also investigated. With the exception of **1.381**, all were found to be active towards *T. cruzi* with IC_{50} values of $<10 \mu\text{M}$, with **1.380** (IC_{50} $1.26 \mu\text{M}$) being the most active, while compounds (**1.375-1.382**) all exhibited activity of $IC_{50} < 0.6 \mu\text{M}$ towards *T. brucei rhodesiense*, with **1.380** being the most active (IC_{50} $0.08 \mu\text{M}$) [109]. The eleven synthetic imido-substituted-1,4-naphthoquinones (**1.385-1.395**) were evaluated for anti-trypanosomal activity towards *T. cruzi*. The most active was **1.387** (IC_{50} $0.70 \mu\text{M}$), while the other compounds exhibited slightly less activity with IC_{50} values up to $6.5 \mu\text{M}$ [111].



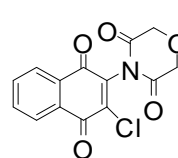
(1.385)



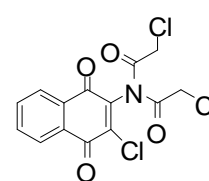
(1.386)



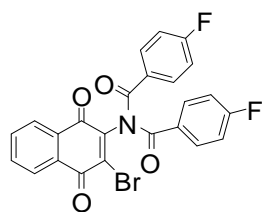
(1.387)



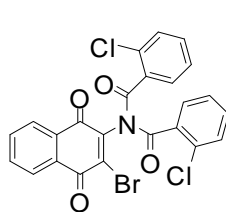
(1.388)



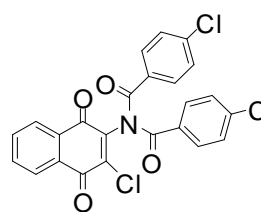
(1.389)



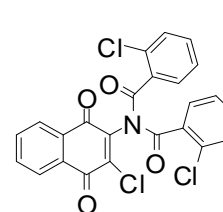
(1.390)



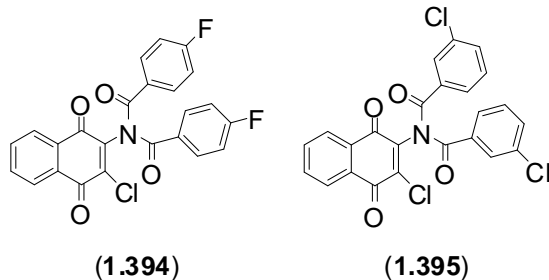
(1.391)



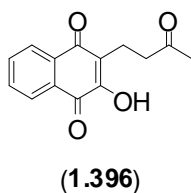
(1.392)



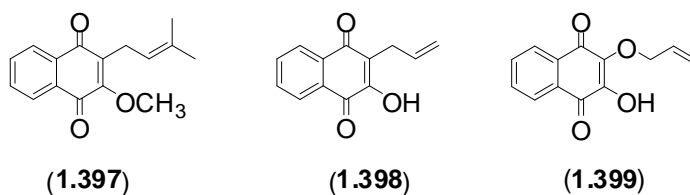
(1.393)



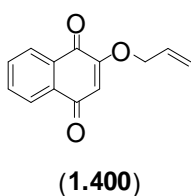
The trypanocidal activity of lapachol (**1.195**) (pg 45) and the related compound (**1.396**) were evaluated and IC_{50} values for **1.195** (31.3 μM) and for **1.396** (35.2 μM) were reported [74].



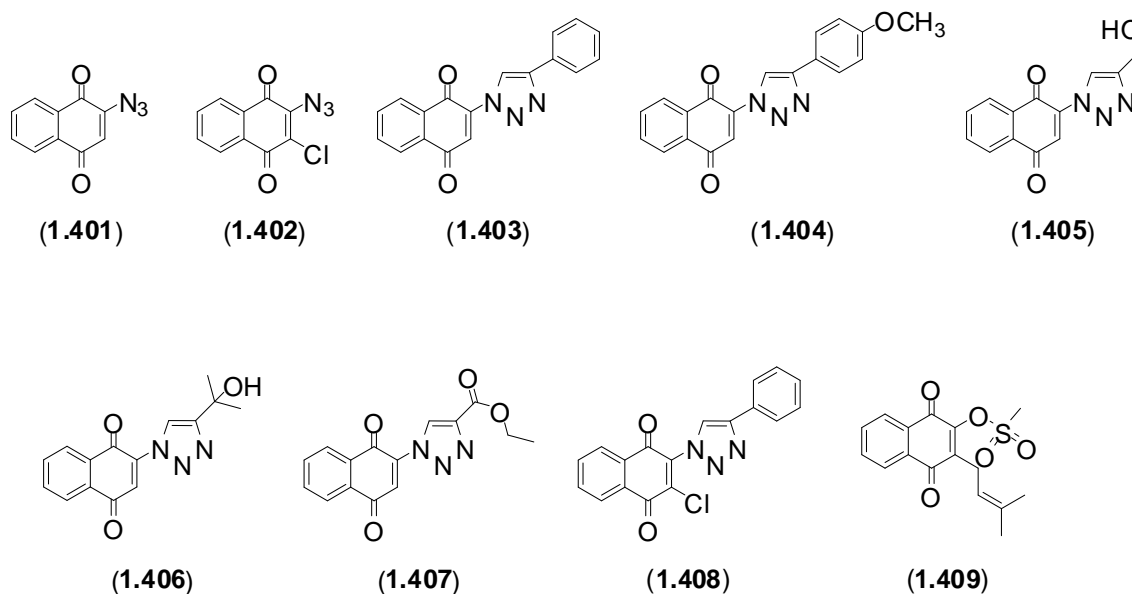
Compounds (**1.397-1.399**) were found to have $ED_{50}/24\text{ h}$ values of between 160 μM and 430 μM [74].



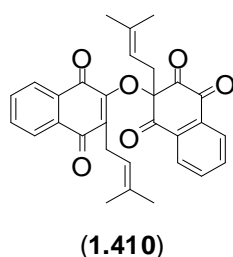
The 1,4-naphthoquinones (**1.194**, **1.197** and **1.400**) were evaluated for activity towards *T. cruzi* epimastigote forms and it was found that **1.194** was the least active (IC_{50} 3.19 μM), while **1.197** (IC_{50} 0.09 μM) and **1.400** (IC_{50} 0.02 μM) were more active [112].



Synthetic azide naphthoquinones (**1.401-1.402**) were used to prepare the triazole naphthoquinones (**1.403-1.408**), as well as the mesyl naphthoquinone (**1.409**), a derivative of lapachol (**1.195**) (pg 45). These compounds were all evaluated for biological activity towards *T. cruzi*, with IC₅₀ values of 41.6 μM (**1.401**), 51.8 μM (**1.402**), 10.9 μM (**1.403**), 45.8 μM (**1.404**), 17.7 μM (**1.405**), 80.2 μM (**1.406**), 67.6 μM (**1.407**), 42.0 μM (**1.408**) and 25.7 μM (**1.409**) [113].

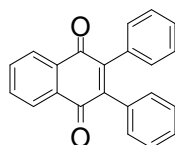


The synthetic naphthoquinone (**1.410**) was found to possess moderate activity towards the trypomastigote forms of *T. cruzi* (IC₅₀ 233 μM) [114].



The naphthoquinone 2,3-diphenyl-1,4-naphthoquinone (**1.411**) was evaluated for *in vitro* and *in vivo* activity towards *T. cruzi*. The *in vitro* activity against epimastigote cell-derived

trypomastigote, as well as intracellular amastigote forms of *T. cruzi* was found to have LD₅₀ values of 2.5 μM, while displaying low toxicity towards normal mammalian cells (LC₅₀ = 130 μM) [115].



(1.411)

1.3.3 Summary

Naphthoquinones have a wide range of activity towards many diseases and for this reason continue to attract interest, particularly in the area of synthetic organic chemistry. The understanding of the mechanism for the biological activity of the naphthoquinones towards different forms of cancer and parasitic diseases is starting to emerge, along with the modes of action. The bioactivity of naphthoquinones requires further research, especially in the development and isolation of novel potent biologically active naphthoquinones that could potentially lead to new pharmaceuticals or leads for drug discovery.

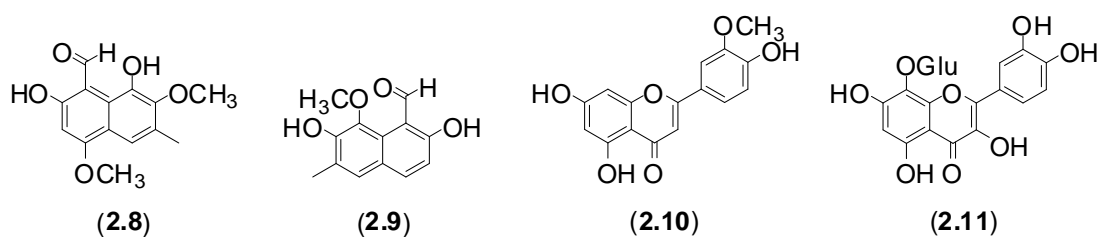
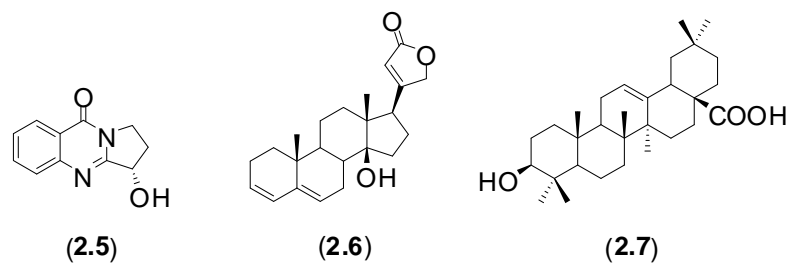
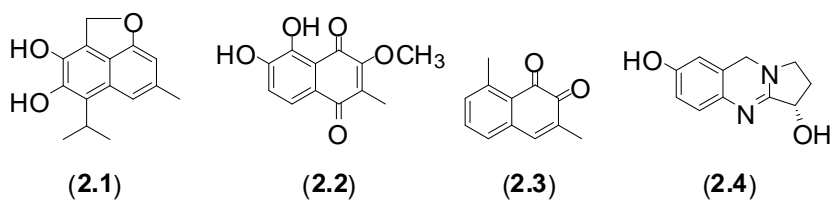
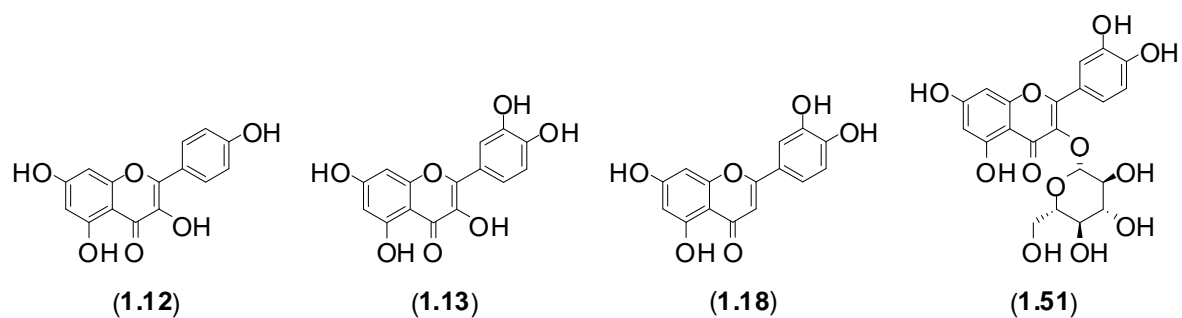
During the course of the research within this thesis, three naphthoquinones and two naphthoquinone glycosides were isolated, as detailed in **Chapter 4**.

Chapter 2

*On-line (HPLC-NMR) and Off-line Phytochemical Profiling of the Australian Plant, *Lasiopetalum macrophyllum**

2.1 Introduction

The plant family Malvaceae, commonly referred to as the Mallow family, consists of two hundred and forty-three genera and 4,225 species that are found worldwide [116]. In 1997, the taxonomy of the family Malvaceae was broadened to include the families Sterculiaceae, Tiliaceae and Bombacaceae [117]. Malvaceae is comprised of many well-known genera including *Gossypium* (cotton) and *Hibiscus* (ornamental), and many of these genera are known to contain biologically active constituents [118, 119]. The Malvaceae has afforded many classes of secondary metabolites, including terpenoids (2.1-2.3) [120], alkaloids (2.4-2.5) [121], steroids (2.6-2.7) [122], naphthalenes (2.8-2.9) [118], and flavonoids (1.12, 1.13, 1.18, 1.51, 2.10-2.12) [118, 122-126]. The genus *Lasiopetalum*, belonging to this family, has not been studied widely in terms of its secondary metabolites, with only fatty acid analyses of seed oils being reported to date [127, 128].



An extract of the Australian plant *L. macrophyllum* was selected for chemical investigation on the basis that very little chemistry had been reported for this genus, together with the fact that the Malvaceae family is known to produce a wide array of structure classes with bioactive properties.

2.2 Experimental

2.2.1 General Experimental

For all general experimental procedures and spectroscopic methods, see the Experimental Chapter **Section 7.1**. All semi-preparative HPLC analyses were performed using a gradient solvent system (0 mins 30% CH₃CN/H₂O; 20 mins 50% CH₃CN/H₂O), with detection at λ_{\max} 254 and 315 nm. Both on-flow and stop-flow HPLC-NMR analyses were performed using gradient HPLC conditions (0-2 mins 30% CH₃CN/D₂O, 20-24 mins 50% CH₃CN/D₂O, 26 mins 30% CH₃CN/D₂O), with detection at λ_{\max} 254 and 315 nm.

2.2.2 Plant material

The plant specimen (stems and leaves) was collected from Troopers Creek in the Grampians National Park, Victoria, Australia on the 23rd September 2006 and identified as *L. macrophyllum* from “*The Grampians in Flower*” monograph [129]. A voucher specimen, designated the code 2006-34, is deposited at the School of Applied Sciences (Discipline of Applied Chemistry), RMIT University. A 2 g portion of the *L. macrophyllum* specimen was extracted with 3:1 MeOH:DCM (40 mL) and evaluated for biological activity as described in the Experimental chapter **Section 7.1.4**. The crude extract was found to display modest P388 activity with an IC₅₀ of 296 μ g/mL, along with minimal anti-bacterial activity towards *Bacillus subtilis*. No activity was detected against *Escherichia coli*, *Pseudomonas aeruginosa*, *Candida albicans*, *Trichophyton mentagrophytes* and *Cladosporium resinae*.



L. macrophyllum

(2006-34)

Kingdom:	Plantae
Phylum:	Magnoliophyta
Class:	Magnoliopsida
Order:	Malvales
Family:	Malvaceae
Genus:	<i>Lasiopetalum</i>
Species:	<i>macrophyllum</i>

2.2.3 Extraction and Isolation

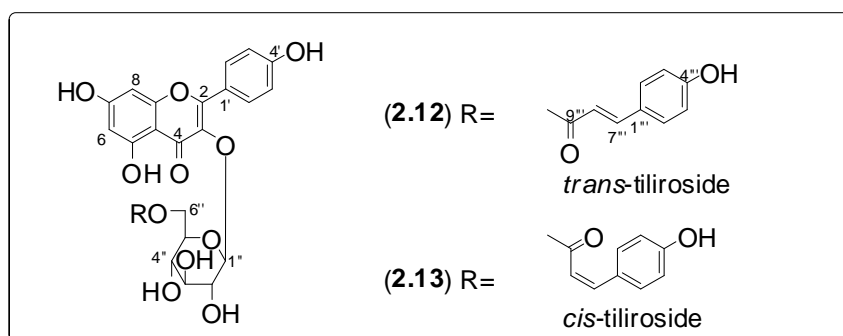
2.2.3.1 Preparation of the extract of *L. macrophyllum* for on-flow and stop-flow HPLC-NMR analysis

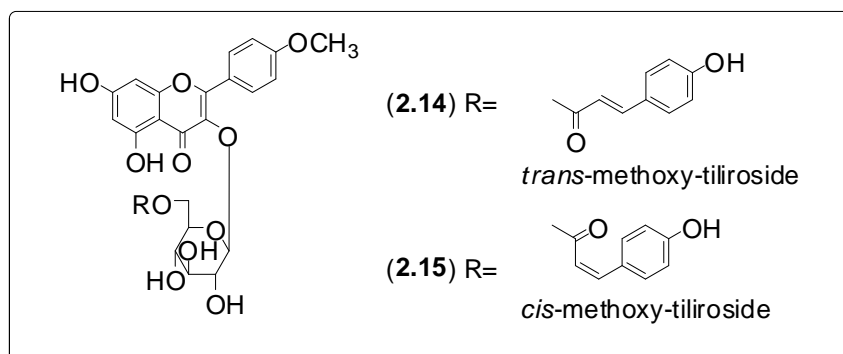
The specimen of *L. macrophyllum* (50 g) was roughly chopped and extracted with 3:1 methanol:dichloromethane (1 L). This extract was then decanted and concentrated under reduced pressure and was then sequentially partitioned (triturated) into dichloromethane followed by methanol. The extracts were then analysed by analytical HPLC using the gradient described in the Experimental chapter **Section 7.1.2**, which led to the development of the HPLC gradient described in **Section 2.2.1**. A portion of the methanol soluble fraction

(72 mg) was re-solubilised in 1 mL 50:50 CH₃CN:D₂O and filtered through a 0.45 μm PTFE membrane filter (HP045 Advantec, Japan). For both the on-flow and stop-flow HPLC-NMR experiments, 50 μL (3,600 μg) of the methanol extract was injected and monitored at λ_{max} 254 and 315 nm. The HPLC-NMR analyses were performed using the HPLC conditions described in **Section 2.2.1**.

2.2.3.2 Preparation of the extract for off-line isolation of secondary metabolites from *L. macrophyllum*

A further extraction of *L. macrophyllum* (100 g) was carried out with 3:1 MeOH:DCM (2 L). This extract was decanted and concentrated under reduced pressure before sequential partitioning into DCM (0.9 g) and MeOH (6.0 g) soluble extracts. A portion (800 mg) of the MeOH extract subjected to C₁₈ Vacuum Liquid Column (VLC) chromatography using a 25% stepwise elution from water to MeOH and then to EtOAc and finally to DCM to afford thirteen fractions. Four fractions were combined due to similarities in the analytical HPLC chromatograms and ¹H NMR spectra, and the combined fraction was filtered through a 0.45 μm PTFE membrane filter (HP045 Advantec, Japan) and subjected to semi-preparative reversed phase HPLC as described in **Section 2.2.1** to yield *trans*-tiliroside (**2.12**) (26 mg, 0.05% dry weight), *cis*-tiliroside (**2.13**) (6 mg, 0.01%), 4'-methoxy-*trans*-tiliroside (**2.14**) (2 mg, 0.004%) and the previously unreported compound, 4'-methoxy-*cis*-tiliroside (**2.15**) (1 mg, 0.002%). Compound (**2.12**) had been isolated previously but its structure had been incorrectly assigned initially [130] as discussed in **Section 2.3**.





2.3 Results and Discussion

For the HPLC-NMR chemical profiling, the plant material was extracted and fractionated as described in **Section 2.2.1**. On-flow HPLC-NMR analysis (**Figure 2.1 [A]**) of the crude methanol extract supported the presence of one major compound. From the HPLC chromatogram and 2D contour plot from the on-flow HPLC-NMR analysis, it was found that along with the major compound (peak 1) three minor compounds (peaks 2 to 4) were also observed (**Figure 2.2**). Similarities in the UV profiles (**Figure 2.2**) of the four HPLC peaks suggested that all four compounds were structurally related. The extracted WET-1D ¹H NMR spectrum of the major component (**Figure 2.1 [B]**), corresponding to peak 1 in **Figure 2.2** contained diagnostic ¹H NMR signals: δ 7.88 (d, J = 9 Hz), δ 7.21 (d, J = 8.5 Hz), δ 6.83 (d, J = 9 Hz) and δ 6.76 (d, J = 8.5 Hz) which indicated the presence of aromatic proton resonances; δ 7.24 (d, J = 16 Hz) and δ 5.92 (d, J = 16 Hz), indicating the presence of a *trans* double bond; and δ 5.03 (d, J = 7.5 Hz), δ 4.11 (d, J = 5.5 Hz), δ 3.38 (m), δ 3.32 (m) and δ 3.21 (m), which were supportive of a sugar moiety. From this the compound was suggested to be an aromatic compound with an attached sugar moiety.

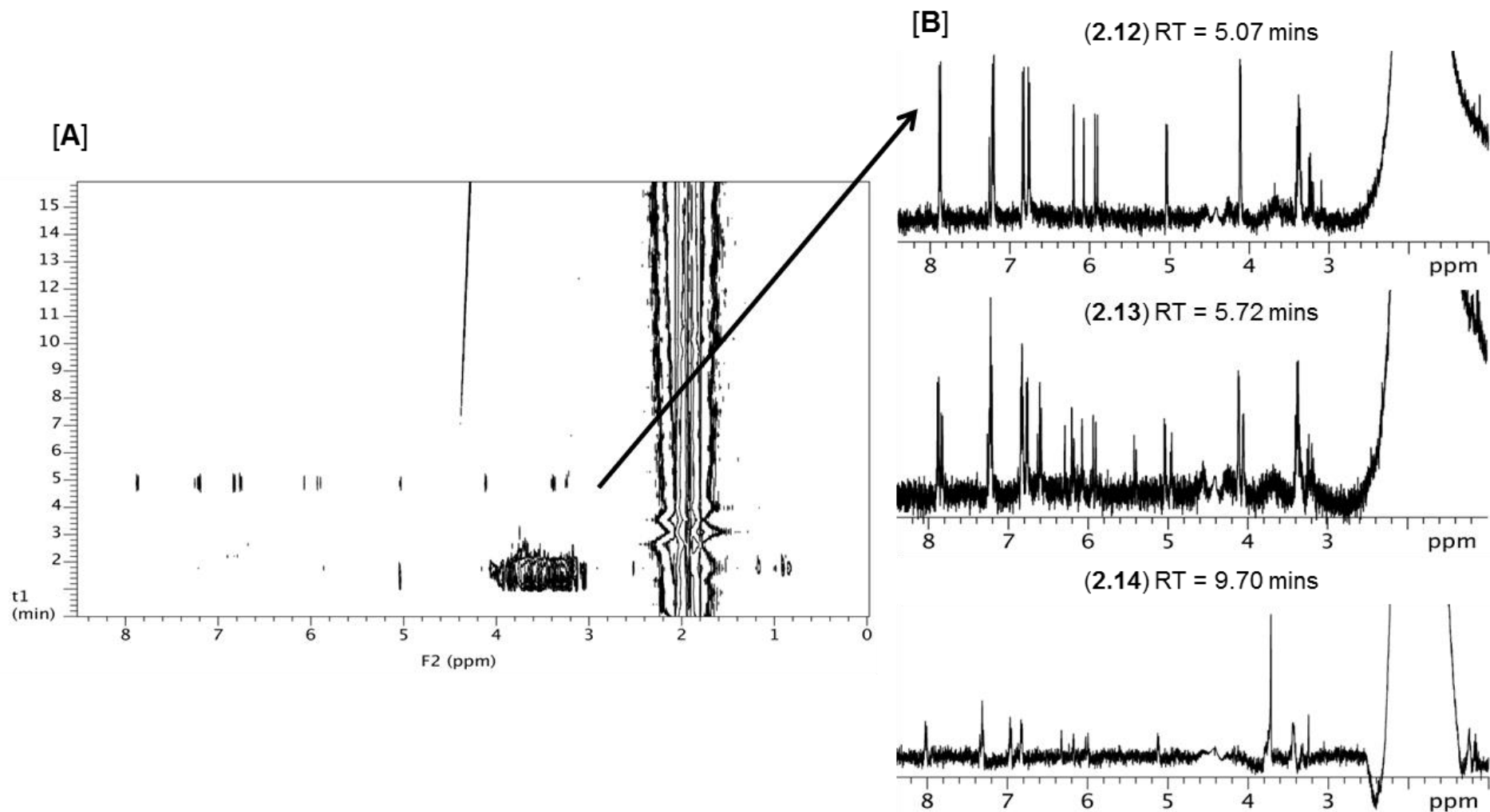


Figure 2.1. [A] 2D HPLC-NMR contour plot showing the major compound (2.12) (on-flow HPLC-NMR) and [B] Extracted WET-1D ¹H NMR spectra of compounds (2.12-2.14) (stop-flow HPLC-NMR).

On the basis of this NMR data and the fact that the family Malvaceae is known to produce flavonoid glycosides [118, 122, 124, 131, 132], this compound was tentatively suggested to be *trans*-tiliroside (**2.12**). Given the relatively poor S/N obtained for the ^1H NMR spectrum of peak 1 in the on-flow HPLC-NMR analysis, together with the fact that the ^1H NMR spectra for the other peaks could not be detected, it was necessary to carry out stop-flow HPLC-NMR analyses. Stop-flow HPLC-NMR analysis enabled extended acquisition times (typically from 20 mins to 16 h) for the WET-1D ^1H NMR experiments.

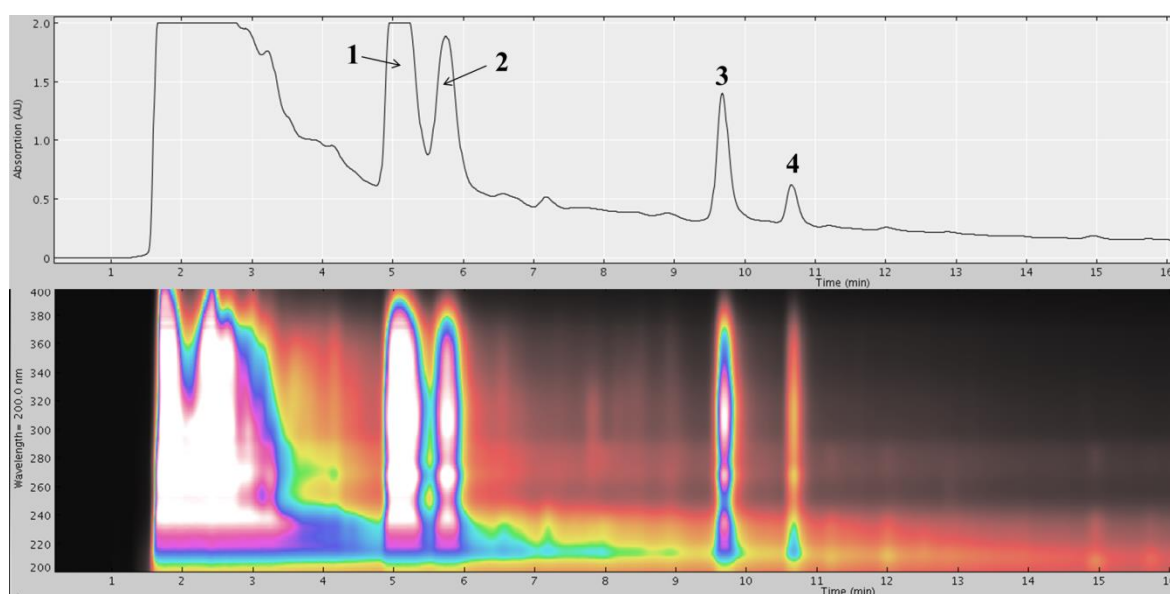


Figure 2.2. HPLC chromatogram and 2D PDA plot of on-flow HPLC-NMR analysis of *L. macrophyllum*.

The 30 minutes acquisition time resulted in a significantly improved S/N WET-1D ^1H NMR spectrum for the major peak, *trans*-tiliroside (**2.12**), as well as allowing the detection of WET-1D ^1H NMR spectra of HPLC peaks 2 and 3 (**Figure 2.2**), as shown in **Figure 2.1 [B]**.

The WET-1D ^1H NMR spectra of peaks 1-3 (**Figure 2.1**) all exhibited resonances consistent with the presence of olefinic and aromatic methines, along with signals associated with a sugar moiety. The elution times of peaks 1 and 2 were very similar, resulting in some overlapping and thus the appearance of signals due to peak 1 (compound **2.12**) in the WET-1D ^1H NMR spectrum of peak 2 (**Figure 2.1**). However, marked differences in the intensities

of the two sets of ^1H NMR signals made it clear which signals belonged to which HPLC peak. Diagnostic ^1H NMR chemical shift differences for peak 2 were observed at δ 6.62 (d, $J = 14.5$ Hz) and δ 5.41 (d, $J = 14.5$ Hz), supporting the presence of *cis* double bond geometry and suggesting that this component was *cis*-tiliroside (**2.13**). Although the WET-1D ^1H NMR S/N for peak 3 was relatively poor (1.5 h acquisition) in comparison with those of compounds **2.12** and **2.13**, several diagnostic features could be extracted. The poor S/N meant that the coupling constant associated with the olefinic signals [δ 7.33 (d, $J \sim 14$ Hz) and δ 6.01 (d, $J \sim 14$ Hz)], could only be estimated and this was similar to that of the *cis* double bond protons in **2.13**. However, the chemical shifts were consistent with the *trans* double bond geometry seen in **2.12** and these, together with the presence of a methoxy signal [δ 3.72, s] indicated that peak 3 was most likely a methoxy derivative of *trans*-tiliroside (**2.12**). Thus peak 3 was tentatively assigned the structure 4'-O-methoxy-*trans*-tiliroside (**2.14**).

Even the prolonged analysis times afforded by stop-flow HPLC-NMR were inadequate to detect the ^1H NMR spectrum of the fourth component (peak 4), although the presence of characteristic UV chromophores at 269 nm and 317 nm indicated that this compound was probably also a related flavonoid glycoside, which was later identified as compound (**2.15**). To unequivocally identify the four secondary metabolites (**2.12-2.15**), off-line purification employing reversed phase HPLC was undertaken.

For the off-line HPLC purification, the plant material was extracted and subjected to the fractionation methodology as described in **Section 2.2.3.2**. Analytical HPLC and ^1H NMR analysis of the methanol-soluble extract confirmed the presence of the flavonoid glycosides that were previously observed in the HPLC-NMR analysis, and from this the isolation of **2.12-2.15** was carried out as described in **Section 2.2.3.2**.

The structure of **2.12** (HPLC peak 1) was confirmed on the basis of 1D (^1H NMR shown in **Figure 2.3**) and 2D NMR spectroscopy (**Table 2.1**) and mass spectrometry. The HR-ESI-MS of **2.12** displayed an m/z at 593.1308 [M-H^-] (calcd. for $\text{C}_{30}\text{H}_{25}\text{O}_{13}$: m/z 593.1295) and an m/z at 595.1440 [M+H^+] (calcd. for $\text{C}_{30}\text{H}_{27}\text{O}_{13}$: m/z 595.1452) consistent with eighteen degrees of

unsaturation and a molecular formula of $C_{30}H_{26}O_{13}$. The ^{13}C NMR spectrum of **2.12** showed the presence of twenty-six discrete signals [thirteen methines (four of these being overlapped and each accounting for two aromatic methines), one methylene and twelve quaternary carbons], as supported by the gHSQCAD 2D NMR experiment. The 1H NMR spectrum (**Figure 2.3**) and the 2D gCOSY NMR spectrum identified the presence of the following moieties: a set of *meta* coupled aromatic methines [δ 6.15, d, $J = 2$ Hz (H-6) and δ 6.38, d, $J = 2$ Hz (H-8)]; two 1,4-disubstituted aromatic rings [δ 7.98, dd, 2H, $J = 1.5, 9$ Hz (H-2'/H-6') and δ 6.85, dd, 2H, $J = 1.5, 9$ Hz (H-3'/H-5')] and [δ 7.37, d, 2H, $J = 8.5$ Hz (H-2''/H-6'') and δ 6.78, d, 2H, $J = 8.5$ Hz (H-3''/H-5'')]; a pair of olefinic methines [δ 7.34, d, $J = 16$ Hz (H-7''') and δ 6.12, d, $J = 16$ Hz (H-8''')] with *trans* coupling and, finally, a sugar moiety containing five deshielded methines [δ 5.45, d, $J = 7.5$ Hz (H-1'') and those occurring between δ 3.16 and δ 3.37, (H-2'', H-3'', H-4'', H-5'')] and one deshielded methylene [δ 4.02, dd, $J = 6.5, 12$ Hz (H-6a'') and δ 4.26, dd, $J = 1.5, 12$ Hz (H-6b'')].

A number of 2D gHMBC NMR experiments were conducted using a range of coupling constants ($J = 2$ Hz, 4 Hz, 6 Hz, 8 Hz, 10 Hz and 12 Hz) in order to optimise the number of HMBC correlations. On the basis of these experiments it was concluded that, for HMBC purposes, the optimal J value for observing correlations in the sugar moiety was 4 Hz, while for the aromatics it was 10 Hz.

In combination with the ^{13}C NMR spectrum, the 2D gHSQC and gHMBC NMR experiments allowed for the complete assignment of **2.12**. The sugar moiety was concluded to be disubstituted at both the anomeric and methylene carbon on the basis of the HMBC correlations observed to both of these carbons. The deshielded sugar methylene resonances at δ 4.02 (H-6a'') and δ 4.26 (H-6b'') showed an HMBC correlation to 166.2 ppm (C-9''') (see **Figure 2.4**), supporting an ester linkage to C-6'' of the sugar.

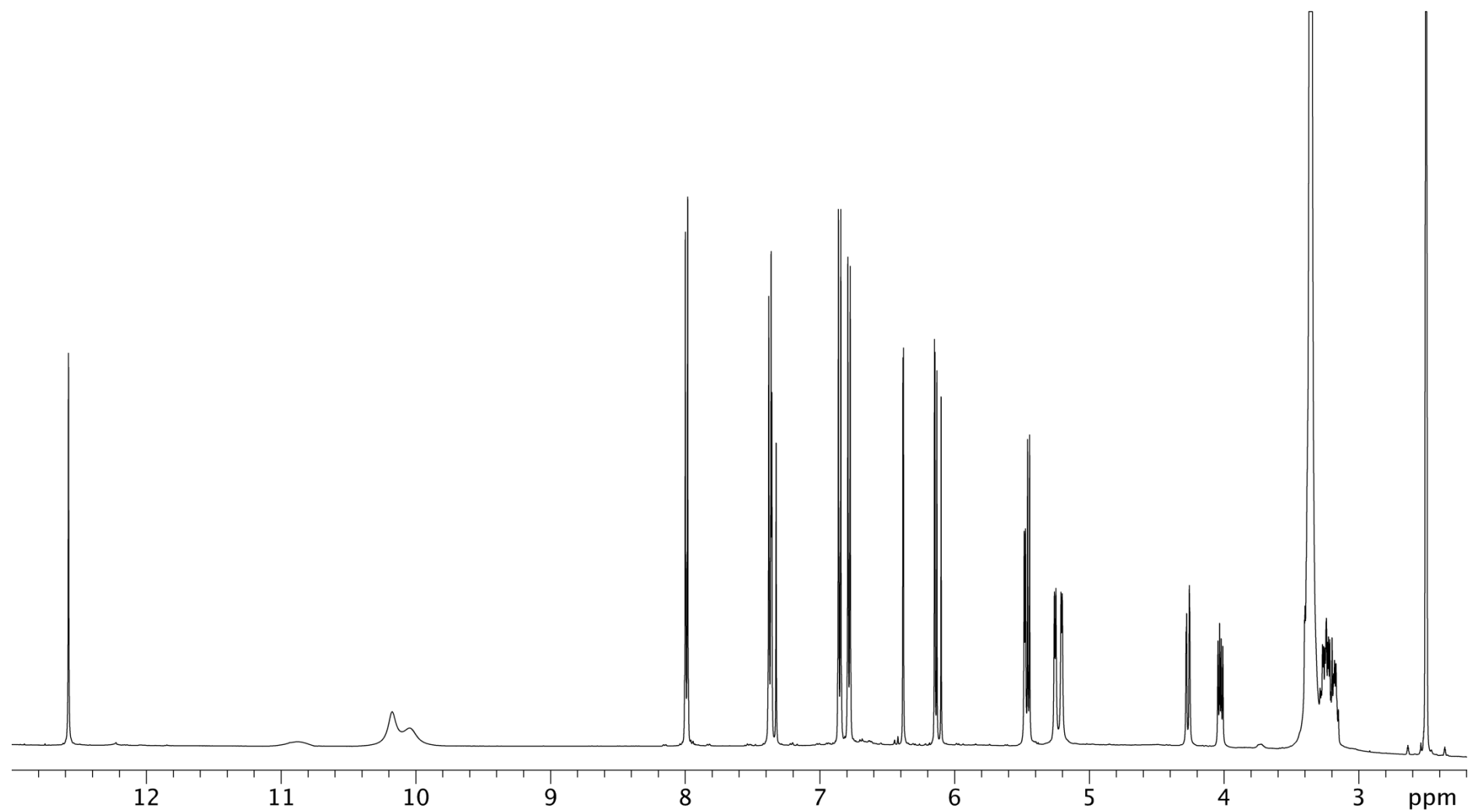


Figure 2.3. ^1H NMR (500 MHz, d_6 -DMSO) spectrum of *trans*-tiliroside (**2.12**).

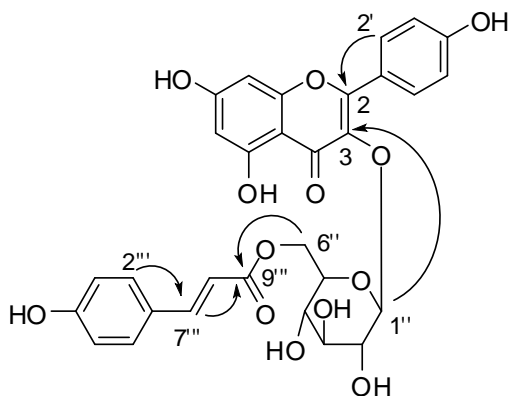


Figure 2.4. Key HMBC correlations for *trans*-tiliroside (**2.12**).

Further HMBC correlations observed between this ester carbon 166.2 ppm (C-9'') and the olefinic methines at δ 7.34 (H-7'') and δ 6.12 (H-8'') (See **Figure 2.4**) unambiguously placed the *trans* double bond adjacent to this ester. This structure fragment could be extended further by considering the HMBC correlations between the aromatic protons at δ 7.37 (H-2''/H-6'') and the olefinic methine carbon at 144.6 ppm (C-7''). A further HMBC correlation between the other methine proton at δ 6.12 (H-8'') and the quaternary carbon at 124.9 ppm (C-1'') suggested a connection of the alkene to one of the two 1,4-disubstituted aromatic rings. This 1,4-disubstituted aromatic ring was probably substituted with a hydroxyl group due to a lack of resonances that would support an alkoxy group, as supported by the HMBC correlation between its aromatic protons δ 7.37 (H-2'') and δ 6.78 (H-3'') and the carbon at 159.8 ppm (C-4''). Together, these HMBC correlations permitted this first structure fragment, attached to a central sugar moiety, to be identified as a *trans*-*p*-coumaroyl moiety as shown in **Figure 2.5**.

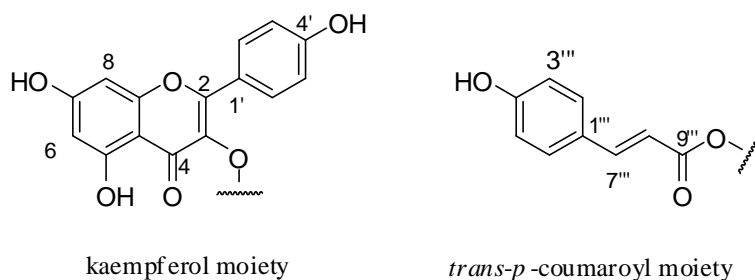


Figure 2.5. Fragments linked to the sugar for the major component (**2.12**).

A second ether linkage from the sugar moiety was identified on the basis of the HMBC correlation observed from the anomeric proton at δ 5.45 (H-1'') to a quaternary carbon at 133.1 ppm (C-3) (See **Figure 2.4**). No other HMBC correlations were observed to C-3, suggesting a high degree of substitution in this portion of the structure. The second of the 1,4-disubstituted aromatic rings was also suggested to be substituted with a hydroxyl moiety on the same basis as that for compound (**2.12**), with correlations observed from the aromatic methines δ 7.98 (H-2') and δ 6.85 (H-3') to the deshielded carbon at 160.0 ppm. A further HMBC correlation, from δ 7.98 (H-2') to 156.4 ppm (C-2), suggested that the 1,4-disubstituted aromatic ring was connected to a deshielded olefinic carbon atom (C-2) as shown in **Figure 2.4**.

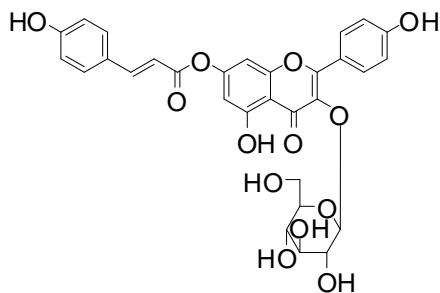
The remaining pair of aromatic protons at δ 6.15 (H-6) and δ 6.38 (H-8) were only *meta* coupled ($J = 2$ Hz) to each other and thus were concluded to be part of a 1,2,3,5-tetra-substituted aromatic ring. These protons displayed HMBC correlations to the quaternary carbons at 103.9 ppm (C-10) and 156.3 ppm (C-9) (**Figure 2.5**). In addition to the carbon at 133.1 ppm (C-3), a further quaternary carbon at 177.4 ppm (C-4) was observed in the ^{13}C NMR spectrum, suggesting that this substructure, attached to the anomeric proton of the sugar moiety, was the flavonol kaempferol (**Figure 2.5**).

The complete NMR data (as given in **Table 2.1**) unequivocally confirmed the structure of **2.12** to be *trans*-tiliroside, a known flavonol glycoside first isolated from *Tilia argenta* [133]. *Trans*-tiliroside was initially reported as compound **2.16** before structural revisions, conducted in 1964 [130], ultimately reassigned it to structure **2.12**. Prior to this structural revision of *trans*-tiliroside, a compound named tribuloside was reported and assigned structure **2.12** in recognition of its difference to structure **2.16** [134]. The revision made it clear that "tribuloside" and the compound initially given structure **2.16** were the same compound, *trans*-tiliroside (**2.12**) [135]. Since this early revision, the "real" compound **2.16** has been isolated from multiple sources [136-140], with the structure determined by 1D and 2D NMR spectroscopy [139].

Table 2.1. ^1H (500 MHz) and ^{13}C (125 MHz) NMR spectroscopic data of *trans*-tiliroside (**2.12**) in d_6 -DMSO.

Position	δ_{H}, J	δ_{C}^a	gCOSY	gHMBC (4 Hz)	gHMBC (8 Hz)	gHMBC (10 Hz)
1	-	-	-	-	-	-
2	-	156.4, s	-	-	-	-
3	-	133.1, s	-	-	-	-
4	-	177.4, s	-	-	-	-
5	-	161.2, s	-	-	-	-
6	6.15, d, $J = 2$ Hz	98.8, d	H-8	C-5, C-7, C-8, C-10	C-5, C-7, C-8, C-10	C-5, C-7, C-8, C-10
7	-	164.2, s	-	-	-	-
8	6.38, d, $J = 2$ Hz	93.7, d	H-6	C-6, C-7, C-9, C-10	C-6, C-7, C-9, C-10	C-6, C-7, C-9, C-10
9	-	156.3, s	-	-	-	-
10	-	103.9, s	-	-	-	-
1'	-	120.8, s	-	-	-	-
2'	7.98, dd, $J = 1.5, 9$ Hz	130.9, d	H-3'	C-2, C-4', C-6'	C-2, C-4', C-6'	C-2, C-3, C-4', C-6'
3'	6.85, dd, $J = 1.5, 9$ Hz	115.1, d	H-2'	C-4', C-5'	C-1', C-4', C-5'	C-1', C-4', C-5'
4'	-	160.0, s	-	-	-	-
5'	6.85, dd, $J = 1.5, 9$ Hz	115.1, d	H-6'	C-3', C-4'	C-1', C-3', C-4'	C-1', C-3', C-4'
6'	7.98, dd, $J = 1.5, 9$ Hz	130.9, d	H-5'	C-2, C-2', C-4'	C-2, C-2', C-4'	C-2, C-2', C-4', C-5'
1''	5.45, d, $J = 7.5$ Hz	101.0, d	H-2''	C-3, C-2'', C-3''	C-3	C-3
2''	3.21 ^b , m	74.1, d	H-1'', 2''-OH	C-1'', C-3''	C-1'', C-3''	C-1'', C-3''
3''	3.24 ^b , m	76.2, d	3''-OH	C-1'', C-2'', C-4''	C-1'', C-4''	C-1'', C-2'', C-4''
4''	3.16 ^b , m	69.9, d	4''-OH	C-3'', C-5'', C-6''	C-3''	C-3'', C-5'', C-6''
5''	3.37 ^b , m	74.2, d	H-6a'', H-6b''	C-1''	C-4''	C-1'', C-3'', C-4''
6a''	4.02, dd, $J = 6.5, 12$ Hz	63.0, t	H-5'', H-6b''	C-5'', C-9''	C-4'', C-5'', C-9''	C-5'', C-9''
6b''	4.26, dd, $J = 1.5, 12$ Hz	-	H-5'', H-6a''	C-4'', C-5'', C-9''	C-4'', C-5'', C-9''	C-4'', C-9''
1'''	-	124.9, s	-	-	-	-
2'''	7.37, d, $J = 8.5$ Hz	130.2, d	H-3'''	C-4''', C-7'''	C-3''', C-4''', C-6''', C-7'''	C-3''', C-4''', C-7'''
3'''	6.78, d, $J = 8.5$ Hz	115.8, d	H-2'''	C-1''', C-4''', C-5'''	C-1''', C-4''', C-5'''	C-1''', C-4''', C-5'''
4'''	-	159.8, s	-	-	-	-
5'''	6.78, d, $J = 8.5$ Hz	115.8, d	H-6'''	C-1''', C-3''', C-4'''	C-1''', C-3''', C-4'''	C-1''', C-3''', C-4'''
6'''	7.37, d, $J = 8.5$ Hz	130.2, d	H-5'''	C-4''', C-7'''	C-2''', C-4''', C-5''', C-7'''	C-4''', C-5''', C-7'''
7'''	7.34, d, $J = 16$ Hz	144.6, d	H-8'''	C-2'''/C-6''', C-8''', C-9'''	C-2'''/C-6''', C-8''', C-9'''	C-2'''/C-6''', C-8''', C-9'''
8'''	6.12, d, $J = 16$ Hz	113.6, d	H-7'''	C-1''', C-9'''	C-1''', C-9'''	C-1''', C-9'''
9'''	-	166.2, s	-	-	-	-
5-OH	12.58, s	-	-	C-5, C-6, C-7, C-10	C-5, C-6, C-10	C-5, C-6, C-7, C-10
7-OH	10.88, bs	-	-	-	-	-
4'-OH	10.18, bs	-	-	-	-	-
2''-OH	5.48, d, $J = 4.5$ Hz	-	H-2''	C-1'', C-2'', C-3''	C-1'', C-2'', C-3''	C-1'', C-2'', C-3''
3''-OH	5.19, d, $J = 5.5$ Hz	-	H-3''	C-2'', C-3'', C-4''	C-2'', C-3'', C-4''	C-2'', C-3'', C-4''
4''-OH	5.24, d, $J = 4.5$ Hz	-	H-4''	C-3'', C-4'' C-5''	C-3'', C-4'' C-5''	C-3'', C-4'' C-5''
4'''-OH	10.05, bs	-	-	-	-	-

^aCarbon assignments based on gHSQCAD and gHMBC NMR experiments. ^bSignals overlapped



(2.16)

misassigned structure of *trans*-tiliroside

A comparison of the NMR data for **2.12** (Table 2.1 and Experimental chapter Section 7.2) with those reported in the literature (d_6 -DMSO and CD_3OD) confirmed that the compound corresponding to HPLC peak 1 was *trans*-tiliroside (**2.12**) [135, 141, 142]. Although the complete 2D NMR assignment of **2.12** is documented in the literature [142], it is worth noting that on one occasion prior to this 2D assignment [143], several of the carbon NMR assignments (namely positions C-5, C-6, C-8 and C-9) were incorrect. The carbon chemical shift assignments were confirmed by our gHSQCAD and gHMBC NMR experiments and are consistent with all other literature NMR reports for **2.12** [135, 141, 142]. The sugar moiety in compound **2.12** was concluded to be a β -D-glucopyranoside on the basis of a comparison of the NMR chemical shifts for this moiety with the literature data [141]. The absolute configuration of the sugar moiety in compound **2.12** has been previously established by both acid and alkali hydrolyses [130, 144]. *Trans*-tiliroside (**2.12**) is known to occur in other Malvaceae species [126, 131, 132, 145-147].

The negative ESI-MS of HPLC peak 2 (**2.13**) was identical to that of **2.12** in that it showed the presence of an ion at m/z 593 $[M-H]^-$, while the positive mode showed the presence of ions at m/z 595 $[M+H]^+$ and m/z 617 $[M+Na]^+$. The 1H NMR spectrum of **2.13** was also very similar to that of **2.12**. Comparison of the spectrum of **2.13** with that of **2.12** indicated that both compounds contained the same kaempferol and glycoside moieties (Table 2.2).

Table 2.2. ^1H (500 MHz) and ^{13}C (125 MHz) NMR spectroscopic data of *cis*-tiliroside (**2.13**) in d_6 -DMSO.

Position	δ_{H}, J	$\delta_{\text{C}}^{\text{a}}$	gCOSY	gHMBC
1	-	-	-	-
2	-	156.5, s	-	-
3	-	133.1, s	-	-
4	-	ND	-	-
5	-	161.1, s	-	-
6	6.17, d, $J = 2.0$ Hz	98.5, d	H-8	C-5, C-7, C-8, C-10
7	-	164.3, s	-	-
8	6.32, d, $J = 2.0$ Hz	93.5, d	H-6	C-6, C-7, C-9, C-10
9	-	156.4, s	-	-
10	-	103.7, s	-	-
1'	-	120.6, s	-	-
2'	7.95, d, $J = 9.0$ Hz	130.6, d	H-3'	C-2, C-4', C-6'
3'	6.84, d, $J = 9.0$ Hz	115.0, d	H-2'	C-1', C-4', C-5'
4'	-	159.7, s	-	-
5'	6.84, d, $J = 9.0$ Hz	115.0, d	H-6'	C-1', C-3', C-4'
6'	7.95, d, $J = 9.0$ Hz	130.6, d	H-5'	C-2, C-2', C-4'
1''	5.40, d, $J = 7.5$ Hz	101.5, d	H-2''	C-3''
2''	3.20 ^b , m	73.8, d	H-1''	-
3''	3.24 ^b , m	75.9, d	3''-OH	-
4''	3.15 ^b , m	69.7, d	4''-OH	-
5''	3.37 ^b , m	74.2, d	H-6a''	-
6a''	4.07, dd, $J = 6.0, 11.0$ Hz	63.0, t	H-5'', H-6b''	C-9''
6b''	4.15, dd, $J = 2.0, 11.0$ Hz		H-6a''	-
1'''	-	125.4, s	-	-
2'''	7.55, d, $J = 8.5$ Hz	132.4, d	H-3'''	C-4''', C-6''', C-7'''
3'''	6.69 ^b , d, $J = 8.5$ Hz	114.6, d	H-2'''	C-1''', C-4''', C-5'''
4'''	-	158.8, s	-	-
5'''	6.69 ^b , d, $J = 8.5$ Hz	114.6, d	H-6'''	C-1''', C-3''', C-4'''
6'''	7.55, d, $J = 8.5$ Hz	132.4, d	H-5'''	C-2''', C-4''', C-7'''
7'''	6.67 ^b , d, $J = 12.5$ Hz	143.5, d	H-8'''	C-2''', C-6''', C-9'''
8'''	5.46 ^b , d, $J = 12.5$ Hz	114.3, d	H-7'''	C-1'''
9'''	-	165.6, s	-	-
5-OH	12.55, s	-	-	-
4'-OH	10.16, bs	-	-	-
2''-OH	5.45 ^b , d, $J = 4.5$ Hz	-	H-2''	-
3''-OH	5.17, d, $J = 5$ Hz	-	H-3''	-
4''-OH	5.22, d, $J = 5.5$ Hz	-	H-4''	C-5''

^a Carbon assignments based on gHSQCAD and gHMBC NMR experiments^b Signals overlapped

ND indicates signals were not detected

Differences were evident in the olefinic methines of the coumaroyl moiety, with a shift from δ 7.34, d, $J = 16$ Hz (H-7''') and δ 6.12, d, $J = 16$ Hz (H-8''') in **2.12** to δ 6.67, d, $J = 12.5$ Hz (H-7''') and δ 5.46, d, $J = 12.5$ Hz (H-8''') in **2.13** as shown in **Figure 2.6**. This change was consistent with a *cis* double bond in the coumaroyl moiety (**Figure 2.6**). In addition, the sugar methylene signals at δ 4.02, dd, $J = 6.5, 12$ Hz (H-6a'') and δ 4.26, dd, $J = 1.5, 12$ Hz (H-6b'') in **2.12** shifted to δ 4.07, dd, $J = 6, 11$ Hz (H-6a'') and δ 4.15, dd, $J = 2, 11$ Hz (H-6b'') in **2.13**, which was also consistent with a change from *trans* to *cis* in the double bond geometry of the coumaroyl moiety. On this basis compound **2.13** was concluded to be *cis*-tiliroside, which was first reported in a mixture with *trans*-tiliroside (**2.12**) in 1995 [148]. The first isolation and characterization of **2.13** was reported in 2004 [142]. Comparison of the NMR data obtained from this study as a mixture with **2.12** in CD₃OD (see Experimental chapter **Section 7.2**) for HPLC peak 2 with that in the literature (reported in CD₃OD) confirmed that this compound was *cis*-tiliroside (**2.13**) [142].

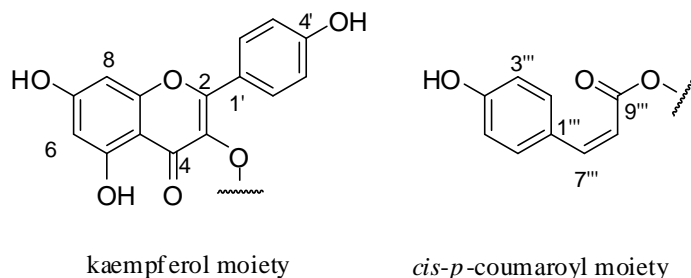


Figure 2.6. Fragments linked to the sugar for the major component (**2.13**).

The negative ESI-MS of the compound responsible for HPLC peak 3 showed the presence of an ion at m/z 607 [M-H]⁻, 14 mass units higher than that of **2.12** and **2.13** and consistent with a molecular formula of C₃₁H₂₆O₁₃ and eighteen degrees of unsaturation. The ¹H NMR spectrum was very similar to that of **2.12**. Once again, the presence of a *trans*-*p*-coumaroyl moiety was indicated by the chemical shifts and coupling constants of the olefinic protons [δ 7.35, d, $J = 16$ Hz (H-7''') and δ 6.17, d, $J = 16$ Hz (H-8''')]. The ¹H NMR chemical shifts of the 1,4-disubstituted aromatic ring associated with the kaempferol moiety [δ 8.06, d, 2H, $J = 8$ Hz

(H-2'/H-6') and δ 6.99, d, 2H, $J = 8$ Hz (H-3'/H-5')] as shown in **Table 2.3**. This evidence and the presence of a deshielded methyl resonance [δ 3.70, s, 3H, (4'-OCH₃)], indicated that **2.14** was a methoxy derivative of **2.12**.

The methoxyl group was positioned on the 1,4-disubstituted aromatic ring of the kaempferol moiety on the basis of the HMBC correlations observed from the methoxyl protons δ 3.70 (4'-OCH₃) and the aromatic protons δ 8.06 (H-2'/H-6') to 161.3 ppm (C-4') (**Figure 2.7** and **Table 2.3**). In turn the aromatic protons δ 8.06 (H-2'/H-6') showed a key correlation to 156.1 ppm (C-2), thereby supporting the positioning of the methoxyl on C-4' of the kaempferol moiety as shown in **Figure 2.7**.

On the basis of this data (**Table 2.3**), it was concluded that HPLC peak 3 was kaempferol-4'-methyl ether-3-O- β -D-(6-O-*trans*-*p*-coumaroyl)-glucopyranoside (**2.14**), which was first reported in 2007 by Morales-Escobar *et al.* [125]. However, the ¹H NMR chemical shifts reported by this group [125] for the *meta*-coupled aromatic methines in the methoxyl kaempferol moiety (δ 6.50, H-6 and δ 6.68, H-8) were markedly higher than those typically observed for kaempferol glycosides, namely δ 6.15 and δ 6.35 [149, 150]. In contrast, the ¹H NMR analysis of **2.14** (**Table 2.3**) is consistent with the typical kaempferol glycoside chemical shifts (δ 6.15 and δ 6.35). A closely related compound, 6'-O-(4'''-methoxy-*trans*-cinnamoyl)-kaempferol-3- β -D-glucopyranoside (**2.17**), reported in 2009 by Choudhary *et al.* [151], for which 2D NMR correlations formed the basis of the structure elucidation argument [151] and their positioning of the methoxyl group on the cinnamoyl moiety was based on a HMBC correlation observed from the methoxyl protons at δ 3.89 to a peak assigned to C-4''' at 161.5 ppm as shown in **Figure 2.8** [151]. The position of attachment of the methoxy moiety in this compound is not unequivocal since no further HMBC correlations from the associated aromatic ring to the remaining section of the cinnamoyl moiety were reported [151].

Table 2.3. ^1H (500 MHz) and ^{13}C (125 MHz) NMR spectroscopic data of 4'-methoxy-*trans*-tiliroside (**2.14**) in d_6 -DMSO.

Position	δ_{H}, J	$\delta_{\text{C}}^{\text{a}}$	gCOSY	gHMBC
1	-	-	-	-
2	-	156.1, s	-	-
3	-	133.4, s	-	-
4	-	ND	-	-
5	-	161.1, s	-	-
6	6.15, s	98.7, d	H-8	C-5, C-7, C-8, C-10
7	-	164.7, s	-	-
8	6.38, d	93.6, d	H-6	C-6, C-7, C-9, C-10
9	-	156.4, s	-	-
10	-	103.9, s	-	-
1'	-	122.4, s	-	-
2'	8.06, d, $J = 7.5$ Hz	130.4, d	H-3'	C-2, C-4', C-6'
3'	6.99, d, $J = 8.5$ Hz	113.3, d	H-2'	C-1', C-4', C-5'
4'	-	161.3, s	-	-
5'	6.99, d, $J = 7.5$ Hz	113.3, d	H-6'	C-1', C-3', C-4'
6'	8.06, d, $J = 7.5$ Hz	130.4, d	H-5'	C-2, C-2', C-4'
1''	5.45, d, $J = 8.0$ Hz	101.8, d	H-2''	C-3
2''	3.23 ^b , m	73.8, d	H-1'', 2''-OH	C-1'', C-3''
3''	3.28 ^b , m	75.7, d	3''-OH	C-4'', C-1''
4''	3.25 ^b , m	69.5, d	4''-OH	C-3''
5''	3.37 ^b , m	73.8, d	H-6a''	C-4''
6a''	4.02, dd, $J = 5.0, 11.0$ Hz	62.4, t	H-5'', H-6b''	C-4'', C-5'', C-9''
6b''	4.28, d, $J = 11.5$ Hz		H-6a''	C-4'', C-5'', C-9''
1'''	-	125.0, s	-	-
2'''	7.40, d, $J = 8.0$ Hz	130.0, d	H-3'''	C-3''', C-4''', C-7'''
3'''	6.78, d, $J = 7.5$ Hz	115.5, d	H-2'''	C-1''', C-4''', C-5'''
4'''	-	159.8, s	-	-
5'''	6.78, d, $J = 7.5$ Hz	115.5, d	H-6'''	C-1''', C-3''', C-4'''
6'''	7.40, d, $J = 8.0$ Hz	130.0, d	H-5'''	C-4''', C-5''', C-7'''
7'''	7.35, d, $J = 16.0$ Hz	144.4, d	H-8'''	C-2'''/C-6''', C-8''', C-9'''
8'''	6.17, d, $J = 16.0$ Hz	113.4, d	H-7'''	C-1''', C-9'''
9'''	-	166.2, s	-	-
4 ¹ -OCH ₃	3.70, s	54.9, q		C-4'
5-OH	12.55, bs	-	-	C-5, C-6, C-10
2''-OH	5.46, m	-	H-2''	C-1'', C-2'', C-3''
3''-OH	5.22, m	-	H-3''	C-2'', C-3'', C-4''
4''-OH	5.26, m	-	H-4''	C-3'', C-4'', C-5''

^a Carbon assignments based on gHSQCAD and gHMBC NMR experiments^b Signals overlapped

ND indicates signals were not detected

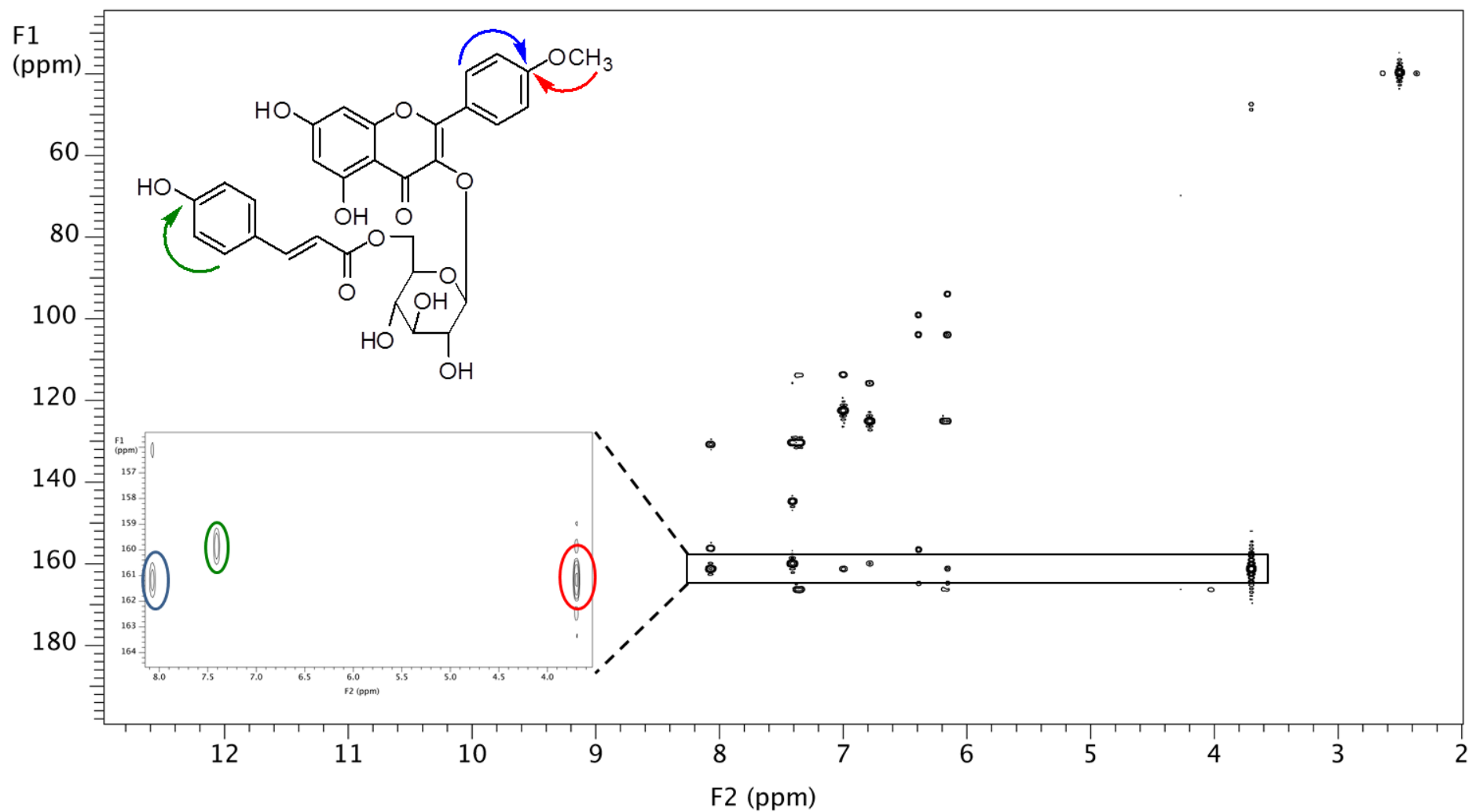


Figure 2.7. 2D gHMBC NMR spectrum of 4'-methoxy-*trans*-tiliroside (**2.14**), showing key correlations.

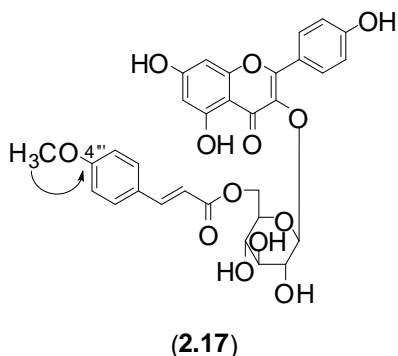


Figure 2.8. HMBC NMR correlation of compound (2.17).

In our study, the original NMR spectra for **2.14** were obtained in d_6 -DMSO. The chemical shifts reported for both **2.14** and **2.17** in the literature [125, 151] were from NMR spectra obtained in CD_3OD . In order to better compare the NMR data, the spectra for **2.14** were re-run in CD_3OD . Comparison of the NMR data obtained for **2.14** in CD_3OD (see Experimental chapter **Section 7.2.2** and **Table 2.4**) with that reported in the literature for compounds **2.14** and **2.17**, indicated that both literature structures had been assigned incorrectly.

The structure of the compound originally reported as 6'-O-(4''-methoxy-*trans*-cinnamoyl)-kaempferol-3-β-D-glucopyranoside (**2.17**), should be revised to kaempferol-4'-methyl ether-3-O-β-D-(6-O-*trans-p*-coumaroyl)-glucopyranoside (**2.14**), on the basis of NMR chemical shift comparisons with the data obtained for **2.14** as shown in **Table 2.4**.

The compound reported in the literature [125] as kaempferol-4'-methyl ether-3-O-β-D-(6-O-*trans-p*-coumaroyl)-glucopyranoside (**2.14**) also requires a structure re-assignment. This structure revision is based on the chemical shifts of the *meta* coupled aromatic protons (δ 6.50 (H-6) and δ 6.68 (H-8)) of the flavonoid moiety [125]. Comparison with literature NMR data [152, 153] for other closely related metabolites (see **Figure 2.9**), shows that these 1H NMR chemical shifts are not consistent with a structure which has two hydroxyl groups at positions 5 and 7 (δ 6.15 (H-6) and δ 6.40 (H-8)). Without access to an authentic sample of the compound incorrectly reported as kaempferol-4'-methyl ether-3-O-β-D-(6-O-*trans-p*-coumaroyl)-glucopyranoside (**2.14**), only a tentative structure re-assignment can be proposed for this compound, which is discussed below [125].

Table 2.4. Chemical shift comparison of **2.14** and literature reports of **2.17** and **2.14** in CD₃OD.

Position	2.14		literature 2.17 [151]		literature 2.14 [125]	
	δ_{H}	δ_{C}	δ_{H}, J	δ_{C}	δ_{H}, J	δ_{C}
1	-	-	-	-	-	-
2	-	158.5, s	-	159.2, s	-	159.3, s
3	-	ND	-	135.1, s	-	136.0, s
4	-	ND	-	179.5, s	-	179.8, s
5	-	ND	-	158.5, s	-	163.5, s
6	6.16, d	99.7, d	6.11, d, $J = 1.8$ Hz	100.3, d	6.50, d, $J = 2.0$ Hz	99.4, d
7	-	165.6, s	-	162.9, s	-	165.8, s
8	6.35, d	94.6, d	6.29, d, $J = 1.8$ Hz	95.0, d	6.68, d, $J = 2.0$ Hz	95.0, d
9	-	157.9, s	-	159.0, s	-	158.9, s
10	-	ND	-	105.2, s	-	106.0, s
1'	-	123.4, s	-	122.4, s	-	122.0, s
2'	8.08, d	131.7, d	7.99, d, $J = 8.6$ Hz	132.1, d	7.95, d, $J = 8.0$ Hz	129.6, d
3'	6.93, d	114.3, d	6.80, d, $J = 8.4$ Hz	116.8, d	7.08, d, $J = 8.0$ Hz	115.7, d
4'	-	162.6, s	-	161.2, s	-	159.0, s
5'	6.93, d	114.3, d	6.80, d, $J = 8.4$ Hz	116.8, d	7.08, d, $J = 8.0$ Hz	115.7, d
6'	8.08, d	131.7, d	7.99, d, $J = 8.6$ Hz	132.1, d	7.95, d, $J = 8.0$ Hz	129.6, d
1''	5.26, d	103.8, d	5.22, d, $J = 7.1$ Hz	104.0, d	5.27, d, $J = 7.8$ Hz	103.5, d
2''	3.46 ^b , m	75.4, d	3.43, dd, d, $J = 9.1,$ 7.5 Hz	75.8, d	3.54, dd, d, $J = 9.5,$ 7.8 Hz	74.0, d
3''	3.44 ^b , m	77.5, d	3.47, d, $J = 7.8$ Hz	77.7, d	3.50, t, $J = 9.5$ Hz	77.8, d
4''	3.38 ^b , m	71.2, d	3.38, t, $J = 9.0$ Hz	71.7, d	3.39, t, $J = 9.5$ Hz	71.6, d
5''	3.41 ^b , m	75.4, d	3.49, m	78.0, d	3.60, m	75.4, d
6a''	4.19, m	63.7, t	4.17, dd, $J = 13.0,$ 3.8 Hz	64.2, t	4.34, dd, $J = 12.0, 4.5$ Hz	64.5, t
6b''	4.30, d		4.27, dd, $J = 12.5,$ 4.4 Hz	-	4.24, dd, $J = 12.0, 3.0$ Hz	-
1'''	-	126.4, s	-	127.0, s	-	125.0, s
2'''	7.35, d	130.9, d	7.32, d, $J = 8.4$ Hz	131.2, d	7.95, d, $J = 8.0$ Hz	129.7, d
3'''	6.82, d	116.5, d	6.78, d, $J = 8.4$ Hz	116.0, d	6.83, d, $J = 8.0$ Hz	116.2, d
4'''	-	160.6, s	-	161.5, s	-	159.5, s
5'''	6.82, d	116.5, d	6.78, d, $J = 8.4$ Hz	116.0, d	6.83, d, $J = 8.0$ Hz	116.2, d
6'''	7.35, d	130.9, d	7.32, d, $J = 8.4$ Hz	131.2, d	7.95, d, $J = 8.0$ Hz	129.7, d
7'''	7.42, d	146.1, d	6.08, t, $J = 16.0$ Hz	146.5, d	7.65, d, $J = 16.0$ Hz	146.0, d
8'''	6.10, d	114.5, d	7.40, d, $J = 15.8$ Hz	114.3, d	6.42, d, $J = 16.0$ Hz	116.1, d
9'''	-	166.3, s	-	168.7, s	-	168.3, s
4'-OCH ₃	3.72, s	55.5, q			3.90, s	58.5, q
4'''-OCH ₃			3.89, s	56.0, q		

a Carbon assignments based on correlations from gHSQCAD and gHMBC NMR spectra

b Sugar moiety proton signals assigned from gHSQCAD NMR spectrum

ND – Not detected in gHMBC NMR experiment

A ^1H NMR comparison of multiple compounds (**2.18-2.22**) from the literature [150, 152] indicated that for the *meta* coupled protons, a hydroxyl or methoxyl substitution at the C-4' or C-3 positions only has a small effect on the chemical shifts of the *meta* coupled aromatic protons as shown in **Figure 2.9**, whereas substitution (methyl-prop-1-enoxyl or methoxyl) at the C-7 position has a significant effect on these protons as shown in **Figure 2.9** [150, 152]. The reported HMBC correlations for the compound reported by Morales-Escobar *et al.* [125], and assigned the structure (**2.14**) showed a correlation from the anomeric proton of the sugar moiety to a quaternary carbon at 133.6 ppm. This correlation immediately eliminated the possibility of the glycoside being substituted at position C-7 (see below).

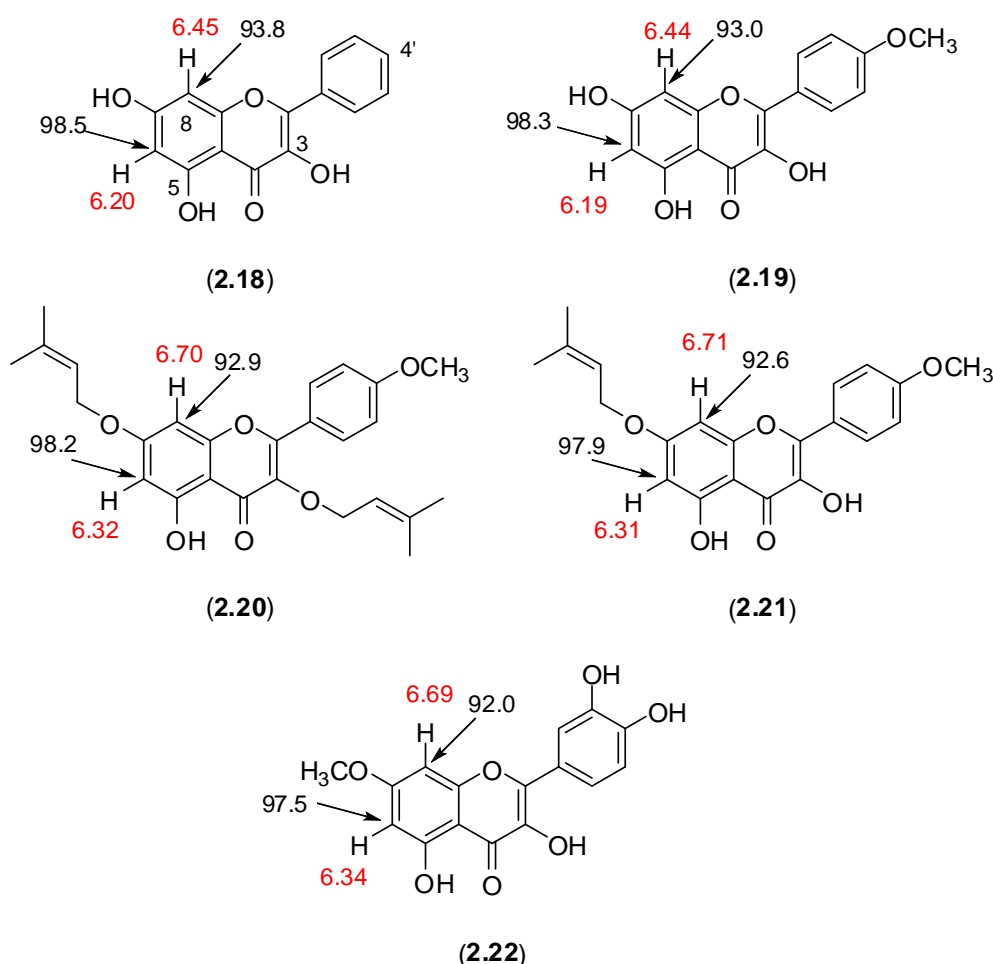


Figure 2.9. Comparison of NMR data for structurally related flavonoids.

As shown in **Figure 2.10**, the chemical shift reported for compound (**2.23**) [154] indicate that a sugar-substituted C-7 quaternary signal would appear near 163 ppm, which is quite different to that of the 133.6 ppm observed for compounds with the sugar moiety attached to C-3 of the kaempferol moiety. The chemical shifts of the methylene protons of the sugar moiety (δ 4.34, δ 4.24) were typical of those of a sugar esterified at C-6" (see compound **2.24** in **Figure 2.10**) and were much higher than those of a terminal sugar moiety (see compound **2.25** in **Figure 2.10**) [155]. This, together with the reported HMBC correlations from the sugar methylene protons to the ester carbon at 168.3 ppm, confirmed that the *p*-coumaroyl moiety was indeed attached at C-6" of the sugar as depicted in compounds (**2.12-2.14**) and compound (**2.24**) (**Figure 2.10**) [153]. Thus, the compound reported by Morales-Escobar *et al.* [125] has the same sugar linkages as **2.14**. Consequently, only a few possibilities remain which could explain the significant differences observed for the *meta* coupled aromatic protons.

One possibility considered was that of a 6,8-dihydroxy-substituted flavonoid instead of a 5,7-dihydroxy-substituted flavonoid. However, neither the ^1H nor the ^{13}C NMR chemical shifts associated with the *meta* coupled aromatic protons (δ 6.50, H-8; δ 6.68, H-6 and 99.4 ppm, C-6; 95.0 ppm C-8) [125] were in accordance with the literature [156] NMR data reported for 6,8-dihydroxy-substituted flavonoids such as compound (**2.27**) (**Figure 2.10**) [156]. In 6,8-dihydroxy flavonoid **2.27**, the aromatic methines in question appear at δ 6.90 (H-5)/104.7 ppm (C-5) and δ 6.81 (H-7)/114.7 ppm (C-7). These large differences in both the ^1H and ^{13}C NMR chemical shifts rule out a 6,8-dihydroxy flavonoid moiety in any revised structure being proposed.

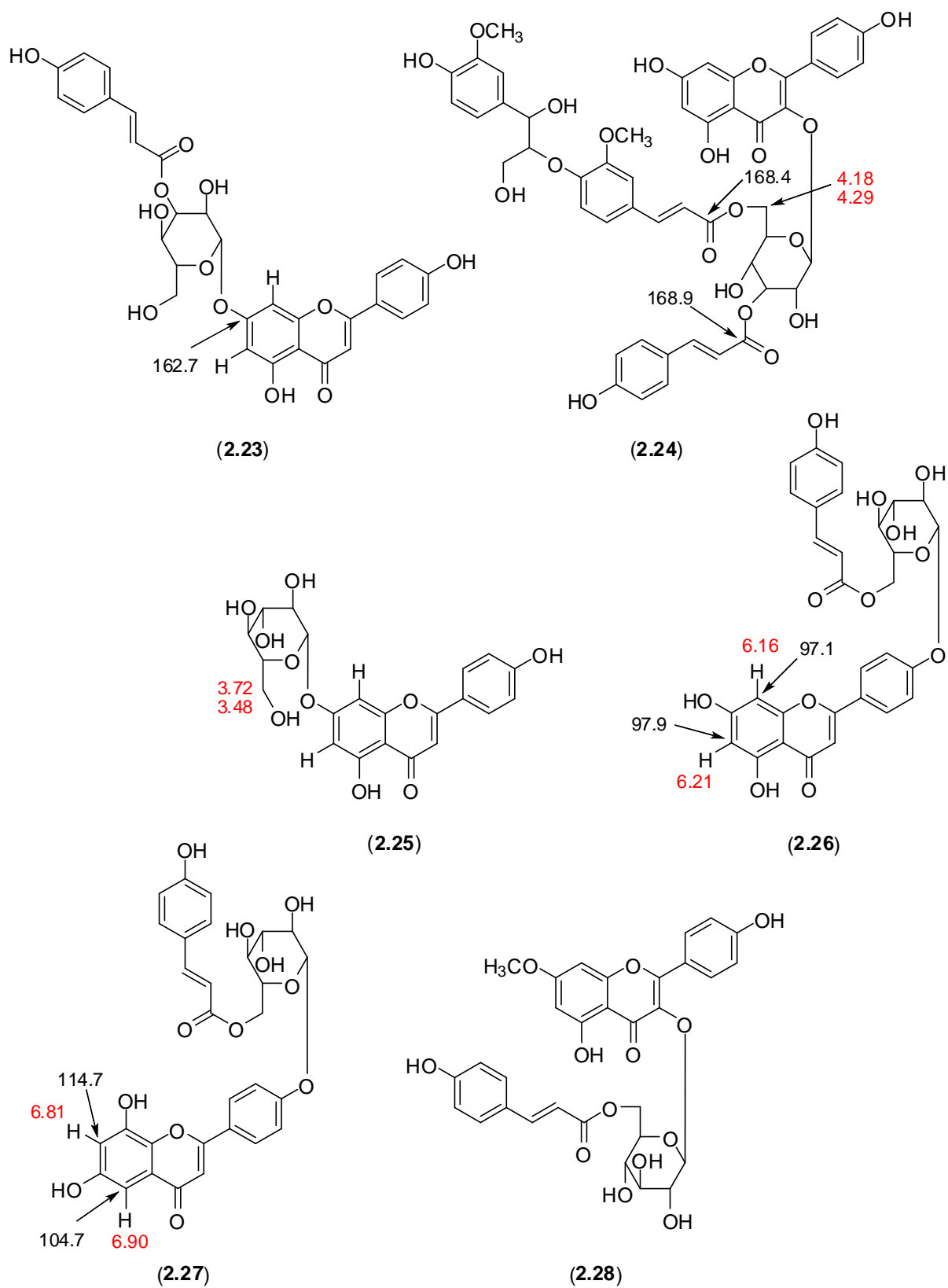


Figure 2.10. Comparison of NMR data for structurally related flavonoids.

After consideration of the NMR data of closely related flavonoids [157], it was concluded that the most likely structure of the compound originally reported as **2.14** by Morales-Escobar *et al.* [125] is kaempferol-7-methyl ether-3-O- β -D-(6-O-*trans-p*-coumaroyl)-glucopyranoside (**2.28**) [157] (**Figure 2.10**). This structure satisfactorily explains the differences observed in chemical shifts for the *meta* coupled aromatic protons on the kaempferol moiety and also supports all the reported HMBC correlations [125]. This proposed structure revision corresponds to a known compound. However a direct NMR comparison was hampered by the use of CD₃OD as the NMR solvent for the compound reported as **2.14** by Morales-Escobar *et al.* [125] and *d*₆-DMSO for **2.28** [157]. For an unequivocal revision to the structure of the compound reported as **2.14**, a complete HMBC re-assessment of an authentic sample would be required.

The HR-ESI-MS of HPLC peak 4 displayed an *m/z* at 607.1461 [M-H]⁻ (calcd. for C₃₁H₂₇O₁₃: *m/z* 607.1452) consistent with a molecular formula C₃₁H₂₈O₁₃ and eighteen degrees of unsaturation. The ¹H NMR and gHSQCAD spectrum (**Figure 2.11**) spectra of peak 4 were very similar to that of **2.13**, with the only noticeable difference being the presence of a new methoxyl resonance (δ 3.77, s, 3H). Like that of *cis*-tiliroside (**2.13**), the ¹H NMR spectrum of peak 4 also indicates the presence of a *cis-p*-coumaroyl moiety [δ 6.67, (H-7'') and δ 5.49, d, *J* = 13.5 Hz (H-8'')]. The coupling constant for the proton at δ 6.67 could not be measured accurately as it was overlapped with the H-3''/H-5'' aromatic protons. The location of the methoxyl moiety was again established on the basis of key HMBC correlations observed from the methoxyl protons at δ 3.77 (4'-OCH₃) and the aromatic methines δ 8.03 (H-2'/H-6') to the carbon at 161.2 ppm (C-4'). The additional HMBC correlation from the aromatic methines δ 8.03 (H-2'/H-6') to the C-2 carbon at 156.0 ppm allowed the methoxyl to be positioned, once again, on the kaempferol moiety. As such, compound **2.15** was identified to be kaempferol-4'-methyl ether-3-O- β -D-(6-O-*cis-p*-coumaroyl)-glucopyranoside. To the best of our knowledge, this represents a new flavonoid glycoside derivative.

A feature that was noted for both the purified *trans*-tiliroside (**2.12**) and *cis*-tiliroside (**2.13**) was that both converted to an equilibrium mixture of the two compounds. This mixture was reminiscent of the initial ratio of the two compounds that occurred in the crude extract (approximately 4:1 *trans*-tiliroside to *cis*-tiliroside). The conversion was much more rapid in CD₃OD than in *d*₆-DMSO and *cis*-tiliroside (3 days) converted to a mixture much more rapidly than *trans*-tiliroside (>3 weeks in CD₃OD). A study was undertaken to determine the stability of *trans*-tiliroside (**2.12**) at different temperatures and various solvents. The conversion was monitored using analytical HPLC, with the most rapid conversion occurring in the presence of methanol at room temperature, where a sample of pure *trans*-tiliroside (**2.12**) converted to a mixture of both isomers. The presence of *cis*-tiliroside (**2.13**) could be detected in this conversion after about 3 weeks. Pure samples of *trans*-tiliroside (**2.12**) in methanol and in ethanol were subjected to UV light (254 nm and 365 nm) for 24 hours at each wavelength, resulting in the ratio of *trans*-tiliroside (**2.12**) to *cis*-tiliroside (**2.13**) isomers increasing from approximately 4:1 to almost 1:1 in both solvents as shown by the analytical HPLC chromatogram of the mixture of *trans*-tilirosde (**2.12**) and *cis*-tiliroside (**2.13**) in **Figure 2.12**. Due to this conversion, particularly in CD₃OD, the optimal NMR solvent for this class of compounds is *d*₆-DMSO as the conversion is substantially slower in this solvent. It is worth noting that most of the literature NMR data for this class of compounds has been reported in CD₃OD.

In order to determine if the methoxy tiliroside derivatives **2.14** and **2.15** were natural products or artefacts of the isolation procedure, two separate small scale (5 g) extractions were conducted in MeOH and EtOH. Both afforded compounds **2.14** and **2.15** in a similar ratio to that detected initially in the crude extract obtained using 3:1 MeOH:DCM, while no ethoxy derivatives were observed in either extraction. This demonstrated that compounds **2.14** and **2.15** are natural products and not artefacts of the isolation procedure.

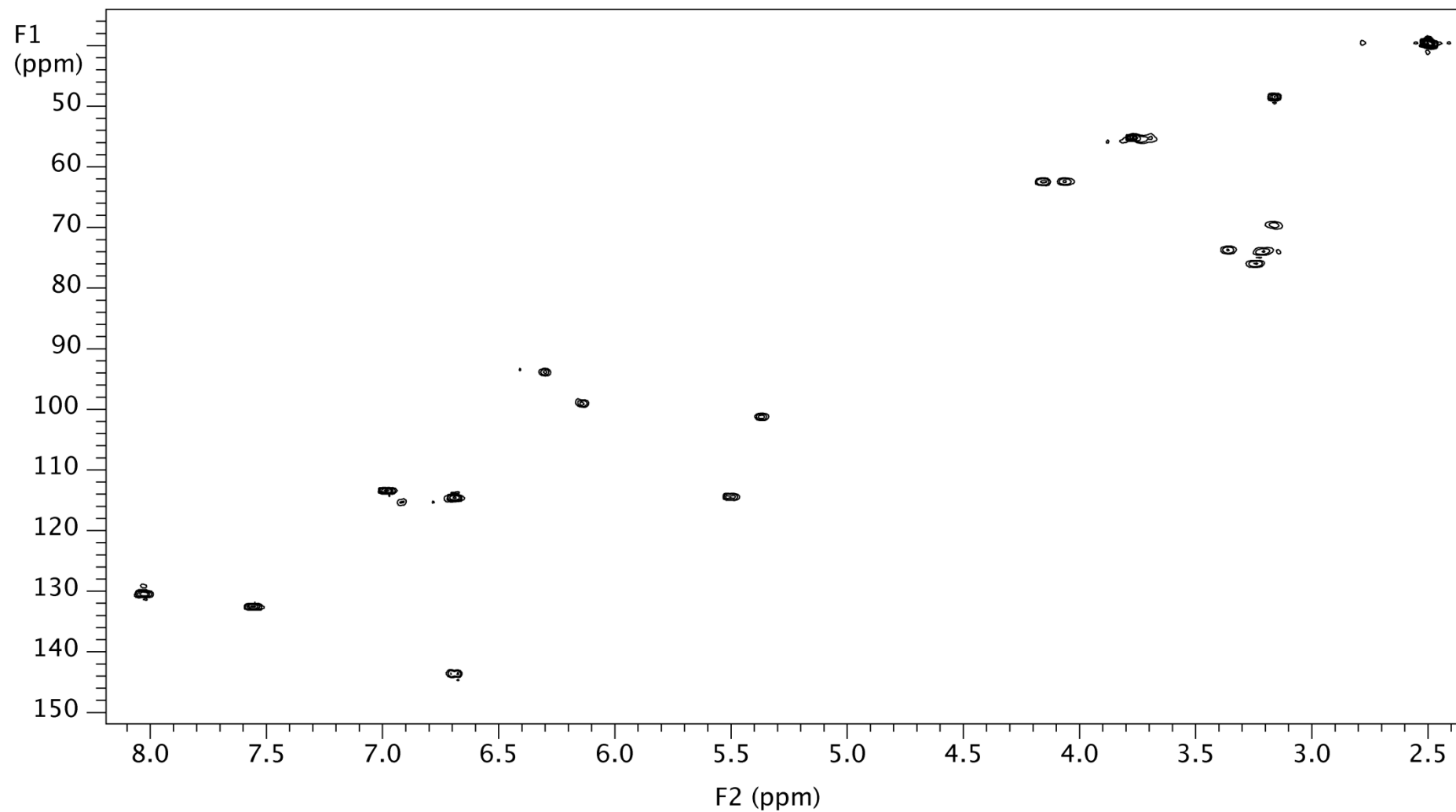


Figure 2.11. 2D gHSQCAD NMR spectrum of kaempferol-4'-methyl ether-3-O- β -D-(6-O-cis-p-coumaroyl)-glucopyranoside (**2.15**).

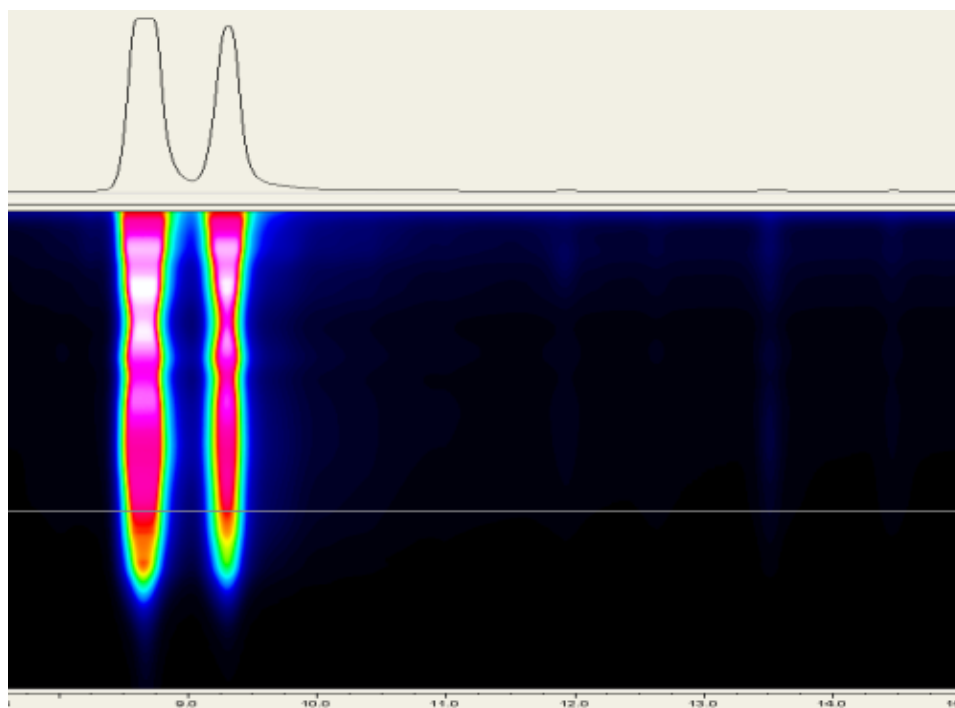


Figure 2.12. Analytical HPLC chromatogram of the UV exposed mixture of **2.12** and **2.13**.

Flavonoids and flavonoid glycosides are a class of secondary metabolites recognised for their important biological activities (Introduction **Section 1.2**) [18, 118, 158]. *Trans*-tiliroside (**2.12**) has been reported to display anti-oxidative properties [159], inhibits cAMP phosphodiesterase [143], exhibits anti-complement, anti-inflammatory and free radical scavenging activities, potent activity towards d-GalN-induced cytotoxicity in hepatocytes, displays cytotoxicity against specific leukaemia cell lines, and also exhibits moderate anti-bacterial activity [132, 147]. It has also been observed that *trans*-tiliroside (**2.12**) can modulate the activity of known anti-bacterial agents, with a reduction of minimum inhibitory concentration (MIC) of at least two fold when *trans*-tiliroside (**2.12**) was incorporated into the growth medium at 32 µg/mL [147]. Mixtures of *trans*-tiliroside (**2.12**) and *cis*-tiliroside (**2.13**) show significant toxicity towards brine shrimp, as well as displaying potent inhibition towards CYP3A4 [142]. The anti-bacterial activity displayed by a mixture of the two compounds has been suggested to be due to the *cis* isomer. In a separate study it was demonstrated that compounds containing the *cis*-coumaroyl moiety are more active than those with the corresponding *trans*-coumaroyl moiety [153, 159]. The crude extract of *L. macrophyllum*

displayed modest cytotoxicity. Owing to the observed tendency of the isolated flavonoid glycosides to form equilibrium mixtures, no cytotoxicity testing was conducted on the isolated secondary metabolites.

2.4 Concluding Remarks

This study demonstrated that on-line and off-line chemical profiling techniques are complementary. The on-line profiling by HPLC-NMR was used to tentatively identify the two major components of the methanol extract of *L. macrophyllum*, as well as one of the minor, related, components. On-line HPLC-NMR provided a chemical profile of the crude methanol extract of the Australian plant *L. macrophyllum*, resulting in the tentative identification of *trans*-tiliroside (**2.12**), *cis*-tiliroside (**2.13**) and 4'-methoxy-*trans*-tiliroside (**2.14**). Subsequent off-line purification permitted the complete structural elucidation of the four flavonoid glycosides (**2.12-2.15**). Compound **2.15** was established to be a new flavonoid glycoside structural derivative. This represents the first report of the isolation of flavonoid glycosides from the genus *Lasiopetalum*. The off-line purification of these compounds was particularly important since the NMR assignment of **2.14**, as reported in the literature, was found to be inconclusive in terms of the position of attachment for the methoxy moiety. Upon detailed examination of the literature NMR data and that obtained for **2.14**, it was concluded that the structures of the two literature compounds reported as kaempferol-4'-methyl ether-3-O- β -D-(6-O-*trans*-*p*-coumaroyl)-glucopyranoside and 6'-O-(4''-methoxy-*trans*-cinnamoyl)-kaempferol-3- β -D-glucopyranoside should be revised. A series of stability studies undertaken concluded that compounds **2.14** and **2.15** interconverted but were not artefacts of the extraction procedure with methanol. The use of HPLC-NMR was found to be particularly suited to the analysis of unstable compounds that convert to equilibrium mixtures, such as those investigated in this study.

Chapter 3

*Phenylphenalenones and Oxabenzochrysenones from the Australian plant *Haemodorum simulans**

3.1 Introduction

Phenylphenalenones (**Figure 3.1**) are secondary metabolites of phenylpropanoid origin which have been found exclusively in the plant families Haemodoraceae, Musaceae, Pontederiaceae and Strelitziaceae [160]. The family Haemodoraceae is predominantly found in the southern hemisphere, with genera such as *Haemodorum* being endemic to Australia and Papua New Guinea [161]. Tetraoxygenated phenylphenalenones and related compounds modified by the formation of an ether bridge between ring A and ring D result in the formation of oxabenzochrysenone (naphthoxanthenones) type structures (**Figure 3.1**). The oxabenzochrysenone structure class of secondary metabolites has also been shown to occur almost exclusively in the family Haemodoraceae [160, 162-167]. The occurrence of the phenylphenalenones and oxabenzochrysenones in families of plants such as Musaceae and Haemodoraceae illustrates their close structural relationship and their importance in being potential chemotaxonomic markers for these families of plants [164, 168].

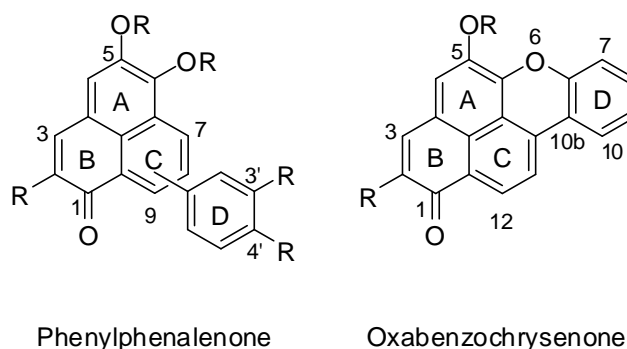
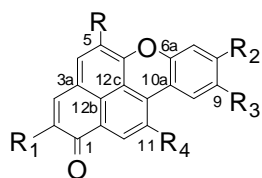
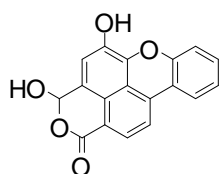


Figure 3.1. General structures and numbering of phenylphenalenones and oxabenzochrysenones.

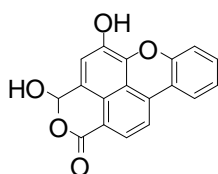
The number of oxabenzochrysenones (**3.1-3.11**) isolated is far fewer than that of the phenylphenalenones (including phenylbenzoisochromenones) (**3.12-3.19**) with the additional fused ring in the former structure class limiting the sites for substitution [162]. The main differences for phenylphenalenones and related compounds are the positioning of the aryl substituent, and degree of oxygenation and functionality, while anhydrides and esters in the B ring also occur. Typically, in the most common phenylphenalenones that have been isolated, the aryl ring is attached to position 7 (**3.15-3.19**) or position 9 (**3.12**) within the D ring, however aryl attachment at position 4 (**3.13-3.14, 3.20-3.21**) and position 8 (**3.22**) have also been identified, along with diphenylphenalenones (**3.23-3.24**).



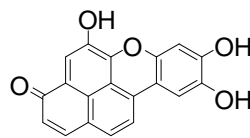
	R	R ₁	R ₂	R ₃	R ₄
3.1	OH	H	H	H	H
3.2	OCH ₃	H	H	H	H
3.3	OH	H	H	H	H
3.4	OH	OCH ₃	H	H	H
3.5	OH	H	H	H	OH
3.6	H	H	OCH ₃	H	H
3.7	OH	H	OH	OH	H
3.8	OCH ₃	H	OCH ₃	OCH ₃	H



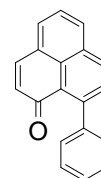
(3.9)



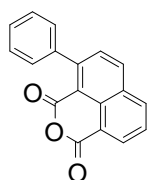
(3.10)



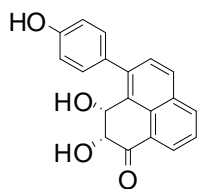
(3.11)



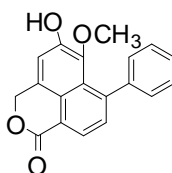
(3.12)



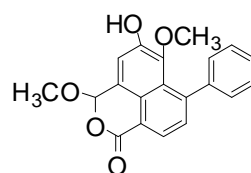
(3.13)



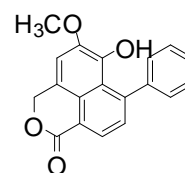
(3.14)



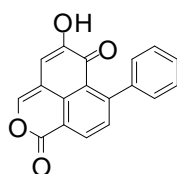
(3.15)



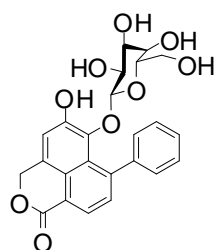
(3.16)



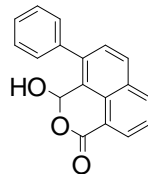
(3.17)



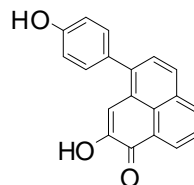
(3.18)



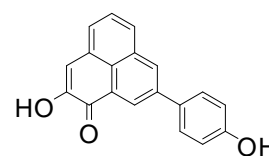
(3.19)



(3.20)



(3.21)

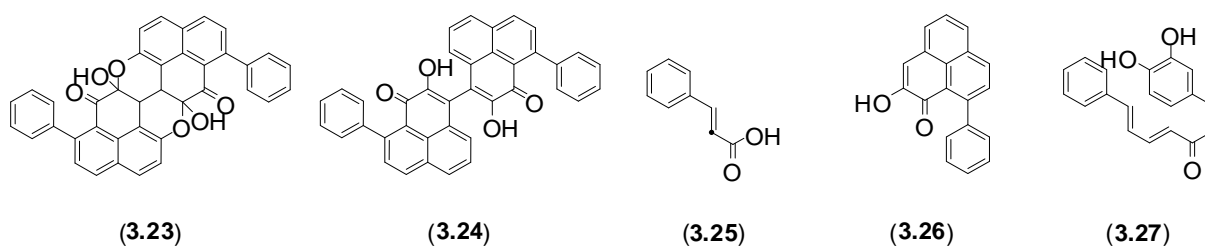


(3.22)

3.1.1 Biosynthesis of phenylphenalenones

The biosynthetic pathway for the formation of phenylphenalenones was first reported as incorporating phenylalanine and tyrosine from the shikimate pathway [169]. This was different to that of the fungal phenalenones which were formed by the acetate-polymalonate pathway [169, 170]. The incorporation of carbon labelled phenylalanine was used to show that the polymalonate pathway was involved in the biosynthesis of phenylphenalenones, with up to 3.8% incorporation of labelled phenylalanine detected [171, 172]. The intermediates involved in the biosynthesis of phenylphenalenones were not discovered until Hölischer and Schneider provided experimental evidence for a diarylheptanoid intermediate [173]. They observed that twenty-four hours after addition of [2-¹³C] cinnamic acid (**3.25**) in root cultures of *Anigozanthos preisii* (Haemodoraceae), isolated anigorufone (**3.26**) showed the presence

of enhanced ^{13}C NMR signals at C-5 and C-8, thereby providing direct evidence of the biosynthetic pathway derived of the phenylalanine pathway [173]. This evidence also supported that the biosynthesis occurs via the diarylheptanoid pathway (**Scheme 3.1**), which was further proved by the addition of $[2-^{13}\text{C}]$ 1-phenyl-7-(3,4-diacetoxyphenyl)hepta-1,3-dien-5-one (**3.27**) to cultured roots of *A. preisii*. When anigorufone (**3.26**) was then isolated enhancements in the ^{13}C NMR signal at C-8 were observed, providing evidence of the diarylheptanoid intermediate [173]. The speed at which incorporation of the labelled precursors was found to occur (within twenty-four hours), would explain why no diarylheptanoid compounds have been isolated from organisms containing phenylphenalenones, as this rapid cyclisation occurs so readily [173].



The origin of the carbon at C-6a in the phenylphenalenone structure class, which corresponds to C4 in the diarylheptanoid intermediate (see **Figure 3.2**), was thought to have come from the incorporation of C-2 from an acetate molecule (**Figure 3.2**), as this carbon could not have come from the *p*-coumaric acid (**Figure 3.2**) molecules in the phenylphenalenone biosynthesis [174]. Multiple experiments using labelled $[^{13}\text{C}_3]$ methionine, $[2-^{13}\text{C}]$ acetate and $[2-^{13}\text{C}]$ malonate allowed for the determination of the origin of the C-6a of the phenylphenalenone nucleus [174]. The incorporation of $[2-^{13}\text{C}]$ acetate into multiple phenylphenalenones showed that acetate is involved in the biosynthesis of phenylphenalenones (**Scheme 3.1**) [174].

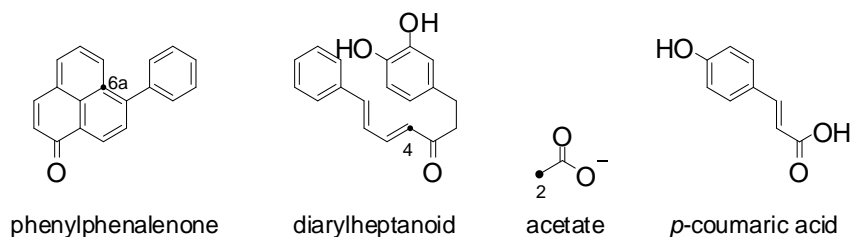


Figure 3.2. Positions corresponding to the acetate incorporation in the biosynthesis of phenylphenalenones.

This led to further studies into the biosynthesis of the phenylphenalenones as there was still uncertainty arising from the incorporation of the saturated phenylpropanoic moiety by either dihydrocinnamic acid or from cinnamic acid (**Figure 3.3**) followed by a post condensation hydrogenation with a second cinnamate moiety [175]. *In vivo* feeding experiments of cultures of *A. preisii* resulted in the identification of reversible interconversions of phenylpropanoids into dihydrophenylpropanoids (**Figure 3.3**), which have roles in the biosynthesis of the phenylphenalenones [175]. The reversible interconversions of the phenyl- and dihydrophenyl- propanoids could lead to the variable ratio of different phenylphenalenones produced [175].

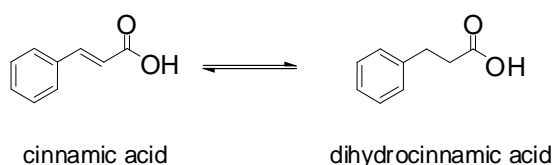
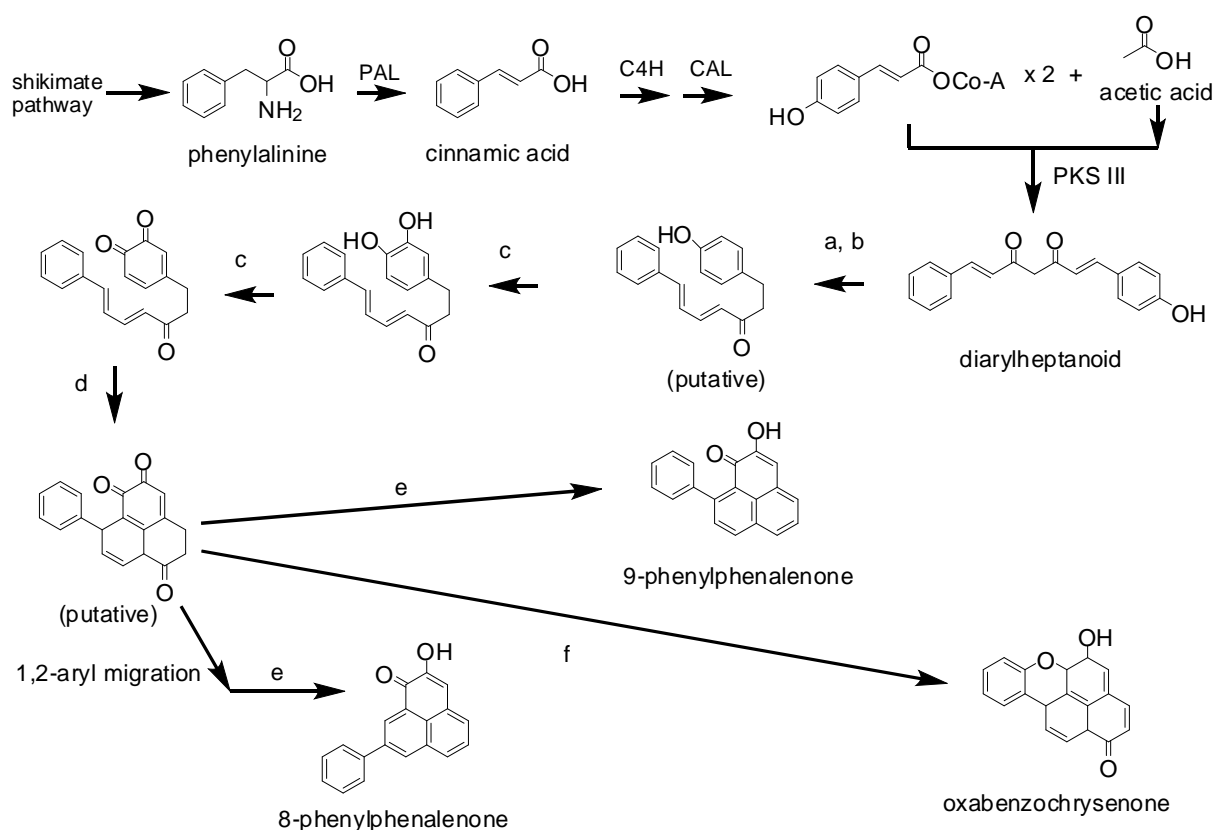


Figure 3.3. Example of the interconversion of a phenylpropanoid into a dihydrophenylpropanoid.

However, the phenylphenalenone biosynthetic pathway would not result in the formation of related phenylphenalenone-type structures such as the phenylbenzochromenone (**3.16**). The formation of these phenylbenzochromenones was suggested to occur via an oxidative step in the phenylphenalenone biosynthetic pathway, or via a Diels-Alder cycloaddition of an

ester intermediate [176]. The use of ^{13}C labelled phenylalanine determined that like that of phenylphenalenones, phenylbenzochromenones were formed through a late branching of the diarylheptanoid pathway [176]. 8-Phenylphenalenones (**3.22**) follow the same biosynthetic pathway, with a diarylheptanoid intermediate, however it was hypothesised that after an intramolecular cycloaddition, a 1,2-aryl migration occurs (**Scheme 3.1**) [177]. Further oxygenation of phenylphenalenones originates from the hydroxyl group of the 4-coumaroyl moiety and is incorporated at the stage of the linear diarylheptanoid, while hydroxyl groups at C-2 are introduced later during the phenylphenalenone biosynthesis [178].

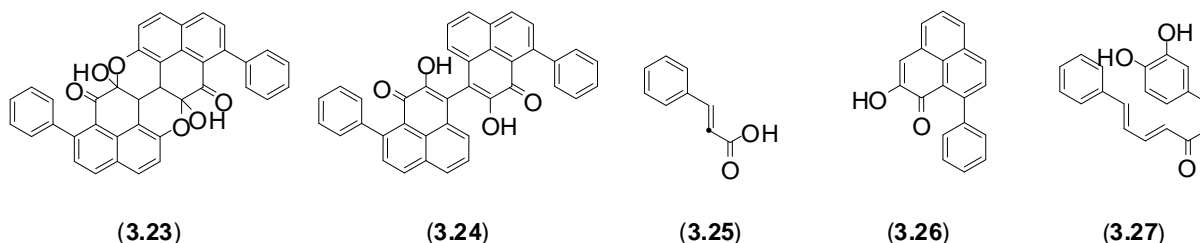


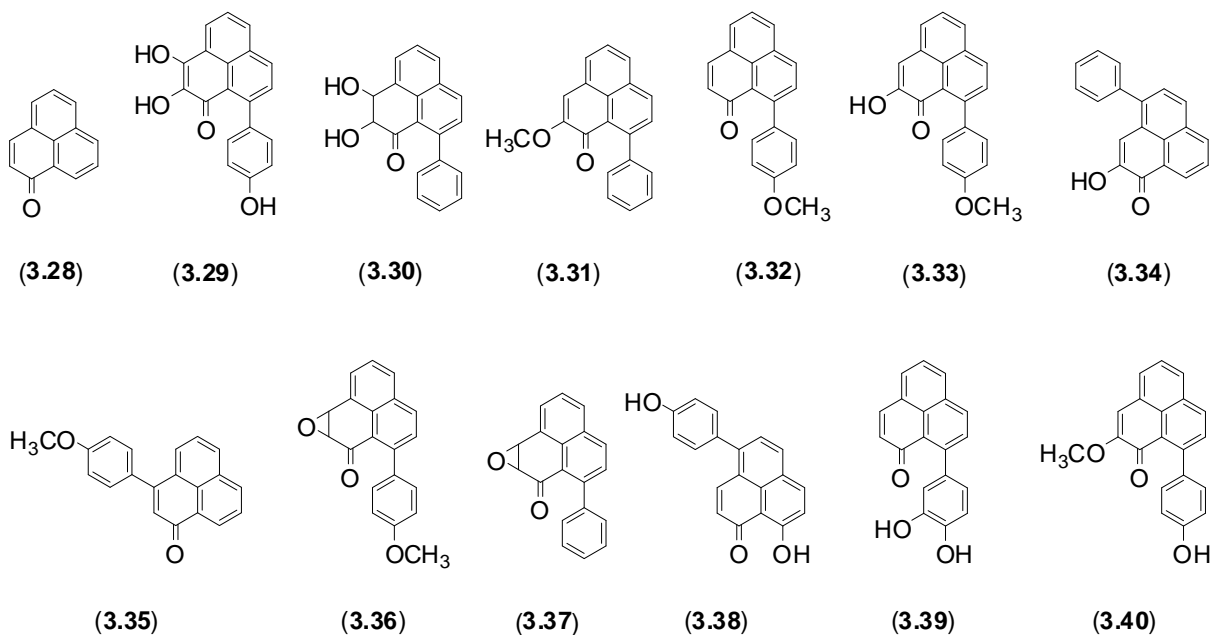
4CL - 4-coumarate CoA ligase; C4H - cinnamate 4-hydroxylase; PAL - phenylalanine ammonia lyase; PKS III – polyketide synthase type III; a) putative reductase (possibly chalcone reductase); b) putative dehydrogenation; c) putative CYP or phenol oxidase; d) putative cyclase (possibly diels-alderase); e) reduction and dehydrogenation; f) putative oxidative phenol coupling.

Scheme 3.1. The biosynthetic pathway for phenylphenalenones (sourced from Schmitt and Schneider [175], Hölscher and Schneider [177], Munde and Maddula *et al* [178], Schmitt and Hölscher *et al* [179] and Brand and Hölscher *et al* [180])

3.1.2 Biological activity of phenylphenalenones

The biological activity of phenylphenalenones has not been thoroughly studied. The activity of phenylphenalenones such as **3.28** and derivatives has been studied more thoroughly, with anti-oxidant activity [181], anti-protozoal activity [182], inhibition of eukaryotic DNA polymerases [183] and inhibition of HIV-1 integrase [184] reported. The first reports of biological activity of phenylphenalenones (**3.26**, **3.29-3.35**), isolated from *Musa acuminata* or derivatives of phenylphenalenones isolated, included growth inhibition of the germination tubes of the fungus *Fusarium oxysporum* f. sp. *cubense* race 4, which is the fungus that causes Panama disease, with increased activity under light exposure [185-188]. Further anti-fungal activity of phenylphenalenones isolated from *Musa* species and synthetic structural derivatives was reported against *Mycosphaerella fijiensis*, with 1H-phenalen-1-one (**3.28**) displaying potent activity, while anigorufone (**3.26**) was the most active natural phenylphenalenone [189, 190]. The anti-parasitic activity of the phenylphenalenones (**3.26**, **3.31-3.37**) was evaluated against *Leishmania donovani* promastigotes and *L. infantum* amastigotes, with **3.26** and **3.31** being the most active against *L. donovani* promastigotes (IC_{50} 12.0 $\mu\text{g/mL}$ and 10.3 $\mu\text{g/mL}$ respectively) while **3.26**, **3.31**, **3.36** and **3.37** possessed activity against *L. infantum* amastigotes (IC_{50} 13.3 $\mu\text{g/mL}$, 10.5 $\mu\text{g/mL}$, 15.6 $\mu\text{g/mL}$ and 17.2 $\mu\text{g/mL}$ respectively) [191]. The plant *M. basjoo* was found to contain phenylphenalenones that exhibit anti-oxidant (**3.21**) and α -glucosidase inhibitory (**3.38-3.39**) activity [192]. Anti-bacterial activity of compound **3.40** was reported against *Bacillus cereus* [193].





In the current study crude extracts originating from two collections of the Australian plant *H. simulans* were selected for chemical investigation on the basis of the presence of minor phenylphenalenone constituents detected from an initial study of this plant species together with the biological activity observed for the crude extracts of the plant [194].

3.2 Experimental

3.2.1 General Experimental

For detailed information on the general experimental procedures and spectroscopic techniques please see the Experimental chapter **Section 7.1**. Both on-flow and stop-flow HPLC-NMR analyses of the 100% hexane silica column fraction were performed using 70% CH₃CN:D₂O, while the HPLC-NMR analyses of the combined 20:80 hexane:DCM and 100% DCM silica column fractions were conducted using 50% CH₃CN:D₂O. Both HPLC-NMR analyses were carried out with detection at λ_{\max} 254 and 290 nm. Semi-preparative reversed phase HPLC was conducted using the methods described in **Section 3.2.3.2**.

3.2.2 Plant material

The plant specimens were collected by Mr. Allan Tinker from the Western Flora Caravan Park, 22 km north of Eneabba (Irwin botanical province), Western Australia (plant license SW008335). The first collection (aerial parts and bulbs) was conducted on the 20th of January 2005 and initially identified as *H. simplex*. This taxonomic classification was subsequently revised to *H. simulans*. A second collection of the bulbs of this plant was conducted on the 20th of February 2007. Voucher specimens designated the codes 2005-01a (bulbs), 2005-01b (aerial parts) and 2007-01 (bulbs) respectively are deposited at the School of Applied Sciences (Discipline of Applied Chemistry), RMIT University.



H. simulans (Voucher code: 2005-01)
(only aerial parts shown)

Kingdom:	Plantae
Phylum:	Magnoliophyta
Class:	Liliopsida
Order:	Commelinidae
Family:	Haemodoraceae
Genus:	<i>Haemodorum</i>
Species:	<i>simulans</i>



H. simulans

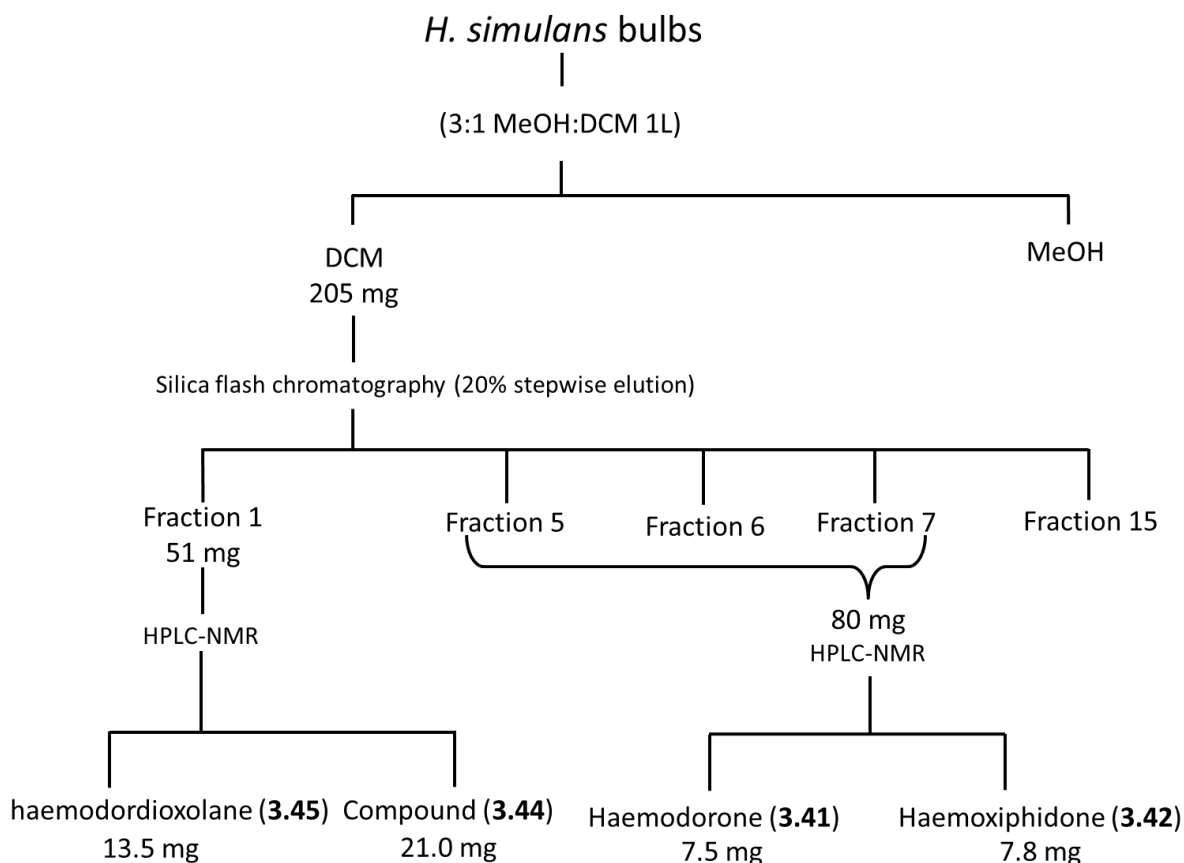
(Voucher code: 2007-01)

A 2 g portion of the initial collection of the *H. simulans* specimen (aerial parts and bulbs) was extracted separately with 3:1 MeOH:DCM (40 mL) and evaluated in several assays (anti-tumour, anti-viral and anti-microbial) at a concentration of 50 mg/mL at the University of Canterbury, Christchurch, New Zealand. The crude extract of the aerial parts displayed moderate cytotoxicity towards P388 with an IC_{50} of 105 $\mu\text{g/mL}$, while the bulbs displayed potent cytotoxicity with an IC_{50} of $<4.9 \mu\text{g/mL}$. Both the aerial parts and the bulbs displayed cytotoxicity towards the BSC-1 cells, and thus it could not be concluded if *Herpes simplex* or *Polio* virus were inhibited (details in the Experimental chapter **Section 7.1.4**). Similar levels of anti-microbial activity were observed between the aerial parts and the bulbs of the plant. Moderate anti-fungal activity towards *Trichophyton mentagrophytes* was observed for both components, with the bulbs being more active of the two, with a zone of inhibition of 5 mm, while a zone of inhibition of 1 mm was observed for the aerial parts. It was also determined that both the aerial parts and bulbs displayed a zone of inhibition of 3 mm against *Bacillus subtilis*. For both extracts it was found that there was no activity towards *Escherichia coli*, *Pseudomonas aeruginosa*, *Candida albicans* or *Cladosporium resinae*.

3.2.3 Extraction and Isolation

3.2.3.1 Preparation of the extract of *H. simulans* for on-flow and stop-flow HPLC-NMR analysis

The first collection of the *H. simulans* bulbs 2005-01a (22 g) was extracted with 3:1 MeOH:DCM (400 mL). This extract was decanted and concentrated under reduced pressure and then subjected to sequential partitioning (trituated) into DCM (97.7 mg) and MeOH (2.24 g) soluble extracts respectively. These bulbs were then re-extracted with a 1:1 mixture of MeOH:DCM (400 mL) and then combined with the initial extract. The second collection of the *H. simulans* bulbs, 2007-01 (36 g) was extracted with 3:1 MeOH:DCM (400 mL). Analysis of the subsequent DCM and MeOH extracts generated from this second collection of the bulbs, indicated that both fractions displayed very similar analytical HPLC chromatograms and ¹H NMR spectra to those obtained from the first collection of the bulbs. On this basis, the DCM and MeOH soluble extracts from the 2007-01 bulbs sample were combined with the DCM and MeOH soluble extracts of the 2005-01 bulbs sample. A portion of the DCM soluble extract (205 mg) was subjected to silica flash chromatography using a 20% stepwise elution as described in the Experimental chapter **Section 7.1**, resulting in fifteen fractions. The enriched 100% hexane fraction (51 mg) and the combined 20:80 hexane:DCM and 100% DCM fractions (36 mg) were selected for HPLC-NMR analysis as shown in **Scheme 3.2**. The 100% hexane fraction was re-solubilised in 1 mL of 70% CH₃CN:D₂O and the combined fraction was re-solubilised in 1 mL of 50% CH₃CN:D₂O and each filtered through a 0.45 μm PTFE membrane filter (HP045 Advantec, Japan). For the HPLC-NMR experiments of the enriched 100% hexane fraction obtained from flash silica chromatography, 50 μL (4,120 μg) was injected, while for the combined fraction as detailed above, 50 μL (3,360 μg) was injected. The HPLC-NMR analyses were carried out using the methods described in **Section 3.2.1**.

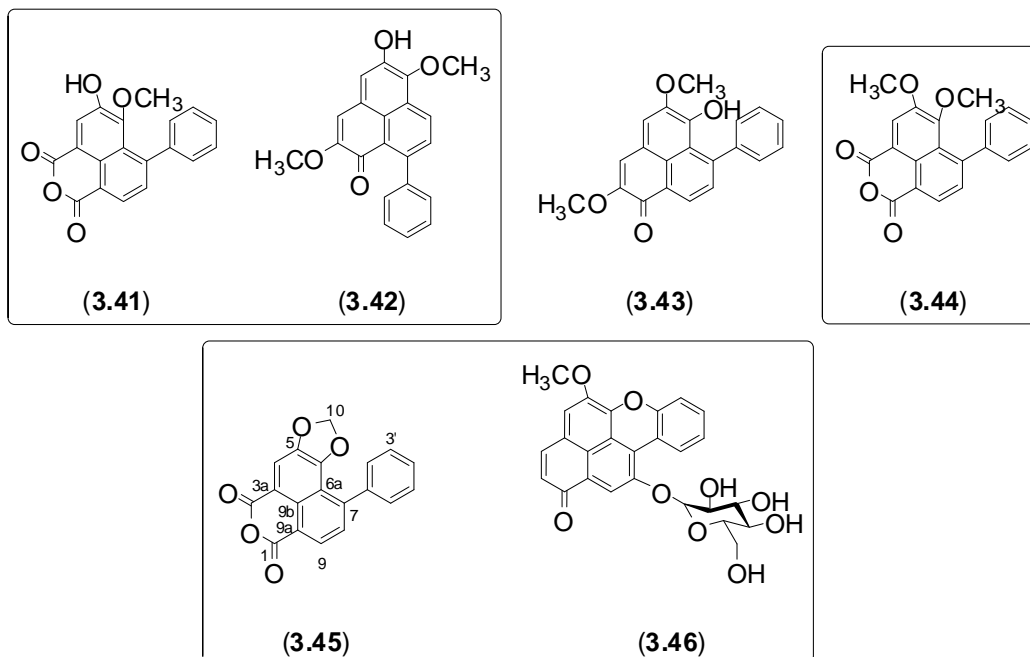


Scheme 3.2. Isolation and purification scheme for the partial identification of secondary metabolites by HPLC-NMR analysis.

3.2.3.2 Preparation of the extract for off-line isolation of secondary metabolites from the bulbs of *H. simulans*

Following the HPLC-NMR analyses, the 100% hexane silica column fraction was subjected to semi-preparative reversed phase HPLC using an isocratic 80% CH₃CN:H₂O solvent system, leading to the isolation of 5,6-dimethoxy-7-phenyl-1*H*,3*H*-naphtho[1,8-*cd*]pyran-1,3-dione (**3.44**) (21.0 mg, 0.10%) and haemodordioxolane (**3.45**) (13.5 mg, 0.06%). Semi-preparative reversed phase HPLC was then carried out on the combined fraction that was subjected to HPLC-NMR analysis, using an isocratic 70% CH₃CN:H₂O solvent system, leading to the isolation of haemoxiphidone (**3.42**) (7.8 mg, 0.03%) and haemodorone (**3.41**) (7.5 mg, 0.03%). Semi-preparative reversed phase HPLC was also conducted on the 80:20

DCM:EtOAc fraction using 70% CH₃CN:H₂O, resulting in the isolation of 5-methoxy-1*H*-naphtho[2,1,8-*mna*]xanthen-1-one (**3.2**) (5.3 mg, 0.02%), while the combined 40:60 and 20:80 DCM:EtOAc fractions was subjected to semi-preparative reversed phase HPLC using isocratic 60% CH₃CN:H₂O conditions to afford 5-hydroxy-2-methoxy-1*H*-naphtho[2,1,8-*mna*]xanthen-1-one (**3.4**) (8.3 mg, 0.04%).



3.2.3.3 Preparation of the extract for off-line isolation of secondary metabolites from the aerial parts of *H. simulans*

The aerial parts of the first collection of *H. simulans*, 2005-01b (26 g) were subjected to the same extraction procedure as the initial extraction of the bulbs described in **Section 3.2.3.21**. The DCM-soluble fraction was subjected to flash silica chromatography using the same 20% stepwise elution profile adopted for the fractionation of the bulbs extract, resulting in fifteen fractions. Subsequent semi-preparative reversed phase HPLC of the 80:20 DCM:EtOAc fraction using isocratic 70% CH₃CN:H₂O conditions yielded 5-methoxy-1*H*-naphtho[2,1,8-*mna*]xanthen-1-one (**3.2**) (8.6 mg, 0.11%), which was also present in the DCM-soluble

fraction of the bulbs of the *H. simulans*. The MeOH soluble extract was subjected to C₁₈ Vacuum Liquid Chromatography (VLC) using a 25% stepwise elution from H₂O to MeOH to EtOAc and finally to DCM resulting in ten fractions. The 100% MeOH and 80:20 MeOH:H₂O fractions were subjected to semi-preparative reversed phase HPLC using 40% CH₃CN:H₂O to afford haemodoroxychrysenose (**3.46**) (23.5 mg, 0.31%).

3.2.4 Acid hydrolysis

Approximately 0.5 mg of haemodoroxychrysenose (**3.46**) was treated with 10 mL of 15% aqueous HCl. The reaction mixtures were heated to 90°C and stirred for six hours. The solution was neutralised by drop-wise addition of 5% aqueous NaOH to which EtOAc was then added. The aqueous partition was evaporated under reduced pressure and the residue spotted on aluminium-backed silica gel TLC plates along with standard samples of β-D-glucopyranose, β-D-galactose, β-D-rhamnose, and β-D-xylose. The TLC plate was developed with *n*-butanol:HOAc:H₂O (3:1:1), air dried and then sprayed with 10% aqueous H₂SO₄, followed by heating in an oven at 110°C. The hydrolysis products from **3.46** exhibited a characteristic spot ($R_f = 0.63$) that was identical with that observed for β-D-glucopyranose.

3.2.5 Crystallography

Crystallographic diffraction data were collected with an Oxford SuperNova diffractometer using Cu radiation ($\lambda = 1.54184 \text{ \AA}$) by Dr Jonathan White at the University of Melbourne. Data were reduced using the CrysAlisPRO software. The temperature of the data collection was maintained at 130 K, using an Oxford Cryostream cooling device. The structure was solved by direct methods, and difference Fourier synthesis and was refined on F^2 (SHELXL-97) [195]. Thermal ellipsoid plot was generated using program ORTEP-3 [196] integrated within the WINGX program suite [197].

3.3 Results and Discussion

As a result of combining extracts of the bulbs of *H. simulans* as well as subsequent silica flash column chromatography fractions as described in **Section 3.2.3.2** and from the subsequent ^1H NMR and analytical HPLC analyses, selected enriched fractions were subjected to HPLC-NMR analysis. On-flow HPLC-NMR analysis of the 100% hexane silica column fraction was carried out as described in **Section 2.2.1** and the results of this can be seen in **Figure 3.4**. On the basis of the on-flow HPLC-NMR analysis of this fraction, two principal compounds were observed, while subsequent stop-flow analysis of this fraction permitted longer acquisition times. The later eluting compound exhibited ^1H NMR resonances and a UV profile consistent with the phenylphenalenone structure class with a maxima at 348 nm (as shown in **Figure 3.5**), while methoxy resonances at δ 3.95 and δ 3.27, together with its extraction characteristics (from 100% hexane fraction of silica column), suggested that this compound could possibly be 5,6-dimethoxy-7-phenyl-1*H*,3*H*-naphtho[1,8-*cd*]pyran-1,3-dione (**3.44**), previously isolated from *H. simulans* [194].

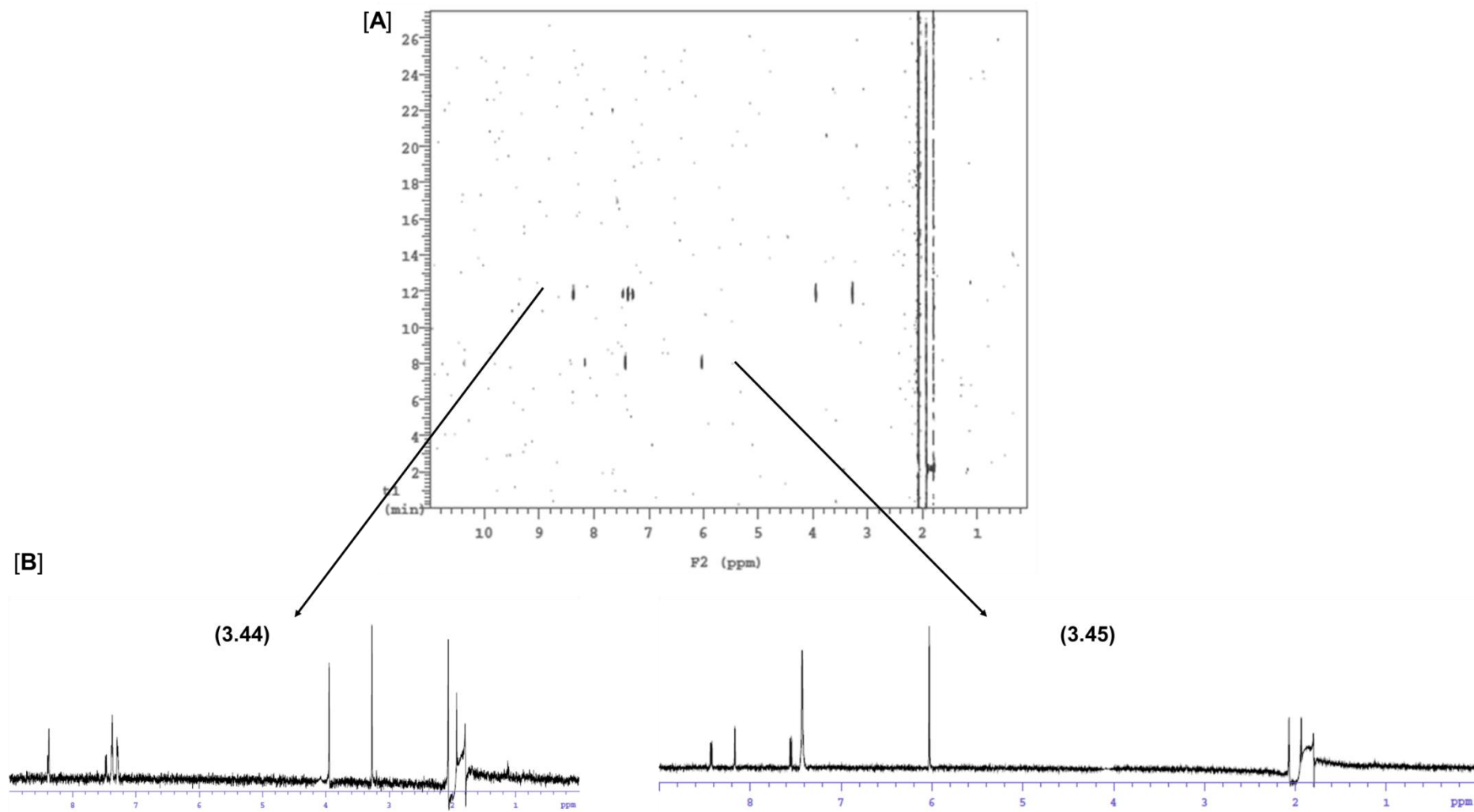


Figure 3.4. [A] 2D HPLC-NMR contour plot showing compounds (3.44 and 3.45) (on-flow HPLC-NMR) and [B] Extracted WET-1D ¹H NMR spectra of compounds (3.44 and 3.45) (stop-flow HPLC-NMR).

The earlier eluting compound displayed the same UV maxima (348 nm) to that of the later eluting compound (see **Figure 3.5**), suggestive of this compound being a phenylphenalenone, together with an unusual singlet at δ 6.03, which integrated as two protons, suggesting the possible presence of a highly deshielded methylene. A literature structure search of the phenylphenalenone structure class returned no matches for such a structural feature [22], suggesting the possibility of a new compound. To determine the identity of this possible new compound, off-line isolation and characterisation would be required.

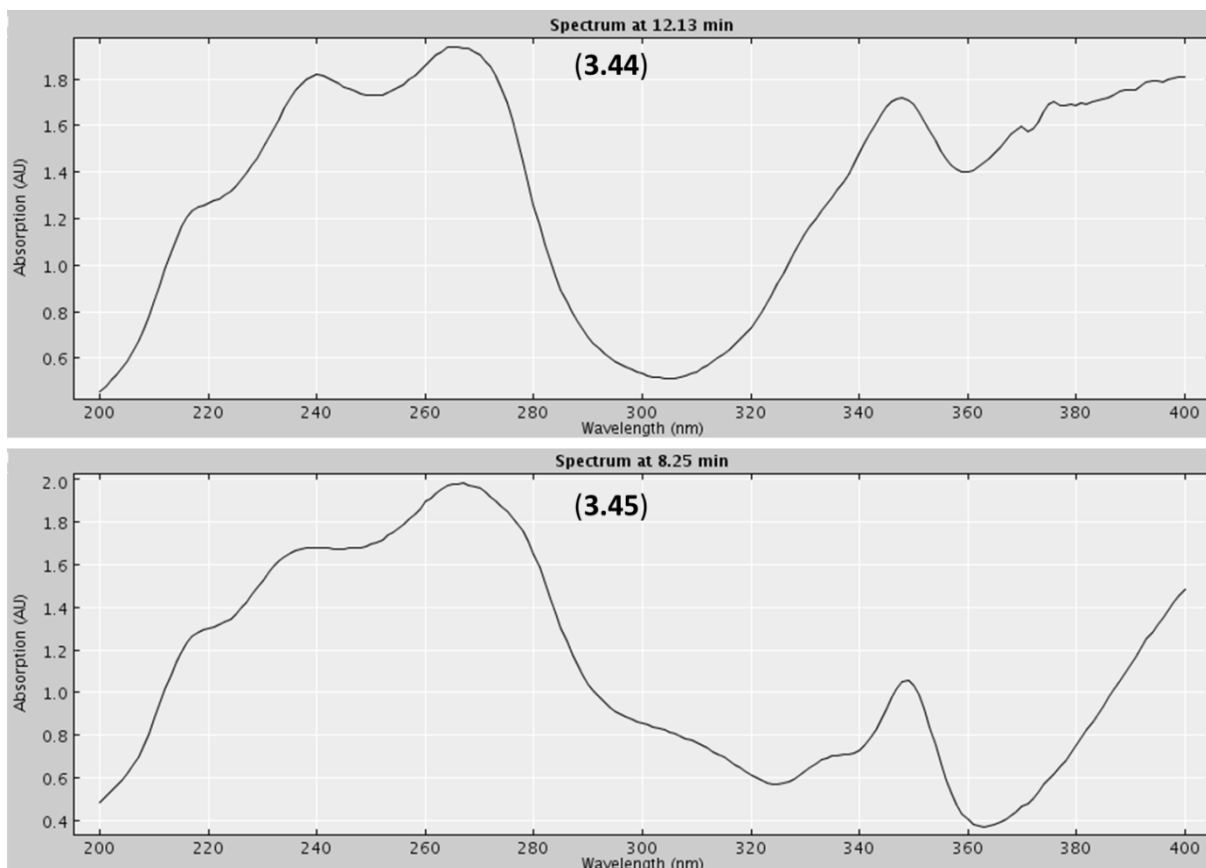


Figure 3.5. UV profiles of **3.44** and **3.45** extracted from HPLC-NMR analysis.

As with the 100% hexane fraction, the combined fraction was also subjected to HPLC-NMR analysis. On-flow analysis and the characteristic UV profile (349 nm for both compounds present) indicated that two phenylphenalenones were present as shown in **Figure 3.6**. Following stop-flow HPLC-NMR analysis, which allowed for improved S/N to be achieved for

the two compounds present, the presence of a methoxy resonance at δ 3.16 together with its extraction characteristics (from combined 20:80 hexane:DCM and 100% DCM fractions), suggested that this compound could possibly be haemodorone (**3.41**), previously isolated from *H. simulans* [194], however off-line isolation and characterisation was required to unequivocally identify this compound and the second compound present.

Off-line isolation of secondary metabolites from the 100% hexane silica fraction was carried out as described in **Section 3.2.3.2**, resulting in the isolation of the known compound 5,6-dimethoxy-7-phenyl-1*H*,3*H*-naphtho[1,8-*cd*]pyran-1,3-dione (**3.44**) and the new compound haemodordioxolane (**3.45**). The combined fraction that was analysed by HPLC-NMR was subjected to semi-preparative reversed phase HPLC to give the known compound haemodorone (**3.41**) and the new compound haemoxiphidone (**3.42**). The 80:20 and 60:40 DCM:EtOAc silica column fractions were combined and semi-preparative reversed phase HPLC using the method described in **Section 3.2.3.2** yielded the known 5-methoxy-1*H*-naphtho[2,1,8-*mna*]xanthen-1-one (**3.2**) along with haemodorone (**3.41**). Analysis of the ^1H NMR and analytical HPLC of the 40:60 and 20:80 DCM:EtOAc silica column fractions led to these fractions to be combined and subjected to semi-preparative reversed phase HPLC using the method described in **Section 3.2.3.2**, resulting in the isolation of the known compound, 5-hydroxy-2-methoxy-1*H*-naphtho[2,1,8-*mna*]xanthen-1-one (**3.4**).

Flash silica chromatography was carried out on the DCM extract of the aerial parts of *H. simulans* as described in **Section 3.2.3.3** to yield fifteen fractions. On the basis of the subsequent analytical HPLC and ^1H NMR data, the 80:20 DCM:EtOAc fraction was subjected to semi-preparative reversed phase HPLC to afford the known compound 5-methoxy-1*H*-naphtho[2,1,8-*mna*]xanthen-1-one (**3.2**), which was also present in the bulbs of the plant. C_{18} Vacuum Liquid Chromatography (VLC) was carried out on the MeOH extract of the aerial parts of *H. simulans* as described in **Section 3.2.3.3**.

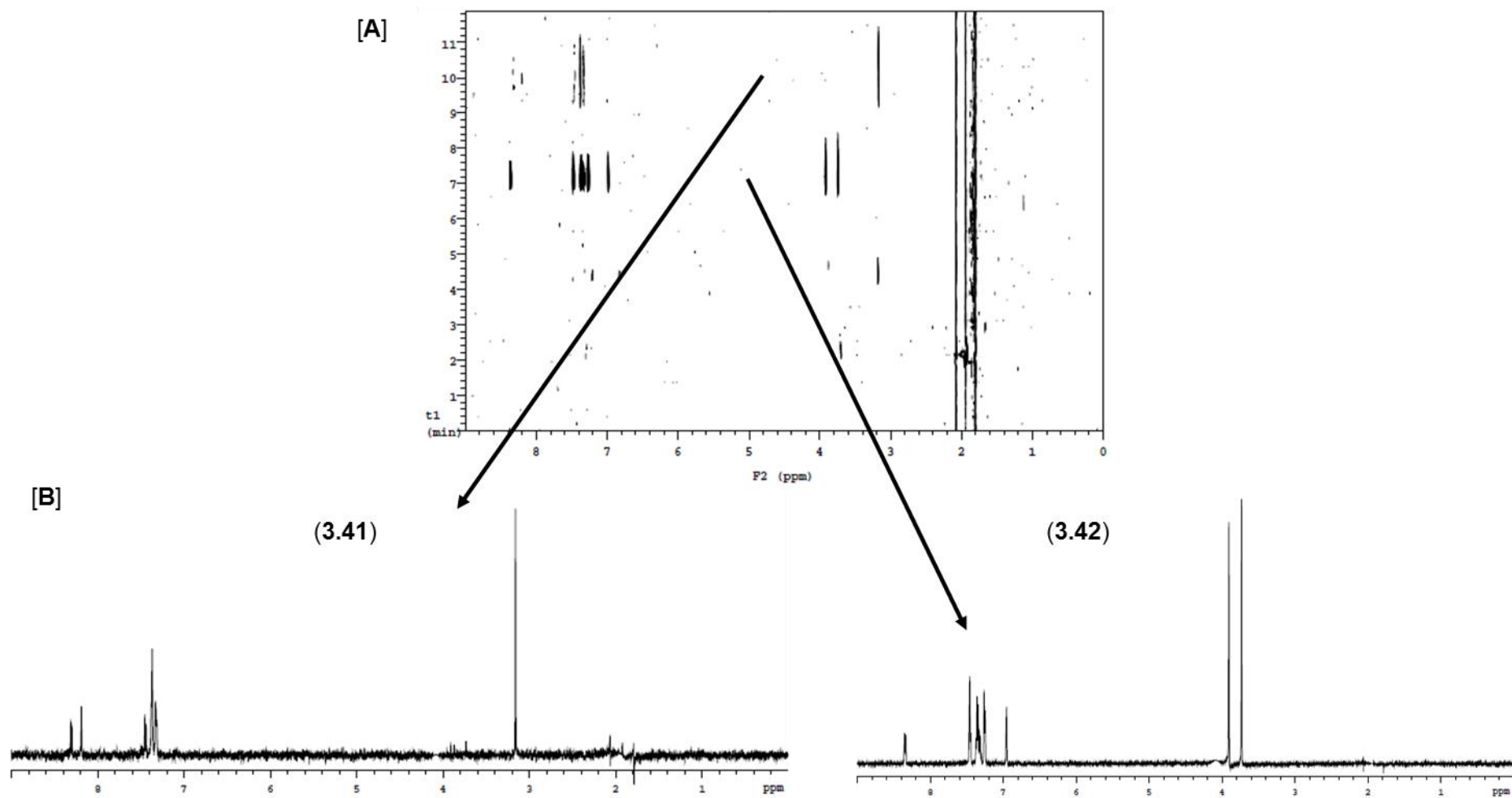


Figure 3.6. [A] 2D HPLC-NMR contour plot (on-flow HPLC-NMR) and [B] Extracted WET-1D ^1H NMR spectra of compounds (3.41 and 3.42) (stop-flow HPLC-NMR).

On the basis of ^1H NMR and analytical HPLC data of the fractions obtained from the VLC C_{18} column chromatography, the 100% MeOH and 80:20 MeOH:H₂O fractions were combined and subjected to semi-preparative reversed phase HPLC, resulting in the isolation of the new compound haemodoroxychrysenose (**3.46**).

The structure of the new compound haemoxiphidone (**3.42**), isolated from the combined 20:80 hexane:DCM and 100% DCM silica column fractions, was determined using 1D and 2D NMR spectroscopy (**Table 3.1**) and mass spectrometry, with the ^1H NMR spectrum provided in **Figure 3.7**. The ESI-MS spectrum of haemoxiphidone (**3.42**) displayed an m/z at 331 $[\text{M}-\text{H}]^-$, consistent with a molecular formula of $\text{C}_{21}\text{H}_{16}\text{O}_4$. In the concurrent study, the HR-ESI-MS analysis was consistent with this mass and molecular formula [198].

The same compound (**3.42**) (based on NMR and HPLC data) was isolated from this plant in an earlier study [194], as well as in an independent and concurrent study of a separate *Haemodorum* species (unpublished results). In the initial study conducted on *H. simulans* this compound was assigned the structure **3.43** (xiphidone) although there were anomalies in the NMR data compared to that reported by Cremona and Edwards [199]. In addition to this anomaly, in two references reporting the structure of xiphidone (**3.43**), it was unclear as to whether this compound was indeed a 7- or a 9- phenylphenalenone [199, 200]. Subsequent references to xiphidone showed inconsistencies in the assignment, with references to this compound being a 7- phenylphenalenone by Opitz *et al.* [164] and also assignment as a 9- phenylphenalenone by Dora *et al.* [201]. In the literature for the compound known as xiphidone (**3.43**), the methoxy moieties are located in the 2- and 5- positions and the ^1H NMR data had been acquired in two different solvents, namely d_6 -DMSO and d_6 -acetone (see **Table 3.2**). Based on this, the ^1H NMR spectrum of the isolated compound that was originally thought to be identical to that of the compound deemed to be xiphidone (**3.43**) from the initial investigation study on this plant [194] was re-acquired in d_6 -acetone to provide a direct comparison to the literature data (**Table 3.2**). Once again, based on a direct comparison to the literature ^1H NMR data for xiphidone (**3.43**) it was concluded that these two compounds were different. This meant that a complete structure re-evaluation would be necessary.

Table 3.1. ^1H (500 MHz) and ^{13}C (125 MHz) NMR data for haemoxiphidone (**3.42**) in d_6 -DMSO.

Position	δ_{H}, J	$\delta_{\text{C}}^{\text{a}}$	gCOSY	gHMBC
1	-	178.9, s	-	-
2	-	152.3, s	-	-
3	7.10, s	111.7, d	-	C-1, C-2, C-9b
3a	-	124.8, s	-	-
4	7.55, s	112.9, d	-	C-3, C-5, C-6, C-9b
5	-	146.6, s	-	-
6	-	141.2, s	-	-
6a	-	125.4, s	-	-
7	8.37, d, $J = 9$ Hz	127.2, d	H-8	C-6, C-6a, C-9, C-9b
8	7.49, d, $J = 9$ Hz	131.2, d	H-7	C-6a, C-9a, C-1'
9	-	144.1, s	-	-
9a	-	127.6, s	-	-
9b	-	119.8, s	-	-
1'	-	142.9, s	-	-
2'	7.27, dd, $J = 1.5, 8.5$ Hz	128.1, d	H-3'	C-9, C-3', C-4'
3'	7.38, dd, $J = 6.5, 7.5$ Hz	128.0, d	H-2'	C-1', C-2'
4'	7.34, dd, $J = 7.0, 7.5$ Hz	126.6, d	-	C-2', C-3', C-5', C-6'
5'	7.27, dd, $J = 6.5, 7.5$ Hz	128.0, d	H-6'	C-1', 6'
6'	7.27, dd, $J = 1.5, 8.5$ Hz	128.1, d	H-5'	C-9, C-4', C-5'
2-OCH ₃	3.76, s	55.3, q	-	C-2
6-OCH ₃	3.95, s	61.2, q	-	C-6'
5-OH	10.05, bs	-	-	C-4, C-5, C-6

^aCarbon assignments based on gHSQCAD and gHMBC NMR experiments

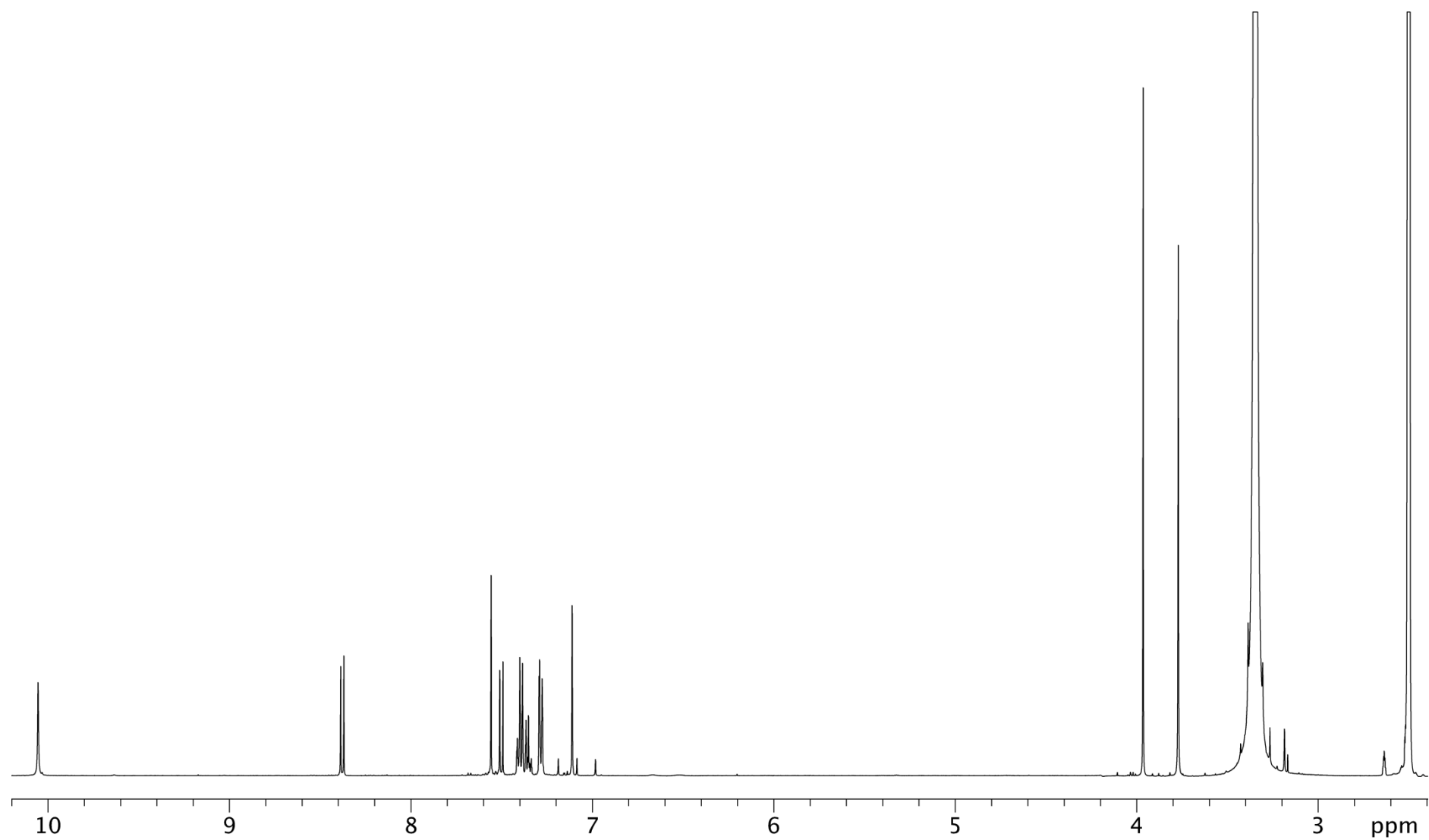


Figure 3.7. ^1H NMR (500 MHz, d_6 -DMSO) spectrum of haemoxiphidone (**3.42**).

Table 3.2. ^1H NMR (500 MHz) comparison of haemoxiphidone (**3.42**) and the literature data for xiphidone (**3.43**) in d_6 -acetone.

3.42 in d_6 -DMSO		3.42 in d_6 -acetone	3.43 in d_6 -acetone [201]
Position	δ_{H}, J	δ_{H}, J	δ_{H}, J
1	-	-	-
2	-	-	-
3	7.10, s	7.04, s	7.37, s
3a	-	-	-
4	7.55, s	7.57, s	6.89, s
5	-	-	-
6	-	-	-
6a	-	-	-
7	8.37, d, $J = 9$ Hz	8.42, d, $J = 8.0$ Hz	8.70, d, $J = 7.7$ Hz
8	7.49, d, $J = 9$ Hz	7.53, d, $J = 8.0$ Hz	7.55, d, $J = 7.7$ Hz
9	-	-	-
9a	-	-	-
9b	-	-	-
1'	-	-	-
2'	7.27, dd, $J = 1.5, 8.5$ Hz	7.33, m	7.41*
3'	7.38, dd, $J = 6.5, 7.5$ Hz	7.40, dd, $J = 6.5, 8.0$ Hz	7.41*
4'	7.34, dd, $J = 7.0, 7.5$ Hz	7.35, m	7.41*
5'	7.27, dd, $J = 6.5, 7.5$ Hz	7.40, dd, $J = 6.5, 8.0$ Hz	7.41*
6'	7.27, dd, $J = 1.5, 8.5$ Hz	7.33, m	7.41*
2-OCH ₃	3.76, s	3.81, s	3.96, s
6-OCH ₃	3.95, s	4.04, s	-
5-OH	10.05, bs	-	-
5-OCH ₃			4.02, s

* signals overlapped

The 2D gHMBC NMR analysis conducted in d_6 -DMSO enabled the unequivocal assignment of the new compound haemoxiphidone (**3.42**). Key HMBC correlations (**Figure 3.8**) were observed from δ 8.37 (H-7), δ 7.55 (H-4) and δ 3.95 (6-OCH₃) to 141.2 ppm (C-6), thereby placing an aromatic proton at position 7 and a methoxy group at position 6. Further correlations from δ 8.37 (H-7) and δ 7.49 (H-8) to 144.1 ppm, supported the presence of the phenyl moiety being located at position 9. In addition, HMBC correlations from the exchangeable hydroxyl proton at δ 10.05 (5-OH) to 122.9 ppm (C-4) and 141.2 ppm (C-6) allowed for the positioning of the hydroxyl group at position 5. In an independent and concurrent study of a separate *Haemodorum* species, haemoxiphidone was also isolated (unpublished results) and in that study the data was acquired in CDCl₃ and a series of single irradiation NOE studies conducted. Both studies were able to unequivocally confirm the structure of haemoxiphidone (**3.42**).

The structure of haemodordioxolane (**3.45**) was determined on the basis of 1D and 2D NMR spectroscopy (**Table 3.3**), mass spectrometry and UV/Vis spectroscopic analysis. The HR-ESI-MS of haemodordioxolane (**3.45**) (see **Figure 3.9**) displayed an m/z at 319.0603 [M+H]⁺ (calcd. for C₁₉H₁₁O₅: m/z 319.0528) consistent with fifteen degrees of unsaturation and a molecular formula C₁₉H₁₀O₅. The ¹H (**Figure 3.10**) and gCOSY NMR spectra identified the presence of a set of overlapped aromatic protons [δ 7.50, m (H-3'/H-5')] and δ 7.48, m (H-2'/H-4'/H-6')], one singlet aromatic proton [δ 8.25, s (H-4)] and two *ortho* aromatic protons [δ 7.65, d, J = 7.5 Hz (H-8) and δ 8.44, d, J = 7.5 Hz (H-9)], along with a singlet proton, which integrated for two protons [δ 6.20, s (H-10)], which were all consistent with that of the phenylphenalenone structure class. The characteristic UV maximum of 368 nm supported the phenylphenalenone structure class [194]. In combination with the ¹³C NMR data, the 2D gHSQCAD (see **Figure 3.11**) and gHMBC NMR experiments allowed for the complete assignment of haemodordioxolane (**3.45**).

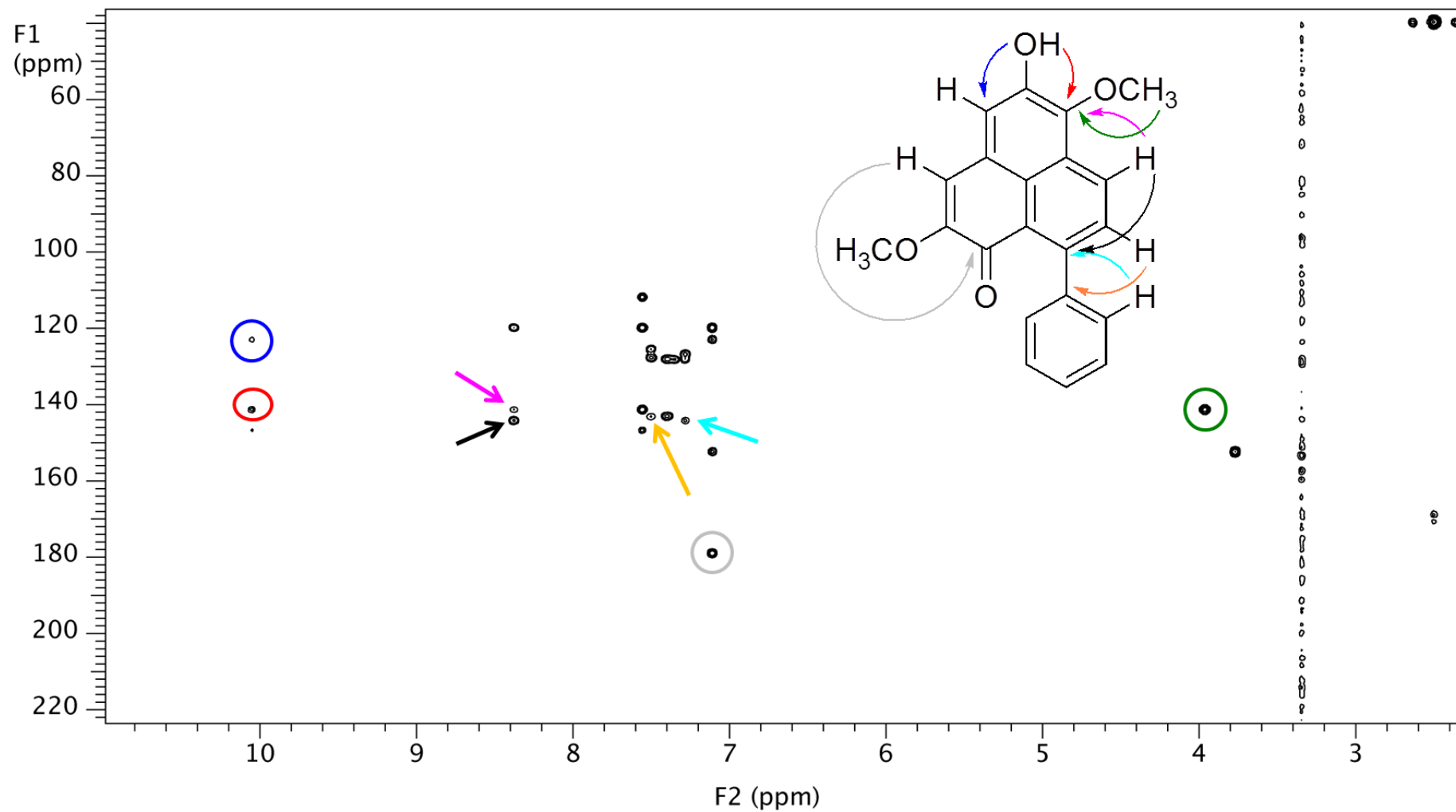


Figure 3.8. 2D gHMBC NMR spectrum showing key correlations of haemoxiphidone (**3.42**).

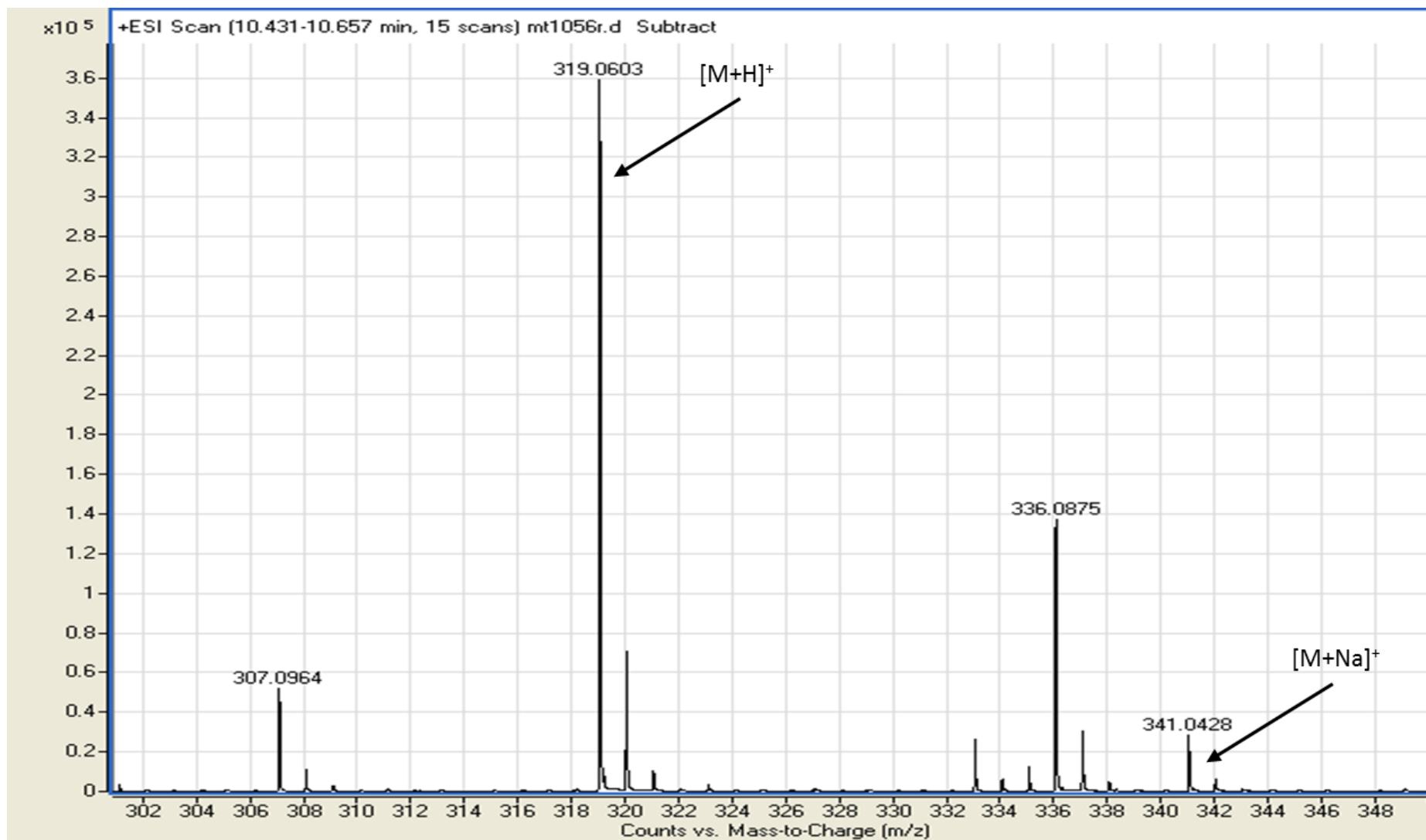


Figure 3.9. HR-ESI-MS (positive mode) spectrum of haemodordioxolane (3.45).

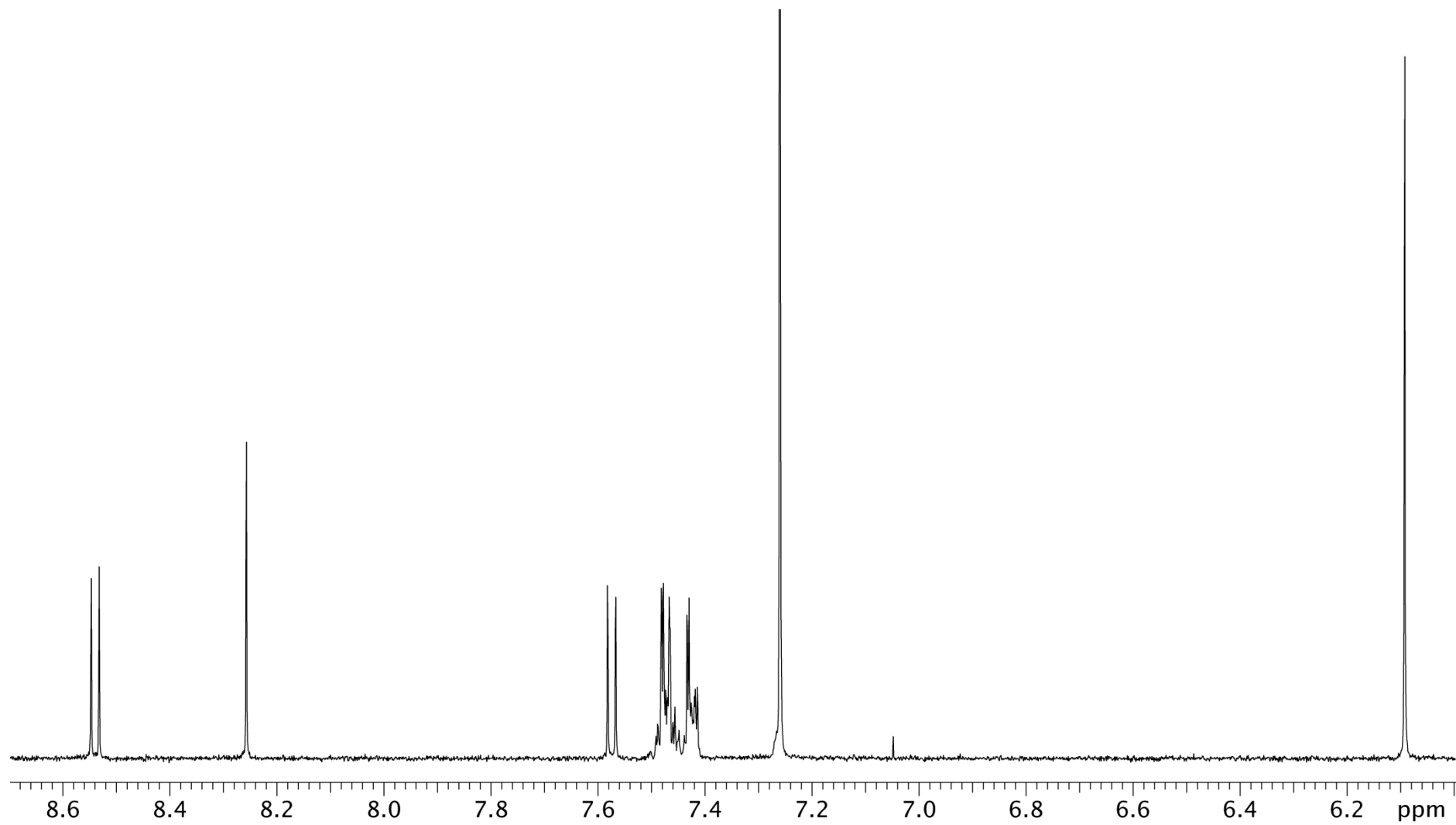


Figure 3.10. ^1H NMR (500 MHz, CDCl_3) spectrum of haemodordioxolane (**3.45**).

It was established through the gHSQCAD NMR experiment that the singlet proton signal at δ 6.20 (H-10) was due to the deshielded methylene protons attached directly to a carbon at 103.2 ppm (C-10), suggestive of a dioxolane moiety. This was confirmed by the HMBC correlations observed from the methylene proton signal at δ 6.20 (H-10) to the aromatic carbons at 145.9 ppm and 149.1 ppm (C-5 and C-6). The lack of protons that could be accounted for in the B ring of the phenylphenalenone (**Figure 3.1**) suggested this was due to the presence of an anhydride [194]. The protons at δ 8.25 (H-4) and δ 8.44 (H-9) displayed HMBC correlations to 160.0 ppm (C-3) and 160.8 ppm (C-1) respectively. The coupling of the *ortho* aromatic protons at δ 7.65 (H-8) and δ 8.44 (H-9), along with the HMBC correlation of δ 8.44 (H-9) to 160.8 ppm (C-1), allowed for the positioning of the phenyl ring at position 7, which was also confirmed by the correlations observed from δ 7.65 (H-8) to 138.9 (C-1') and from δ 8.44 (H-9) and δ 7.50 (H-2'/H-6') to 143.7 ppm (C-7). This allowed for the unequivocal assignment of haemodordioxolane (**3.45**) as the structure of this compound, which was isolated as very fine needle crystals. These crystals were analysed by single crystal X-ray analysis at the Australian synchrotron, however the crystals did not diffract and no crystal structure could be obtained.

The compound isolated from the MeOH extract of the stems and leaves, haemodoroxychrysenose (**3.46**) was determined using 1D and 2D NMR spectroscopy (**Table 3.4**), along with mass spectrometry and UV-Vis spectroscopy. The HR-ESI-MS of **3.46** displayed a peak at m/z 479.1337 [M+H]⁺ (calcd. for C₂₆H₂₃O₉: m/z 479.1342) consistent with a molecular formula C₂₆H₂₂O₉, with 16 degrees of unsaturation. The UV-Vis spectrum displayed a maximum at λ 537 nm, consistent with an oxabenzochrysenone structure class [162, 164, 165, 200, 202].

Table 3.3. ^1H (500 MHz) and ^{13}C (125 MHz) NMR data for haemodordioxolane (**3.45**).

d_6 -DMSO					CDCl_3			
Position	δ_{H}, J	δ_{C}^a	gCOSY	gHMBC	δ_{H}, J	δ_{C}^a	gCOSY	gHMBC
1	-	160.8, s	-	-	-	160.9, s	-	-
2	-	-	-	-	-	-	-	-
3	-	160.0, s	-	-	-	160.1, s	-	-
3a	-	112.3, s	-	-	-	112.4, s	-	-
4	8.25, s	115.0, d	-	C-3, C-5, C-6, C-9b	8.26 s	116.1, d	-	C-3, C-5, C-6, C-9b
5	-	145.9 [^] , s	-	-	-	146.2 [^] , s	-	-
6	-	149.1 [^] , s	-	-	-	149.5 [^] , s	-	-
6a	-	118.3, s	-	-	-	118.8, s	-	-
7	-	143.7, s	-	-	-	144.1, s	-	-
8	7.65, d, $J = 7.5$	129.5, d	H-9	C-6a, C-9a, C-1'	7.57 d, $J = 7$ Hz	129.3, d	H-9	C-6a, C-9a, C-1'
9	8.44, d, $J = 7.5$	131.4, d	H-8	C-1, C-7, C-9b	8.54 d, $J = 7$ Hz	132.3, d	H-8	C-1, C-7, C-9b
9a	-	115.4, s	-	-	-	116.4, s	-	-
9b	-	128.3, s	-	-	-	129.5, s	-	-
10	6.20, s	103.2, t	-	C-5, C-6	6.09, s	102.9, t	-	C-5, C-6
1'	-	138.8, s	-	-	-	139.1, s	-	-
2'	7.49, m *	127.7, d	-	C-7, C-4', C-6'	7.48 m*	127.8, d [#]	-	C-7, C-4', C-6'
3'	7.52, m **	129.2, d	-	C-1', C-5'	7.43 m**	128.5, d ^{##}	-	C-1', C-5'
4'	7.49, m *	127.7, d	-	C-2', C-6'	7.47 m***	127.8, d [#]	-	C-2', C-6'
5'	7.52, m **	129.2, d	-	C-1', C-3'	7.43 m**	128.5, d ^{##}	-	C-1', C-3'
6'	7.49, m *	127.7, d	-	C-7, C-2' C-4'	7.48 m*	127.8, d [#]	-	C-7, C-2' C-4'

^aCarbon assignments based on gHSQCAD and gHMBC NMR experiments

*, **, # and ## signals overlapped

[^] signals interchangeable

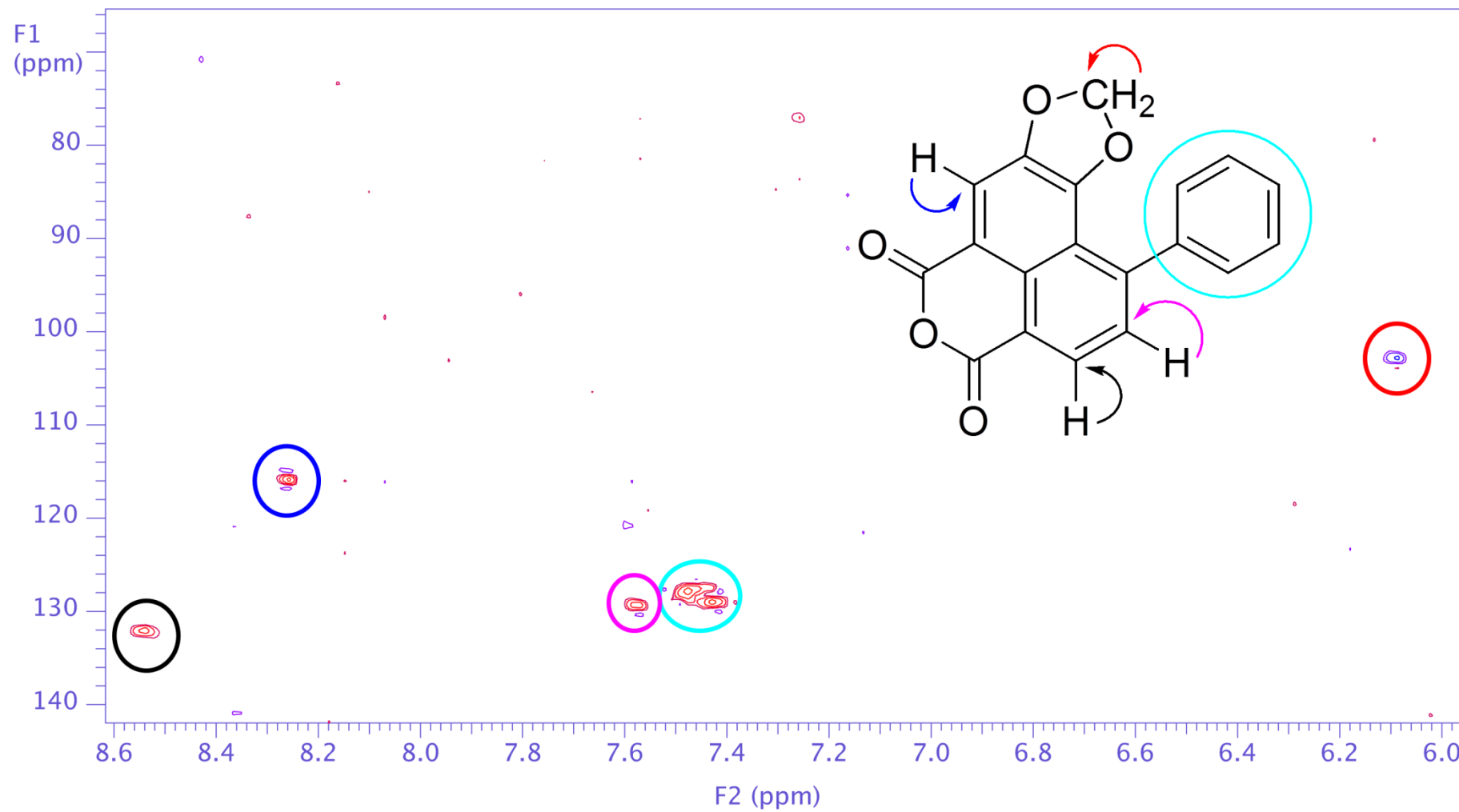


Figure 3.11. 2D gHSQCAD NMR spectrum of haemodordioxolane (**3.45**).

Table 3.4. ^1H (500 MHz) and ^{13}C (125 MHz) NMR data for haemodoroxychrysenose (**3.46**) in d_6 -DMSO

Position	δ_{H}, J	$\delta_{\text{C}}^{\text{a}}$	gCOSY	gHMBC	NOESY	ROESY
1	-	182.3, s	-	-	-	-
2	6.72, d, $J = 9.5$ Hz	126.2, d	H-3	C-3a, C-12a	H-3	H-3
3	8.06, d, $J = 9.5$ Hz	140.9, d	H-2	C-1, C-4, C-12b	H-2	H-2
3a	-	119.4*, s	-	-	-	-
4	8.10, s	119.2, d	-	C-3, C-3a, C-5, C-5a, C-12b	5-OCH ₃	5-OCH ₃
5	-	142.2, s	-	-	-	-
5a	-	140.8, s	-	-	-	-
6	-	-	-	-	-	-
6a	-	151.2, s	-	-	-	-
7	7.49, dd, $J = 1.5, 8.5$ Hz	117.0, d	H-8	C-6a, C-9, C-10a	H-8	H-8
8	7.59, ddd, $J = 1.5, 8.0, 8.5$ Hz	131.5, d	H-7, H-9	C-6a, C-10	H-7, H-9	H-7, H-9
9	7.37, ddd, $J = 1.5, 8.0, 8.5$ Hz	124.6, d	H-8, H-10	C-7, C-10, C-10a	H-8, H-10	H-8, H-10
10	9.24, dd, $J = 1.5, 8.5$ Hz	130.0, d	H-9	C-6a, C-8, C-10b	H-9	H-9
10a	-	118.3, s	-	-	-	-
10b	-	119.4*, s	-	-	-	-
11	-	150.6, s	-	-	-	-
12	8.48, s	119.4*, d	-	C-1, C-10a, C-10b, C-11, C-12a, C-12b	-	-
12a	-	127.9, s	-	-	-	-
12b	-	117.5, s	-	-	-	-
12c	-	121.1, s	-	-	-	-
1'	5.39, d, $J = 8.0$ Hz	101.3, d	2'	C-11	H-12	H-12, H-3'
2'	3.58, m	73.4, d	H-1', H-3', 2'-OH	C-1'	H-3'	2'-OH
3'	3.46, m	77.3, d	H-2', H-4', 3'-OH	-	H-2'	-
4'	3.32, m	69.2, d	H-3', H-5', 4'-OH	-	-	-
5'	3.42, m	76.6, d	H-4'	C-3'	H-6a'	-
6a'	3.58, m	60.4, t	H-6b', 6'-OH	C-5'	H-5', H-6b'	-
6b'	3.70, m		H-6a', 6'-OH	-	H-6a'	-
5-OCH ₃	4.08, s	56.7, q	-	C-5	H-4	H-4
2'-OH	5.61, d, $J = 5.5$ Hz	-	H-2'	C-1'	-	-
3'-OH	5.26, d, $J = 4.5$ Hz	-	H-3'	-	-	-
4'-OH	5.10, d, $J = 5.5$ Hz	-	H-4'	-	-	-
6'-OH	4.56, t, $J = 5.5$ Hz	-	H-6a', H-6b'	-	-	-

^aCarbon assignments based on ^{13}C , DEPT, gHSQCAD and gHMBC NMR experiments* ^{13}C at 119.4 ppm overlapped

The ^1H (**Figure 3.12**) and gCOSY NMR spectra identified the presence of two singlet aromatic protons [δ 8.10, s (H-4)] and [δ 8.48, s (H-12)], a pair of *ortho* aromatic protons [δ 6.72, d, $J = 9.5$ Hz (H-2) and δ 8.06, d, $J = 9.5$ Hz (H-3)], along with four aromatic protons [δ 7.37, ddd, $J = 1.5, 8.0, 8.5$ Hz (H-9), δ 7.49, dd, $J = 1.5, 8.5$ Hz (H-7), δ 7.59, ddd, $J = 1.5, 8.0, 8.5$ Hz (H-8) and δ 9.24, dd, $J = 1.5, 8.5$ Hz (H-10)], a methoxy group [δ 4.08, s (5-OCH₃)] and resonances consistent with a sugar moiety including four methines at [δ 5.39, d, $J = 8$ Hz (H-1') and those occurring between δ 3.32 and δ 3.57, (H-2'', H-3'', H-4'', H-5'')] and one methylene [δ 3.58, m, (H-6a') and δ 3.70, m, (H-6b')]. Also observed were the exchangeable hydroxy moieties of the sugar unit at [δ 4.56, t, $J = 5.5$ Hz (6'-OH), δ 5.61, d, $J = 5.5$ Hz (2'-OH), δ 5.26, d, $J = 4.5$ Hz (3'-OH), δ 5.10, d, $J = 5.5$ Hz (4'-OH)].

The 2D gHSQCAD and gHMBC NMR experiments allowed for the complete assignment of haemodoroxychrysenose (**3.46**). The HSQCAD (see **Figure 3.13**) and HMBC correlations observed from δ 8.48 (H-12) allowed for the positioning of the carbonyl moiety at position C-1 (182.3 ppm) as shown in **Figure 3.14**. Additional correlations from δ 8.48 (H-12) to quaternary carbons at 119.4 ppm (C-10b) and 150.6 ppm (C-11) (**Figure 3.14**) showed that further substitution of the C ring was present. The *ortho*-coupled aromatic proton at δ 8.06 (H-3) displayed a correlation to 182.3 ppm (C-1) as shown in **Figure 3.14**, placing both *ortho*-coupled aromatic protons δ 8.06 and δ 6.72 (H-3 and H-2 respectively) in ring B (**Figure 3.1**).

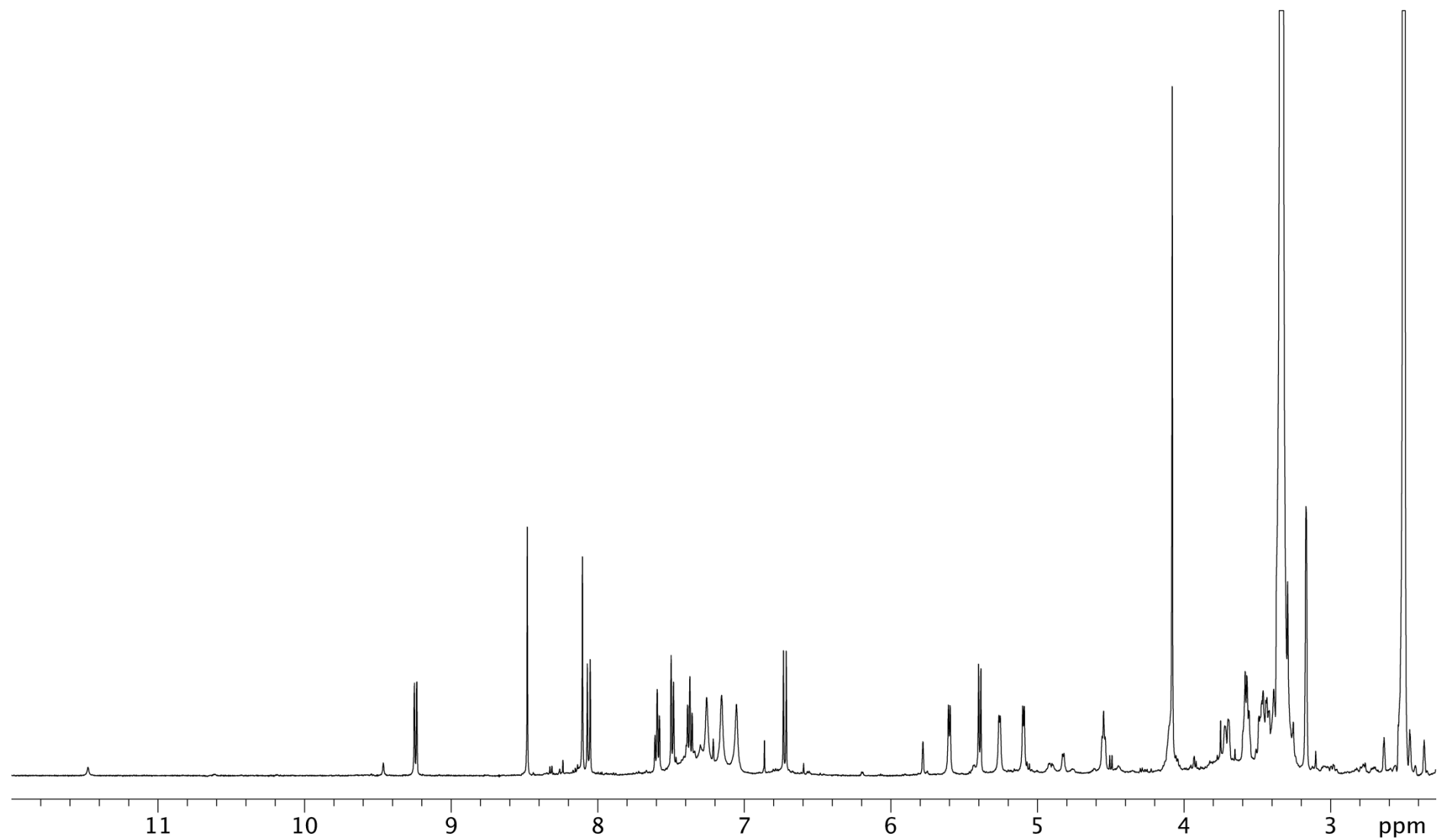


Figure 3.12. ¹H NMR (500 MHz, CDCl₃) spectrum of haemodoroxchrysenose (**3.46**).

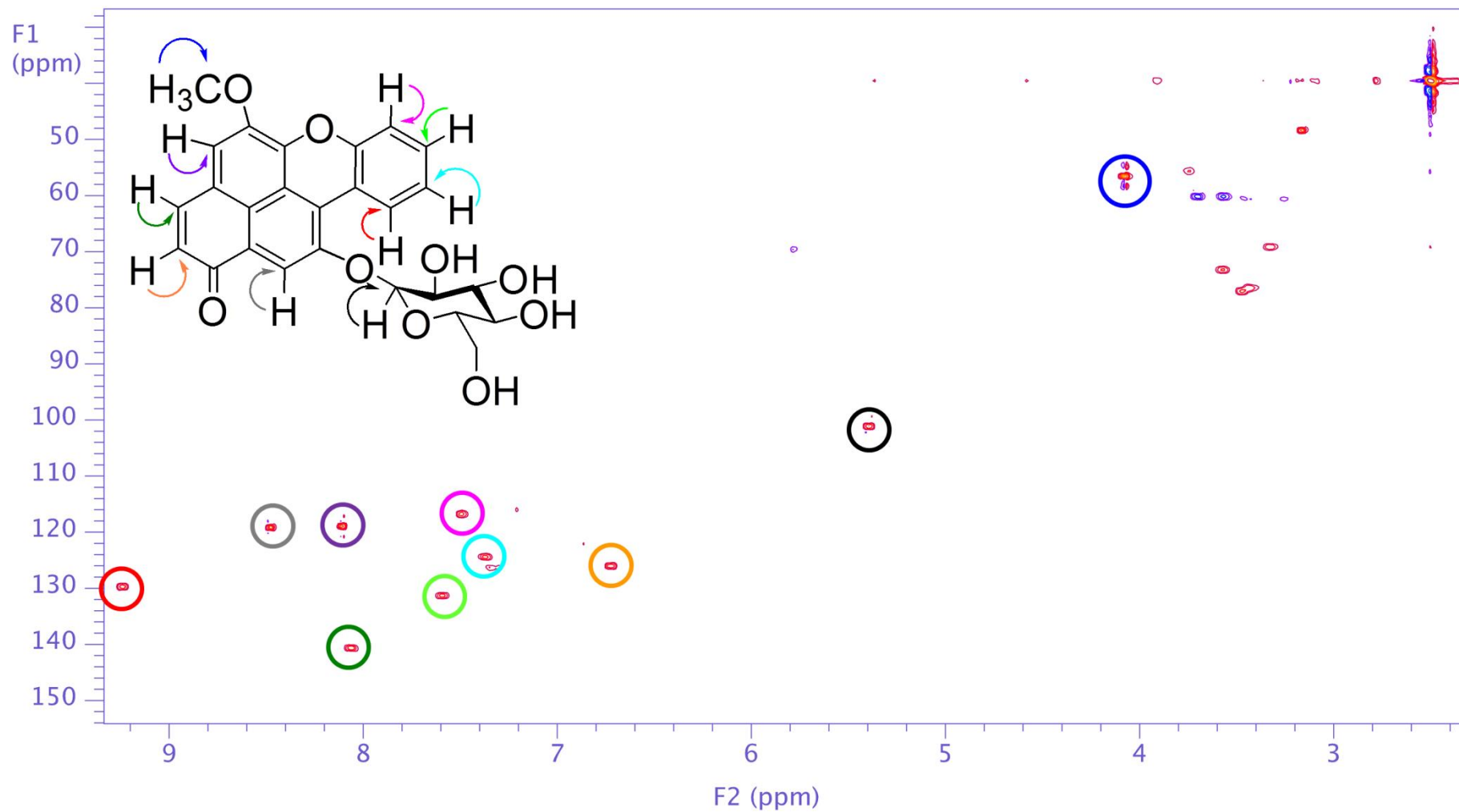


Figure 3.13. 2D gHSQCAD NMR spectrum of haemodoroxychrysenose (**3.46**).

Correlations from the singlet methine at δ 8.10 (H-4) to 140.9 ppm (C-3), 140.8 ppm (C-5a) and 142.2 ppm (C-5), along with the correlation of the methoxy at δ 4.08 (5-OCH₃) to 142.2 ppm (C-5), allowed for the positioning around the A ring shown in **Figure 3.1**. The remaining coupled aromatic protons [δ 7.49 (H-7), δ 7.59 (H-8), δ 7.37 (H-9) and δ 9.24 (H-10)] were found to be due to the D ring of the oxabenzochrysenone-type structure (**Figure 3.1**). The HMBC correlation from δ 5.39 (H-1') to 150.6 ppm (C-11) (**Figure 3.14**) linked the sugar moiety to the ring C carbon at position 11 (see **Figure 3.1**). The positioning of the methoxy and sugar moieties was further supported by NOESY and ROESY NMR enhancements between δ 5.39 (H-1') and δ 8.48 (H-12), along with correlations between δ 8.10 (H-4) and δ 4.08 (5-OCH₃) (see **Table 3.4**). The TOCSY NMR correlation observed between δ 8.06 (H-3) and δ 8.10 (H-4) also supported the fact that the sugar moiety was not positioned at the alternative 2 position of the oxabenzochrysenone structure, see **Figure 3.1**.

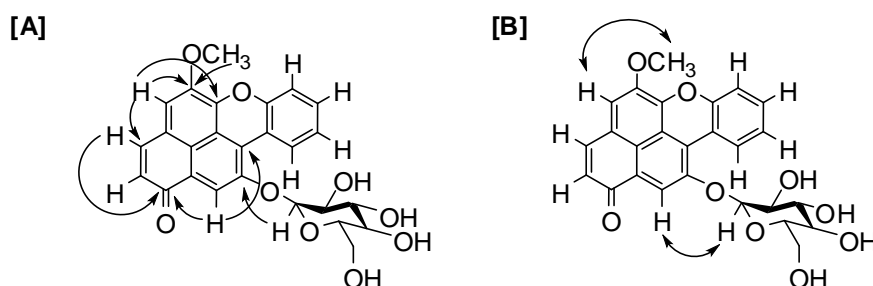


Figure 3.14. [A] Key HMBC correlations and [B] key NOESY and ROESY enhancements observed for haemochrysenone (**3.46**).

The 1D and 2D NMR data, along with ESI-MS data for 5-methoxy-1*H*-naphtho[2,1,8-*mna*]xanthen-1-one (**3.2**) [162], 5-hydroxy-2-methoxy-1*H*-naphtho[2,1,8-*mna*]xanthen-1-one (**3.4**) [164], haemodorone (**3.41**) and 5,6-dimethoxy-7-phenyl-1*H*,3*H*-naphtho[1,8-*cd*]pyran-1,3-dione (**3.44**) [194], were consistent with literature data.

5,6-dimethoxy-7-phenyl-1*H*,3*H*-naphtho[1,8-*cd*]pyran-1,3-dione (**3.44**) was isolated from the 100% hexane fraction from the silica column chromatography, which was the fraction that

also contained **3.45** and upon drying, fine fluorescent crystals were obtained. This allowed for the first single crystal X-ray diffraction study of **3.44** to be carried out. Compound **3.44** crystallises as a hemihydrate, with the water oxygen situated on a 2-fold axis of symmetry, forming a hydrogen bond with carbonyl oxygen O1: O(6)-H(6') 0.823(5)(9) Å, O1...H6, 2.174(14) Å, O1...O6 2.982(4) Å and O1...H6...O6 167(6)°. A thermal ellipsoid plot of **3.44** depicting 20% ellipsoids as determined by X-ray crystallographic analysis is given in **Figure 3.15**. Full details are provided in **Section 3.2.5**.

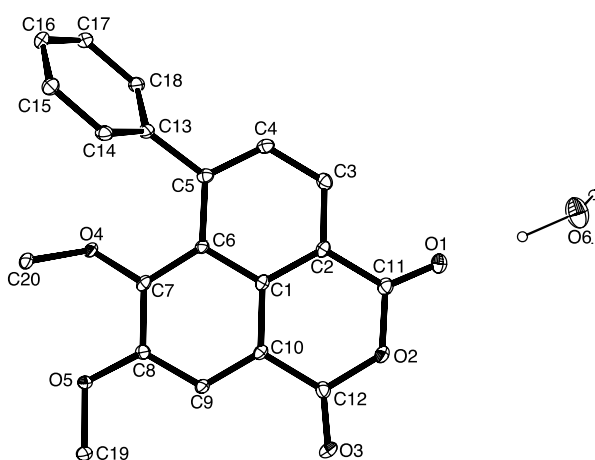


Figure 3.15. Single crystal X-ray structure (ORTEP) of **3.44**.

3.4 Conclusion

This study describes the on-line HPLC-NMR profiling of an enriched fraction that led to the isolation of the new phenylphenalenones, haemodordioxolane (**3.45**) and haemoxiphidone (**3.42**), from the bulbs of *H. simulans* together with the isolation of the new oxabenzochrysenone glycoside, haemodoroxychrysenose (**3.46**) from the aerial parts. Several previously reported compounds (**3.2**, **3.4**, **3.41** and **3.44**) were also isolated and identified. In addition this study has resulted in the first reported single crystal X-ray analysis for compound (**3.44**). The biological activity of all compounds was evaluated in the P388 anti-tumour assay and concluded that all compounds were inactive in this assay.

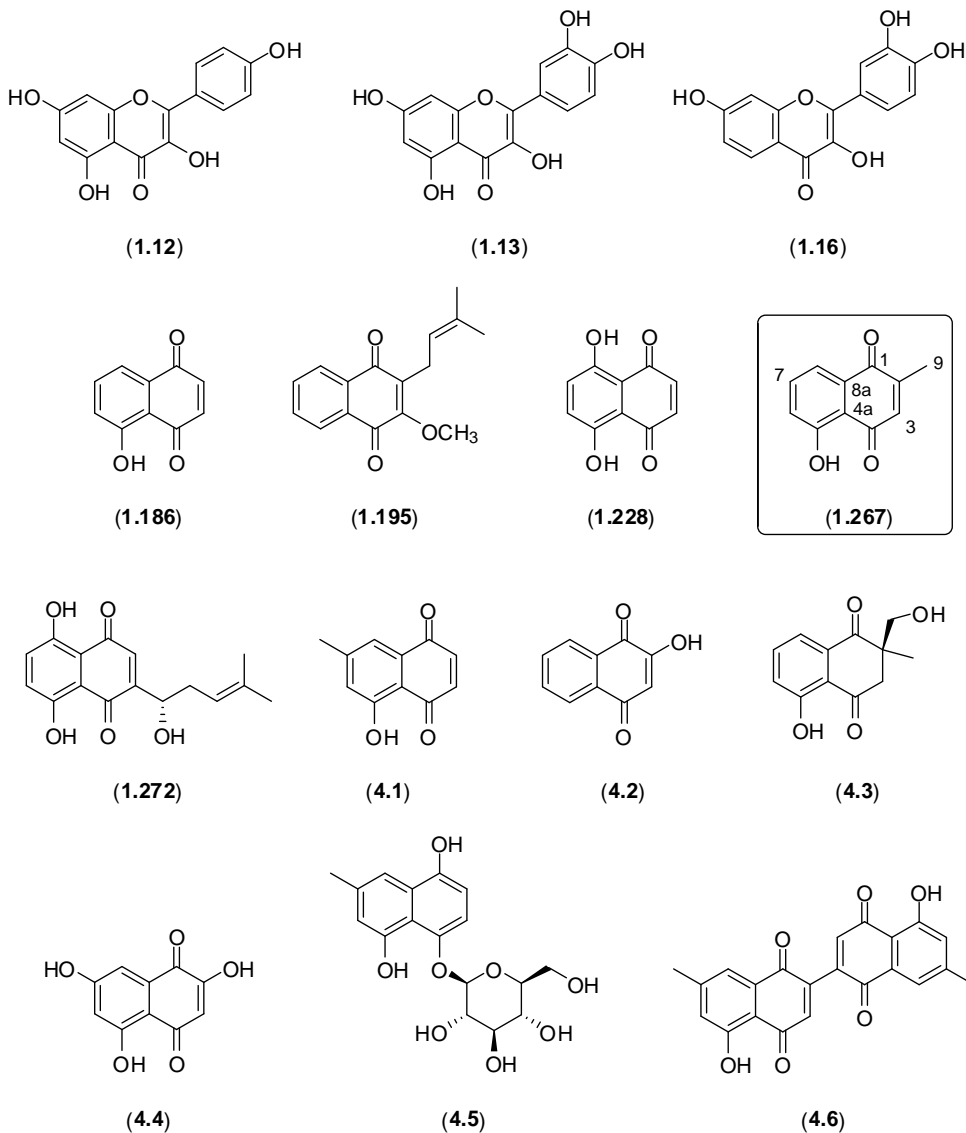
Chapter 4

*On-line and off-line chemical profiling of the Australian plant, *Drosera erythrorhiza* subspecies *magna**

4.1 Introduction

Plants belonging to the family Droseraceae, which consist of three genera (*Drosera*, *Dionaea* and *Aldrovanda*), have been used for centuries as traditional medicines [203]. Applications include the use of extracts in the treatment of asthma, bronchitis, whooping cough, for paroxysmal and hacking coughs, in addition to being used in anticancer treatment [204-209]. *Drosera* is one of the largest genera of carnivorous plants and is commonly known as “*the sundews*”. Members of *Drosera* spp. secrete a sticky substance from their leaves that traps prey [210, 211]. There are greater than one hundred species of *Drosera* found worldwide, with the largest species distribution occurring within Australia. Plants of the *Drosera* genus have been used throughout Europe for the treatment of respiratory problems, whilst the Australian Aboriginal people have utilised the bulbs in their dyes [212, 213]. Extracts have been shown to possess anti-fertility, anti-inflammatory, spasmolytic and anti-microbial activities [214-217]. Plants of the family Droseraceae are known to produce two principal classes of secondary metabolites, namely flavonoids such as compounds (1.12, 1.13 and

1.16) and naphthoquinones such as compounds (1.186, 1.195, 1.228, 1.267, 1.272 and 4.1-4.10) [75, 206, 218-221].



In continuing the application of hyphenated spectroscopic approaches to rapidly assess the chemistry of Australian plants, crude extracts (from the bulbs and aerial parts) of the Australian carnivorous plant *D. erythrorhiza* subspecies *magna* were assessed for anti-tumour, anti-viral and anti-microbial activities. This plant was selected for an on-line HPLC-NMR chemical profiling study on the basis of previous chemistry reported from the family Droseraceae as well as the broad range of activity displayed by the crude extracts.

4.2 Experimental

4.2.1 General Experimental

For all general experimental procedures and spectroscopic methods, see the Experimental Chapter **Section 7.1**. Semi-preparative reversed phase HPLC purification of plumbagin (**1.267**) was conducted using isocratic conditions consisting of 25% CH₃CN/H₂O, while for the remaining compounds, a gradient method of (0 mins 30% CH₃CN/H₂O; 20 mins 50% CH₃CN/H₂O) was used (monitored at λ_{\max} 254 and 300 nm). Both on-flow and stop-flow HPLC-NMR analyses were performed using gradient HPLC conditions (0 mins 30% CH₃CN/D₂O; 20 mins 50% CH₃CN/D₂O), with detection at λ_{\max} 254 and 300 nm. An authentic sample of plumbagin (**1.267**), derived from *Plumbago indica* (CAS number 481-42-5) was purchased from Sigma Aldrich.

4.2.2 Plant material

The plant was identified as *D. erythrorhiza* subspecies *magna* (Droseraceae) and collected by Mr Allan Tinker on 6th of July 2004, from the Western Flora Caravan Park, 22 km north of Eneabba (Irwin botanical district) in Western Australia (plant licence for scientific or other prescribed purposes SW008335). The plant material was physically separated into its aerial and bulbaceous components. Voucher specimens designated the codes 2004-44a (bulbaceous roots) and 2004-44b (aerial parts) are deposited at the School of Applied Sciences (Discipline of Applied Chemistry), RMIT University. Samples (2 g) of both the bulbs (voucher sample 2004-44a) and aerial (2004-44b) components of the plant were extracted with 3:1 MeOH:DCM and sequentially partitioned (trited) into DCM and MeOH soluble crude extracts, which were then evaluated for biological activity as described in the Experimental chapter **Section 7.1.4**. Both extracts showed anti-tumour activity against the P388 (Murine leukaemia) cell line (IC₅₀ of 4.9 μ g/mL for the bulb extract and 8.8 μ g/mL for the aerial component extract) as well as displaying significant anti-viral activity towards *Herpes simplex* type 1 and *Polio* virus type 1. In addition, both extracts exhibited potent

broad spectrum anti-fungal activity towards *Candida albicans*, *Trichophyton mentagrophytes* and *Cladosporium resinae* with inhibition zones (radius of inhibition outside the 6 mm diameter application disc) of 15, 15 and 10 mm respectively, while exhibiting significant and selective anti-bacterial activity towards *Bacillus subtilis* (10 mm zone of inhibition). Both of the crude extracts were inactive against *Escherichia coli* and *Pseudomonas aeruginosa*. All compounds isolated (**1.267** and **4.7-4.10**) were evaluated for P388 anti-tumour activity, while compounds **1.267** and **4.7-4.8** were assessed for anti-microbial activity and compounds **4.7-4.8** were tested for anti-viral activity (**Table 4.1**).



D. erythrorhiza subspecies *magna* (Voucher code: 2004-44)

Kingdom:	Plantae
Phylum:	Equisetophyta
Class:	Equisetopsida
Order:	Caryophyllales
Family:	Droseraceae
Genus:	<i>Drosera</i>
Species:	<i>erythrorhiza</i>
Subspecies:	<i>magna</i>

Table 4.1. Biological evaluation of *D. erythroziza* subspecies *magna* compounds isolated.

Compound	Anti-tumour assay	Anti-viral assays				Anti-microbial assays (Zone of inhibition in mm)					
	P388 ($\mu\text{g/mL}$)	HSV	HSV Cyt	PV	PV Cyt	BS	CA	TM	CR	EC	PA
Plumbagin (1.267)	0.52	NT	NT	NT	NT	12	20	10	3	NT	NT
Droserone (4.7)	< 12.5	ND	ND	No virus inhibition	50% cytotoxic zone observed	ND	ND	ND	ND	ND	ND
Hydroxydroserone (4.8)	4.25	U	100% cytotoxic zone observed	U	100% cytotoxic zone observed	5	ND	6	ND	ND	ND
Drosersone-5-O- β -glycoside (4.9)	1.01	NT	NT	NT	NT	NT	NT	NT	NT	NT	NT
Hydroxydroserone-5-O- β -glycoside (4.10)	3.72	NT	NT	NT	NT	NT	NT	NT	NT	NT	NT

^a All compounds tested at 1 mg/mL.

^b The inhibition zones are the radius of inhibition outside the 6 mm diameter application disc.

U = unable to see if there was any virus present because of the cytotoxicity.

NT = Not tested; ND = No activity detected; Cyt = cytotoxicity; P388 = Murine leukaemia cell line; HSV = DNA *Herpes simplex virus* type 1; PV = RNA *Polio virus* type 1; BS = *Bacillus subtilis*; CA = *Candida albicans*; TM = *Trichophyton mentagrophytes*; CR = *Cladosporium resinae*; EC = *Escherichia coli*; PA = *Pseudomonas aeruginosa*
The P388 standard used was mitomycin C (sigma M0503) with an IC_{50} of 183 ng/mL.

The anti-viral standard used was 30 μL of 0.005 mg/mL didemnum B which displayed cytotoxicity against both viruses at this concentration.

The standard reference compounds for the anti-microbial assays included 10 μg gentamicin (Difco 6423890) which showed a 10 mm zone of inhibition against *E. coli* and *P. aeruginosa*, 30 μg of chloramphenicol (Difco 61338910) which showed a 12 mm zone of inhibition against *Bacillus subtilis*, and 100 IU units of nystatin (Difco 6753890), which showed zones of inhibition of 12 mm, 6 mm and 10 mm against *Candida albicans*, *Trichophyton mentagrophytes*, and *Cladosporium resinae* respectively.

4.2.3 Extraction and Isolation

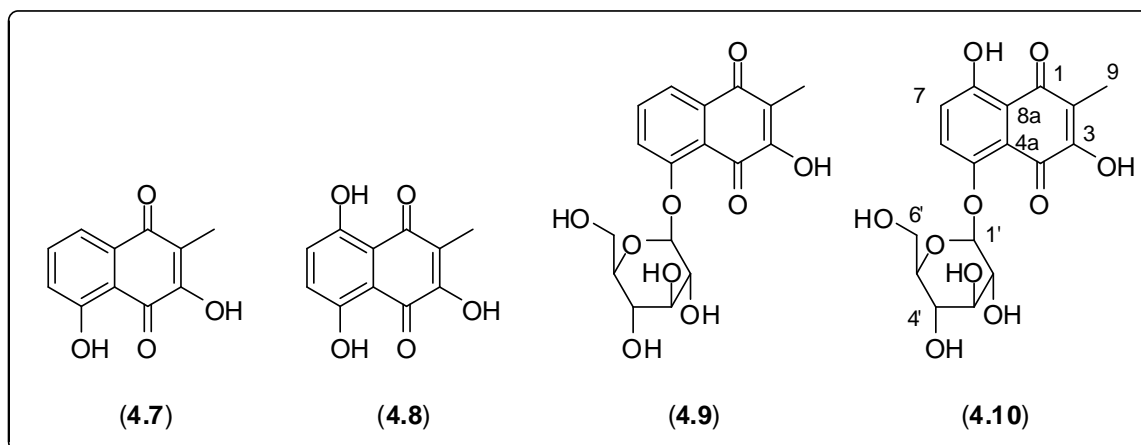
4.2.3.1 Preparation of the extract of *D. erythrorhiza* subspecies *magna* for on-flow and stop-flow HPLC-NMR analysis

A portion of the bulbs of the plant *D. erythrorhiza* subspecies *magna* (12.67 g) was initially extracted using 3:1 MeOH:DCM (400 mL) and then sequentially partitioned (triturated) into EtOAc (748 mg) and H₂O (204 mg) soluble extracts. The bulbs were then re-extracted using 3:1 MeOH:DCM (400 mL), before being sequentially partitioned (triturated) into DCM (150 mg) and MeOH (536 mg) soluble extracts. Analytical HPLC analysis indicated similarities in the compounds present in the initial EtOAc extract and the MeOH extract from the re-extraction and so were combined. Part (96 mg) of this combined extract was dissolved in 40% CH₃CN/D₂O and subjected to HPLC-NMR analysis using the method described in **Section 2.2.1**.

4.2.3.2 Preparation of the extract for off-line isolation of secondary metabolites from *D. erythrorhiza* subspecies *magna*

Off-line isolation of the compounds observed in HPLC-NMR analysis was carried out using the combined extracts used for HPLC-NMR analysis. A portion of this combined extract (300 mg) was subjected to size exclusion chromatography using the method described in the Experimental chapter **Section 7.1** to afford twenty-four fractions. Subsequent analytical HPLC and ¹H NMR analysis of the fractions led to six fractions being combined and subjected to reversed phase semi-preparative HPLC. This was conducted using the gradient described in **Section 2.2.1**, which resulted in the isolation of the four structurally related naphthoquinones: droserone (**4.7**) (15.2 mg, 0.25%), hydroxydroserone (**4.8**) (13.8 mg, 0.23%), droserone-5-O-β-glycoside (**4.9**) (8.6 mg, 0.14%) and hydroxydroserone-5-O-β-glycoside (**4.10**) (5.8 mg, 0.10%). The aerial parts of the *D. erythrorhiza* subspecies *magna* plant were extracted using 3:1 MeOH:DCM (300 mL), and then sequentially partitioned (triturated) into DCM, MeOH and H₂O fractions. Analytical reversed phase HPLC of the MeOH

extract of the aerial parts of the plant indicated that a further naphthoquinone was present. The MeOH extract was fractionated by size exclusion chromatography as described in the Experimental chapter **Section 7.1** resulting in five fractions. Two of these fractions were combined before being subjected to reversed phase semi-preparative HPLC as described in **Section 2.2.1**, which afforded plumbagin (**1.267**) (5.4 mg, 0.31%).



4.3 Results and Discussion

The analytical HPLC chromatograms of the crude EtOAc extract and the re-extracted MeOH extract were similar and were therefore combined. These extracts both showed the presence of two early-eluting compounds, as well as two later-eluting compounds. HPLC-NMR analysis was undertaken and on the basis of the on-flow HPLC-NMR analysis three peaks were apparent in the HPLC chromatogram (**Figure 4.1**), whilst in the 2D NMR contour plot one major compound was present as well as one further compound (see **Figure 4.2**). The early-eluting peak was not observed in the on-flow HPLC-NMR analysis due to its low abundance in the extract. In HPLC-NMR there most often is a requirement to overload the analytical HPLC in order to achieve sufficient S/N for the NMR analysis and this frequently results in poor resolution/separation in the chromatography, as shown in **Figure 4.1**.

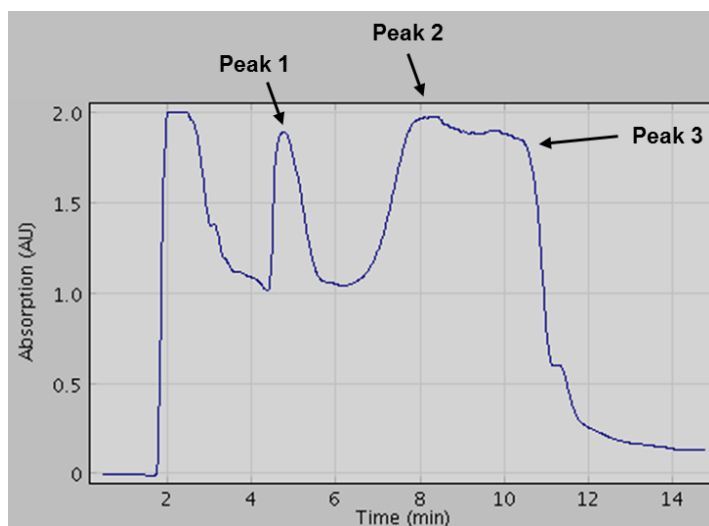


Figure 4.1. HPLC chromatogram obtained from the on-flow HPLC-NMR analysis of the crude extract of *D. erythrorhiza* subspecies *magna*.

As shown in **Figure 4.2**, the changing solvent composition associated with the gradient method used in the HPLC-NMR analysis results in a chemical shift drift. This is evident for the major component which was observed to change in chemical shift by ~ 0.1 ppm over the thirty seconds that it took to elute. This chemical shift drift is expected to occur when employing a gradient HPLC method for HPLC-NMR analysis [222]. It was necessary to conduct stop-flow HPLC-NMR to permit longer acquisition times for the other two minor components observed in the HPLC chromatogram.

Analysis of the WET-1D ^1H NMR spectra (**Figure 4.3**) from stop-flow HPLC-NMR of the early-eluting peak showed the presence of a sugar moiety (δ 3.20- δ 3.80, m) together with aromatic resonances (δ 6.80- δ 7.70) as shown in **Figure 4.3**. A comparison with the initial analytical HPLC analysis led to the suspicion that the first, early-eluting peak in the HPLC-NMR was, in fact, two co-eluting compounds. The ^1H NMR spectra of the two later-eluting compounds (peak 2 and peak 3 in **Figure 4.1**) showed some similarities to that of the early co-eluting compounds but did not exhibit any resonances associated with a sugar moiety. The ^1H NMR of the first of the later-eluting compounds (**4.7**) showed the presence of a set of three aromatic protons [δ 7.48, t, $J = 7$ Hz (H-7); δ 7.34, d, $J = 7.5$ Hz (H-8) and δ 6.97, m, $J = 8.5$ Hz (H-6)] together with a methyl singlet [δ 1.79, (H-9)].

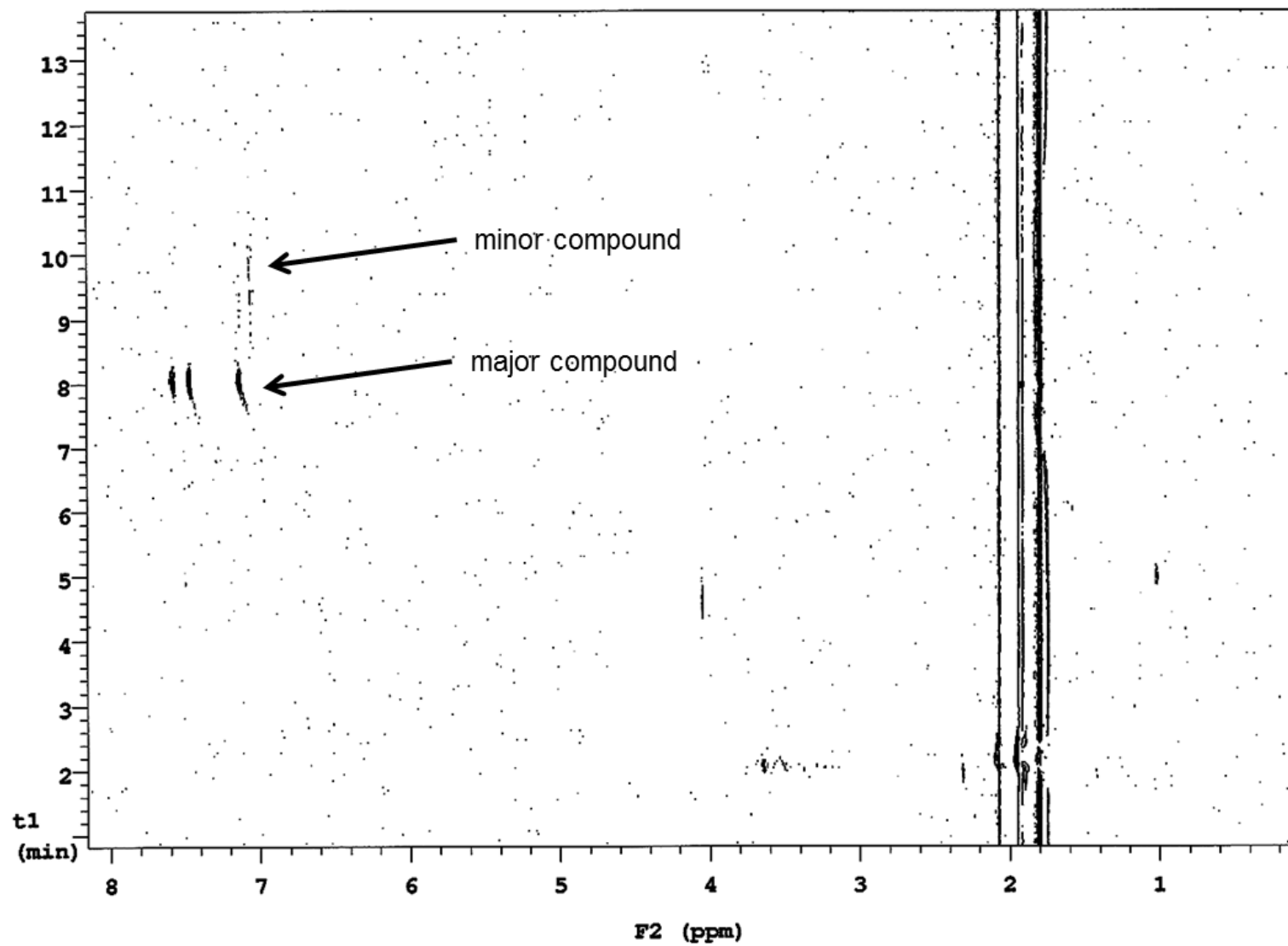


Figure 4.2. On-flow 2D HPLC-NMR contour plot showing the presence of the major compound (4.7) and one of the minor compounds (4.8).

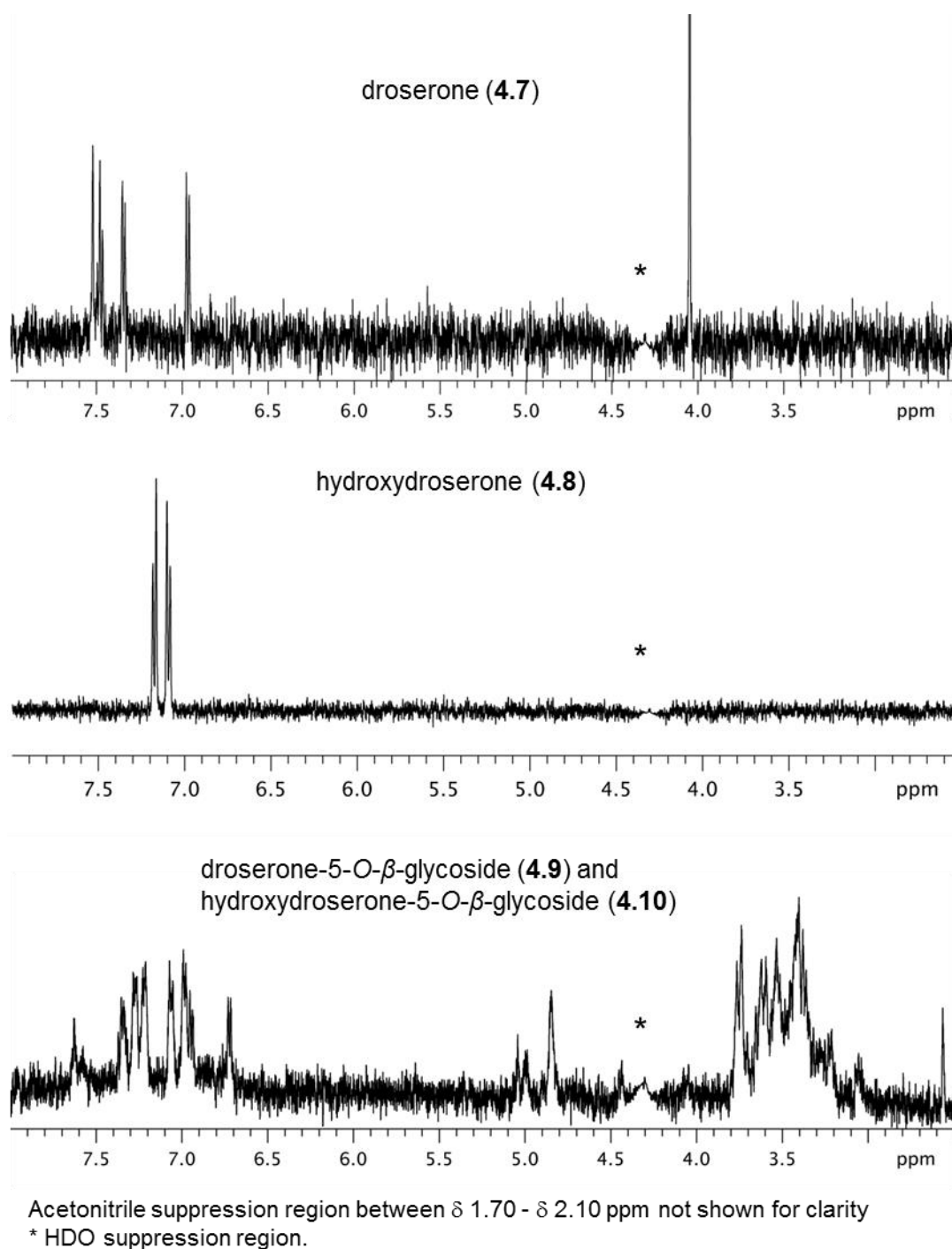


Figure 4.3. WET-1D ^1H NMR spectra of the peaks observed in the stop-flow HPLC-NMR analysis.

The second of the later-eluting compounds (4.8) displayed resonances similar to that of 4.7 but exhibited only two aromatic protons [δ 7.17, d, J = 9 Hz and δ 7.09, d, J = 9 Hz], along with a methyl singlet [δ 1.79, s]. These chemical shifts, together with the UV maxima at approximately 270 nm (**Figure 4.4**), were consistent with the naphthoquinone structure class.

Given the known chemistry produced by *Drosera* spp. it was suspected that these two compounds were the naphthoquinones, droserone (**4.7**) and hydroxydroserone (**4.8**).

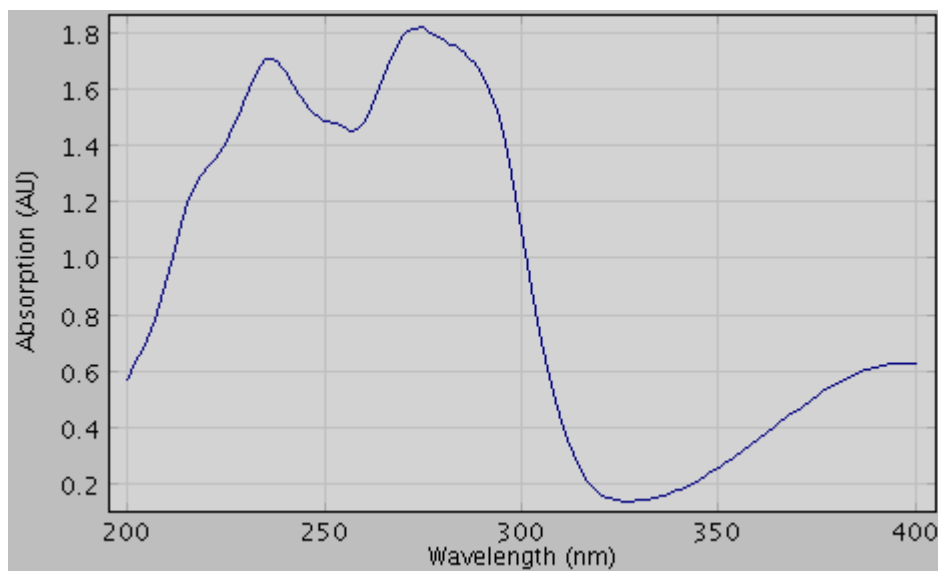


Figure 4.4. Extracted UV profile of the major component observed in the HPLC-NMR analyses.

Off-line isolation was necessary in order to identify which compounds were responsible for the biological activity observed in the crude extract. This would also permit an unequivocal identification of the four secondary metabolites indicated by the initial analytical HPLC analysis. Off-line isolation of compounds from both the bulbs and aerial parts were undertaken separately as described in **Section 4.2.3.2**. The structures of the naphthoquinones and the corresponding glycosides (**1.267** and **4.7-4.10**) were determined on the basis of 1D and 2D NMR analysis, along with mass spectrometry.

The negative mode ESI-MS of the compound isolated from the aerial parts of the plant (**1.267**), displayed an m/z at 187 [M-H]⁻, consistent with a molecular formula of C₁₁H₈O₃ and eight degrees of unsaturation. Comparison of the ¹H and ¹³C NMR spectra with those of naphthoquinones known to occur in Droseraceae, indicated that the secondary metabolite was plumbagin (**1.267**) [223, 224]. An authentic sample of plumbagin was purchased from Sigma Aldrich and used to confirm that the compound isolated from the aerial parts of the

plant was plumbagin. NMR and mass spectrometric data was identical to that of the authentic sample as shown in **Table 4.2**.

The negative mode ESI-MS of the second peak detected in the HPLC-NMR analysis (**4.7**), displayed an m/z of 203 $[M-H]^-$, consistent with a molecular formula of $C_{11}H_8O_4$ and eight degrees of unsaturation. On the basis of the 1D and 2D NMR analyses along with a comparison of NMR data to the literature, it was concluded that this secondary metabolite was in fact droserone (**4.7**) [207, 225-227]. While 1H NMR (**Figure 4.5**) assignments were found to be consistent with those in the literature, it was evident that the ^{13}C NMR chemical shift literature reassignments for the carbons at positions C-6 and C-8 was necessary (see **Figure 4.6**).

Table 4.2. 1H (500 MHz) and ^{13}C NMR (125 MHz) chemical shift comparison of isolated and authentic plumbagin (**1.267**) in d_6 -DMSO.

Position	Isolated plumbagin		Authentic plumbagin	
	δ_H, J	δ_C	δ_H, J	δ_C
1	-	184.4, s	-	184.4*, s
2	-	149.4, s	-	ND
3	6.98 dd, $J = 3.0, 1.5$ Hz	135.2, d	6.98 bs	135.2, d
4	-	190.1, s	-	190.1*, s
4a	-	114.9, s	-	ND
5	-	160.1, s	-	160.1, s
6	7.32 dd, $J = 8.5, 1.0$ Hz	123.8, d	7.32 d, $J = 7.0$ Hz	123.8, d
7	7.72 dd, $J = 8.5, 7.5$ Hz	137.0, d	7.73 dd, $J = 8.0, 8.0$ Hz	136.5, d
8	7.53 dd, $J = 7.5, 1.0$ Hz	118.7, d	7.53 d, $J = 7.5$ Hz	118.7, d
8a	-	132.0, s	-	131.9, s
9	2.09 d, $J = 1.5$ Hz	16.0, q	2.10 bs	15.9, q
5-OH	11.86 s	-	11.85, s	-

bs indicates a broad singlet

ND indicates signals were not detected

* indicates these signals were just visible from the baseline noise

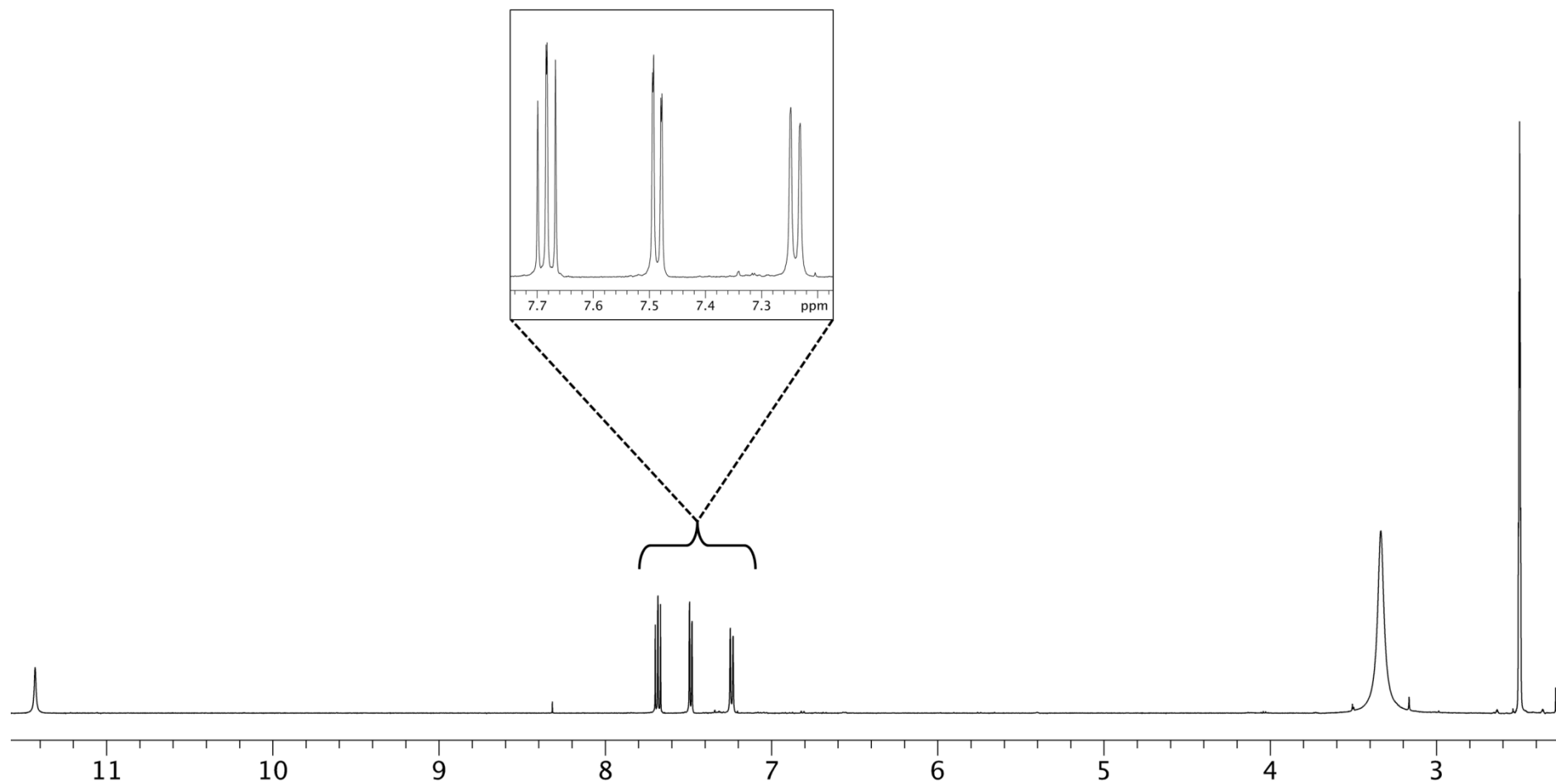


Figure 4.5. ^1H NMR (500 MHz, d_6 -DMSO) spectrum of droserone (**4.7**).

In the literature [227], C-6 is assigned as 118.1 ppm while C-8 is assigned as 122.7 ppm. On the basis of the direct $^1J_{C-H}$ correlations observed in the gHMBC NMR experiment (**Figure 4.7**) the correct assignment of these carbons has been revised to C-6 (122.7 ppm) and C-8 (118.2 ppm) respectively.

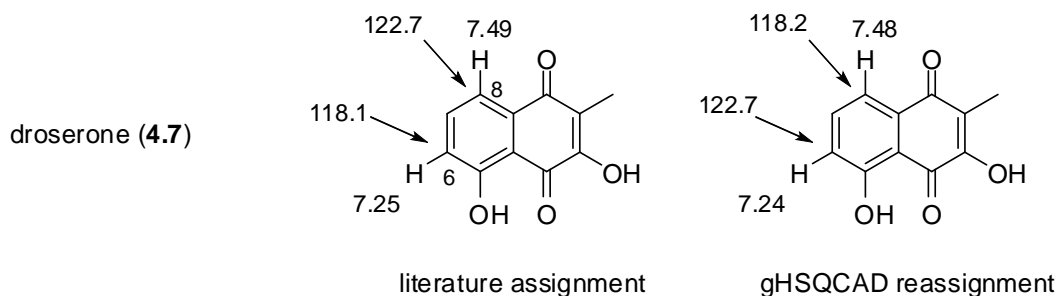


Figure 4.6. Literature ^{13}C NMR assignments and re-assignments of positions C-6 and C-8 for droserone (**4.7**).

The second naphthoquinone (**4.8**) isolated from the bulbs of the plant displayed an m/z of 219 $[M-H]^-$ in the negative mode ESI-MS, which was consistent with $C_{11}H_8O_5$ and eight degrees of unsaturation. NMR comparison with droserone (**4.7**) suggested this was hydroxydroserone (**4.8**), while a comparison with literature data confirmed this [219, 228].

The two glycosides (**4.9-4.10**) which co-eluted in the HPLC-NMR analysis (**Figure 4.3**) were suggested to be the glycosides of droserone (**4.7**) and hydroxydroserone (**4.8**) by comparison of the stop-flow WET-1D 1H NMR and off-line 1H NMR spectra and on the basis of biosynthetic origin considerations. This was further supported by the negative mode ESI-MS analyses of **4.9** and **4.10** which displayed an m/z of 365 $[M-H]^-$, and 381 $[M-H]^-$, consistent with masses corresponding to the glycosides of droserone (**4.7**) and hydroxydroserone (**4.8**) respectively. On the basis of direct NMR comparisons to the literature [219, 227], it was established that these were in fact droserone-5-O- β -glycoside (**4.9**) and hydroxydroserone-5-O- β -glycoside (**4.10**).

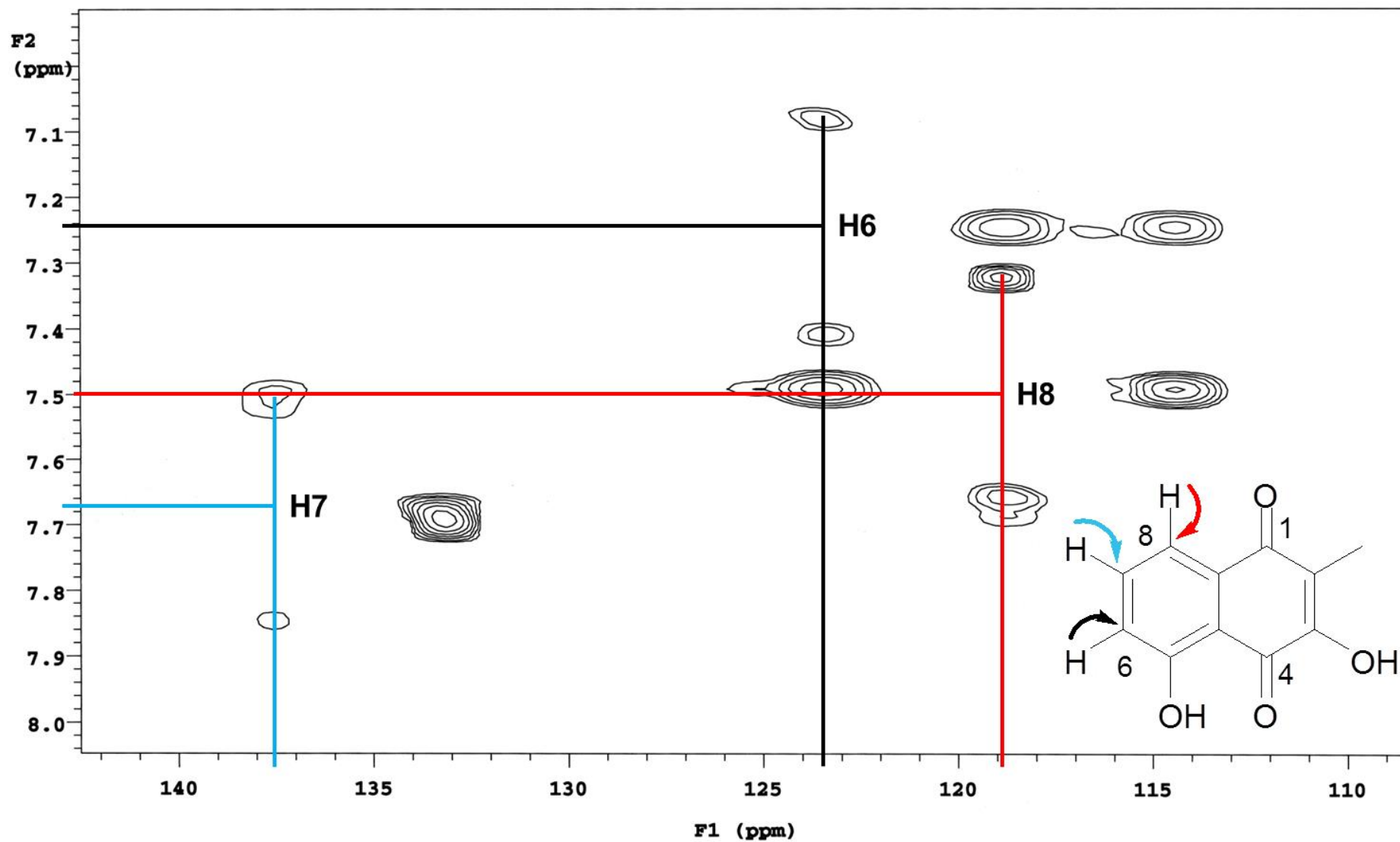


Figure 4.7. Expansion of 2D gHMBC NMR spectrum, displaying the direct $^1J_{C-H}$ correlations for the assignment of droserone (4.7).

Although ^1H NMR chemical shifts for droserone-5- O - β -glycoside (**4.9**) were consistent with the literature data as shown in **Figure 4.8**, the data from the gHSQCAD (See **Figure 4.9**) and gHMBC NMR experiments established that the ^{13}C NMR chemical shifts previously assigned [227] to positions C-6 and C-8 in the structure of droserone-5- O - β -glycoside (**4.9**) should (as in the case of droserone (**4.7**)) be reversed as shown in **Figure 4.8**.

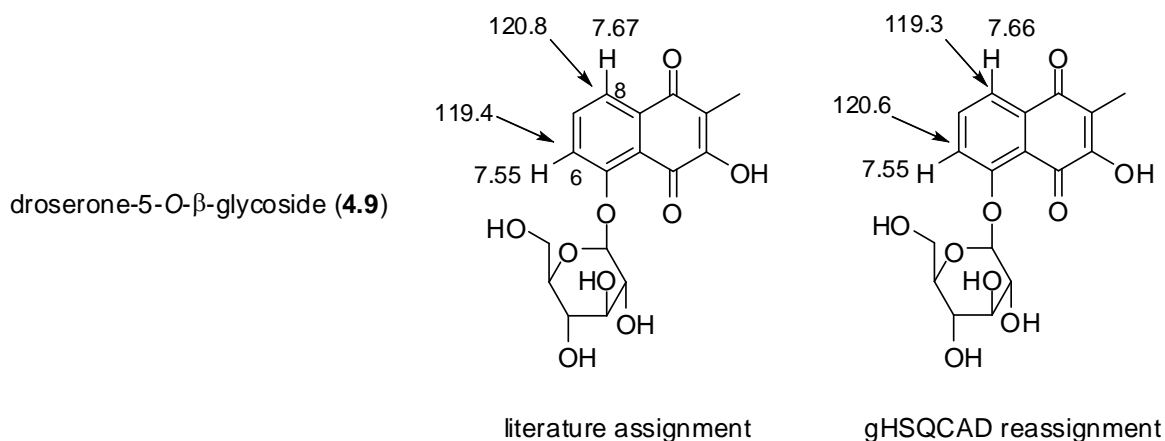


Figure 4.8. Literature ^{13}C NMR assignments and re-assignments of positions C-6 and C-8 for droserone-5- O - β -glycoside (**4.9**).

The complete assignment of hydroxydroserone-5- O - β -glycoside (**4.10**) using 1D and 2D NMR analysis (See **Table 4.3**) confirmed the structure, with the ^1H NMR spectrum shown in **Figure 4.10**. The positioning of the sugar moiety was determined on the basis of a chemical shift comparison with droserone-5- O - β -glycoside (**4.9**), droserone (**4.7**), hydroxydroserone (**4.8**) as shown in **Figure 4.11**, and the literature data for hydroxydroserone-5- O - β -glycoside (**4.10**) [219]. It was observed that when the hydroxy at position C-5 was changed to a sugar moiety (for instance in the case of droserone (**4.7**) and droserone-5- O - β -glycoside (**4.9**)), the ^{13}C NMR chemical shift of the carbonyl at C-4 decreased markedly (**Figure 4.11**).

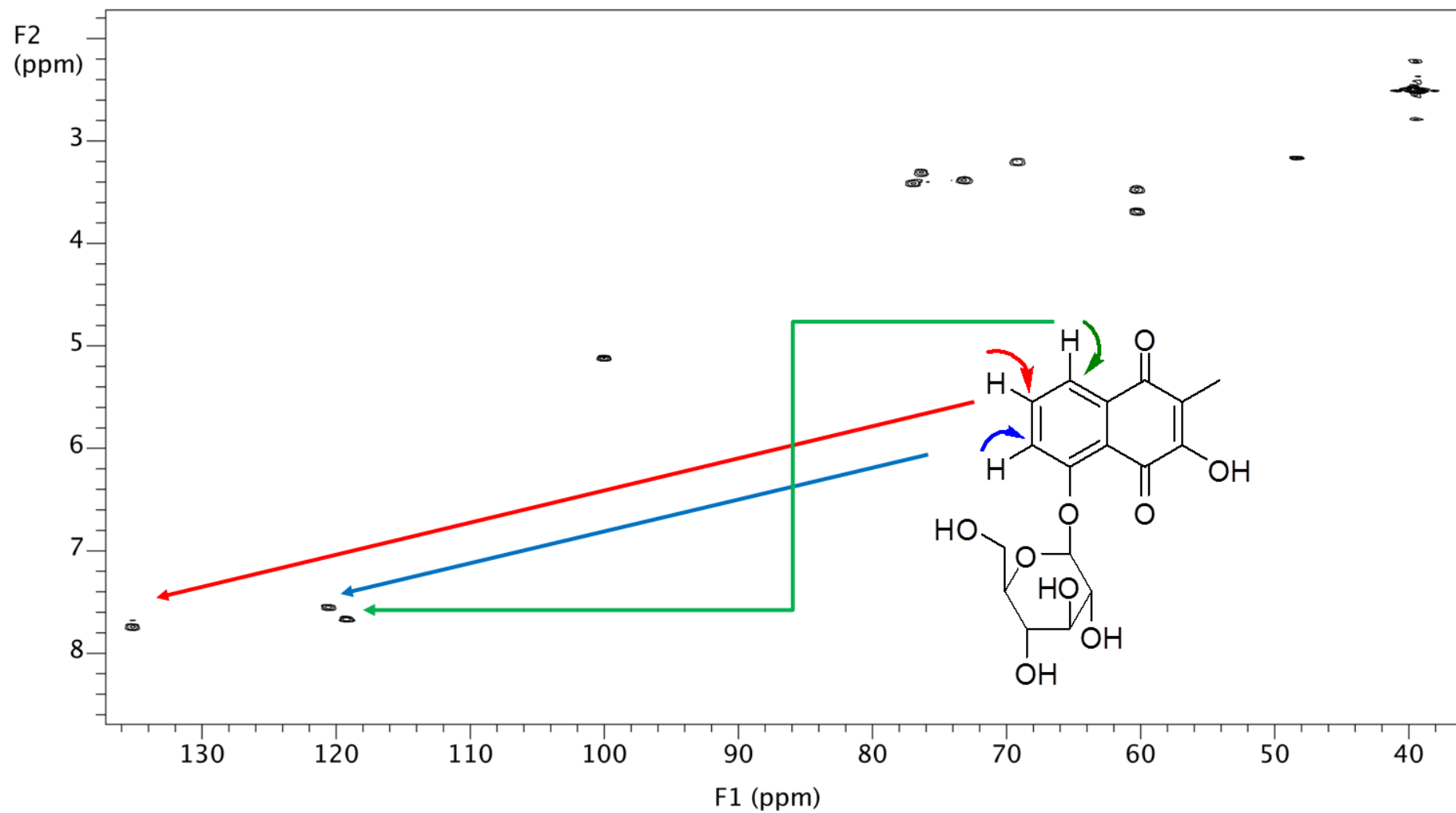


Figure 4.9. 2D gHSQCAD NMR spectrum of droserone-5-O-β-glycoside (4.9).

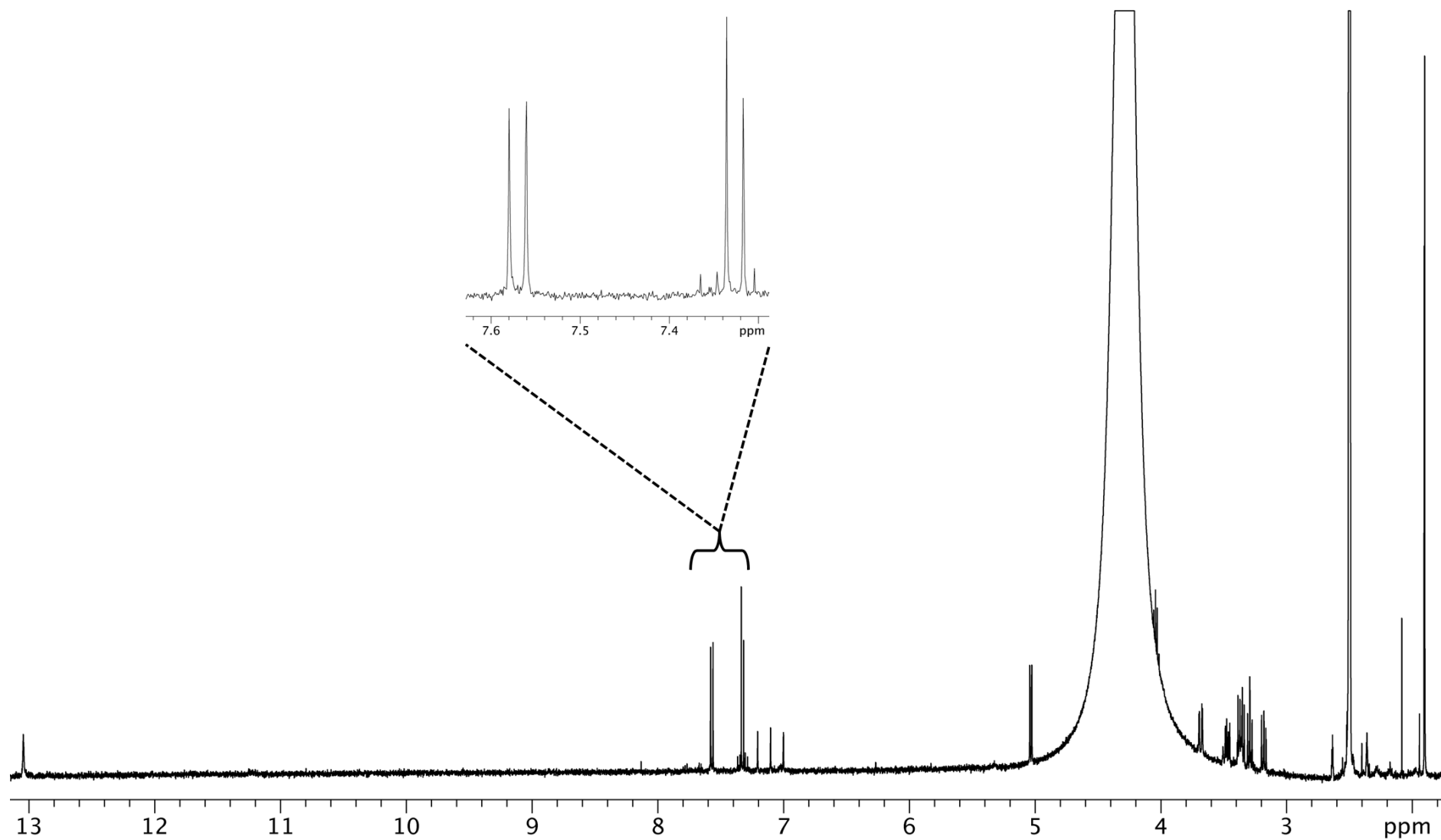


Figure 4.10. ^1H NMR (500 MHz, d_6 -DMSO) spectrum of hydroxydroserone-5-O- β -glycoside (4.10).

While the carbon at C-4 was not observed in the NMR experiments of **4.10**, the chemical shift for C-1 (191.2 ppm) of **4.10** was similar to that of the chemical shift observed for C-1 of hydroxydroserone (**4.8**) (188.8 ppm), indicating that the sugar moiety was not at C-8. This left only position C-5 for the positioning of the sugar moiety as illustrated in **Figure 4.11**.

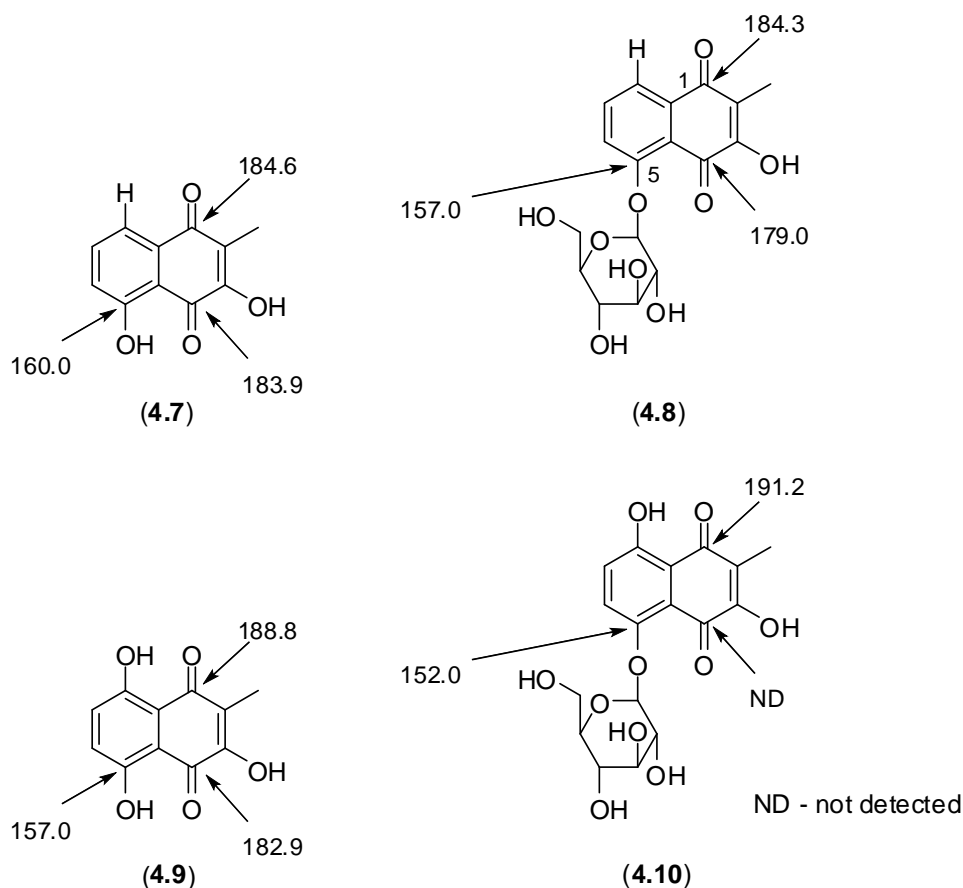


Figure 4.11. Key ^{13}C NMR assignments allowing the sugar moiety for hydroxydroserone-5-O- β -glycoside (**4.10**) to be positioned.

A selective 1D NOE enhancement observed for the proton at δ 7.56 (H-6) to the anomeric proton (H-1') at δ 5.02 (**Figure 4.12**), positioned the sugar moiety adjacent to the proton at δ 7.56 (H-6), while from the 2D gCOSY NMR experiment, H-6 was coupled to the proton at δ 7.32 (H-7). The HMBC correlations from δ 13.05 (8-OH) to 113.7 ppm (C-8a), 126.9 (C-7) and 156.3 (C-8) (**Figure 4.12**), enabled unequivocal assignment of hydroxydroserone-5-O- β -glycoside (**4.10**). Based on this data (as well as the gHSQCAD NMR experiment), both ^1H

and ^{13}C assignments in the literature [219] for positions C-6 and C-7 should be reversed. The sugar moieties of **4.10** and **4.11** had been previously established on the basis of a hydrolysis and subsequent TLC analysis, together with the interpretation of the coupling constants [219, 227].

Table 4.3. ^1H (500 MHz) and ^{13}C (125 MHz NMR spectroscopic data of hydroxydroserone-5-*O*- β -glycoside (**4.10**) in d_6 -DMSO.

Position	δ_{H}, J	$\delta_{\text{C}}^{\text{a}}$	gCOSY	gHMBC	1D NOE
1	-	191.2, s	-	-	-
2	-	118.0, s	-	-	-
3	-	157.9, d	-	-	-
4	-	ND	-	-	-
4a	-	116.9, s	-	-	-
5	-	152.0, s	-	-	-
6	7.56 d, $J = 9.5$ Hz	125.5, d	H-7	C-4a, C-5, C-8	H-1'
7	7.32 d, $J = 9.5$ Hz	126.9, d	H-6	C-5, C-8, C-8a	-
8	-	156.3, s	-	-	-
8a	-	113.7, s	-	-	-
9	1.89, s	8.3, q	-	C-1, C-2, C-3	-
1'	5.02 d, $J = 7.0$ Hz	101.7, d	H-2'	C-5	-
2'	3.35 m	73.2, d	H-1'	C-1', C-3'	-
3'	3.29 m	76.2, d	-	C-2', C-4'	-
4'	3.19 m	69.2, d	H-5'	C-3', C-6'	-
5'	3.37 m	77.0, d	H-4', H-6'b	C-6'	-
6'	3.47 m	60.4, t		C-5'	-
	3.69 dd, $J = 11.5, 1.5$ Hz		H-5'		
3-OH	11.22, s	-	-	-	-
8-OH	13.05, s	-	-	C-7, C-8, C-8a	-
2'-OH	ND	-	-	-	-
3'-OH	ND	-	-	-	-
4'-OH	ND	-	-	-	-
5'-OH	ND	-	-	-	-
6'-OH	ND	-	-	-	-

ND indicates signals were not detected

^a Carbon assignments based on gHSQCAD and gHMBC NMR experiments

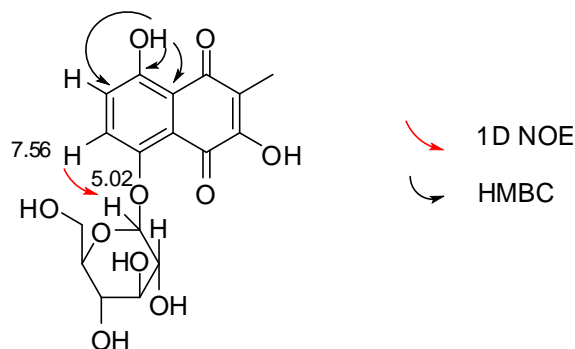


Figure 4.12. Key HMBC correlations and single irradiation NOE NMR enhancement observed in the unequivocal assignment of hydroxydroserone-5-O- β -glycoside (**4.10**).

Of the isolated compounds, plumbagin (**1.267**) displayed the most potent and broad spectrum anti-tumour and anti-microbial activity (**Table 4.1**). It was observed that hydroxydroserone (**4.8**) and its 5-O- β -glycoside (**4.10**) had similar P388 activity, while droserone-5-O- β -glycoside (**4.9**) exhibited a greater than 10 fold increase in P388 activity compared to droserone (**4.7**). While the glycosides were not tested for anti-microbial activity, it was observed that hydroxydroserone (**4.8**) exhibited slight inhibition against *Bacillus subtilis* (5 mm zone of inhibition) and *Trichophyton mentagrophytes* (6 mm), however droserone (**4.7**), displayed no activity against these strains. Plumbagin (**1.267**) is well known for its wide range of biological activities (See Introduction **Section 1.3**) including anti-malarial, anti-microbial, anti-fungal, anti-inflammatory activity and cytotoxicity [75, 229-233]. Droserone (**4.7**) is also known to exhibit slight anti-plasmodial and seed germination activity [231, 232].

4.4 Concluding Remarks

In this study, HPLC-NMR was successfully implemented to rapidly profile secondary metabolites present in the crude extracts of the bulbs of the Australian carnivorous plant, *D. erythrorhiza* subspecies *magna*, resulting in the partial identification of two naphthoquinones (**4.7**) and (**4.8**) and a mixture of the two corresponding naphthoquinone glycosides (**4.9**) and (**4.10**). Subsequent off-line isolation of compounds from the bulb extracts permitted the

unequivocal identification of compounds **4.7-4.10**. As a result of this study, several ^{13}C NMR chemical shift reassignments were established for compounds **4.7**, **4.9** and **4.10**. Chemical investigation of the aerial parts of *Drosera erythrorhiza* subspecies *magna* led to the isolation of plumbagin (**1.267**). Of all the compounds isolated, plumbagin (**1.267**) was observed to possess the greatest anti-tumour and anti-microbial activity, with this potent broad spectrum activity being consistent with the known activity of plumbagin (**1.267**).

Chapter 5

*On-line and Off-line Methodologies for the Identification of Secondary Metabolites from the Marine Red Alga *Plocamium angustum**

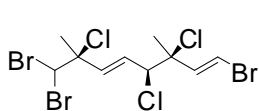
5.1 Introduction

The marine environment has, to date, proven to be a valuable resource for the search of new bioactive secondary metabolites [234-236]. The sheer biodiversity of the marine environment has resulted in the discovery of a vast array of unique secondary metabolites, many of which possess potent biological activities [10, 11, 234, 236, 237]. One feature that differs between marine secondary metabolites compared to plant secondary metabolites is the very common incorporation of halogens into marine secondary metabolites, especially those derived from marine red algae.

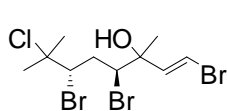
Crude extracts of marine organisms are frequently composed of a complex mixture of compounds, so that any insight into the structure class(es) of the secondary metabolites present is invaluable. To assist in the search and identification of new compounds, hyphenated methodologies (e.g., GC-MS and HPLC-MS) are often employed. The

application of HPLC-NMR has been demonstrated as being able to offer valuable insight into the structure class and the range of secondary metabolites present in a crude extract. This has been successfully demonstrated in a number of chemical profiling studies conducted within the MATNAP research group at RMIT University, both on marine and terrestrial extracts and also in monitoring chemical interconversions [238-241]. HPLC-NMR is advantageous in that it has the ability to separate components *in situ* and is a non-destructive technique. This allows for the full recovery of all components for any further studies such as bioassays or mass spectrometry. It is also an invaluable method of analysis for compounds that are unstable [242].

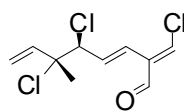
Plocamium is a genus of red algae that has been highly studied, with forty-seven species known to date [8, 243, 244]. Some species of *Plocamium* are found in various worldwide locations such as *P. cartilagineum*, while others such as *P. angustum* are found in specific regions (New Zealand and South Eastern Australia). The genus *Plocamium* is known to produce a vast array of acyclic and cyclic polyhalogenated monoterpenes (5.1-5.21) for which the main differences are associated with the position, orientation and degree of halogen incorporation [238, 245-260]. Of the species of *Plocamium*, *P. cartilagineum* has been studied more widely than any other species, with forty-three compounds having been reported to date [8]. The first reported acyclic polyhalogenated monoterpene was tribromotrichloromonoterpene (5.1), discovered in 1973 from the digestive system of the sea hare of *Aplysia californica* [245]. The structure of this polyhalogenated monoterpene was determined on the basis of X-ray diffraction and it was noted that during analysis, discolouration of the crystal was observed as it yellowed over time, and reflections declined, suggesting decomposition. This was the first naturally occurring compound with such a high degree of halogenation, while it was later determined that the true source of this polyhalogenated terpene was in fact *P. coccineum* [246].



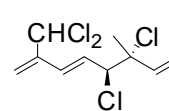
(5.1)



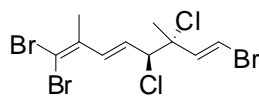
(5.2)



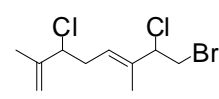
(5.3)



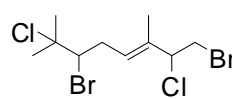
(5.4)



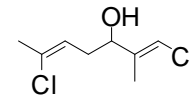
(5.5)



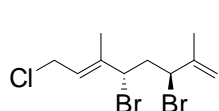
(5.6)



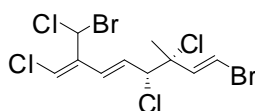
(5.7)



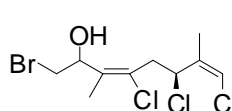
(5.8)



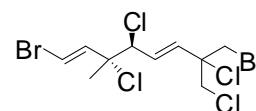
(5.9)



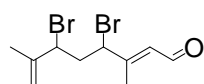
(5.10)



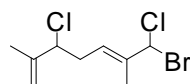
(5.11)



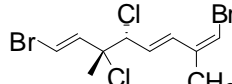
(5.12)



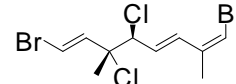
(5.13)



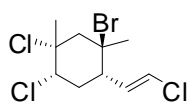
(5.14)



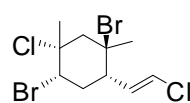
(5.15)



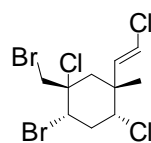
(5.16)



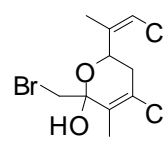
(5.17)



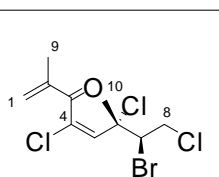
(5.18)



(5.19)

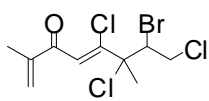


(5.20)

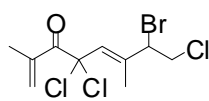


(5.21)

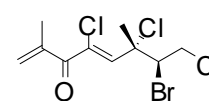
plocamenone
(revised structure)



(5.22)



(5.23)



(5.24)

isoplocamenone
(previously assigned
structure of plocamenone)

The species *P. angustum* is endemic to New Zealand and Australia and has not been as widely studied, with only four secondary metabolites having been reported (5.6, 5.7, 5.20, 5.21) to date [254, 256]. An extract of the red alga *P. angustum* was selected for chemical investigation on the basis of the potent cytotoxicity and significant anti-microbial activities

displayed by the crude extract. In addition, chemical investigation of the alga was motivated by the fact that this genus is known to produce a wide array of polyhalogenated monoterpenes, some of which possess bioactive properties, together with the fact that this species has not been extensively studied [258, 261-267].

5.2 Experimental

5.2.1 General Experimental

For all general experimental procedures and spectroscopic methods, see the Experimental chapter **Section 7.1**. Analytical HPLC method development was conducted on the crude DCM extract and isocratic 70% CH₃CN:H₂O found to be most suited for this separation. HPLC-NMR was conducted at 70% CH₃CN:D₂O with detection at λ_{\max} 254 and 290 nm. Semi-preparative HPLC was conducted using an isocratic solvent system (65% CH₃CN/H₂O) and UV detection at λ_{\max} 254 nm and 290 nm.

5.2.2 Algal material

A specimen of *P. angustum* was collected on 22nd January 2006 from the Borough of Queenscliff near Pt. Lonsdale, Victoria. Two further specimens of the alga were obtained on 13th December 2009 from the same location as the initial collection, with this collection a targeted collection undertaken by Dr Gerald Kraft. The three separate specimens were identified by Dr Gerald Kraft. Voucher specimens designated the codes 2006-04, 2009-14 and 2009-15 respectively are deposited at the School of Applied Sciences (Discipline of Applied Chemistry), RMIT University. A 2 g portion of the frozen *P. angustum* specimen (voucher specimen 2006-04) was extracted with 3:1 MeOH:DCM (40 mL) and evaluated for biological activity as described in **Section 7.1.4**. This crude extract exhibited potent cytotoxicity (IC₅₀ <4.9 µg/mL, see **Table 5.1**), broad spectrum anti-fungal activity against *Candida albicans* (10 mm zone of inhibition), *Trichophyton mentagrophytes* (10 mm zone

of inhibition), and *Cladosporium resinae* (20 mm zone of inhibition) as well as selective anti-bacterial activity against *Bacillus subtilis* (15 mm zone of inhibition). In addition the crude extract also showed a 100% cytotoxic zone when tested against *Herpes simplex* type 1 and *Polio* virus type 1, meaning that it was not possible to distinguish if there was any virus inhibition at all. Further collections of *P. angustum* (voucher codes 2009-14 and 2009-15) were also subjected to cytotoxicity screening, with one of the two collections having an IC₅₀ of <4.9 µg/mL, while the other extract possessed an IC₅₀ of 22.7 µg/mL. All cytotoxicity results are given in **Table 5.1**.



P. angustum

(Voucher code: 2006-04)

Kingdom:	Plantae
Phylum:	Rhodophyta
Class:	Florideophyceae
Subclass:	Rhodymeniophycidae
Order:	Plocamiales
Family:	Plocamiaceae
Genus:	<i>Plocamium</i>
Species:	<i>angustum</i>

Collected by Dr Sylvia Urban, Dr Rick Tinker, Dr Daniel Dias and Mrs Priyanka Reddy



P. angustum

(Voucher code: 2009-14)



P. angustum

(Voucher code: 2009-15)

Table 5.1. Summary of the P388 cytotoxicity of plocamenone (**5.21**) and isoplocamenone (**5.24**) isolated from three separate specimens of *P. angustum*.

Specimen Voucher Code	P388 cytotoxicity IC ₅₀ (µg/mL)
2006-04 (crude extract)	<4.9
2009-14 (crude extract)	<4.9
2009-15 (crude extract)	22.7
plocamenone (5.21) (obtained from 2006-04)	0.158*
plocamenone (5.21) (obtained from 2009-14)	<0.098
plocamenone (5.21) (obtained from 2009-15)	<0.098
mixture of 5.21 and 5.24 (obtained from 2009-14)	<0.098

* Purity of isolated plocamenone was lower on this occasion.

5.2.3 Extraction and Isolation

5.2.3.1 Preparation of the extract of *P. angustum* for on-flow and stop-flow HPLC-NMR analysis

The specimen of *P. angustum* (voucher specimen 2006-04) (50 g) was roughly chopped and extracted with 3:1 MeOH:DCM (1 L). This extract was then decanted and concentrated under reduced pressure and was then sequentially partitioned (trituated) into DCM, MeOH and H₂O soluble extracts respectively. A portion of the DCM extract (64.3 mg) was re-solubilised in 1 mL 70:30 CH₃CN:D₂O and filtered through a 0.45 µm PTFE membrane filter (HP045 Advantec, Japan). For both on-flow and stop-flow HPLC-NMR analyses 50 µL injections (3,217 µg per injection) of the DCM extract was injected using the conditions described in **Section 2.2.1**.

5.2.3.2 Preparation of the extract for off-line isolation of secondary metabolites from *P. angustum*

The remaining algal material (125 g) was extracted using 1 L of 3:1 MeOH:DCM. The crude extract was decanted and concentrated under reduced pressure and then sequentially partitioned (trituated) into DCM, MeOH and H₂O soluble extracts respectively. The DCM extract from the HPLC-NMR analysis was combined with this DCM extract to give a combined DCM fraction (510 mg), which was subjected to flash silica column chromatography using the method described in **Section 7.1**, resulting in sixteen fractions. On the basis of the analytical HPLC analysis and the ¹H NMR spectra one fraction was found to contain the two compounds observed from the HPLC-NMR analysis. Subsequent off-line purification of this fraction was achieved using semi-preparative reversed phase HPLC using the method described in **Section 5.2.1**, to afford plocamenone (**5.21**) (30 mg, 0.15%) and isoplocamenone (**5.24**) (2 mg, 0.01%). While plocamenone (**5.21**) was observed to be a very stable secondary metabolite, isoplocamenone (**5.24**) degraded rapidly. Further to this, it was found that the latter degraded much more rapidly once

purified than when it was present as a mixture with plocamenone (**5.21**). Owing to the degradation observed it was necessary to undertake re-collections of the alga. A separate fraction containing a mixture of plocamenone (**5.21**) and isoplocamenone (**5.24**) (4:1) was obtained from a combination of the two re-collected specimens of the alga, using the same isolation procedure as described for the initial isolation (45 mg, 0.38%). This mixture was utilised for subsequent NMR analysis, HR-GC-MS analysis as well as for the biological screening.

5.3 Results and Discussion

P. angustum was extracted as outlined in **Section 5.2.3.1**. ^1H NMR analysis showed the presence of possibly one major metabolite, while from analytical HPLC analysis, two closely eluting peaks were observed. From this, analytical HPLC method development was undertaken as shown in **Figure 5.1** in order to obtain suitable separation conditions for HPLC-NMR analysis to be undertaken.

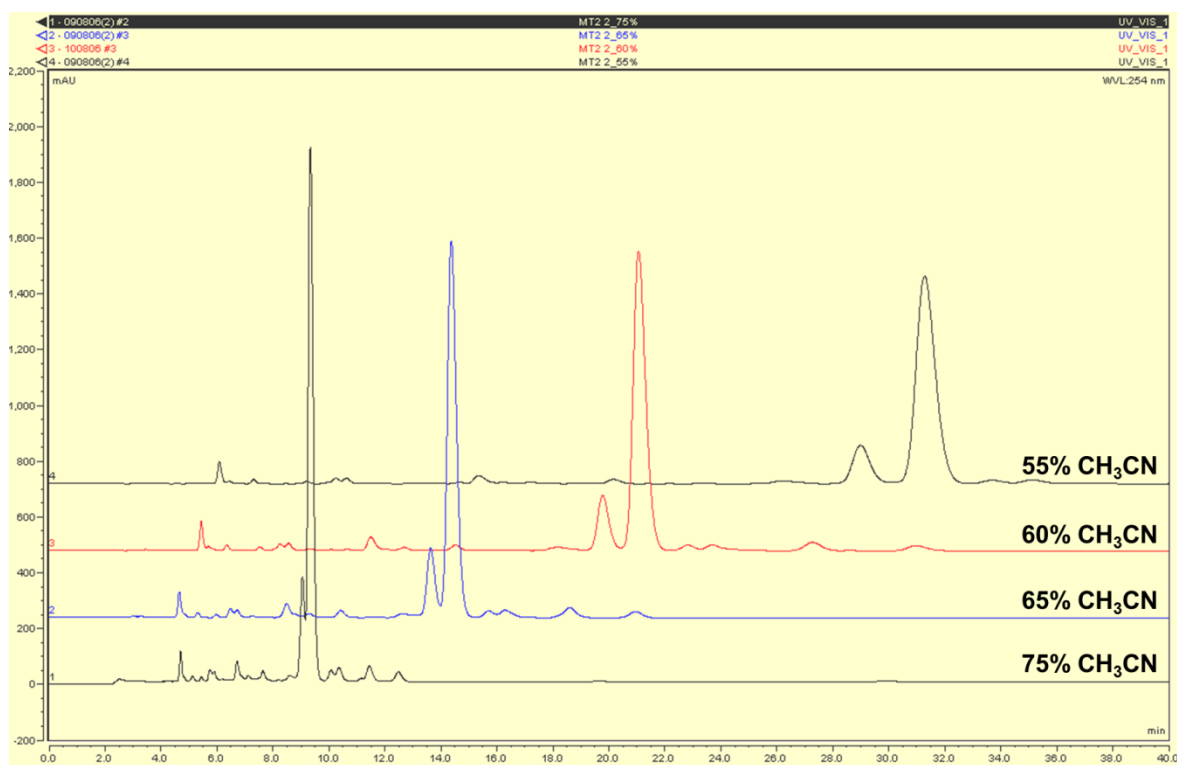


Figure 5.1. Analytical HPLC method development for the DCM extract of *P. angustum*.

On the basis of this HPLC method development, taking into consideration the total run time and separation, 70% CH₃CN:D₂O was selected for the HPLC-NMR analyses. Chemical profiling was conducted employing HPLC-NMR in an attempt to identify the class of secondary metabolites present. HPLC-NMR chemical profiling was achieved using both on-flow and stop-flow analyses. On-flow HPLC analysis clearly indicated the presence of two structurally related secondary metabolites as shown in **Figure 5.2**. Given that the genus *Plocamium* is known to produce polyhalogenated monoterpenes, it was proposed that the compounds present in the crude extract were most likely of this structure class. This was also supported by the presence of the deshielded ¹H NMR chemical shift at δ 4.44 which is characteristic of a halogenated methine.

Stop-flow HPLC-NMR analysis was also carried out in an attempt to elucidate the structures of the two polyhalogenated monoterpenes, previously observed in the on-flow HPLC-NMR analysis. In the stop-flow mode, selected chromatographic peaks can be trapped in the HPLC-NMR flow cell for an indefinite period, thereby allowing for extended acquisition times and consequently greatly improved sensitivity and resolution in the resulting WET-1D ¹H NMR spectra. The major secondary metabolite **5.21** present in the DCM fraction was now subjected to stop-flow HPLC-NMR analysis, whereby acquisition of a WET-1D ¹H NMR spectrum (1 min) (**Figure 5.2**), together with a WET-2D gCOSY (47 min) (**Figure 5.3**) and a gHSQCAD (4 h) (**Figure 5.4**) NMR experiment were carried out. On the basis of the WET-2D gCOSY NMR spectrum obtained (**Figure 5.3**), protons at δ 4.44 (H-7), δ 4.18 (H-8b) and δ 3.74 (H-8a) all shared correlations, suggestive of a methine and methylene with non-equivalent protons. In addition, an aromatic proton at δ 6.18 (H-1b) showed a correlation to the terminal singlet methyl at δ 1.82 (H-9). This NMR data was consistent with the acyclic polyhalogenated monoterpene structure class that has previously been reported from this red alga genus [235, 250, 264, 268].

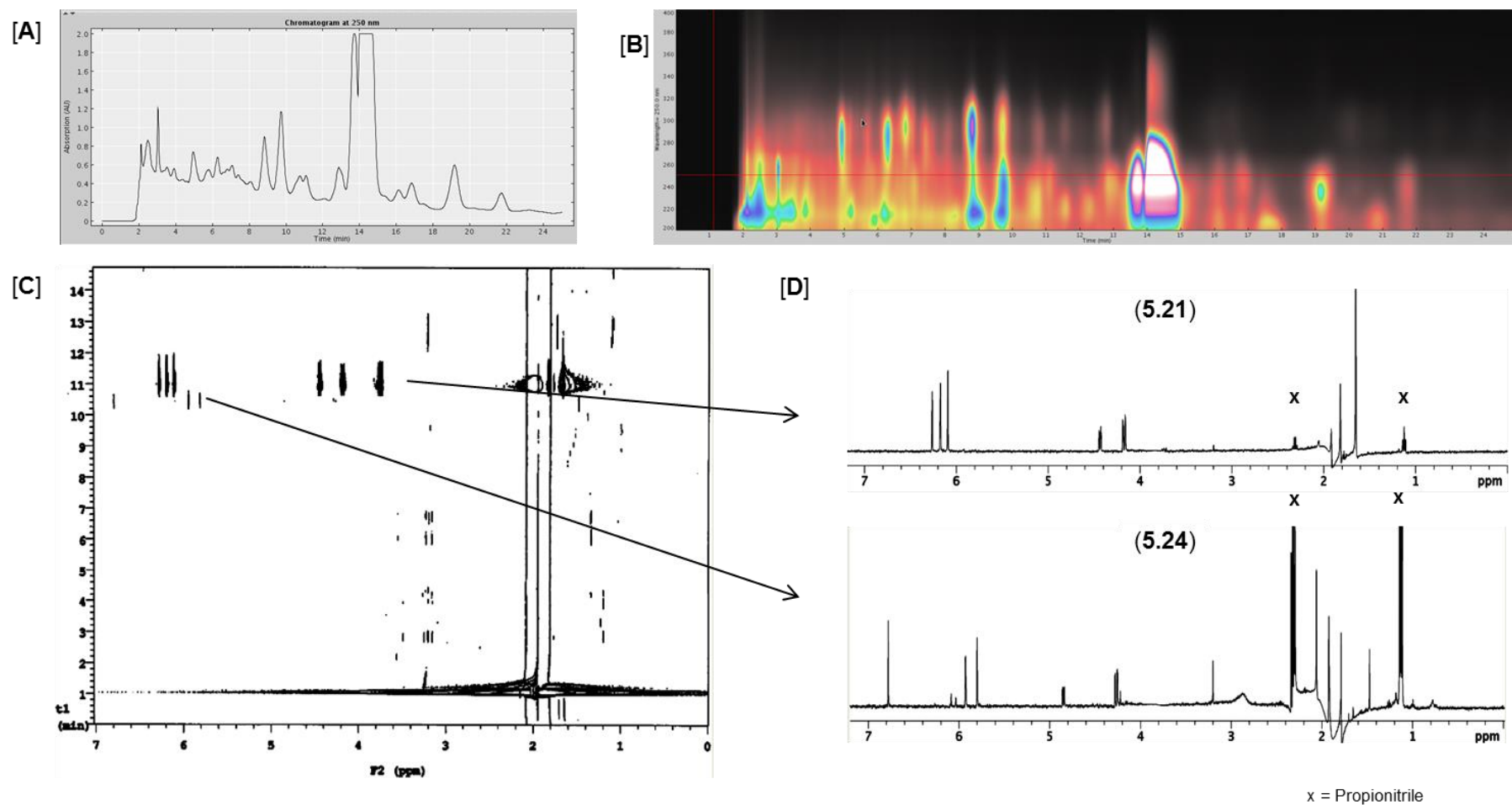


Figure 5.2. [A] HPLC chromatogram of the HPLC-NMR analysis (UV detection at λ_{max} 250 nm), [B] HPLC 2D contour plot of the HPLC-NMR analysis (200-400 nm), [C] On-flow HPLC-NMR contour plot of the DCM extract of *P. angustum* and [D] Stop-flow HPLC-NMR WET-1D ^1H NMR spectra of compounds (5.21 and 5.24).

The WET-2D gHSQCAD NMR experiment (**Figure 5.4**) showed the presence of an olefinic methine (δ 6.26 to 134.0 ppm), an exocyclic double bond (δ 6.18 and δ 6.09 to 133.2 ppm), a deshielded methine (δ 4.44 to 63.5 ppm), a deshielded methylene (δ 4.18 to 48.0 ppm) as well as a singlet methyl (δ 1.65 to 27.9 ppm), while the peak at δ 3.74 observed in the gCOSY was not evident in the WET-1D or gHSQCAD NMR experiments was due to this peak being completely suppressed under the residual water suppression region. On the basis of the analysis of this NMR data, in consultation with the MarinLit database, it was proposed that the major component was plocamenone, an acyclic polyhalogenated monoterpene previously isolated from *P. angustum* (**5.21**) [255, 269]. For this compound to be unequivocally identified, it would be necessary to obtain further NMR spectroscopic evidence of the compound's connectivity, along with mass spectrometric data.

The minor component (**5.24**) that was observed in the on-flow HPLC-NMR analysis was also subjected to stop-flow HPLC-NMR analysis. This allowed for an extended WET-1D ^1H NMR spectrum (20 min) to be acquired (**Figure 5.2**). It was evident that some of the signals in the WET-1D ^1H NMR spectrum were either partially or completely suppressed (under the suppressed HDO peak). Also the low abundance of **5.24** meant that any further WET-2D NMR experiments that were acquired in the stop-flow HPLC-NMR mode failed to provide any conclusive connectivity. It was necessary to undertake an off-line isolation and analysis of this compound in order for its complete structure to be elucidated. In addition, the significant cytotoxicity and anti-microbial activities observed for the crude extract of this marine alga further supported the need for an off-line investigation in order to evaluate and determine the nature of the bioactive compound(s).

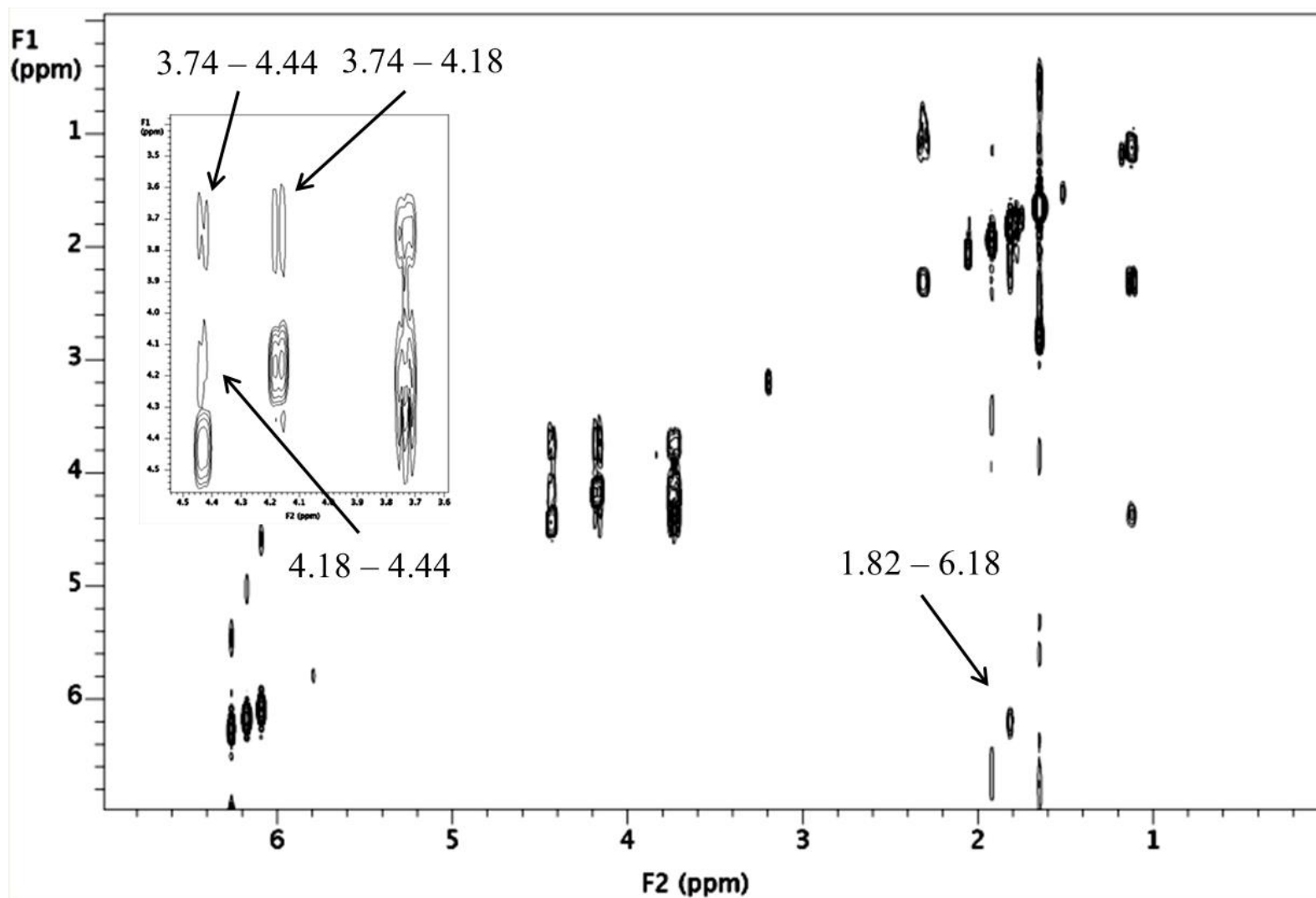


Figure 5.3. Stop-flow HPLC-NMR WET-2D gCOSY NMR spectrum of plocamenone (5.21).

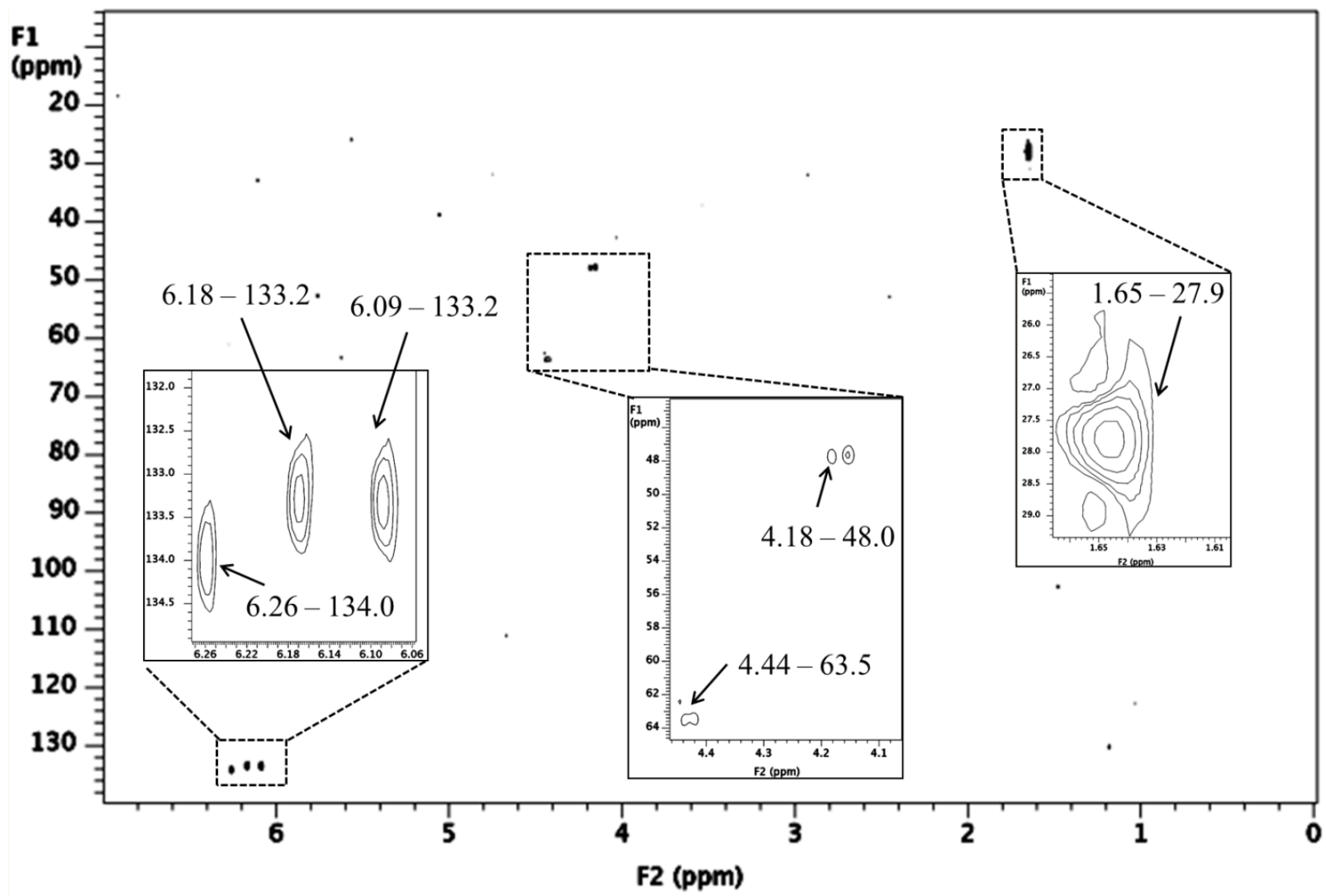


Figure 5.4. Stop-flow HPLC-NMR WET-2D gHSQCAD NMR spectrum of plocamenone (5.21).

The off-line isolation of the secondary metabolites from the red alga *P. angustum* was conducted using the extraction as outlined in **Section 5.2.3.2**. The DCM partitioned fraction was further fractionated by flash silica chromatography to afford sixteen fractions, one of which consisted of the two secondary metabolites previously observed in the HPLC-NMR analyses. This fraction was further purified using semi-preparative reversed phase HPLC (see **Figure 5.5**) using the conditions described in **Section 2.2.1** to afford plocamenone (**5.21**) and the minor structurally related secondary metabolite, isoplocamenone (**5.24**). In the purification of **5.24**, the compound was isolated either as a separate unstable compound or as a mixture with **5.21**, since the stability of **5.24** could be prolonged when isolated as a mixture.

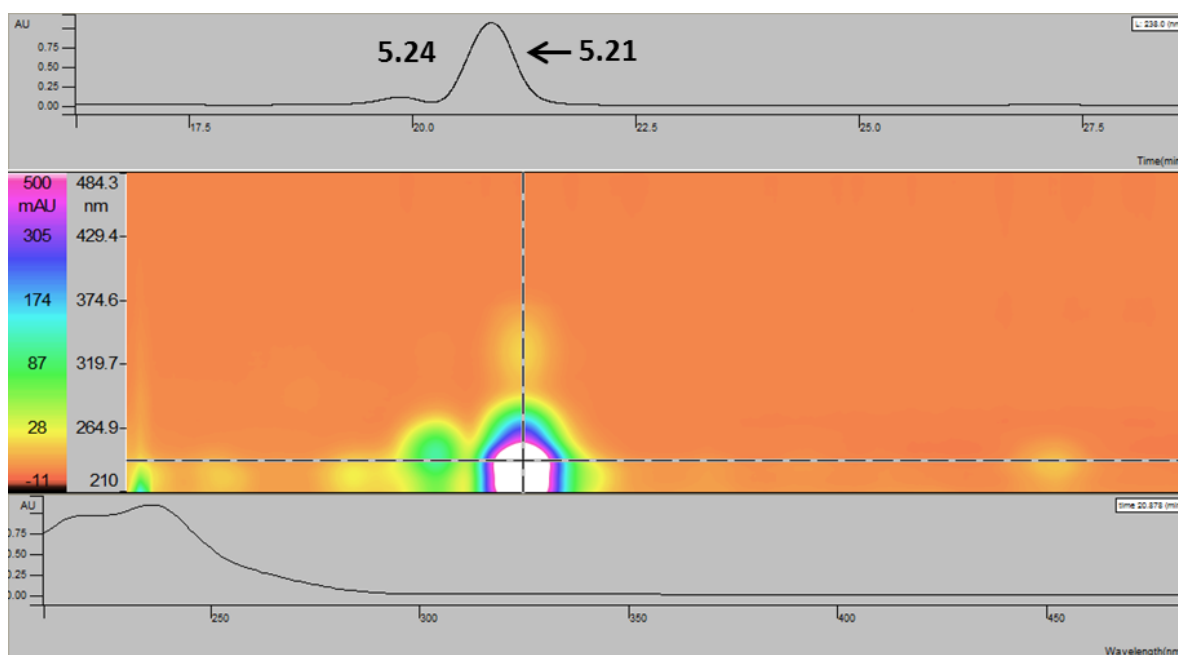


Figure 5.5. Semi-preparative HPLC chromatogram with 2D contour plot showing the isolation of plocamenone (**5.21**) and isoplocamenone (**5.24**), as well as the extracted UV profile of the major compound, plocamenone (**5.21**).

The structure of plocamenone (**5.21**) was established by 1D (^1H NMR given in **Figure 5.6**) and 2D NMR analysis (see **Table 5.2**), along with mass spectrometry. 2D NMR experiments confirmed the structure of plocamenone, a marine secondary metabolite

previously reported as possessing structure (**5.24**), isolated from *P. angustum* [254-256, 269, 270].

The structure of plocamenone has been the focus of several structural revisions. Plocamenone was first reported in 1979 and proposed as **5.22** [254], but in the same year the structure was revised to **5.24** [255]. In 1983 the structure was revised back to **5.22**, and then in 1984 further revisions to **5.23** were concluded [256, 270]. This structure was deemed to be incorrect and was again revised back to **5.24** [269]. In 1997 the structure was again incorrectly described as **5.23** [271] and finally in 2010 plocamenone was once again reported as **5.24** [272]. While all NMR chemical shifts were consistent with those given in literature sources [254, 256, 270], no complete 2D NMR analysis was reported in the structural elucidation/revisions. This is the first complete 2D NMR assignment of plocamenone, and the first assignment of its double bond geometry, which has revised the structure of plocamenone from (**5.24**) to (**5.21**).

Table 5.2. ^1H (500 MHz) and ^{13}C (125 MHz) NMR data for plocamenone (**5.21**) in CDCl_3 .

position	δ_{H} <i>J</i>	δ_{C}	gCOSY	gHMBC
1	6.13, s	131.3, t	H-10	C-2, C-3, C-10
2	-	141.8, s	-	-
3	-	191.5, s	-	-
4	-	129.9, s	-	-
5	6.20, s	133.4, d	-	C-3, C-4, C-6, C-7, C-9
6	-	69.0, s	-	-
7	4.36, dd, <i>J</i> = 3, 9 Hz	62.2, d	H-8a, H-8b	C-6, C-8, C-9
8a	3.72, dd, <i>J</i> = 9, 12 Hz	46.4, t	H-7, H-8b	C-7
8b	4.24, dd, <i>J</i> = 3, 12 Hz		H-7, H-8a	C-6
9	1.75, s	26.9, q	-	C-5, C-6, C-7
10	1.95, s	16.6, q	H-1	C-1, C-2, C-3

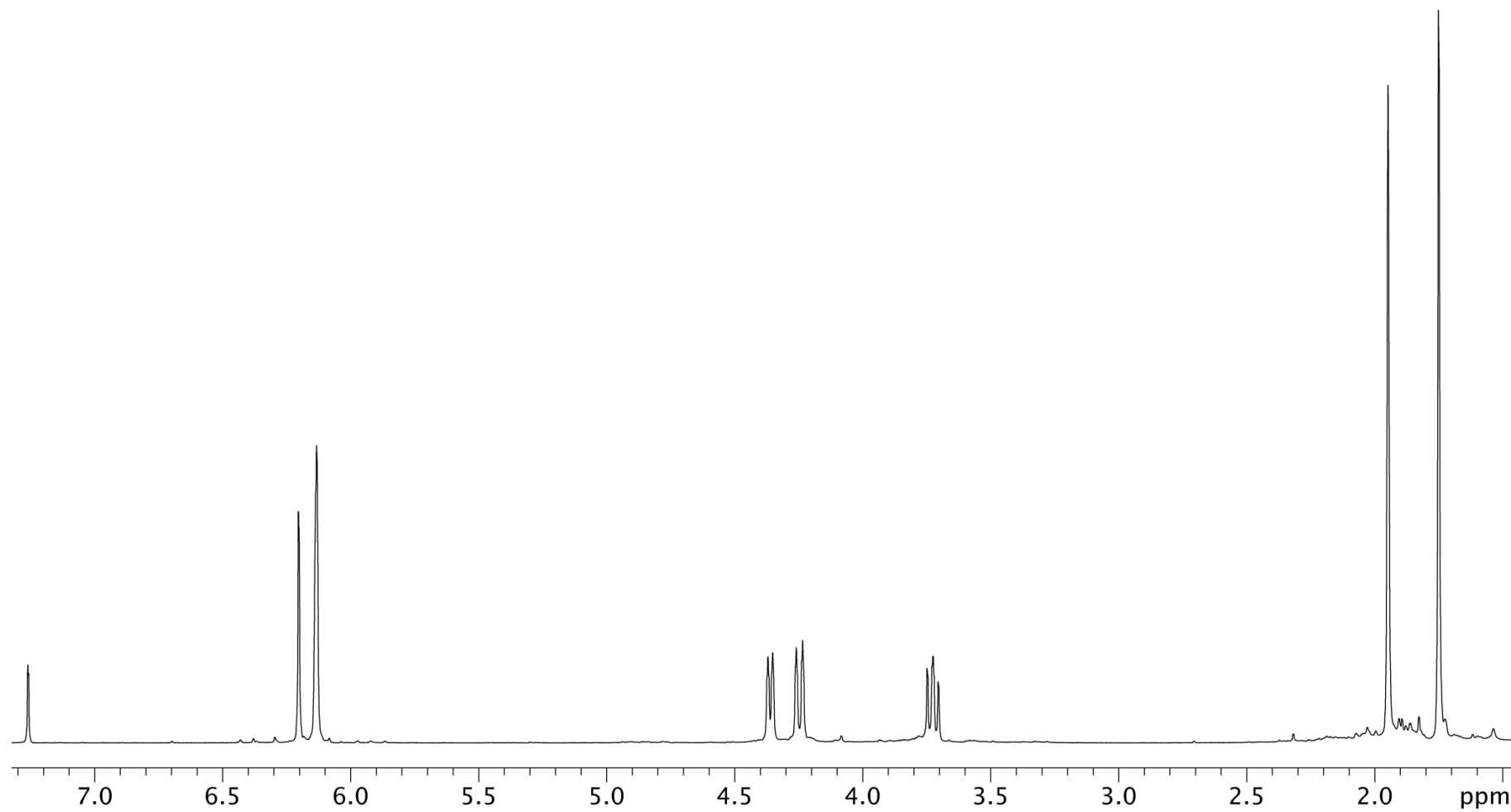


Figure 5.6. ^1H NMR (500 MHz, CDCl_3) spectrum of plocamenone (**5.21**).

The assignment of *R* or *S* configurations to stereogenic centers in halogenated monoterpenes is not a trivial matter. Fortunately, in 1975 Mynderse and Faulkner observed, for compounds whose structures were confirmed by X-ray crystallography, that the ^1H NMR chemical shift of the position 10 methyl varied in a predictable manner depending on the relative configurations at positions 6 and 7 [248, 259, 266, 268, 273-276]. Crews expanded these rules by making use of the more reliable and more discernible differences in ^{13}C NMR chemical shifts for the position 10 methyl carbon atom [275]. Here a chemical shift difference of 3 ppm between the (*R*, *S*) and (*R*, *R*) configurations have been reported, in particular chemical shifts of ca. δ 28 and 25 are characteristic of $6R^*$, $7R^*$ (or $6S^*$, $7S^*$) and $6S^*$, $7R^*$ (or $6R^*$, $7S^*$) relative configurations, respectively [275]. As such the relative configuration for plocamenone was assigned in 1985 by applying the empirical rules of Mynderse and Faulkner and Crews to the proton and carbon chemical shifts of the methyl group (H-10, δ 1.75; C-10, 26.8 ppm). In particular, the chemical shift of δ 26.8 ppm was consistent with a $6R^*$, $7R^*$ (or $6S^*$, $7S^*$) relative configuration. While these chemical shifts supported an *RS* configuration, attempts to employ calculated ^1H NMR chemical shifts to resolve the double bond geometry of plocamenone were not fruitful [269].

The minor analogue isoplocamenone (**5.24**) was subjected to similar analyses to that of plocamenone (**5.21**). However, owing to the instability of this compound, particularly in CDCl_3 , a complete characterisation in this NMR solvent was only possible when acquired as a mixture of **5.24** and **5.21** (^1H NMR spectrum shown in **Figure 5.7**). Subsequent re-isolations of **5.24** were carried out, in an attempt to characterise and identify the compound, however the instability of this compound continually resulted in rapid degradation being observed after each isolation attempt. ESI-MS analysis of **5.24** was only possible if undertaken immediately after semi-preparative reversed phase HPLC purification, providing that the fraction containing the compound was not evaporated to dryness.

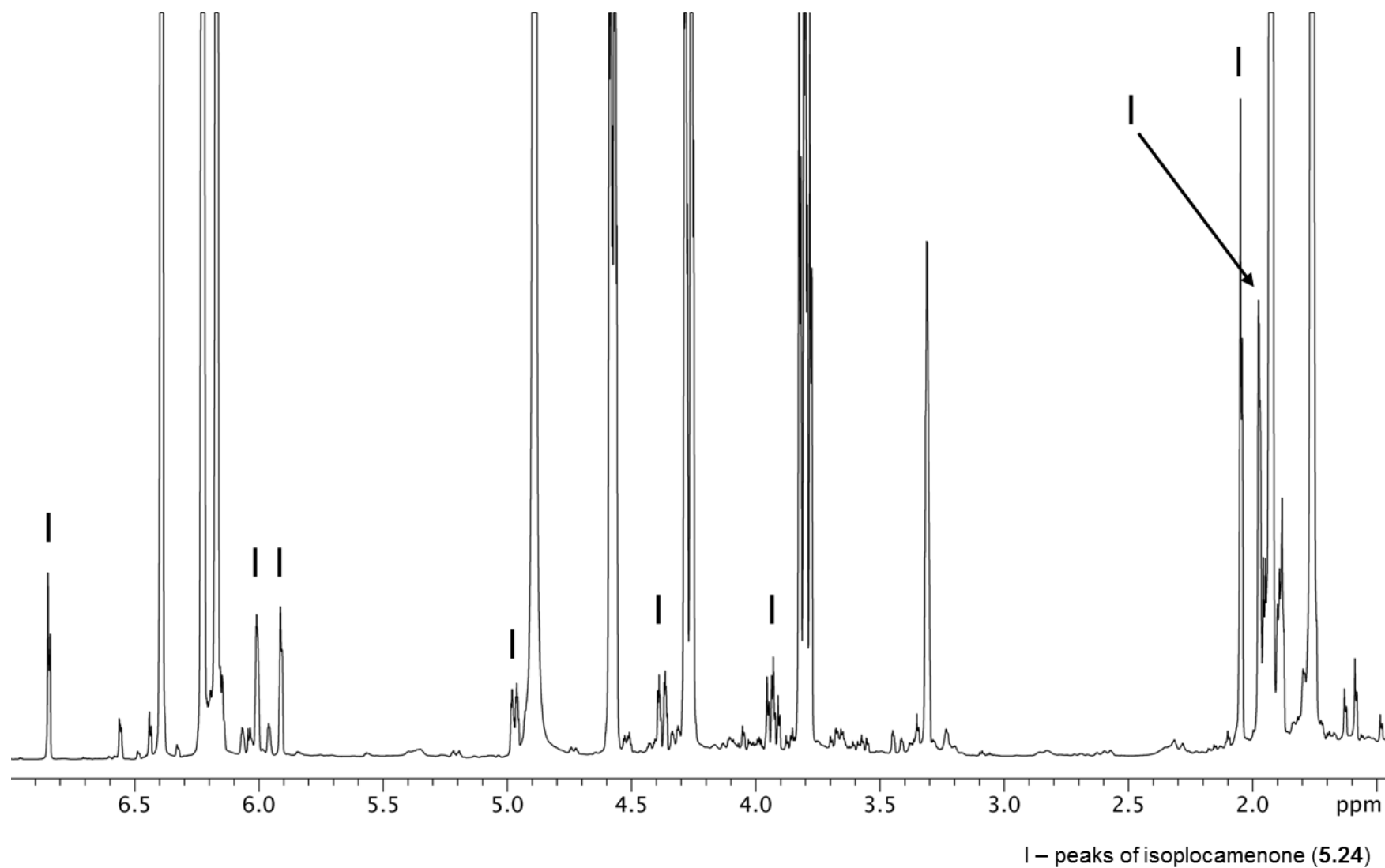


Figure 5.7. ^1H NMR (500 MHz, CD_3OD) spectrum of isoplocamenone (5.24) in a mixture with plocamenone (5.21).

Table 5.3. ^1H (500 MHz) and ^{13}C (125 MHz) NMR data for isoplocamenone (**5.24**) in CD_3OD .

Position	δ_{H} (J in Hz)	$\delta_{\text{C}}^{\text{a}}$, mult	gCOSY	gHMBC
1a	5.92, d, $J = 2.0$ Hz	129.1, t	H-10	C-2, C-3, C-10
1b	6.02, d, $J = 2.0$ Hz			
2	-	143.3, s	-	-
3	-	192.1, s	-	-
4	-	133.5, s	-	-
5	6.85, s	140.9, d	-	C-3, C-4, C-6, C-7, C-9
6	-	69.8, s	-	-
7	4.97, dd, $J = 3.0, 9.0$ Hz	61.6, d	H-8a, H-8b	C-6, C-8, C-9
8a	3.94, dd, $J = 9.0, 12.0$ Hz	47.1, t	H-7, H-8b	C-7
8b	4.38, dd, $J = 3.0, 12.0$ Hz		H-7, H-8a	C-6
9	2.05, s	26.3, q	-	C-5, C-6, C-7
10	1.98, s	18.0, q	H-1	C-1, C-2, C-3

^aCarbon NMR assignments based on gHSQCAD and gHMBC NMR experiments

The positive mode ESI-MS of **5.24** displayed an m/z of 335 $[\text{M}+\text{H}]^+$, which was isobaric with that observed for plocamenone (**5.21**), with an isotopic ratio and splitting also comparable to that of plocamenone (**5.21**). HR-GC-MS analysis of **5.24** was carried out on a sample also containing **5.21** with the chromatographic peak of **5.24** displaying an m/z of 298.9397 $[\text{M}-\text{Cl}]^+$, consistent with $\text{C}_{10}\text{H}_{12}\text{O}^{35}\text{Cl}_2^{81}\text{Br}$ (calculated for 298.9403). It was noted that this compound's stability could be prolonged when isolated in the presence of plocamenone (**5.21**) and so it was decided that this minor secondary metabolite would be isolated as a mixture with **5.21** to permit further characterisation and identification to be carried out. It must be noted that even in a mixture, this minor compound degraded within two weeks. On the basis of the NMR analyses conducted on the mixture of plocamenone (**5.21**) and isoplocamenone (**5.24**) in CD_3OD , complete characterisation was possible by

NMR analysis. Extensive analysis of the 1D and 2D NMR data (**Table 5.3**), in combination with the mass spectrometric evidence, established that the minor analogue had the same connectivity as that of plocamenone (**5.21**) and was an isomer of this compound.

Owing to the instability of **5.24**, any further separation and characterisation could not be conducted as a means to ascertain the structure of this minor structural analogue. Comparison of the NMR data indicated that the most significant chemical shift differences for plocamenone (**5.21**) and the minor analogue **5.24** in CD₃OD (**Table 5.4**) were observed for the ¹H NMR chemical shifts at positions 1a, 1b, 5, 7 and 10, whilst the greatest differences in the ¹³C NMR chemical shifts were evident at positions 1, 4 and 5.

Table 5.4. ¹H and ¹³C NMR chemical shift differences for plocamenone (**5.21**) and isoplocamenone (**5.24**) (500 MHz, CD₃OD).

Position	plocamenone (5.21)		isoplocamenone (5.24)		Differences (ppm)	
	δ_{H}	$\delta_{\text{C}}^{\text{a}}$	δ_{H}	$\delta_{\text{C}}^{\text{a}}$	$\Delta\delta_{\text{H}}$	$\Delta\delta_{\text{C}}$
1a	6.17, s	132.3, (t)	5.91, s	129.0, (t)	+0.26	+3.3
1b	6.23, s		6.00, s		+0.23	
2	-	143.3, (s)	-	143.5, (s)		-0.2
3	-	193.2, (s)	-	192.3, (s)		+0.9
4	-	130.5, (s)	-	133.7, (s)		-3.2
5	6.39, s	134.7, (d)	6.84, s	140.8, (d)	-0.45	-6.1
6	-	70.7, (s)	-	69.7, (s)		+1.0
7	4.57, dd, (3, 9.5)	63.5, (d)	4.97, dd, (2.5, 9)	61.5, (d)	-0.40	+2.0
8a	3.80, dd, (9.5, 12)	47.6, (t)	3.93, dd, (9, 13)	47.1, (t)	-0.13	+0.5
8b	4.27, dd, (3, 12)		4.37, dd (2.5, 13)		-0.10	
9	1.93	16.6, (q)	1.97, s	18.0, (q)	-0.04	-1.4
10	1.76	27.6, (q)	2.05, s	26.2, (q)	-0.29	+1.4

^a Carbon assignments based on gHSQCAD and gHMBC NMR experiments.

Inspection of ^1H and ^{13}C NMR chemical shifts reported for structurally related halogenated terpenes such as compounds (5.25-5.28) (Figure 5.8) established that a configurational change of the stereogenic centers only results in small chemical shift differences being observed [248, 250, 275]. Given that the ^1H and ^{13}C NMR chemical shift differences between plocamenone (5.21) and the minor analogue 5.24 (Table 5.4) were much greater than for those observed for changes around stereogenic centers, it was concluded that the structures of 5.21 and 5.24 did not differ by a relative configuration change. This ultimately led to the conclusion that the two structures differed in terms of their double bond geometry. Since the double bond geometry of plocamenone had not been previously established, the isolation of this isomer provided an opportunity to resolve this structural feature.

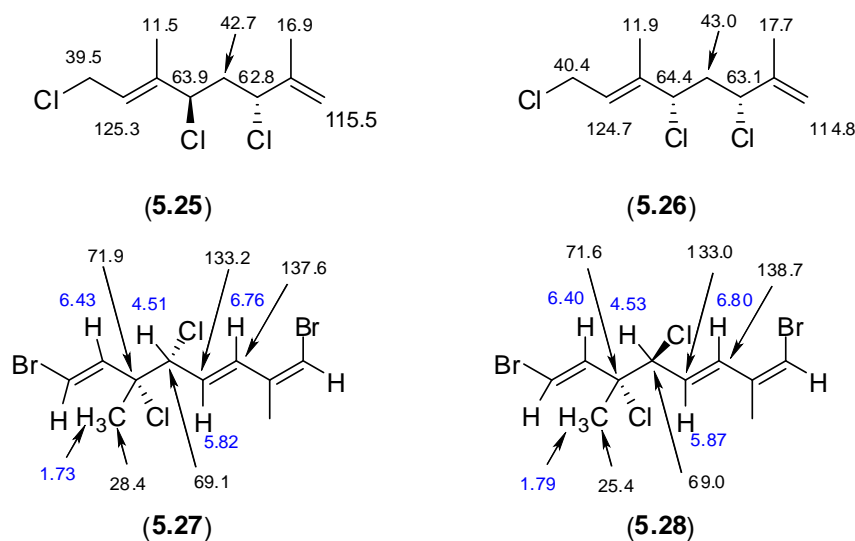


Figure 5.8. ^1H and ^{13}C NMR chemical shift comparisons of configurational isomers.

A change in the double bond geometry from *E* to *Z* can have a significant effect on ^1H NMR chemical shifts. This was apparent when comparing the NMR data for the polyhalogenated compounds (5.29–5.31) [248]. From these compounds (5.29-5.31) it was observed that once again a configurational change had little effect on surrounding chemical shifts when comparing compounds 5.29 and 5.30, while comparison of the chemical shifts of compounds 5.30 and 5.31, the change in double bond geometry from *E*

to *Z* has a significant effect on surrounding chemical shifts, with a difference of 0.26 ppm observed for the α position between compounds **5.30** and **5.31** [248].

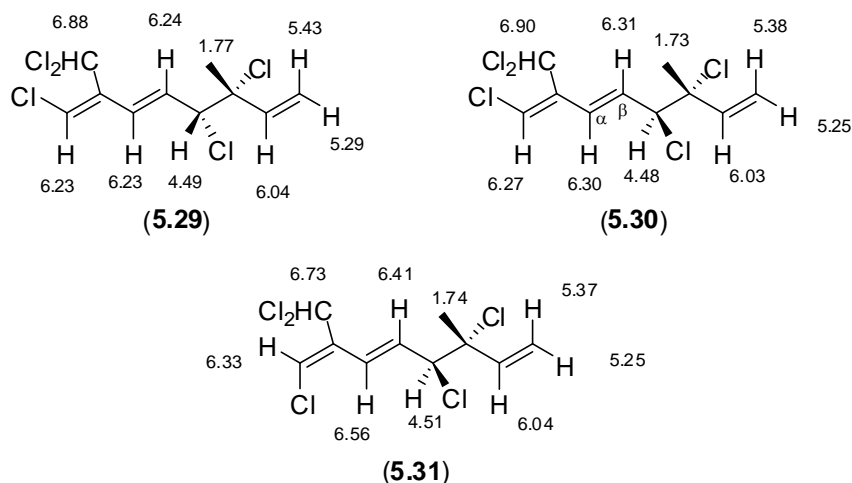
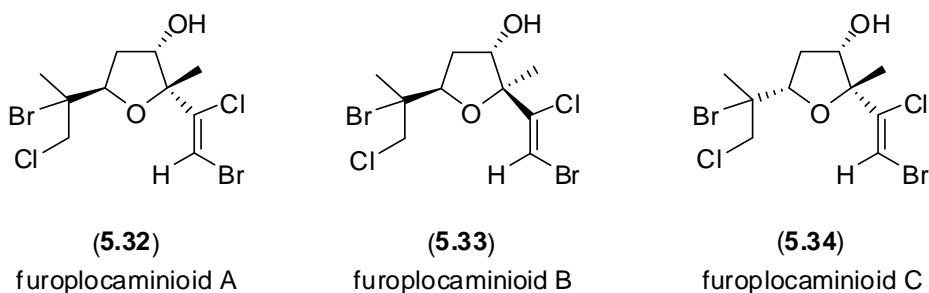


Figure 5.9. ^1H NMR comparison of configurational and double bond isomers.

In trisubstituted olefins it has been documented that the olefinic carbons of the *E* isomer reside at a higher field [277] and in the case of 1,2-disubstituted ethylenes the rule $\delta E < \delta Z$ is observed in the ^{13}C NMR data of the olefinic carbons [278, 279]. In addition, the regiochemistry of furoplocamioids A to C (**5.32–5.34**), which possess a 1,2-dihalovinyl system were determined on the basis of the ^{13}C NMR chemical shifts of the substituted vinyl carbon [280].



A range of model compounds clearly established that the chemical shift of the olefinic proton and associated carbon resonance in trisubstituted olefinic systems are deshielded for compounds with *Z* geometry. This trend is in line with the differences observed in the

^1H and ^{13}C NMR chemical shifts of plocamenone (**5.21**) and isoplocameone (**5.24**), for the olefinic H-5 and the associated olefinic carbon resonances at C-4 and C-5 (**Table 5.4**). Further to this, the geometry of the double bond could be assigned by comparison of the observed chemical shifts for the olefinic H-5 to those calculated either through NMR prediction software such as Advanced Chemistry Development (ACD) labs™ and ChemDraw™ [281, 282] or those calculated from tables of substituent shielding constants which support compound (**5.24**) as being the *Z* isomer of plocamenone (**5.21**) [247, 283-285]. This trend for both the ^1H and ^{13}C NMR chemical shifts for the *E* isomer to be more shielded than for the corresponding *Z* isomer is also evident in the structure of cartilagineal (**5.3**) [247].

On the basis of the significant chemical shift differences observed for the olefinic ^1H and ^{13}C NMR resonances for plocamenone (**5.21**) and the minor analogue as seen in **Table 5.4**, it was concluded that the minor analogue **5.24** was the *Z* double bond geometric isomer of plocamenone (**5.21**). This meant that the double bond geometry that had been previously depicted in the structure of plocamenone should now be revised to an *E* configuration. This isomer **5.24** has been attributed the name isoplocamenone and on biosynthetic grounds the same relative configuration is assigned to both isoplocamenone (**5.24**) and plocamenone (**5.21**). The ^1H and ^{13}C NMR chemical shifts of the position 10 methyl support an *RS* configuration for both compounds [248].

It is worth noting that HPLC-NMR analysis of *P. angustum* was essential in recognising the existence of the closely related plocamenone structural analogue **5.24** and greatly assisted in the eventual isolation and identification of this unstable compound. It may be speculated that isoplocamenone (**5.24**) could potentially arise as an artefact formed under the extraction conditions. To study this phenomenon, a portion of the frozen alga was extracted with DCM and immediately analysed by analytical HPLC. This confirmed the presence of both plocamenone (**5.21**) and isoplocamenone (**5.24**) in the crude extract. This was also supported by the detection of both compounds in the crude extracts analysed by HPLC-NMR which were also conducted on the frozen alga and immediately

analysed. On the basis of this evidence, it is suggested that both compounds are natural products. The isolation of double bond isomers from the one organism has been documented on other occasions especially in marine algae [248, 286, 287].

Plocamenone (**5.21**) has been previously reported to exhibit cytotoxicity in the AMES test, as well anti-bacterial activity towards *Escherichia coli* [255, 271]. Plocamenone (**5.21**) as well as a mixture of plocamenone (**5.21**) and isoplocamenone (**5.24**) were subjected to biological screening as detailed in **Section 5.2.2**. It was observed that the initial plocamenone (**5.21**) isolated possessed significant cytotoxicity in the P388 murine leukemia cell assay, with an observed IC₅₀ of 0.158 µg/mL (**Table 5.1**). The IC₅₀ for the anti-tumour compound adriamycin, also known as doxorubicin, was 0.031 µg/mL in this assay. Plocamenone (**5.21**) also showed activity when tested as an inhibitor of bacterial and fungal pathogens. It was observed that at a concentration of 30 µg/mL, plocamenone (**5.21**) inhibited the growth of *Bacillus subtilis*, *Candida albicans* and *Cladosporium resinae* with inhibition zones (radius of inhibition outside the 6 mm diameter application disc) of 10, 2 and 6 mm zones respectively. At a concentration of 30 µg/mL the standard compound chloramphenicol had an inhibition zone of 12 mm against *B. subtilis* and the standard compound nystatin had inhibition zones of 12 mm against both *C. albicans* and *C. resinae*. The reported activity towards *E. coli* of plocamenone (**5.21**) [271] was not observed in this biological activity screening of plocamenone (**5.21**), however the reason for this is unclear.

Subsequent biological testing of a highly purified sample of plocamenone (**5.21**) isolated from the two re-collected specimens of the alga, along with a mixture of plocamenone (**5.21**) and isoplocamenone (**5.24**) (present in a ratio of approximately 4:1) both displayed an IC₅₀ of <97.5 ng/mL (**Table 5.1**). Owing to the instability of isoplocamenone (**5.24**), this compound was only able to be tested as a mixture with plocamenone (**5.21**). However, given the greater abundance of **5.21** (4:1), the activity observed for the mixture of the two compounds is presumed to be due to the major compound, plocamenone (**5.21**).

5.4 Concluding Remarks

HPLC-NMR chemical profiling of the red alga *P. angustum* with subsequent off-line HPLC isolation resulted in the identification of plocamenone (**5.21**), together with a new, unstable double bond isomer, isoplocamenone (**5.24**). The complete structures of plocamenone (**5.21**) and isoplocamenone (**5.24**) were established on the basis of extensive 2D NMR analysis and by recognising chemical shift trends for closely related trisubstituted olefins. This represents the first complete structure assignment for plocamenone (**5.21**) leading to a structural revision for this compound, along with its selective anti-bacterial activity towards *Bacillus subtilis* and moderate broad spectrum anti-fungal activity. The use of HPLC-NMR to conduct this study clearly demonstrated that it is an invaluable method for the analysis of unstable compounds.

Chapter 6

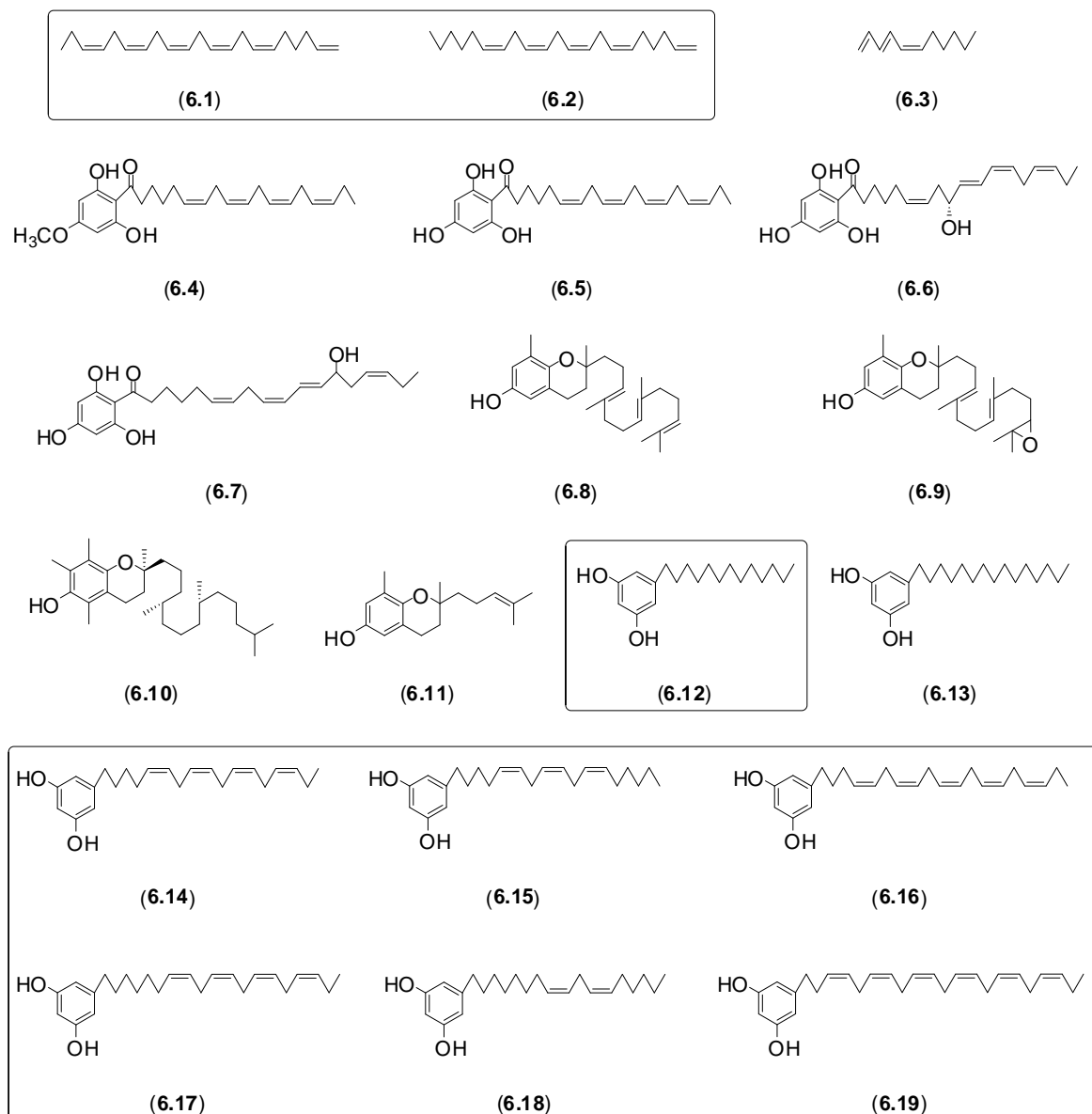
*HPLC-NMR Chemical Profiling and Dereplication Studies of the Marine Brown Alga, *Cystophora torulosa**

6.1 Introduction

To date, the genus *Cystophora* consists of twenty-six accepted species, all of which have been extensively studied [288]. The genus is endemic to Australasia with most species only found around Australia [289]. A range of structural classes of compounds have been reported from various species of *Cystophora* including polyenes (6.1-6.3), phloroglucinol derivatives (6.4-6.7), polyprenyl chromans (6.8-6.11), resorcinol derivatives (6.12-6.15), farnesylacetone derivatives (6.20-6.31), carotenoids (6.32), steroids (6.33), meroditerpenes (6.34), isoprenoid dihydroquinones (6.35-6.37), tetraprenyltoluquinols (6.38-6.39) amongst others [289-292].

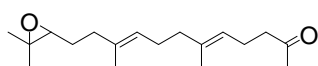
The first study conducted on a species of the genus *Cystophora* was in 1977, with four classes of compounds reported [293]. This included two polyenes (6.1-6.2), a phloroglucinol derivative (6.4), five polyprenyl chromans (6.5-6.9) and four resorcinols (6.12-6.15), which were all isolated from *Cystophora torulosa* [293]. In an earlier report of

the isolation of secondary metabolites from the brown alga *Sargassum tortile*, it was established that polyprenyl chromans similar to compounds **6.8** and **6.9** stimulate the settling and metamorphosis of *Coryne uchidai* larvae [294].

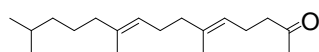


Later it was discovered that the farnesylacetone epoxide (**6.20**) reported from *C. moniliformis*, displayed anti-convulsant activity in mice [295]. The phloroglucinol derivatives (**6.5-6.6**) isolated from *C. moniliformis* displayed potent inhibition of oxidative phosphorylation, while the resorcinol derivative (**6.14**) from *C. torulosa* showed only slight inhibition of oxidative phosphorylation [296]. The study of four different species of

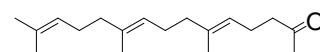
Cystophora afforded many secondary metabolites [297], including phloroglucinol derivatives (6.5-6.6) from *C. monilifera* and polyenes (6.1-6.2) as well as the phloroglucinol (6.5) from *C. congesta* [297]. Within the same study, it was found that *C. expansa* contained the phloroglucinols (6.4-6.5), as well as δ -tocotrienol (6.8), while *C. scalaris* afforded the phloroglucinols (6.4-6.5) [297]. The isoprenoid dihydroquinones (6.35-6.37) were isolated from an unknown species of *Cystophora* from Western Australia [298]. A further study of *C. moniliformis* afforded α -tocotrienol (6.10) as well as compounds (6.22-6.25 and 6.40-6.46) [299]. The crude extract of *C. congesta* was found to possess cardiovascular activity in hypertensive rats [300], however it was from an inactive fraction that the phloroglucinol trimer (6.47) was isolated [300], with a separate report of polymeric phloroglucinol derivatives similar to that of 6.47 being isolated from the same species [301]. The sperm attraction of cystophorone (6.3), isolated from *C. siliquosa*, was established in 1984 [302] with activity within the range of other hormone systems in brown algae [302]. A number of carotenoids such as 6.32 were then isolated in 1987 from the two species *C. retroflexa* and *C. torulosa* [303]. A year later, a number of sesquiterpenes (6.26-6.28), related to farnesylacetone as well as the cyclic sesquiterpene (6.48) were isolated from *C. moniliformis*, where preliminary feeding studies suggested that geranylacetone (6.29) was a deterrent of *Tripnerstes gracilis* and *Subninella undulata* [304].



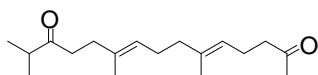
(6.20)



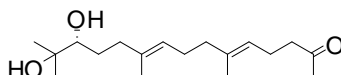
(6.21)



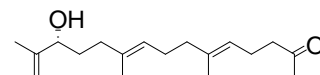
(6.22)



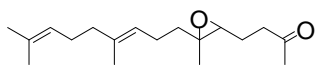
(6.23)



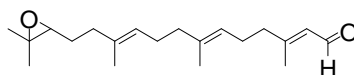
(6.24)



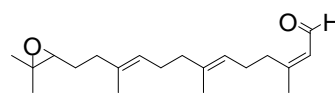
(6.25)



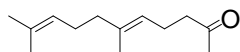
(6.26)



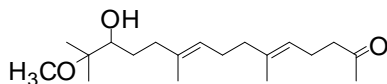
(6.27)



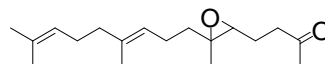
(6.28)



(6.29)

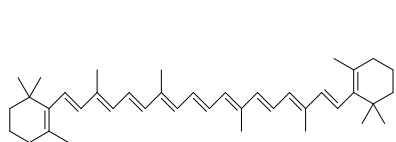


(6.30)

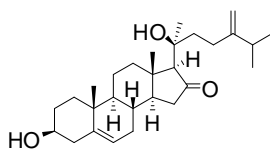


(6.31)

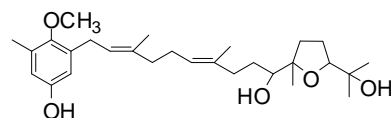
C. torulosa and *C. retroflexa* were also found to contain a number of phlorotannins such as **6.49** [305-308], while steroids like **6.33** and meroditerpenes such as **6.34** were isolated in 1998 from *C. brownii* [291]. In 2006, a study of *C. fibrosa* from South Africa yielded the tetraprenyltoluquinols (**6.38-6.39**) [292], however it was suggested by the authors that the species *C. fibrosa* should be moved into the *Cystoseira* genus due to the presence of these secondary metabolites [292]. The first report of the isolation of compounds from the species *C. harveyi* was in 2007 with the isolation of atractylochromene (**6.11**), a known anti-inflammatory agent, pycnanthuquinone C (**6.50**), as well as (**6.35** and **6.37**) [309]. In this latter study [309] it was also reported that extracts containing atractylochromene (**6.11**) have been used in the treatment of rheumatic diseases, digestive ailments, mild diarrhoea and influenza, while extracts known to contain (**6.35**) have been used for the treatment of dysentery, fever, arthritis and apoplexia [309]. The related pycnanthuquinones A (**6.51**) and B (**6.52**), isolated from the African plant, *Pycnanthus angolensis* were shown in a previous report to possess anti-hyperglycemic activity in mice [310]. The highly studied *C. moniliformis* was studied further in 2008, with the isolation of the two new epimeric terpene diols, namely monilforminol A and B (**6.53-6.54**) along with a farnesylacetone derivative (**6.30**) [311]. In this study it was established that a mixture of compounds **6.41** and **6.42** displayed moderate P388 anti-tumour activity and moderate anti-fungal activity towards *Trichophyton mentagrophytes*. In 2010, the farnesylacetone epoxide (**6.31**) from *C. moniliformis* and the phloroglucinol derivative (**6.7**) were reported from *C. scalaris* [312].



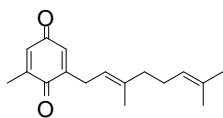
(6.32)



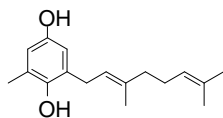
(6.33)



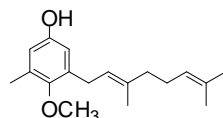
(6.34)



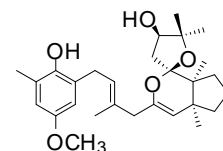
(6.35)



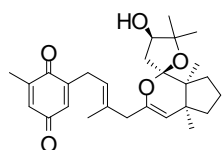
(6.36)



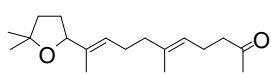
(6.37)



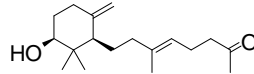
(6.38)



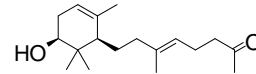
(6.39)



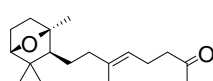
(6.40)



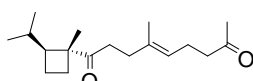
(6.41)



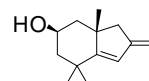
(6.42)



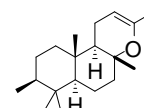
(6.43)



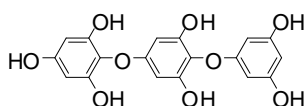
(6.44)



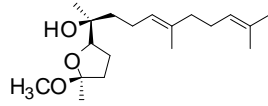
(6.45)



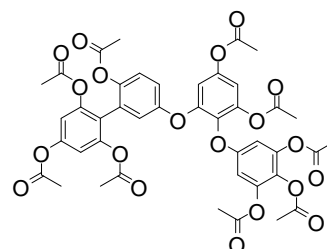
(6.46)



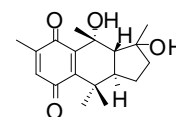
(6.47)



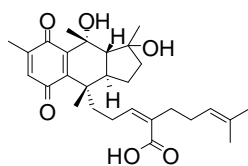
(6.48)



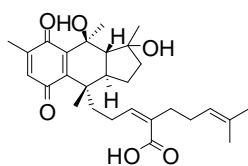
(6.49)



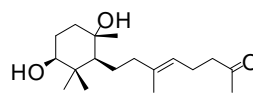
(6.50)



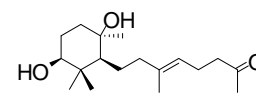
(6.51)



(6.52)



(6.53)



(6.54)

Databases are an invaluable resource to assist in the dereplication of compounds that are present in an organism (marine or terrestrial). In particular, databases such as the Dictionary of Natural Products [7] and the MarinLit database [8] are extremely useful due to their ability to search using structural information (e.g. UV profiles, molecular mass,

NMR spectra, etc.), structures/substructures and/or taxonomic classification, or on the basis of other bibliographic information. While the Dictionary of Natural Products has a very broad scope in that it allows searches to be conducted for both marine and terrestrial organisms (~170,000 compounds) [7], the MarinLit database is more specific in that it deals only with the literature for compounds that have been reported from marine sources and comprises >5,200 compounds isolated from approximately 6,000 species, spanning 2,200 genera and thirty-nine phyla [8]. The use of the MarinLit database in assisting to determine the structure class(es) of compound(s) that are present in specific genera/genus and species can provide insight into the classes of compounds that are likely to be present/occur in a specific organism and is therefore an invaluable aid in the dereplication of marine natural products .

In this chapter, a dereplication exercise was conducted on the crude extract of the southern Australian marine brown alga *C. torulosa*. The specimen was selected for chemical profiling due to the highly studied nature of the genus in an effort to identify the class(es) of compounds present and/or rapidly identify these compounds. The crude DCM extract was subjected to HPLC-NMR chemical profiling for the rapid determination of the class(es) of compounds present in this alga. The dereplication exercise was carried out in conjunction with the use of the MarinLit database and was successful in identifying two principal classes of secondary metabolites. Following ESI-MS or GC-MS of the small scale isolations of the compounds present, a total of nine secondary metabolites could be identified.

6.2 Experimental

6.2.1 General Experimental

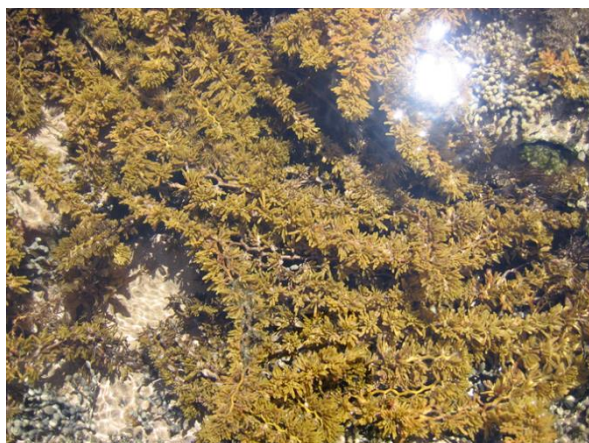
For detailed information on the general experimental procedures and spectroscopic techniques refer to the Experimental chapter **Section 7.1**. Analytical HPLC method

development was conducted on the crude DCM extract, using isocratic conditions consisting of 80% CH₃CN:H₂O providing good separation of the early eluting group of compounds. For the two later eluting compounds 100% CH₃CN provided sufficient separation, however this was not suitable for the HPLC-NMR analysis as some D₂O is required to maintain a lock. It was established that 90% CH₃CN:H₂O was suitable for the HPLC-NMR analysis of these later components. On-flow HPLC-NMR analyses were conducted on the crude DCM extract using isocratic HPLC conditions obtained via analytical HPLC method development (80% CH₃CN:D₂O for the identification of the early eluting compounds and 90% CH₃CN:D₂O for the identification of the later eluting compounds), with detection at λ_{max} 230 and 254 nm. A single analytical reversed phase HPLC collection was conducted to isolate a small quantity of the minor secondary metabolites (**6.1-6.2**, **6.12**, **6.15-6.19**) to permit ESI-MS or GC-MS analyses to be carried out. These analytical HPLC collections were conducted using 90% CH₃CN:H₂O for the off-line isolation of **6.12**, **6.15-6.19** and 100% CH₃CN for the isolation of **6.1-6.2** with detection at λ_{max} 220 and 254 nm in both cases. Semi-preparative reversed phase HPLC was conducted using isocratic conditions consisting of 90% CH₃CN:H₂O for the off-line isolation of the major secondary metabolite (**6.14**) with detection at λ_{max} 220 and 254 nm.

6.2.2 Algal material

A specimen of *C. torulosa* was collected on 22nd of January 2006 from the Borough of Queenscliff near Pt. Lonsdale, Victoria, Australia and the specimen was identified by Dr Gerald Kraft. A voucher specimen designated the code 2006-10 is deposited at the School of Applied Sciences (Discipline of Applied Chemistry), RMIT University. For detailed information on the biological assays refer to the Experimental chapter **Section 7.1.4**. A 2 g sample of the *C. torulosa* specimen was extracted using 3:1 MeOH:DCM and evaluated for biological activity. The crude extract displayed cytotoxicity against the P388 (Murine leukaemia) cell line with an IC₅₀ of 23.9 $\mu\text{g/mL}$. The extract also showed a 25% anti-viral zone of inhibition for *Herpes simplex* type 1 and a 75% zone of inhibition against

the *Polio* virus type 1. The crude extract showed no anti-microbial activity against *Escherichia coli*, *Bacillus subtilis*, *Pseudomonas aeruginosa*, *Candida albicans*, *Trichophyton mentagrophytes* and *Cladosporium resinae*.



C torulosa

(Voucher code: 2006-10)

Kingdom:	Chromista
Phylum:	Ochrophyta
Class:	Phaeophyceae
Order:	Fucales
Family:	Sargassaceae
Genus:	<i>Cystophora</i>
Species:	<i>torulosa</i>

Collected by Dr Sylvia Urban, Dr Rick Tinker, Dr Daniel Dias and Mrs Priyanka Reddy

6.2.3 Extraction and Isolation

6.2.3.1 Preparation of the crude extract of *C. torulosa* for on-flow HPLC-NMR analysis

A frozen sample of *C. torulosa* (120 g) was extracted with 3:1 MeOH:DCM (1 L). This extract was decanted and concentrated under reduced pressure and sequentially partitioned (triturated) into DCM (748.4 mg) and MeOH (1.2 g) soluble fractions respectively. A portion of the DCM fraction (112 mg) was concentrated under reduced pressure and then re-solubilised using 100% HPLC-NMR grade CH₃CN and then filtered through a 0.45 µm PTFE membrane filter (HP045 Advantec, Japan). For on-flow HPLC-NMR experiments 50 µL (5,600 µg) of the DCM extract was injected using the conditions described in **Section 6.2.1**.

6.2.3.2 Preparation of the crude extract of *C. torulosa* for off-line isolation of secondary metabolites from *C. torulosa*

A portion of the crude DCM extract (50 mg) that was used to conduct the HPLC-NMR analysis was also subjected to a single analytical reversed phase HPLC collection using the methods described in **Section 6.2.1** to conduct a small scale isolation of the resorcinol derivatives (**6.12**, **6.14-6.19**) and polyenes (**6.1-6.2**). This was undertaken to permit ESI-MS or GC-MS analyses to be conducted for each of the secondary metabolites. After the dereplication exercise had been completed a further portion of the DCM extract (100 mg) was subjected to semi-preparative reversed phase HPLC in an effort to conduct off-line isolation and structure confirmation of the major component (**6.14**). Semi-preparative reversed phase HPLC was conducted using the methods as described in **Section 6.2.1** to afford compound (**6.14**) (6.8 mg, 0.04%).

6.3 Results and Discussion

The marine alga *C. torulosa* was extracted as outlined in **Section 6.2.3.1**. The analytical HPLC chromatogram showed the presence of what appeared to be one main class of compounds, while a second class was present as shown in **Figure 6.1**. This was concluded on the basis of the extracted UV profiles of the major compound and a minor late eluting compound as shown in **Figure 6.2**. On this basis, separate analytical HPLC methods were developed for each of the two classes of compounds present as described in **Section 6.2.1**. Chemical profiling methodologies were undertaken to identify firstly the classes of compounds present and to attempt to identify each component present. The methodology used for this chemical profiling is given in **Scheme 6.1**.

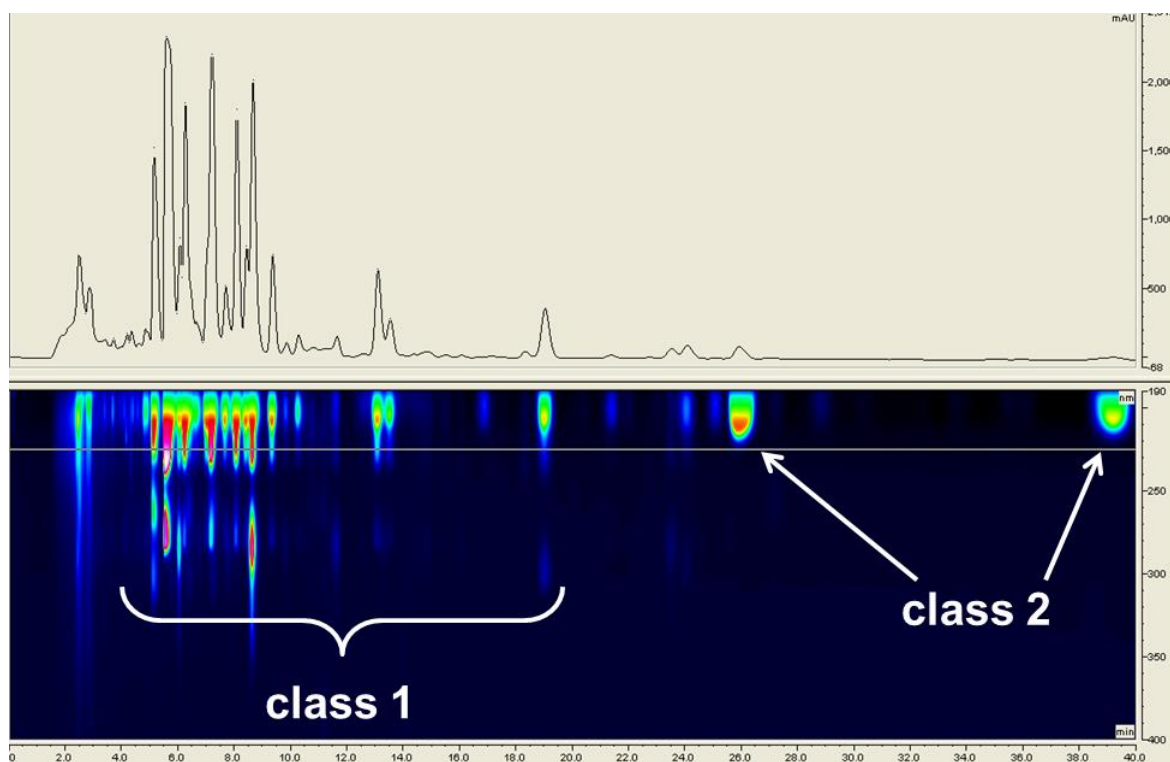
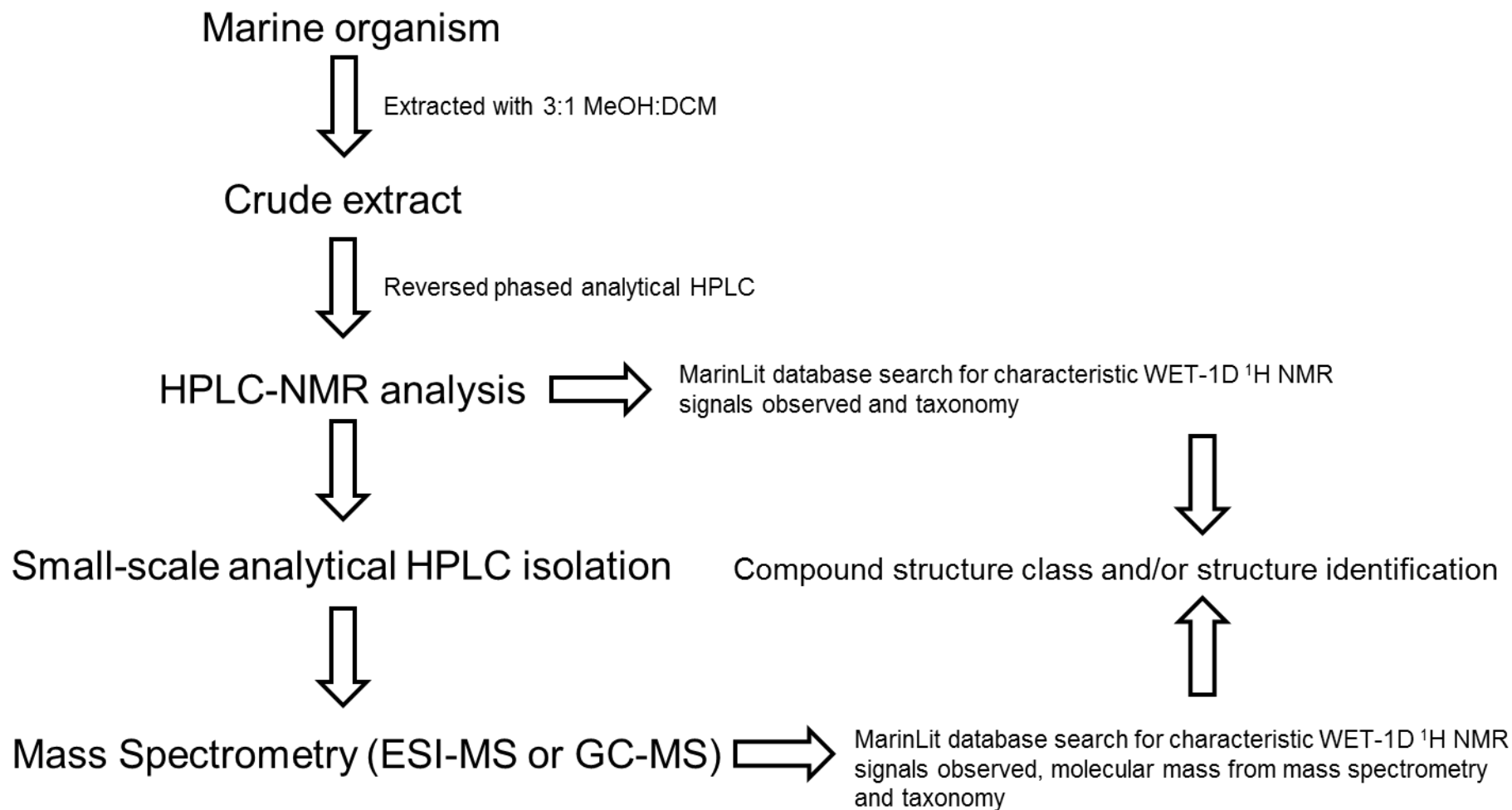


Figure 6.1. Analytical HPLC chromatogram of the crude DCM extract of *C. torulosa* showing the presence of two distinct classes of compounds.



Scheme 6.1. Methodologies used for the chemical profiling of *C. torulosa*.

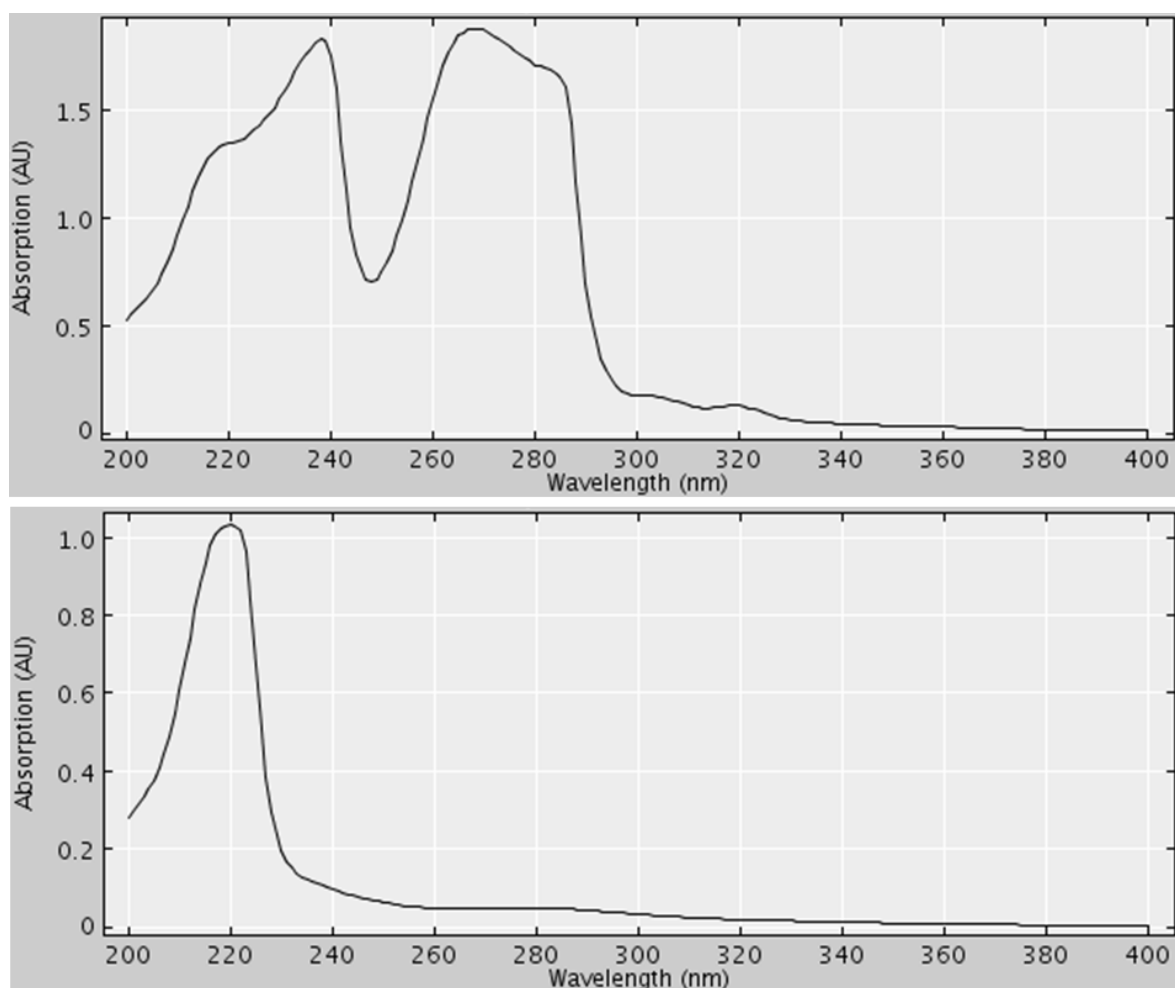


Figure 6.2. Extracted UV profiles of the two classes of compounds observed in the analytical HPLC analysis of the crude extract.

On-flow HPLC-NMR chemical profiling of the earlier eluting compounds (**Figure 6.3**) was undertaken using the DCM extract and the method described in **Section 6.2.1**.

On the basis of the 2D contour plot (**Figure 6.3**) obtained from the on-flow HPLC-NMR analysis of the crude extract, five secondary metabolites were detected. It could be concluded these five compounds were structurally related, as they had very similar WET-1D ^1H NMR spectra as illustrated in **Figure 6.3**, as well as similar UV profiles. In the on-flow HPLC-NMR trace, the major compound (**6.14**) displayed the presence of a characteristic triplet methyl signal at δ 0.86, two aromatic singlets at δ 6.07 and δ 6.01, overlapping proton signals at δ 2.70 and δ 5.28, and signals consistent with a straight chain alkane between δ 2.40 and δ 1.25.

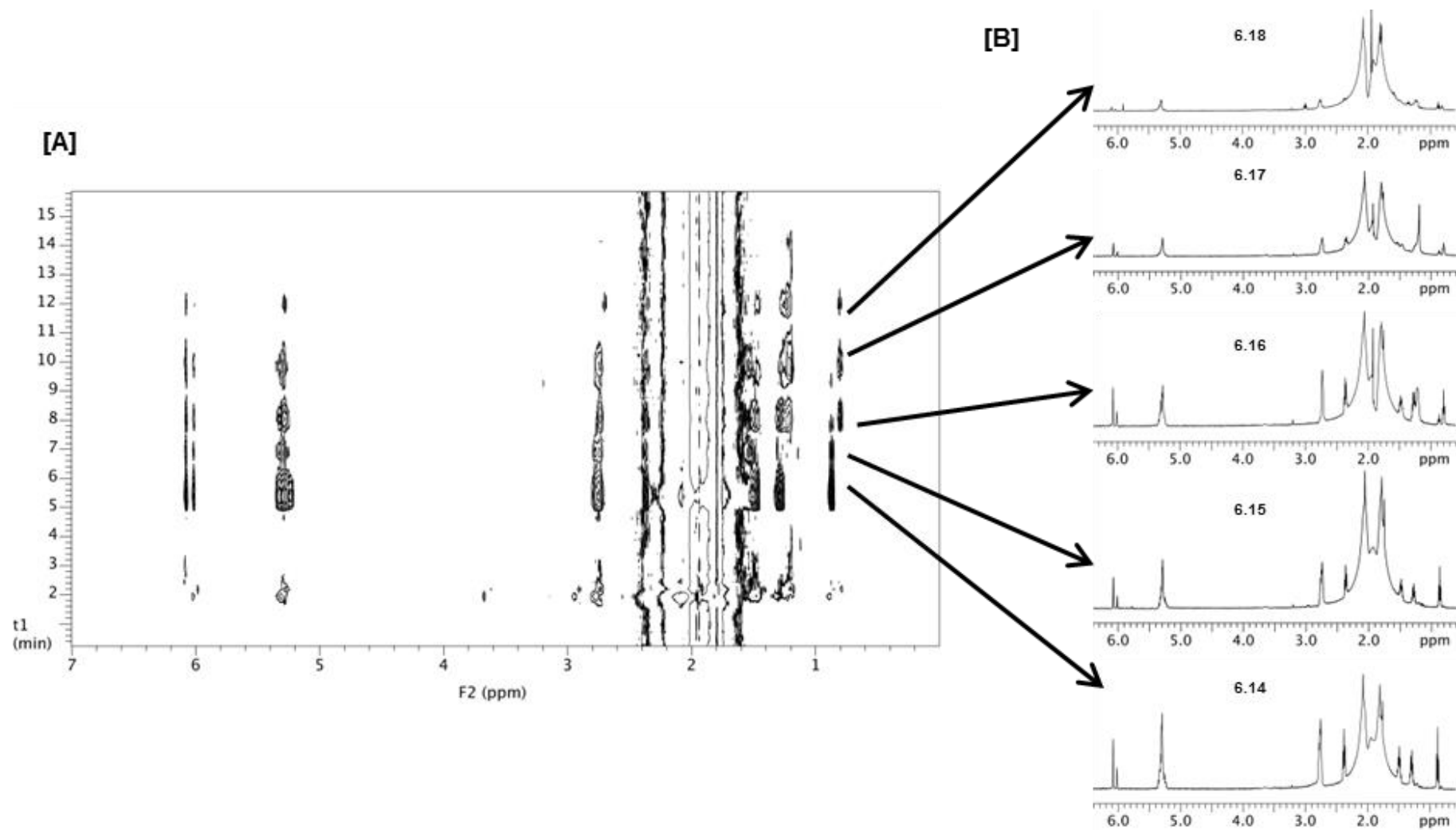


Figure 6.3. [A] On-flow 2D HPLC-NMR contour plot showing the presence of five structurally related compounds (6.14-6.18) and [B] Extracted WET-1D ¹H NMR spectra of compounds (6.14-6.18) from the on-flow HPLC-NMR analysis.

On the basis of this information, the MarinLit database [8] was used to conduct searches of marine natural products reported from brown algae of the genus *Cystophora* that contained the diagnostic triplet methyl. This search profile is given in **Figure 6.4** and it can be seen that six possible compounds were identified, with both resorcinol and phloroglucinol derivatives displaying the characteristic triplet methyl and aromatic moieties that were observed in the on-flow HPLC-NMR analysis. In the major compound the two aromatic protons present in the NMR spectrum integrated for a total of three aromatic protons. This indicated that the major compound was in fact a resorcinol derivative as given in **Figure 6.5**, which shows two different types of aromatic protons whilst phloroglucinol derivatives only possess one distinct aromatic proton chemical shift integrating for a total of two protons (**Figure 6.5**). Owing to the similarities for the remaining compounds observed in the HPLC-NMR analysis, this allowed the five early eluting secondary metabolites to be identified as being structurally related resorcinol derivatives. It was however not possible to unequivocally identify each resorcinol derivative definitively without a corresponding mass.

A small-scale off-line isolation of the compounds present would be required in order to identify each of the resorcinol derivatives present. This would then permit either ESI-MS or GC-MS analyses to be conducted to obtain a most likely molecular mass of each of the compounds. For this, a single analytical reversed phase HPLC injection was undertaken to obtain sufficient quantities for ESI-MS. Upon acquisition of the ESI-MS it was observed that the negative mode ESI-MS of the major secondary metabolite (**6.14**) exhibited an $[M-H]^-$ at an m/z of 339, indicating a molecular weight of 340 g/mol. This mass was added to the previous search criteria (ie. taxonomy and characteristic triplet methyl from the WET-1D 1H NMR spectrum) in the MarinLit database. This reduced the number of possibilities to a single resorcinol derivative (**6.14**) as given in **Figure 6.6**.

[A] Microsoft FoxPro

File Edit Window Help

Search Profile

BIBLIOGRAPHIC DATA

clear all

COMPOUND DATA AND
(AND operations only)

1 CH3(t)

TAXONOMY DATA AND
(OR operations only)

Genus IS Cystophora

do search

SUBSTRUCTURE AND

Use ChemOffice to carry out a substructure search.
When completed, use the Collect script in Chemfinder
to create a results file in tfr.txt.

Then use **recover results** to retrieve these results.

There are currently 0 structures in the search results file.

home screen

[B] Microsoft FoxPro

File Edit Window Help

4006/1

cystophorene

resorcinol

1-(trihydroxyphenyl)octadecatetraeno

phloroglucinol

trihydroxyphenyl-hydroxyoctadecatetraeno

Cancel

The image shows two screenshots of a Microsoft FoxPro application. Screenshot [A] displays a 'Search Profile' window with four search criteria sections: 'BIBLIOGRAPHIC DATA' (empty), 'COMPOUND DATA' (1 CH3(t)), 'TAXONOMY DATA' (Genus IS Cystophora), and 'SUBSTRUCTURE' (instructions on using ChemOffice and Chemfinder). Buttons for 'clear all', 'do search', and 'home screen' are visible. Screenshot [B] shows the search results, displaying chemical structures for 'cystophorene', 'resorcinol', '1-(trihydroxyphenyl)octadecatetraeno', and 'phloroglucinol', along with their corresponding names and a 'Cancel' button.

Figure 6.4. [A] Search parameters input into the MarinLit database for the class of compounds observed from the HPLC-NMR analysis [B] Compounds in the MarinLit database that conform to the search parameters in [A].

The off-line small scale analytical HPLC isolation resulted in a total of seven resorcinol derivatives being isolated, two more than were observed by HPLC-NMR analysis and were subjected to ESI-MS analysis. These two further secondary metabolites were present in the extract in very low quantities which is why they were not observed in the HPLC-NMR analysis. These two minor additional compounds had the same UV profile as the other resorcinol derivatives.

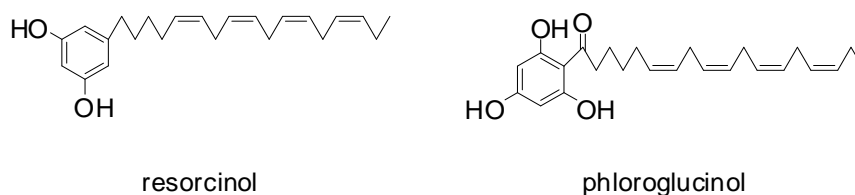


Figure 6.5. Resorcinol and phloroglucinol derivatives

When the WET-1D ^1H NMR and/or ESI-MS results for each of the minor resorcinol derivatives were entered into the MarinLit database without specifying the genus *Cystophora* so as to broaden the search profile, the compounds were identified as **6.12** and **6.15-6.19** as shown in **Figure 6.7** and **Table 6.1** [293, 313]. The NMR and ESI-MS data for **6.14** was in accordance with the previously reported data for this compound [293]. The resorcinol derivatives (**6.12**, **6.14-6.15**) had been previously reported from *C. torulosa* [293], while compounds (**6.16-6.19**) were described from the sponge *Haliclona* sp. [313]. The identity of the two compounds that were not visible from the HPLC-NMR analysis, but were isolated off-line for ESI-MS analysis (**6.12** and **6.19**), were tentatively assigned as indicated in **Table 6.1**.

In order to validate and confirm the identity of these resorcinol derivatives, as determined from the chemical profiling of the crude extract by HPLC-NMR, it was decided that the major compound would be subjected to off-line purification by semi-preparative reversed phase HPLC followed by a complete characterisation by NMR spectroscopy and mass spectrometry. Following the purification, a complete 2D NMR characterisation of the major secondary metabolite was achieved as shown in **Table 6.2**.

[A]

[B]

Figure 6.6. [A] Search parameters from the MarinLit database for the major compound observed in the HPLC-NMR analysis including ESI-MS mass [B] Single compound from MarinLit that conformed to the search parameters entered for the major compound.

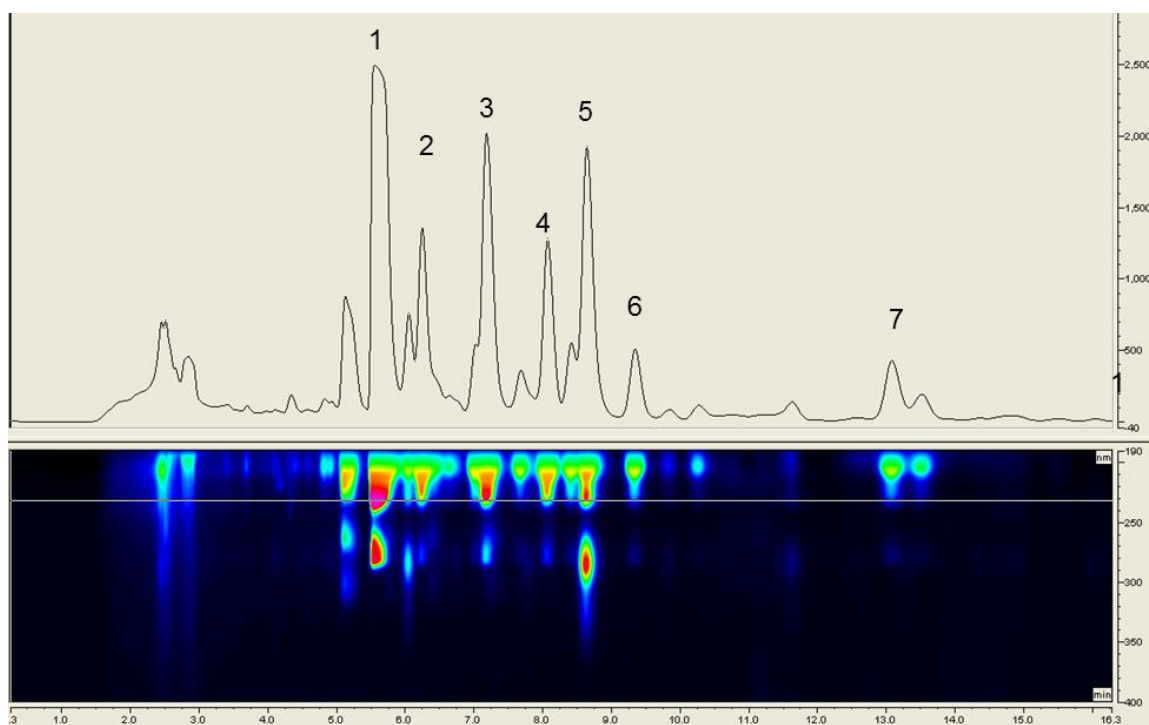


Figure 6.7. HPLC chromatogram showing the seven compounds (see **Table 6.1**) collected from the analytical HPLC, resulting in the identification of the resorcinols (**6.12**, **6.14-6.19**).

Given the overlapped nature of the aliphatic region of compound **6.14**, the 2D H_2BC spectrum was utilised to confirm the results obtained from the gCOSY. The H_2BC was especially useful in the assignment of positions 4, 5, 15 and 16, where overlap in the 1H NMR chemical shifts means that interpretation of the gCOSY spectrum is impossible due to this overlap. While the 1H NMR chemical shifts were overlapped, the corresponding ^{13}C NMR chemical shifts were different, allowing positions 4, 5, 15 and 16 to be assigned.

A comparison of the WET-1D 1H NMR spectrum and the off-line purified 1H NMR, along with the ESI-MS of the major component are provided in **Figure 6.8**. This showed that the on-line WET-1D 1H NMR was comparable to that of the off-line 1H NMR spectrum for this compound. The 2D NMR and ESI-MS unequivocally confirmed the structure of the major compound (**6.14**) deduced from the dereplication exercise.

Table 6.1. Resorcinol derivatives as isolated from the crude extract of *C. torulosa* with the seven compounds collected (see **Figure 6.7**), their mass from ESI-MS and their identified structure based on MarinLit database searching.

Peak number	Compound	Mass	Structure
1	6.14	340	
2	6.16	366	
3	6.15	342	
4	6.17	368	
5	6.12*	292	
6	6.18	344	
7	6.19*	392	

* not observed in the HPLC-NMR analysis

Table 6.2. ^1H (500 MHz) and ^{13}C (125 MHz) NMR spectroscopic data of the major resorcinol derivative (**6.14**) in CDCl_3 .

Position	δ_{H}, J	$\delta_{\text{C}}^{\text{a}}$	gCOSY	gHMBC
1	2.50, t, $J = 7.5$ Hz	35.6, t	H-2	C-2, C-3, C-1', C-2', C-6'
2	1.60, tt, $J = 7.5, 7.5$ Hz	30.6, t	H-1, H-3	C-1, C-3, C-4, C-1'
3	1.39, tt, $J = 7.5, 7.5$ Hz	29.1, t	H-2, H-4	C-1, C-2, C-4, C-5
4	2.09 ^b , dt, $J = 7.5, 7.0$ Hz	27.0, t	H-3, H-5	C-2, C-3, C-5, C-6
5	5.37 ^b , m	130.0, d	H-4	C-3, C-4
6	5.37 ^b , m	127.8, d	H-7	C-4
7	2.83 ^b , m	25.6 ^c , t	H-6, H-8	C-5, C-9
8	5.37 ^b , m	127.9 ^c , d	H-7	-
9	5.37 ^b , m	128.4 ^c , d	H-10	-
10	2.83 ^b , m	25.5 ^c , t	H-9, H-11	C-8, C-12
11	5.37 ^b , m	128.5 ^c , d	H-10	-
12	5.37 ^b , m	128.0 ^c , d	H-13	-
13	2.83 ^b , m	25.6 ^c , t	H-12, H-14	C-11, C-15
14	5.37 ^b , m	127.0, d	H-13	C-16
15	5.37 ^b , m	132.1, d	H-16	C-16, C-17
16	2.07 ^b , dq, $J = 7.5, 7.0$ Hz	20.5, t	H-15, H-17	C-14, C-15, C-17
17	0.97, t, $J = 7.5$ Hz	14.3, q	H-16	C-15, C-16
1'	-	145.8, s	-	-
2'	6.23, s	108.0, d	-	C-1, C-3', C-4', C-6'
3'	-	156.6, s	-	-
4'	6.17, bs	100.2, d	-	-
5'	-	156.6, s	-	-
6'	6.23, s	108.0, d	-	C-1, C-2', C-4', C-5'

^a Carbon assignments based on gHSQCAD and gHMBC NMR experiments^b Signals overlapped

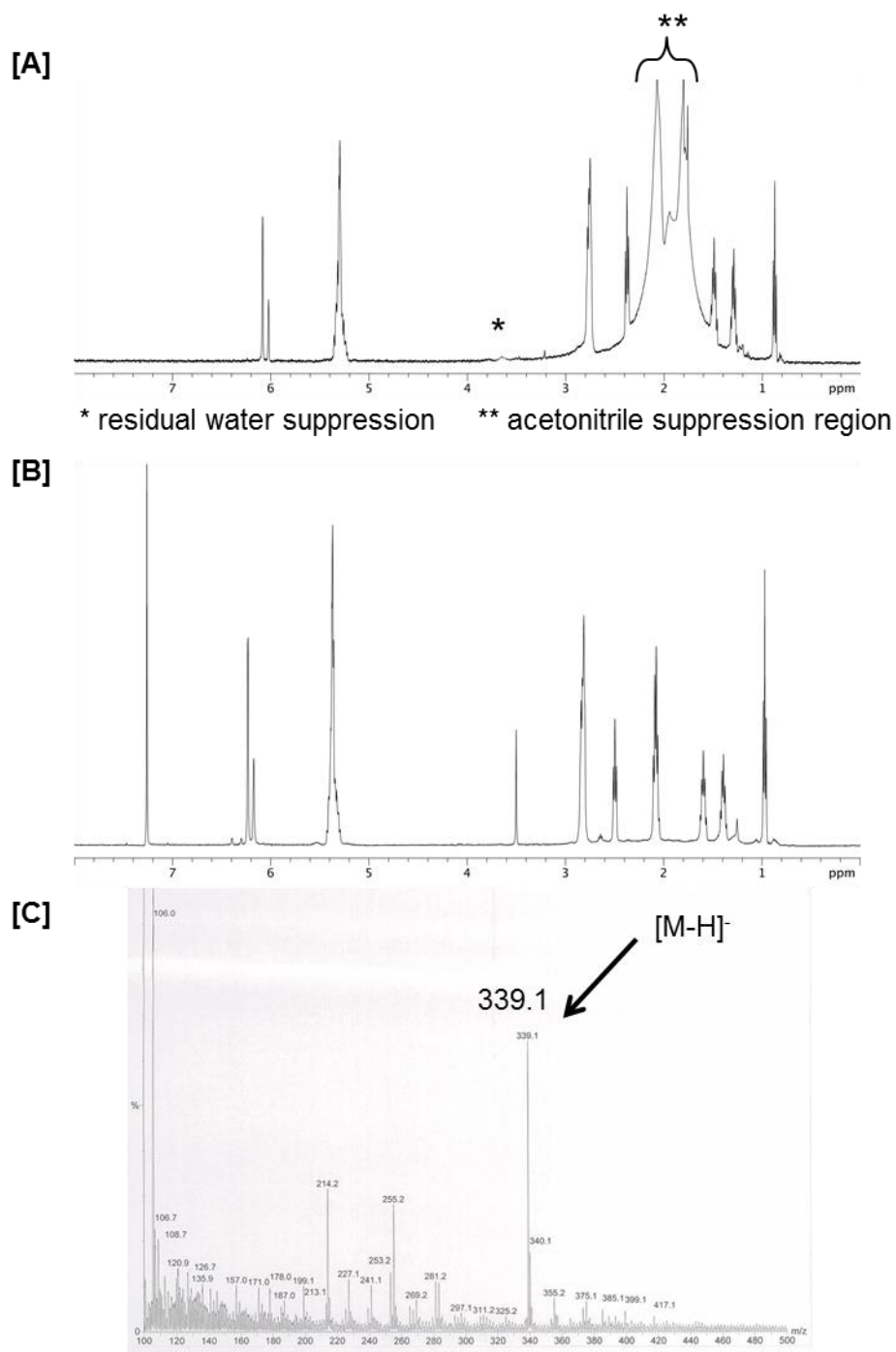


Figure 6.8. **[A]** WET-1D ^1H NMR spectrum of the major compound (**6.14**) **[B]** Off-line ^1H NMR (500 MHz, d_6 -DMSO) spectrum of compound (**6.14**) and **[C]** ESI-MS (negative mode) of compound (**6.14**).

The on-flow HPLC-NMR analysis of the later eluting compounds was undertaken using the method as described in **Section 6.2.1**, with the analytical HPLC obtained from HPLC method development given in **Figure 6.9**.

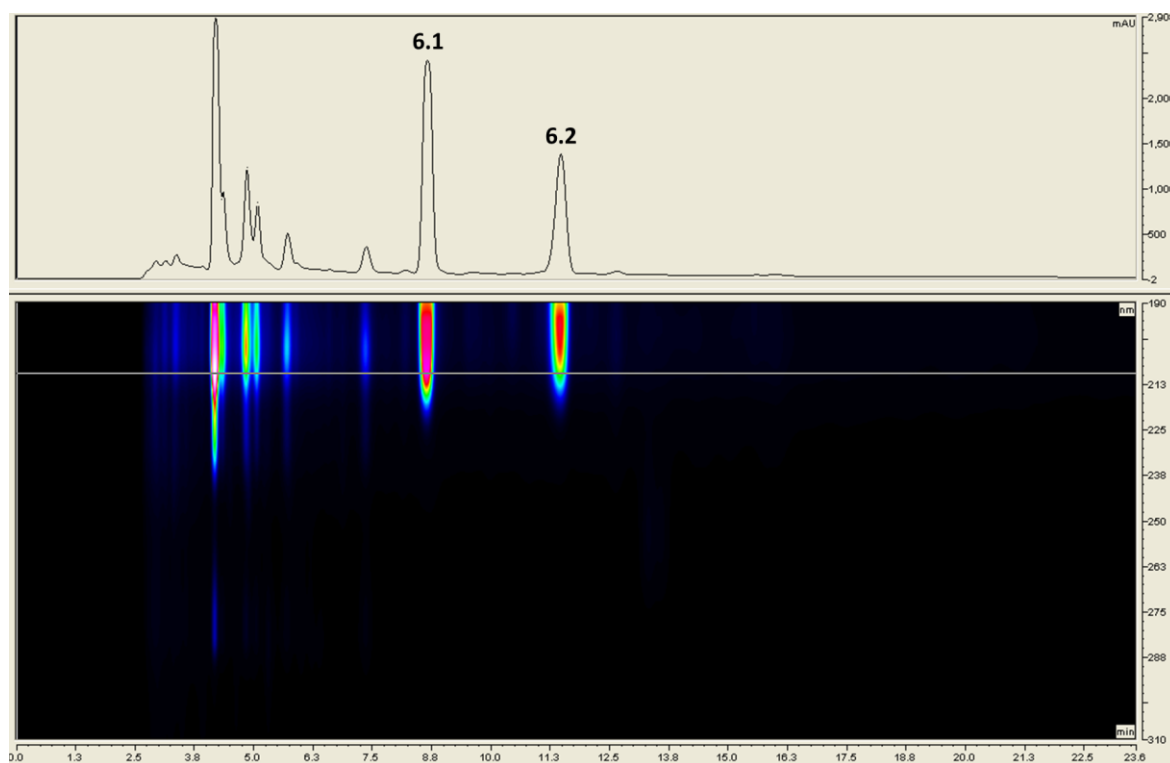


Figure 6.9. Analytical HPLC chromatogram (100% CH₃CN) of the later eluting compounds (**6.1** and **6.2**) in the crude extract of *C. torulosa*.

It was evident that the resorcinol derivatives observed in the previous on-flow HPLC-NMR analysis were overlapped between 4 and 6 minutes as shown in **Figure 6.9**. On the basis of the on-flow HPLC-NMR analysis it was recognised that the two compounds were structurally related to one another as shown in **Figure 6.10**. These two compounds shared similarities with that of the resorcinol derivatives, primarily the presence of the triplet methyl signal in the ¹H NMR spectrum, however they did not contain the aromatic protons at approximately δ 6.00 and δ 6.10. On the basis of the lack of these signals, it was suggested that these compounds were most likely of the polyene structure class.

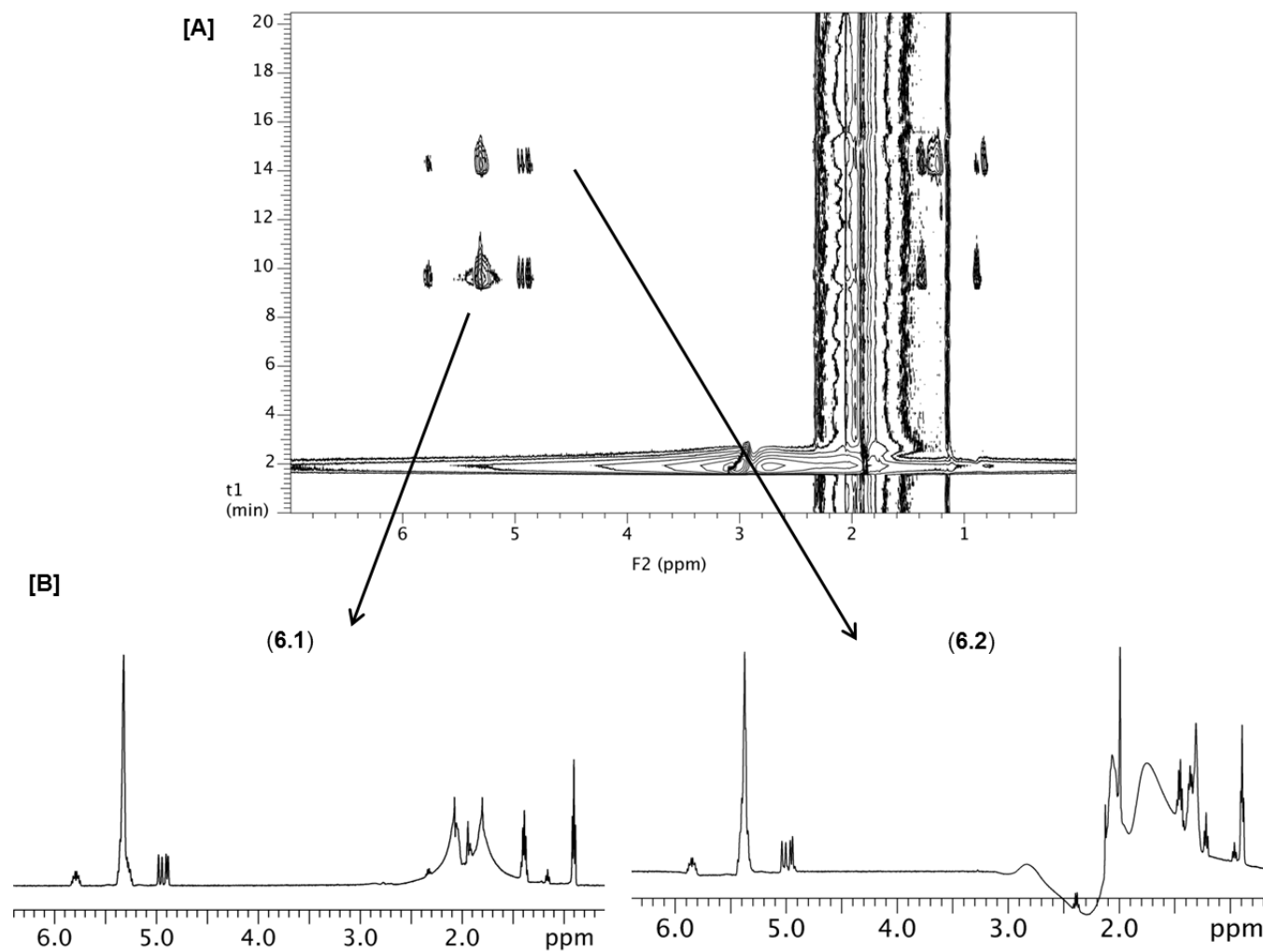




Figure 6.10. [A] On-flow 2D HPLC-NMR contour plot showing the two structurally related compounds (**6.1** and **6.2**) and [B] Extracted WET-1D ¹H NMR spectra of compounds (**6.1** and **6.2**) from the on-flow HPLC-NMR analysis.

The MarinLit database confirmed that this structure class had been previously reported from the *Cystophora* genus. This is illustrated in **Figure 6.4** whereby the triplet methyl signal and the *Cystophora* genus were entered into the search profile in the MarinLit database to give the polyene structure class (**6.3**) as one of the six possibilities.

The crude extract was then subjected to analytical reversed phase HPLC in order to isolate a small quantity of the polyenes for GC-MS analysis using the method described in **Section 6.2.1** (GC-MS of **6.1** shown in **Figure 6.11**). By searching the diagnostic triplet methyl NMR signal and the mass obtained from GC-MS the identification of the polyenes as (**6.1** and **6.2**) was possible as shown in **Table 6.3**. The WET-1D ^1H NMR spectra and GC-MS analyses were comparable with the literature data [293]. However, the MarinLit database indicated that these compounds had not been reported from the genus *Cystophora* (see **Figure 6.4**), but it did indicate that the polyenes **6.1** and **6.2** had been previously reported from the brown alga *Fucus vesiculosus* [314] as shown in **Figure 6.12**. A further review of the literature using Scifinder Scholar [22] established that these compounds had actually been isolated and reported from a *Cystophora* sp. [293].

Table 6.3. Polyenes isolated and identified from *C. torulosa*.

Compound	GC-MS	Structure
6.1	284	
6.2	286	

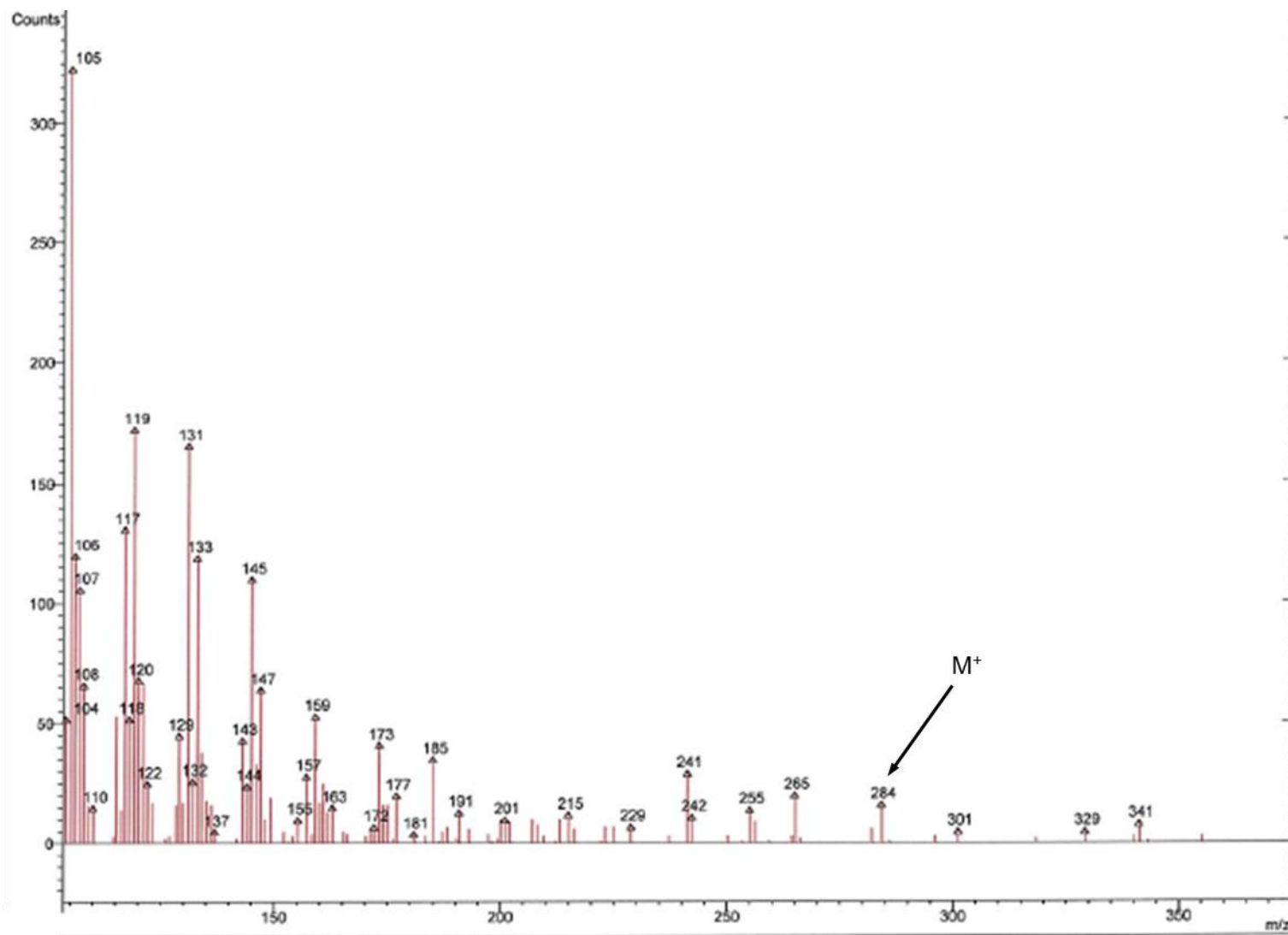


Figure 6.11. Mass Spectrum obtained from the GC-MS of the polyene (6.1)

[A] Microsoft FoxPro Search Profile

BIBLIOGRAPHIC DATA

COMPOUND DATA AND (AND operations only)
 Mass FROM 284 TO 285 AND 1 CH3(t)

TAXONOMY DATA AND (OR operations only)

SUBSTRUCTURE AND

Use ChemOffice to carry out a substructure search. When completed, use the Collect script in Chemfinder to create a results file in trf.bt. Then use recover results to retrieve these results.

There are currently 0 structures in the search results

home screen

trivial names:	#	name	formula	mas
1	MATCH	C21H32	284.2504	
3		C21H34	286.2660	

view all structures print

TAXONOMY DATA

phylum	class	order	family	genus
Chromophycota	Phaeophyceae	Fucales	Fucaceae	Fucus vesiculosus

Article # 10835
 Record # 5 of 6

[B] Microsoft FoxPro

Chemical structures shown:

- 4523/2a
- 4523/2b
- 4532/5
- 6-chlorolauthisa-3Z,11-dien-1-yne-diol (4735/1)
- 6-chlorolauthisa-3E,11-dien-1-yne-diol (4735/2)
- 6,10-dichlorolauthisa-3,9,11-trien-1-yne (5898/6)
- 2-methoxy-6Z-hexadecenoic acid (10835/1)
- 2-methoxy-6Z-hexadecenoic acid (11996/1)
- bisepoxy-chloro-hydroxypentadecaenyne
- tanikolide (C₁₁H₂₃)

[C] Microsoft FoxPro Search Results

BIBLIOGRAPHIC DATA

Title: Isolation of heneicosane-1,6,9,12,15,18-hexene and -1,6,9,12,15-pentene from the alga *Fucus vesiculosus*

Authors: Hasegawa TG, Hills IR

Keywords: Chemical conversion Journal: Chem. Commun.

COMPOUND DATA

trivial names:	#	name	formula
1	MATCH	C21H32	284.2504
3		C21H34	286.2660

TAXONOMY DATA

phylum	class	order	family	genus
Chromophycota	Phaeophyceae	Fucales	Fucaceae	Fucus vesiculosus

Article # 10835
 Record # 5 of 6

[D] Microsoft FoxPro

Chemical structures shown:

- 10835/1 (C₂H₅)
- 10835/3 (C₅H₁₁)

Figure 6.12. [A] Search parameters from the MarinLit database entered for the first polyene (6.1) observed in the HPLC-NMR analysis [B] Compounds in the MarinLit database that conform to the search parameters entered [C] Reference details of the polyene (6.1) matching search criteria and [D] The two polyenes (6.1 and 6.2) identified from matching reference.

The limitation of databases such as MarinLit, is that while the polyenes had actually been previously isolated from *Cystophora* spp. [293], only one polyene (**6.3**), that was not isolated in this study, appeared in the MarinLit database search profile for the triplet methyl signal observed for all of the compounds observed from HPLC-NMR analysis as given in **Figure 6.4**. Anomalies such as this one are common when searching specific databases and it serves as a warning to be thorough with the use of various databases and to search the literature extensively for all possible compounds.

Due to the fact that the secondary metabolites identified in this study were only isolated in minute quantities (sufficient for on-line HPLC-NMR and ESI-MS or GC-MS), together with the fact that the major compound (**6.14**) was found to degrade over time, these compounds were not evaluated for any biological activity.

6.4 Concluding remarks

This study utilised on-line HPLC-NMR as a means of chemical profiling a crude DCM soluble extract of the brown algae *C. torulosa*. On the basis of two separate on-flow HPLC-NMR analyses of the crude extract, it was concluded that two classes of compounds were present in the crude extract. Analysis of the earlier eluting compounds led to the partial identification of the major component, namely the resorcinol derivative (**6.14**) with the assistance of the MarinLit database, while the additional compounds present also possessed similar ¹H NMR spectra, suggestive of a group of structurally related resorcinol derivatives being present. Analysis of the later eluting compounds allowed for the partial identification of the two compounds as being of the polyene structure class. Subsequent small-scale analytical HPLC collections and analyses of these two classes of compounds permitted the ESI-MS or GC-MS spectra to be obtained, which, in turn allowed for the determination of the compounds as being the polyenes (**6.1** and **6.2**), and the resorcinol derivatives (**6.12**, **6.14-6.19**) in conjunction with the use of the MarinLit database. To confirm that the dereplication exercise was successful semi-preparative reversed phase HPLC was employed to obtain sufficient

quantities of the major resorcinol derivative (**6.14**) that permitted a complete 2D NMR assignment of this compound to be carried out. All the compounds identified in this *Cystophora* sp. had been previously reported from other *Cystophora* spp.

Chapter 7

Experimental

7.1 General Experimental

All organic solvents used were Analytical Reagent (AR), UV Spectroscopic, HPLC or HPLC-NMR grades, with milli-Q water also used. Silica flash chromatography was carried out with Merck™ silica gel (60-120 mesh), using a 20% stepwise solvent elution system from 100% hexane to 100% DCM to 100% EtOAc and finally 100% MeOH, unless otherwise specified. C₁₈ Vacuum Liquid Chromatography (VLC) was performed using a 25% stepwise elution using 100% H₂O to 100% MeOH and finally to 100% DCM. Size exclusion chromatography was performed using Sephadex LH-20 (Sigma™) using 100% MeOH as the eluent. Melting points (uncorrected) were determined on a Gallenkamp Melting Point apparatus. All % yields of compounds isolated were calculated using dry weight of the organism.

7.1.1 Spectroscopic Analyses

Optical rotation measurements were carried out using either a Jasco DIP-1000 digital polarimeter with 1.2 mL cell, set to Na 589 nm wavelength, or a Perkin-Elmer 241 MC polarimeter, at the sodium wavelength of 589 nm, a slit width of 1 nm and an integral of 1 second per reading. UV-Vis spectra were obtained on a Varian Cary 50 Bio Spectrophotometer or on a Varian 1C Spectrophotometer, while UV profiles were also

extracted from HPLC (PDA detection) in the way of a 2D contour plot (both from a Dionex analytical HPLC system or a Varian semi-preparative HPLC system). IR spectra were obtained as a film using NaCl discs (CHCl_3 or dried EtOH as solvent, then solvent evaporated) on a Perkin-Elmer, Spectrum One FTIR Spectrometer. NMR spectra (^1H , 500 MHz and ^{13}C , 125 MHz) were acquired on a 500 MHz Varian INOVA NMR Spectrometer, using referencing for each of the solvent signals, CDCl_3 (δ 7.26, 77.0 ppm), CD_3OD (δ 3.31, 49.0 ppm), d_6 -acetone (δ 2.05) and d_6 -DMSO (δ 2.50, 39.5 ppm). 1D and 2D NMR included ^1H , ^{13}C , DEPT, 1D NOE, gCOSY, gHSQCAD, gHMBC, NOESY, ROESY, TOCSY and CIGAR experiments. ESI-MS analyses were conducted on a Micromass Platform II Mass Spectrometer, equipped with a LC-10AD Shimadzu solvent pump, using a solvent system of 50% $\text{CH}_3\text{CN}/\text{H}_2\text{O}$ at a flow rate of 0.2 mL/min. The analyses were conducted in both positive and negative ionisation modes and a cone voltage of 20 V-30 V. HR-ESI-MS was carried out on an Agilent 6200 Series TOF system (ESI operating conditions of 8 L/min N_2 , 350°C drying gas and 4000 V capillary voltage) with an Agilent 1200 Series LC solvent pump (100% CH_3OH at a flow rate of 0.1 mL/min) in positive or negative ionisation modes (where the instrument was calibrated with the Agilent Tuning Mix using purine and HP-0921 as reference compounds). GC-MS analyses were carried out on two instruments, the first being a Hewlett Packard 56890/5973 GC-MS Mass Selective Detector using a BPX 5 30 m x 0.25 mm ID d_f of 0.25 μ GC column at a constant column flow of 1.0 mL/min, with a temperature program (0-1 min 70°C, 22-27 min 280°C). The parameters for the GC included an injector temperature of 250°C, detector temperature of 260°C with injector port set to standard split/splitless mode, while the mass spectrometer was set to electron impact (EI) analysing over the mass range of m/z 40-600. The second GC-MS system utilised was a Varian Saturn 2200 GC-MS-MS and Varian CP-3800 Gas Chromatograph using a Varian VF-5ms 30 m x 0.25 mm ID d_f of 0.25 μ GC column at a constant flow of 1.0 mL/min, using a temperature gradient (0-1 min 60°C, 20-30 min 260°C). The GC parameters included an injector temperature of 250°C, with the injector port using the standard split/splitless mode, while the

mass spectrometer was set to electron impact (EI) analysing over the mass range of m/z 40-400. HR-GC-MS analysis was carried out on a Waters GCT Premier GC-Time-of-Flight (TOF) system using a BPX5 30 m x 0.25 mm ID column with a column flow of 1.0 mL/min and a temperature method (0-0.5 min 40°C, 18-24 min 320°C). The GC parameters included an injector temperature of 250°C with injector port set to standard split/splitless mode, while mass spectrometer was set to the electron impact (EI) analysing over the mass range of m/z 40-500. Crystallographic diffraction data were collected with an Oxford SuperNova diffractometer using Cu radiation ($\lambda = 1.54184 \text{ \AA}$) by Dr Jonathan White at the University of Melbourne. Data were reduced using the CrysAlisPRO software. The temperature of the data collection was maintained at 130 K, using an Oxford Cryostream cooling device. The structure was solved by direct methods, and difference Fourier synthesis and was refined on F^2 (SHELXL-97) [195]. Thermal ellipsoid plot was generated using program ORTEP-3 [196] integrated within the WINGX program suite [197].

7.1.2 Analytical and semi-preparative HPLC

All analytical and semi-preparative HPLC analyses were conducted in the reversed phase (RP) mode. Analytical HPLC analyses were performed on a Dionex P680 pump with a PDA100 UV detector, using Chromeleon software. All analytical HPLC was initially conducted using the gradient (0-2 min 10% CH₃CN/H₂O; 14-24 min 75% CH₃CN/H₂O; 26-30 min 100% CH₃CN; 32-40 min 10% CH₃CN/H₂O) as outlined in **Figure 7.1**, unless otherwise stated. These analyses were carried out using a Phenomenex Prodigy ODS (3) C₁₈ 100Å 250 mm x 4.6 mm (5 μ) column, Phenomenex Gemini ODS (3) C₁₈ 100Å 250 x 4.6 mm (5 μ) or a Phenomenex Luna ODS (3) C₁₈ 100Å 250 mm x 4.6 mm (5 μ) column and a flow rate of 1.0 mL/min. Semi-preparative HPLC was conducted on two instruments, the first being a Varian Prostar 210 pump equipped with a Varian Prostar 355 PDA detector using STAR LC Workstation Version 6.0 software, with a Phenomenex Prodigy ODS (3) C₁₈ 100Å 250 mm x 10 mm (5 μ) column and a flow rate of 3.5 mL/min. The second semi-preparative HPLC system used was a Dionex P680 pump with a UVD340U PDA detector and a Foxy Jr.

fraction collector. The HPLC column was a Phenomenex Gemini C₁₈ 100Å 250 mm x 4.6 mm (5 μ) column.

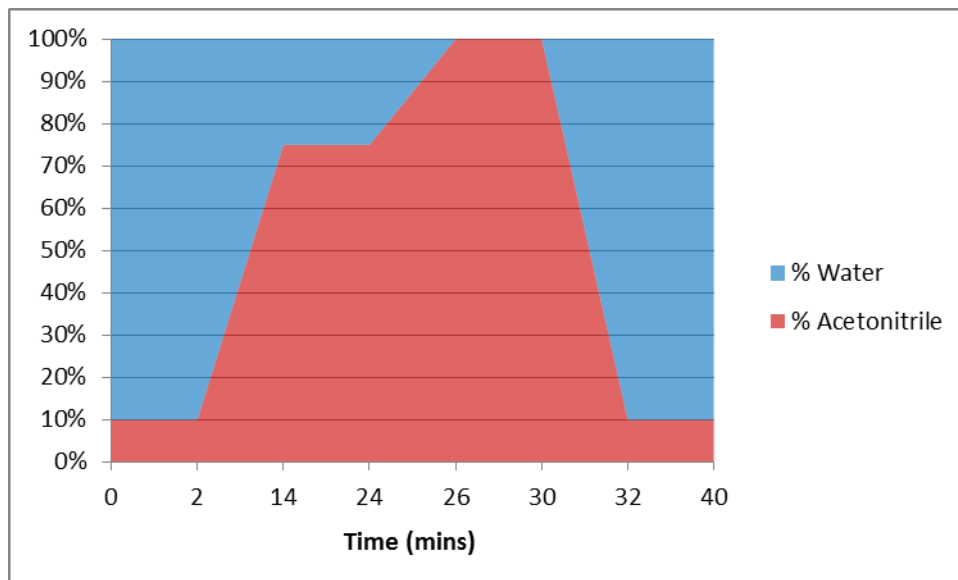


Figure 7.1. Analytical HPLC gradient used for all initial analytical HPLC analyses.

7.1.3 HPLC-NMR

HPLC-NMR solvents used were HPLC-NMR grade CH₃CN (Chromasol V[®]), and D₂O (99.9%). HPLC-NMR analyses were carried out on a Varian Unity INOVA 500 MHz NMR Spectrometer, with a Varian ¹H[¹³C] pulsed field gradient flow-probe with a 60 μL flow cell, connected to a Varian Prostar 230 pump with a Varian Prostar 335 PDA detector and a Prostar AS430 Autosampler (injection volume of 50 μL). The CORBA[™] server communication was used between the HPLC pump and NMR and then operated using the VNMRJ software (version VNMRJ 2.1b). All HPLC-NMR analyses were conducted on a Varian Polaris C₁₈ 150 mm x 4.6 mm (5 μ) column at either a flow rate of 0.8 mL/min or 1.0 mL/min. Varian WET solvent suppression [315] was used to suppress the CH₃CN and its satellites, as well as the residual water peaks arising from D₂O.

7.1.4 Biological Activity Assays

For all biological activity assays, crude extracts were tested at 50 mg/mL and individual compounds tested at 1 mg/mL unless otherwise specified. The three types of activity assessed included anti-tumour (P388 Murine Leukaemia cell line), anti-viral (*Herpes simplex* type 1 and *Polio* type 1) and anti-microbial (three anti-bacterial and three anti-fungal assays). All activity studies were conducted at the University of Canterbury, Christchurch, New Zealand, by Ms Gill Ellis.

7.1.4.1 Anti-tumour (P388 Murine Leukaemia Cell Line) Assay

Anti-tumour activity was determined by use of a two-fold dilution series of the crude extract or compound, and incubated for 72 hours with P388 cells. The concentration required of the given sample was determined using the absorbance values from when yellow MTT tetrazolium dye is reduced by healthy cells to purple MTT formazan as shown in **Figure 7.2**, expressed as an IC_{50} (ng/mL). This is achieved by determination of the concentration required to inhibit P388 cell growth by 50% compared to the control cells. For referencing purposes, the standard P388 inhibitor mitomycin C (M0503) was used, which has an IC_{50} value of 0.183 $\mu\text{g/mL}$.

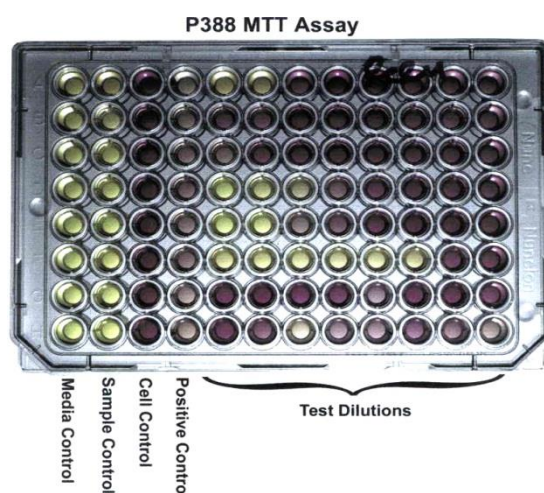


Figure 7.2. Micro-titre (96 well) plate with control and test dilutions showing the colour change due to inhibition.

7.1.4.2 Anti-microbial Activity Assays

The three anti-bacterial assays included inhibition of *Escherichia coli* (G-ve ATCC 25922), *Bacillus subtilis* (G+ve ATCC 19659) and *Pseudomonas aeruginosa* (G-ve ATCC 27853), while the three anti-fungal assays assessed inhibition towards *Candida albicans* (ATCC 14053), *Trichophyton mentagrophytes* (ATCC 28185) and *Cladosporium resinae*. Both anti-bacterial and anti-fungal activities were determined using the same procedure. The inoculum was prepared when a loop of the specific assay cells were transferred from a fresh culture in 10 mL of sterile water. After vortexing the vial until a cell density of 10^8 colony forming units per mL was formed, which was done by comparison with 5% BaCl₂ standard. The inoculated sample was then added to 100 mL of Müller Hinton or Potato Dextrose agar and mixed, allowing for a final cell density of 10^7 colonies per mL of solution. Five mL of this solution was added to an 85 mm petri dish and allowed to cool. The crude extracts and compounds were pipetted onto 6 mm discs of filter paper and allowed to dry. Upon drying the discs were placed on the petri dishes, as well as controls, and incubated for 24 hours. The zone of inhibition for each assay was determined in millimetres from the edge of the disc as shown in **Figure 7.3**. For referencing of anti-bacterial activity, gentamicin (10 µg) (Difco 6423890) displays zones of inhibition of 10 mm against *E. coli* and *P. aeruginosa*, while chloramphenicol (30 µg) (Difco 61338910) displays a zone of inhibition of 12 mm against *Bacillus subtilis*. For anti-fungal activity, nystatin (100 IU units) (Difco 6753890) displays zones of inhibition of 12 mm, 6 mm and 10 mm against *Candida albicans*, *Trichophyton mentagrophytes* and *Cladosporium resinae* respectively.



Figure 7.3. Zones of inhibition of anti-microbial assays.

7.1.4.3 Anti-viral (*Herpes simplex virus* and *Polio virus*) Assays

Anti-viral activity was established by pipetting the crude extract or compound on a 6 mm diameter filter paper disc and the solvent evaporated. The disc was then placed onto BSC-1 cells (African Green Monkey kidney) that had been infected with the *Herpes simplex virus* type 1 or RNA *Polio virus* type 1 and incubated. The radius of the anti-viral activity and/or cytotoxic zones, as well as the type of cytotoxicity were examined with an inverted microscope after 24 hours. As a reference, didemnum B (30 μ L of 0.005 mg/mL) displays activity against both *Herpes simplex* and *Polio* viruses at this concentration.

7.1.5 Miscellaneous

7.1.5.1 Photography

All photos of organisms were taken by Dr Sylvia Urban, Mr Allan Tinker, Dr Rick Tinker, Dr Gerald Kraft and Mr Michael Timmers.

7.1.5.2 Chemical Structures

Structures were drawn using ChemDraw Ultra Version 10.0, for details see <http://www.cambridgesoft.com>.

7.1.5.3 Crystal structure data analysis

For crystal structure data obtained, Mercury 3.0 was used to visualise the structure in 3D. For further information regarding the Mercury program, see http://www.ccdc.cam.ac.uk/free_services/mercury/. Associate Professor Jonathan White (School of Chemistry, The University of Melbourne, Victoria, 3010, Australia) conducted all single X-ray analyses and lodged the cif data with the Cambridge Crystallographic Data Centre (CCDC).

7.2 Chapter 2 Experimental

7.2.1 Chapter 2 HPLC-NMR Characterisation (from stop-flow HPLC-NMR)

Trans-tiliroside (**2.12**)

HPLC-NMR (WET-1D, 500 MHz, δ) 7.88 (2H, d, $J = 9$ Hz, H2'/H6'), 7.24 (1H, d, $J = 16$ Hz, H7'''), 7.21 (2H, d, $J = 8.5$ Hz, H2'''/H6'''), 6.83 (2H, d, $J = 9$ Hz, H3'/H5'), 6.76 (2H, d, $J = 8.5$ Hz, H3'''/H5'''), 6.20 (1H, d, $J = 1.5$ Hz, H8), 6.07 (1H, d, $J = 1.5$ Hz, H6), 5.92 (1H, d, $J = 16$ Hz, H8'''), 5.03 (1H, d, $J = 7.5$ Hz, H1''), 4.11 (2H, d, $J = 5.5$ Hz, H6''), 3.38 (2H, m, H3''/H5''), 3.23 (1H, m, H2''), 3.21 (1H, m, H4'').

Cis-tiliroside (**2.12**)

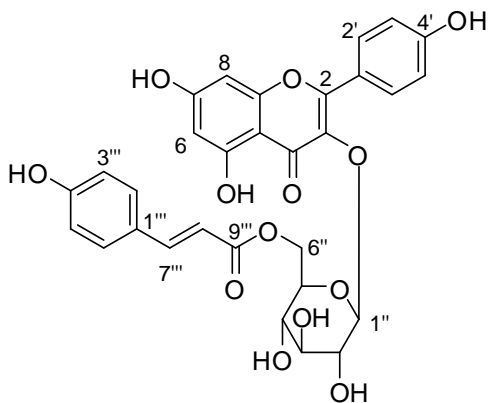
HPLC-NMR as a mixture with **2.12** in a ratio of 1:4 [compound **2.13**:compound **2.12**] (WET-1D, 500 MHz, δ) 7.83 (d, $J = 9$ Hz, H2'/H6'), 6.62 (d, $J = 14.5$ Hz, H7'''), 6.60 (d, $J = 9$ Hz, H3'/H5'), 6.45 (s, H8), 6.18 (s, H6), 5.41 (d, $J = 14.5$ Hz, H8'''), 4.96 (d, $J = 7.5$ Hz, H1''), 4.06 (d, $J = 5$ Hz, H6''), 3.43-3.20 (m, H2''/H3''/H4''/H5''), remaining signals overlapped with **2.12** or suppressed, while integration was not possible.

4'-Methoxy-*trans*-tiliroside (**2.14**)

HPLC-NMR (WET-1D, 500 MHz, δ) 8.02 (d, $J = 8.5$ Hz, H2'/H6'), 7.33 (d, $J = 14.5$ Hz, H7'''), 7.31 (d, $J = 7.5$ Hz, H2'''/H6'''), 6.97 (d, $J = 8.5$ Hz, H3'/H5'), 6.83 (d, $J = 7.5$ Hz, H3'''/H5'''), 6.33 (s, H8), 6.18 (s, H6), 6.01 (d, $J = 14.5$ Hz, H8'''), 5.13 (d, $J = 7.5$ Hz, H7'''), 3.72 (s, 4'-OCH₃), 3.44 (m), 3.25 (m), all other signals suppressed, while integration was not possible.

7.2.2 Chapter 2 Off-line Characterisation

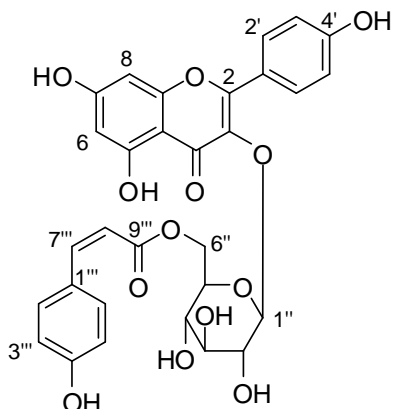
Trans-tiliroside (**2.12**), also known as kaempferol-3-O- β -D-(6-O-*trans*-*p*-coumaroyl)-glucopyranoside



Isolated as yellow fibrous crystals; m.p. 260-265°C; $[\alpha]_D^{21} -33^\circ$ (c 0.164, MeOH); IR (film) ν_{\max} cm⁻¹: 3367, 1655, 1605, 1509, 1443, 1359, 1260, 1207, 1179; UV (EtOH) λ_{\max} (nm) 205, 229 shoulder (sh), 269, 300 sh, 317, 350 sh ($\epsilon = 3924, 2488, 2049, 2400, 2665, 1434$ respectively); ¹H NMR (500 MHz, *d*₆-DMSO) and ¹³C NMR (125 MHz, *d*₆-DMSO) are detailed in **Table 2.1**; ¹H NMR present as a mixture with **2.13** (500 MHz, CD₃OD, δ) 7.99 (2H, d, $J = 9$ Hz, H-2'/H-6'), 7.40 (1H, d, $J = 16$ Hz, H-7'''), 7.32 (2H, d, $J = 9$ Hz, H-2'''/H-6'''), 6.82 (2H, d, $J = 9$ Hz, H-3'/H-5'), 6.80 (2H, d, $J = 9$ Hz, H-3'''/H-5'''), 6.32 (1H, s, H-8), 6.13 (1H, s, H-6), 6.07 (1H, d, $J = 16$ Hz, H-8'''), 5.24 (1H, d, $J = 7$ Hz, H-1''), 4.29 (1H, d, $J = 11.5$ Hz, H-6b''), 4.19 (1H, m, H-6a''), 3.44* (1H, m, H-2''), 3.43* (1H, m, H-3''), 3.39* (1H, m, H-5''), 3.31* (1H, m, H-4'') * indicates overlapping signals; ¹³C NMR (obtained from gHSQCAD and gHMBC

NMR experiments, CD₃OD, ppm) 161.4 (C, C-4'), 161.0 (C, C-4'''), 159.1 (C, C-2), 146.5 (CH, C-7'''), 131.9 (CH, C-2'/C-6'), 130.9 (CH, C-2'''/C-6'''), 126.9 (C, C-1'''), 116.4 (CH, C-3'''/C-5'''), 115.8 (CH, C-3'/C-5'), 114.4 (CH, C-8'''), 103.7 (CH, C-1''), 99.9 (CH, C-6), 94.6 (CH, C-8), 77.6 (CH, C-3''), 75.5 (CH, C-2''/C-5''), 71.4 (CH, C-4''), 63.9 (CH₂, C-6''), all other carbons were not detected; ESI-MS (negative): *m/z* 593 [M-H]⁻, (positive): *m/z* 595 [M+H]⁺, 617 [M+Na]⁺; HR-ESI-MS displayed an *m/z* at 593.1308 [M-H]⁻ (calcd. for C₃₀H₂₅O₁₃: *m/z* 593.1295) and an *m/z* at 595.1440 [M+H]⁺ (calcd. for C₃₀H₂₇O₁₃: *m/z* 595.1452).

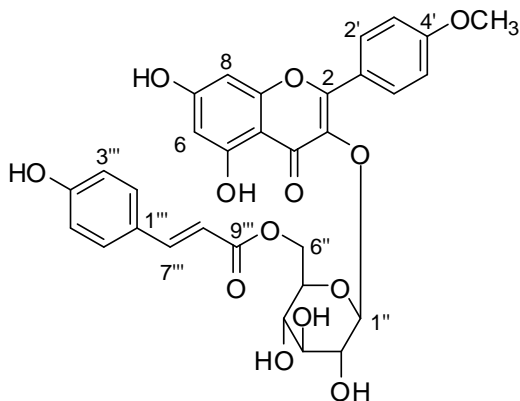
Cis-tiliroside (**2.13**) also known as kaempferol-3-O-β-D-(6-O-*cis*-*p*-coumaroyl)-glucopyranoside



Isolated as a yellow powder; ¹H NMR (500 MHz, *d*₆-DMSO) and ¹³C NMR (125 MHz, *d*₆-DMSO) are detailed in **Table 2.2**; ¹H NMR present as a mixture with **2.12** (500 MHz, CD₃OD, δ) 7.96 (2H, d, *J* = 9 Hz, H-2'/H-6'), 7.51 (2H, d, *J* = 8.5 Hz, H-2'''/H-6'''), 6.82 (2H, d, *J* = 9 Hz, H-3'/H-5'), 6.69 (1H, d, *J* = 12.5 Hz, H-7'''), 6.67 (2H, d, *J* = 8.5 Hz, H-3'''/H-5'''), 6.32 (1H, s, H-8), 6.19 (1H, s, H-6), 5.50 (1H, d, *J* = 12.5 Hz, H-8'''), 5.20 (1H, d, *J* = 7.5 Hz, H-1''), 4.29 (1H, d, *J* = 11.5 Hz, H-6b''), 4.19 (1H, m, H-6a''), 3.44* (1H, m, H-2''), 3.43* (1H, m, H-3''), 3.39* (1H, m, H-5''), 3.31* (1H, m, H-4'') * indicates overlapping signals; ¹³C NMR (obtained from gHSQCAD NMR experiment present as a mixture with **2.12** in a ratio of 1:2 [compound **2.13**: compound **2.12**], CD₃OD, ppm): 145.0 (CH, C-7'''), 133.5 (CH, C-2'''/C-6'''), 131.9 (CH, C-2'/C-6'), 115.8 (CH, C-3'/C-5'), 115.8 (CH, C-8'''), 115.4 (CH, C-3'''/C-5'''), 103.6 (CH, C-1''),

99.7 (CH, C-6), 94.5 (CH, C-8), 77.6 (CH, C-3''), 75.4 (CH, C-2''/C-5''), 71.4 (CH, C-4''), 63.9 (CH₂, C-6''), all other carbons were not detected; ESI-MS (negative): m/z 593 [M-H]⁻, (positive): m/z 595 [M+H]⁺, 617 [M+Na]⁺.

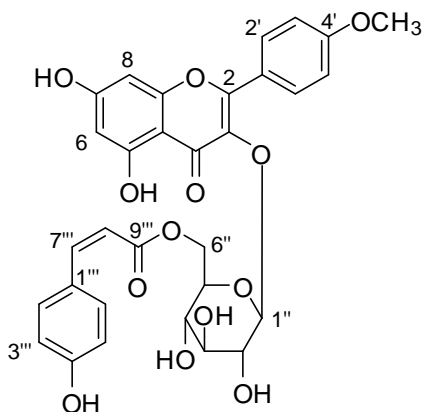
4'-Methoxy-*trans*-tiliroside (**2.14**) also known as kaempferol-4'-methyl ether 3-O-β-D-(6-O-*trans*-*p*-coumaroyl)-glucopyranoside



Isolated as a yellow powder; ¹H NMR (500 MHz, *d*₆-DMSO, δ) 12.51 (brs, 5-OH), 8.06 (2H, d, $J = 8$ Hz, H-2'/H-6'), 7.40 (2H, d, $J = 8$ Hz, H-2'''/H-6'''), 7.35 (1H, d, $J = 16$ Hz, H-7'''), 6.99 (2H, d, $J = 8$ Hz, H-3'/H-5'), 6.78 (2H, d, $J = 8$ Hz, H-3'''/H-5'''), 6.38 (1H, s, H-8), 6.17 (1H, d, $J = 16$ Hz, H-8'''), 6.15 (1H, s, H-6), 5.46 (1H, m, 2''-OH), 5.45 (1H, d, $J = 8$ Hz, H-1''), 5.26 (m, 4''-OH), 5.22 (m, 3''-OH), 4.28 (1H, d, $J = 11.5$ Hz, H-6b''), 4.02 (1H, dd, $J = 5.0, 11$ Hz, H-6a''), 3.70 (3H, s, 4'-OCH₃), 3.37* (1H, m, H-5''), 3.28* (1H, m, H-3''), 3.25* (1H, m, H-4''), 3.23* (1H, m, H-2'') * indicates overlapping signals; ¹³C NMR (125 MHz, *d*₆-DMSO, ppm): 166.2 (C, C-9'''), 164.7 (C, C-7), 161.3 (C, C-4'), 161.1 (C, C-5), 159.8 (C, C-4'''), 156.4 (C, C-9), 156.1 (C, C-2), 144.4 (CH, C-7'''), 133.4 (C, C-3), 130.4 (CH, C-2'/C-6'), 130.0 (CH, C-2'''/C-6'''), 125.0 (C, C-1'''), 122.4 (C, C-1'), 115.5 (CH, C-3'''/C-5'''), 113.4 (CH, C-8'''), 113.3 (CH, C-3'/C-5'), 103.9 (C, C-10), 101.8 (CH, C-1''), 98.7 (CH, C-6), 93.6 (CH, C-8), 75.7 (CH, C-3''), 73.8 (CH, C-2''/C-5''), 69.5 (CH, C-4''), 62.4 (CH₂, C-6''), 54.9 (CH₃, 4'-OCH₃), not detected (C-4); ¹H NMR present as a mixture with **2.15** (500 MHz, CD₃OD, δ) 8.08 (2H, d, $J = 9$ Hz, H-2'/H-6'), 7.42 (1H, d, $J = 16$ Hz, H-7'''), 7.35 (2H, d, $J = 9$ Hz, H-2'''/H-6'''), 6.93 (2H,

d, $J = 9$ Hz, H-3'/H-5'), 6.82 (2H, d, $J = 9$ Hz, H-3'''/H-5'''), 6.35 (1H, d, $J = 1.5$ Hz, H-8), 6.16 (1H, d, $J = 1.5$ Hz, H-6), 6.10 (1H, d, $J = 16$ Hz, H-8'''), 5.26 (1H, d, $J = 6.5$ Hz, H-1''), 4.30 (1H, d, $J = 11.5$ Hz, H-6b''), 4.19 (1H, m, H-6a''), 3.72 (3H, s, 4'-OCH₃), 3.46* (1H, m, H-2''), 3.44* (1H, m, H-3''), 3.41* (1H, m, H-5''), 3.38* (1H, m, H-4'') * indicates overlapping signals; ¹³C NMR (obtained from gHSQCAD and gHMBC NMR experiments, CD₃OD, ppm): 166.3 (C, C-9'''), 165.6 (C, C-7), 162.6 (C, C-4'), 160.6 (C, C-4'''), 158.5 (C, C-2), 157.9 (C, C-9), 146.1 (CH, C-7'''), 131.7 (CH, C-2'/C-6'), 130.9 (CH, C-2'''/C-6'''), 126.4 (C, C-1'''), 123.4 (C, C-1'), 116.5 (CH, C-3'''/C-5'''), 114.5 (CH, C-8'''), 114.3 (CH, C-3'/C-5'), 103.8 (CH, C-1''), 99.7 (CH, C-6), 94.6 (CH, C-8), 77.5 (CH, C-3''), 75.4 (CH, C-2''/C-5''), 71.2 (CH, C-4''), 63.7 (CH₂, C-6''), 55.5 (CH₃, 4'-OCH₃), C3, C4, C5 and C10 not detected; ESI-MS (negative): m/z 607 [M-H]⁻.

4'-Methoxy-*cis*-tiliroside (**2.15**), kaempferol-4'-methyl ether-3-O-β-D-(6-O-*cis*-*p*-coumaroyl)-glucopyranoside



Isolated as a yellow powder; IR (film) ν_{\max} cm⁻¹: 3342, 2919, 2851, 1651, 1605, 1510, 1456, 1371, 1358, 1302, 1259, 1181; UV (MeOH) λ_{\max} (nm) 204, 224 sh, 268, 299 sh, 313, 354 sh ($\epsilon = 4522, 2899, 2254, 2238, 2389, 1357$ respectively); ¹H NMR (500 MHz, *d*₆-DMSO, δ): 12.48 (brs, 5-OH), 8.03 (2H, d, $J = 9$ Hz, H-2'/H-6'), 7.55 (2H, d, $J = 8$ Hz, H-2'''/H-6'''), 6.99 (2H, d, $J = 8.5$ Hz, H-3'/H-5'), 6.67* (1H, H-7'''), 6.67* (2H, d, $J = 9$ Hz, H-3'''/H-5'''), 6.30 (1H,

s, H-8), 6.14 (1H, s, H-6), 5.49 (1H, d, $J = 13.5$, H-8'''), 5.48 (1H, m, 2''-OH), 5.38 (1H, d, $J = 7.5$ Hz, H-1''), 5.26 (m, 4''-OH), 5.20 (m, 3''-OH), 4.15 (1H, m, H-6b''), 4.06 (1H, dd, $J = 5.5, 11.5$ Hz H-6a''), 3.77 (3H, s, 4'-OCH₃), 3.36* (1H, m, H-5''), 3.24* (1H, m, H-3''), 3.23* (1H, m, H-2''), 3.16* (1H, m, H-4'') * indicates overlapping signals; ¹³C NMR (obtained from gHSQCAD and gHMBC NMR experiments, d₆-DMSO, ppm): 165.5 (C, C-9'''), 161.2 (C, C-4'), 158.8 (C, C-4'''), 156.7 (C, C-9), 156.0 (C, C-2), 143.5 (CH, C-7'''), 133.3 (C, C-3), 132.5 (CH, C-2'''/C-6'''), 130.4 (CH, C-2'/C-6'), 125.3 (C, C-1'''), 122.4 (C, C-1'), 114.5 (CH, C-3'''/C-5'''), 114.3 (CH, C-8'''), 113.3 (CH, C-3'/C-5'), 103.5 (C, C-10), 101.2 (CH, C-1''), 99.0 (CH, C-6), 93.8 (CH, C-8), 75.9 (CH, C-3''), 73.9 (CH, C-2''), 73.7 (CH, C-5''), 69.5 (CH, C-4''), 62.4 (CH₂, C-6''), 55.2 (CH₃, 4'-OCH₃), not detected (C-4, C-5, C-7); ¹H NMR present as a mixture with **2.14** in a ratio of 1:2 [compound **2.15**: compound **2.14**] (500 MHz, CD₃OD, δ) 8.04 (2H, d, $J = 9$ Hz, H-2'/H-6'), 7.55 (2H, d, $J = 8.5$ Hz, H-2'''/H-6'''), 6.93 (2H, d, $J = 9$ Hz, H-3'/H-5'), 6.72 (1H, d, $J = 13$ Hz, H-7'''), 6.69 (2H, d, $J = 8.5$ Hz, H-3'''/H-5'''), 6.35 (1H, d, $J = 2$ Hz, H-8), 6.21 (1H, d, $J = 2$ Hz, H-6), 5.53 (1H, d, $J = 13$ Hz, H-8'''), 5.17 (1H, d, $J = 7$ Hz, H-1''), 4.17 (2H, m, H-6''), 3.77 (3H, s, 4'-OCH₃), 3.30-3.47* (4H, m, H-2''/H-3''/H-4''/H-5'') * indicates overlapping signals; ¹³C NMR present as a mixture with **2.14** in a ratio of 1:2 [compound **2.15**: compound **2.14**] (obtained from gHSQCAD NMR experiment, CD₃OD, ppm): 145.1 (CH, C-7'''), 133.6 (CH, C-2'''/C-6'''), 131.7 (CH, C-2'/C-6'), 115.6 (CH, C-8'''), 115.4 (CH, C-3'''/C-5'''), 114.3 (CH, C-3'/C-5'), 104.0 (CH, C-1''), 99.7 (CH, C-6), 94.6 (CH, C-8), 63.7 (CH₂, C-6''), 54.3 (CH₃, 4'-OCH₃), all other carbons were not detected; HR-ESI-MS (negative): m/z at 607.1461 [M-H]⁻ (calcd. for C₃₁H₂₇O₁₃: m/z 607.1452); ESI-MS (negative): m/z 607 [M-H]⁻, (positive): m/z 609 [M+H]⁺, 630 [M+Na]⁺.

7.3 Chapter 3 Experimental

7.3.1 Chapter 3 HPLC-NMR Characterisation (from on-flow and stop-flow HPLC-NMR)

Haemodorone (**3.41**)

HPLC-NMR (WET-1D, 500 MHz, 60:40 CH₃CN:D₂O, on-flow HPLC-NMR, δ) 8.31 (1H, d, $J = 7.5$ Hz), 8.19 (1H, s), 7.45 (1H, d, $J = 7.5$ Hz), 7.37 (3H, m), 7.33 (2H, m), 3.16 (3H, s).

Haemoxiphidone (**3.42**) also known as 5-Hydroxy-2,6-dimethoxy-9-phenyl-phenalen-1-one

HPLC-NMR (WET-1D, 500 MHz, 60:40 CH₃CN:D₂O, on-flow HPLC-NMR, δ) 8.35 (1H, d, $J = 8.0$ Hz), 7.46 (1H, s), 7.45 (1H, d, $J = 8.0$ Hz), 7.35 (2H, d, $J = 7.5, 7.5$ Hz), 7.32 (1H, dd, $J = 7.0, 7.0$ Hz), 7.26 (2H, d, $J = 8.0$ Hz), 6.96 (1H, s), 3.91 (3H, s), 3.73 (3H, s).

5,6-dimethoxy-7-phenyl-1*H*,3*H*-naphtho[1,8-*cd*]pyran-1,3-dione (**3.44**)

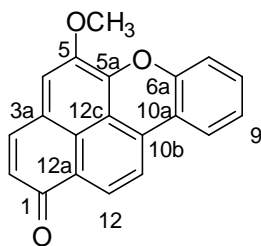
HPLC-NMR (WET-1D, 500 MHz, 80:20 CH₃CN:D₂O, stop-flow HPLC-NMR, δ): 8.39 (1H, d, $J = 7.5$ Hz), 8.38 (1H, s), 7.48 (1H, d, $J = 7.5$ Hz), 7.38 (3H, m), 7.29 (2H, m), 3.95 (3H, s), 3.27 (3H, s).

Haemodordioxolane (**3.45**)

HPLC-NMR (WET-1D, 500 MHz, 80:20 CH₃CN:D₂O, stop-flow HPLC-NMR, δ): 8.43 (1H, d, $J = 7.5$ Hz), 8.17 (1H, s), 7.55 (1H, d, $J = 7.5$ Hz), 7.43 (5H, s), 6.03 (2H, s).

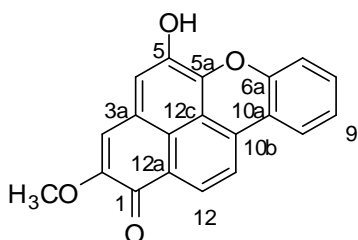
7.3.2 Chapter 3 Off-line Characterisation

5-methoxy-1*H*-naphtho[2,1,8-*mna*]xanthen-1-one (3.2)



Isolated as an orange powder; IR (film) ν_{\max} cm^{-1} : 3423, 2956, 2922, 2851, 1608, 1575, 1558, 1465, 1407, 1381, 1309; UV (c, 0.038 mg/mL in EtOH) λ_{\max} (nm) 233, 278, 313, 522 ($\epsilon = 5021, 1887, 1097, 1761$ respectively); ^1H NMR (500 MHz, d_6 -DMSO, δ) 8.55 (1H, d, $J = 8.0$ Hz, H-12), 8.46 (1H, d, $J = 8.0$ Hz, H-10), 8.42 (1H, d, $J = 8.0$ Hz, H-11), 8.22 (1H, s, H-4), 8.09 (1H, d, $J = 10.0$ Hz, H-3), 7.67 (1H, ddd, $J = 8.0, 7.5, 1.0$ Hz, H-8), 7.59 (1H, d, $J = 8.5$ Hz, H-7), 7.46 (1H, dd, $J = 8.0, 7.5$ Hz, H-9), 6.75 (1H, d, $J = 10.0$ Hz, H-2), 4.10 (3H, s, 5-OCH₃). ^{13}C (125 MHz, d_6 -DMSO, ppm) 183.2 (s, C-1), 151.7 (s, C-6a), 142.6 (s, C-5), 141.5 (s, C-5a), 141.0 (d, C-3), 133.1 (s, C-10b), 132.9 (d, C-8), 131.1 (d, C-12), 127.6 (d, C-2), 127.5 (s, C-12a), 125.6 (d, C-9), 125.0 (d, C-10), 121.9 (s, C-12b), 120.9 (d, C-4), 120.1 (s, C-3a), 119.7 (s, C-12c), 119.2 (s, C-10a), 118.4 (d, C-7), 117.0 (d, C-11), 57.3 (q, 5-OCH₃); ESI-MS (positive): m/z 301 [M+H]⁺.

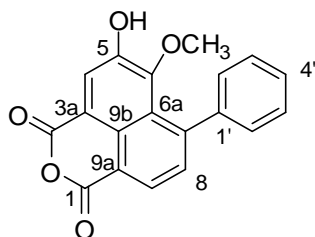
5-hydroxy-2-methoxy-1*H*-naphtho[2,1,8-*mna*]xanthen-1-one (3.4)



Isolated as a purple powder; IR (film) ν_{\max} cm^{-1} : 3346, 3219, 2922, 2851, 1731, 1665, 1608, 1575, 1558, 1454, 1391, 1366, 1219; UV (c, 0.035 mg/mL in EtOH) λ_{\max} (nm) 237, 255 sh,

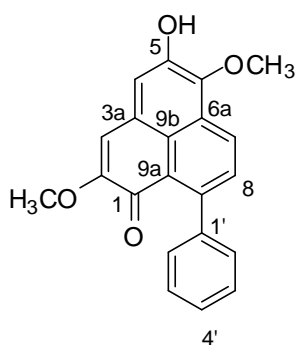
276 sh, 317, 364, 384, 544 ($\epsilon = 8884, 6472, 4512, 3277, 1679, 1715, 1995$ respectively); ^1H NMR (500 MHz, d_6 -DMSO, δ) 10.24 (1H, bs, 5-OH), 8.54 (1H, d, $J = 8.0$ Hz, H-12), 8.41 (1H, d, $J = 7.5$ Hz, H-10), 8.34 (1H, d, $J = 8.0$ Hz, H-11), 7.81 (1H, s, H-4), 7.63 (1H, dd, $J = 8.5, 7.0$ Hz, H-8), 7.51 (1H, d, $J = 8.5$ Hz, H-7), 7.40 (1H, dd, $J = 8.0, 7.0$ Hz, H-9), 7.40 (1H, s, H-2), 3.87 (3H, s, 2-OCH₃). ^{13}C (125 MHz, d_6 -DMSO, ppm) 177.3 (s, C-1), 153.0 (s, C-2), 151.9 (s, C-6a), 140.5 (s, C-5), 137.6 (s, C-5a), 133.1 (s, C-10b), 132.8 (d, C-8), 130.4 (d, C-12), 127.4 (s, C-12c), 125.1 (d, C-9), 125.0 (d, C-10), 122.5 (d, C-4), 120.7 (s, C-3a), 120.3 (s, C-12a), 119.1 (s, C-10a), 118.3 (d, C-7), 117.6 (s, C-12b), 116.7 (d, C-11), 113.2 (d, C-3), 55.9 (q, 2-OCH₃); ESI-MS (positive): m/z 317 [M+H]⁺.

Haemodorone (3.41)



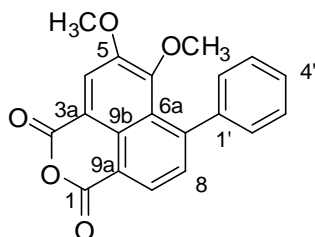
Isolated as a yellow powder; ^1H NMR (500 MHz, d_6 -DMSO, δ) 8.53 (1H, d, $J = 8.0$ Hz, H-9), 8.45 (1H, s, H-4), 7.66 (1H, d, $J = 8.0$ Hz, H-8), 7.49 (5H, s, H-2', H-3', H-4', H-5', H-6'), 3.16 (3H, s, H-10); ESI-MS (positive): m/z 321 [M+H]⁺.

Haemoxiphidone (**3.42**) also known as 5-Hydroxy-2,6-dimethoxy-9-phenyl-phenalen-1-one



Isolated as a yellow powder; m.p. 282-286°C; ^1H NMR (500 MHz) and ^{13}C (125 MHz) in d_6 -DMSO as well as the 2D COSY and HMBC correlations are detailed in **Table 3.1**; ^1H NMR (500 MHz) in d_6 -acetone described in **Table 3.1**; ESI-MS (negative): m/z 331 $[\text{M-H}]^-$.

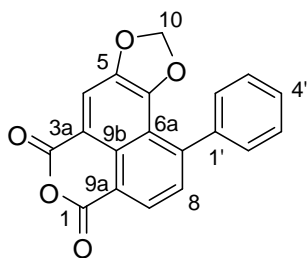
5,6-dimethoxy-7-phenyl-1*H*,3*H*-naphtho[1,8-*cd*]pyran-1,3-dione (**3.44**)



Isolated as fine fluorescent yellow crystals; Crystal data, $\text{C}_{20}\text{H}_{14}\text{O}_5 \cdot 0.5(\text{H}_2\text{O})$, $M = 343.32$, $T = 130.0(2)$ K, $\lambda = 1.5418$, Monoclinic, space group $\text{C}2/c$, $a = 18.455(2)$, $b = 8.077(1)$, $c = 21.455(2)$, Å, $\beta = 105.72(1)^\circ$, $V = 3078.7(6)$ Å³, $Z = 8$, $D_c = 1.481$ mg M^{-3} , $\mu(\text{Cu-K}\alpha) 0.904$ mm⁻¹, $F(000) = 1432$, crystal size 0.45 x 0.05 x 0.03 mm. 5526 reflections measured, 2765 independent reflections ($R_{\text{int}} = 0.071$) the final R was 0.0585 [$I > 2\sigma(I)$] and $wR(F^2)$ was 0.1488 (all data). Crystallographic data for **3.44** has been deposited at the Cambridge Crystallographic Data Centre (CCDC 912701)* 12 Union Road, Cambridge, CB2 1EZ, UK (www.ccdc.cam.ac.uk/data_request/cif); m.p. (uncorr.) 256-258°C; ^1H NMR (500 MHz, CDCl_3 , δ) 8.51 (1H, d, $J = 7.0$ Hz, H-9), 8.42 (1H, s, H-4), 7.55 (1H, d, $J = 7.0$ Hz, H-8), 7.42 (3H, m, H-3', H-4', H-5'), 7.35 (2H, m, H-2', H-6'), 4.06 (3H, s, 5-OCH₃), 3.38 (s, 6-OCH₃). ^{13}C

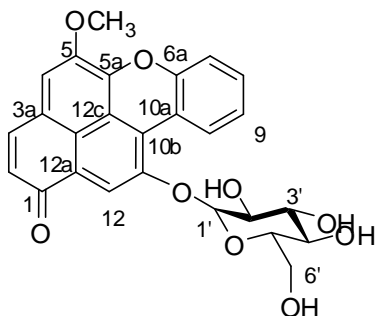
(125 MHz, CDCl₃, ppm) 160.8 (s, C-1), 160.6 (s, C-3), 151.8 (s, C-6), 150.9 (s, C-4), 146.7 (s, C-7), 142.2 (s, C-1'), 131.3 (d, C-9), 130.7 (d, C-8), 128.2 (d, C-2', C-6'), 127.9 (s, C-9b), 127.3 (d, C-3', C-4', C-5'), 125.9 (s, C-6a), 123.7 (s, C-3a), 120.6 (d, C-4), 117.9 (s, C-9a), 60.9 (q, 6-OCH₃), 56.9 (q, 5-OCH₃); ESI-MS (positive): *m/z* 335 [M+H]⁺.

Haemodordioxolane (**3.45**) also known as 1-phenyl-5,8,10-trioxa-cyclopenta[*a*]phenalene-4,6-dione



Isolated as a fluorescent yellow needles; m.p. (uncorr.) 215-218°C; IR (film) ν_{\max} cm⁻¹: 2956, 2926, 2854, 1770, 1728, 1679, 1463, 1379, 1265; UV (c, 0.033 mg/mL in EtOH) λ_{\max} (nm) 220 sh, 254, 314 sh, 327, 368, 421 sh (ϵ = 7430, 5083, 1137, 1272, 1081, 242 respectively); ¹H NMR (500 MHz) and ¹³C (125 MHz) *d*₆-DMSO and CDCl₃ details as well as the 2D COSY and HMBC correlations are detailed in **Table 3.2**; ESI-MS (positive): *m/z* 319 [M+H]⁺, HR-ESI-MS displayed an *m/z* at 319.0603 [M+H]⁺ (calcd. for C₁₉H₁₁O₅: *m/z* 319.0606).

Haemodoroxychysenose (**3.46**) also known as 11-O- β -D-glucopyranosyloxy-5-methoxy-6-oxabenzochrysen-1-one



Isolated as a fluorescent pink powder; m.p. (uncorr.) 155-160°C; $[\alpha]_{\text{D}}^{25} +16.2^\circ$ (c, 3.8 mg/mL in MeOH); IR (film) ν_{max} cm^{-1} : 3383, 2956, 2921, 2851, 1731, 1593, 1564, 1415, 1380, 1358, 1318; UV (c, 0.033 mg/mL in EtOH) λ_{max} (nm) 236 sh, 266 sh, 288 sh, 371 sh, 402, 537 ($\epsilon=$ 8217, 3900, 3399, 882, 731, 2581 respectively); ^1H NMR (500 MHz, d_6 -DMSO) and ^{13}C (125 MHz, d_6 -DMSO) details as well as the 2D COSY and HMBC correlations are detailed in **Table 3.3**; ESI-MS (positive): m/z 479 $[\text{M}+\text{H}]^+$, HR-ESI-MS displayed an m/z at 479.1337 $[\text{M}+\text{H}]^+$ (calcd. for $\text{C}_{19}\text{H}_{11}\text{O}_5$: 479.1342).

7.4 Chapter 4 Experimental

7.4.1 Chapter 4 HPLC-NMR Characterisation (from stop-flow HPLC-NMR)

Droserone (**4.7**)

HPLC-NMR (WET-1D, 500 MHz, stop-flow HPLC-NMR, δ) 7.48 (dd, $J = 8.5, 7.5$ Hz, H-7), 7.34 (d, $J = 7.5$ Hz, H-8), 6.97 (d, $J = 8.5$ Hz, H-6), 1.74 (s, H-9) signal partially suppressed in CH_3CN region.

Hydroxydroserone (**4.8**)

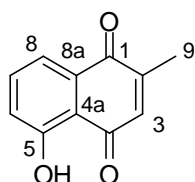
HPLC-NMR (WET-1D, 500 MHz, stop-flow HPLC-NMR, δ) 7.17 (d, $J = 9$ Hz, H-6), 7.09 (d, $J = 9$ Hz, H-7), 1.79 (s, H-9) signal partially suppressed in CH_3CN region.

Co-eluting droserone-5-*O*- β -glycoside (**4.9**) and Hydroxydroserone-5-*O*- β -glycoside (**4.10**)

HPLC-NMR (WET-1D, 500 MHz, stop-flow HPLC-NMR, δ) 7.65-6.70 (m), 5.04 (m), 5.00 (s), 4.85 (s), 3.20-3.80 (m), 1.80 (s, H-9) signal partially suppressed in CH_3CN region.

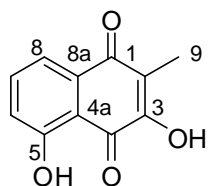
7.4.2 Chapter 4 Off-line Characterisation

Plumbagin (**1.267**)



Isolated as a stable brown oil; ^1H NMR (500 MHz, d_6 -DMSO, δ) and ^{13}C (125 MHz, d_6 -DMSO) details in **Table 4.2**; ESI-MS (negative): m/z 203 [M-H].

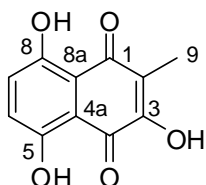
Droserone (**4.7**)



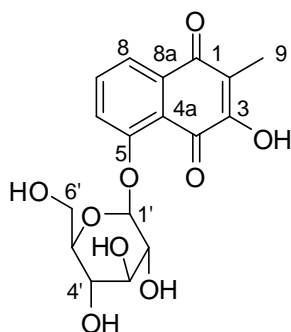
Isolated as a stable yellow oil; ^1H NMR (500 MHz, d_6 -DMSO, δ) 11.43 (bs, 5-OH), 7.69 (dd, $J = 7.5, 8.0$ Hz, H-7), 7.48 (dd, $J = 1.0, 7.5$ Hz, H-8), 7.24 (dd, $J = 1.0, 8.0$ Hz, H-6), 1.91 (s, H-9). ^{13}C (125 MHz, d_6 -DMSO, ppm) 184.6 (s, C-1), 183.9 (s, C-4), 160.0 (s, C-5), 155.5 (s, C-3), 136.8 (d, C-7), 132.4 (s, C-8a), 122.7 (d, C-6), 120.3 (s, C-2), 118.2 (d, C-8), 113.6 (s, C-

4a), 8.7 (q, C-9), 3-OH not detected; ^1H NMR (500 MHz, CDCl_3 , δ) 7.61 (dd, $J = 8.0, 8.0$ Hz, H-7), 7.29 (d, $J = 8.0$ Hz, H-8), 7.23 (d, $J = 8.0$ Hz, H-6), 2.08 (s, H-9), 3-OH and 5-OH not detected; ESI-MS (negative): m/z 203 $[\text{M-H}]^-$.

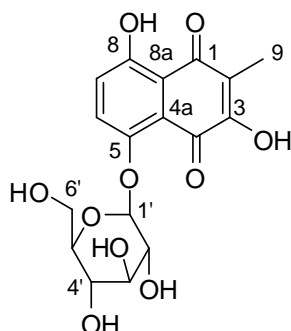
Hydroxydroserone (4.8)



Isolated as a stable brown oil; ^1H NMR (500 MHz, d_6 -DMSO, δ) 12.95 (s, 8-OH), 11.73 (s, 5-OH), 7.34 (d, $J = 9.3$ Hz, H-7), 7.27 (d, $J = 9.3$ Hz, H-6), 1.93 (s, H-9); ^{13}C (125 MHz, d_6 -DMSO, ppm) 188.8 (s, C-1), 182.9 (s, C-4), 157.0 (s, C-5), 156.0 (s, C-8), 155.3 (s, C-3), 129.9 (d, C-7), 127.2 (d, C-6), 120.2 (s, C-2), 110.9* (s, C-4a), 110.8* (s, C-8a), 8.1 (q, C-9), 3-OH not detected; ^1H NMR (500 MHz, CDCl_3 , δ) 12.83 (s, bs, 8-OH), 7.27 (d, $J = 9.3$ Hz, H-6), 7.16 (d, $J = 9.3$ Hz, H-7), 2.10 (s, H-9); ^{13}C (125 MHz, CDCl_3 , ppm) 188.9 (s, C-1), 182.1 (s, C-4), 157.5 (s, C-5), 157.0 (s, C-8), 154.0 (s, C-3), 131.3 (d, C-7), 127.4 (d, C-6), 121.6 (s, C-2), 110.7 (s, C-8a), 110.2 (s, C-4a), 8.3 (q, C-9), 3-OH and 5-OH not detected; ESI-MS (negative): m/z 219 $[\text{M-H}]^-$. * Chemical shifts interchangeable

Droserone-5-*O*- β -glycoside (**4.9**)

Isolated as a stable yellow/brown oil; ^1H NMR (500 MHz, d_6 -DMSO, δ) 10.84 (bs, 3-OH), 7.74 (dd, $J = 8, 8$ Hz, H-7), 7.66 (d, $J = 8$ Hz, H-8), 7.55 (d, $J = 8$ Hz, H-6), 5.12 (d, $J = 8.0$ Hz, H-1'), 3.69 (d, $J = 11$ Hz, H-6'b), 3.48 (m, H-6'a), 3.41 (m, H-5'), 3.38 (m, H-2'), 3.29 (m, H-3'), 3.20 (m, H-4'), 1.89 (s, H-9). ^{13}C (125 MHz, d_6 -DMSO, ppm); 184.3 (s, C-1), 179.0 (s, C-4), 157.0 (s, C-5), 155.9 (s, C-3), 135.2 (d, C-7), 133.9 (s, C-8a), 120.6 (d, C-6), 119.3 (d, C-8), 117.9 (s, C-4a), 117.3 (s, C-2), 100.0 (d, C-1'), 76.9 (d, C-5'), 76.3 (d, C-3'), 73.2 (d, C-2'), 69.2 (d, C-4'), 60.3 (t, C-6'), 8.3 (q, C-6'), 2'-OH, 3'-OH, 4'-OH, 5'-OH and 6'-OH not detected; ESI-MS (negative): m/z 203 $[\text{M-H}]^-$.

Hydroxydroserone-5-*O*- β -glycoside (**4.10**)

Isolated as a stable brown oil; ^1H NMR (500 MHz, d_6 -DMSO, δ) and ^{13}C (125 MHz, d_6 -DMSO) details in **Table 4.3**; ESI-MS (negative): m/z 203 $[\text{M-H}]^-$.

7.5 Chapter 5 Experimental

7.5.1 Chapter 5 HPLC-NMR Characterisation (from stop-flow HPLC-NMR)

Plocamenone (5.21)

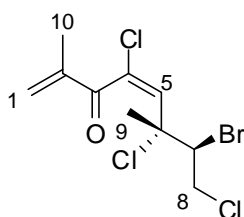
HPLC-NMR (WET-1D, 500 MHz, 70% CH₃CN/D₂O, δ); 6.26 (s, H-5), 6.18 (s, H-1b), 6.09 (s, H-1a), 4.44 (dd, $J = 2.5, 9.5$ Hz, H-7), 4.18 (dd, $J = 2.5, 13$ Hz, H-8b), 3.74 (dd, $J = 9.5, 13$ Hz, H-8a), 1.82 (s, H-9)*, 1.65 (s, H-10); HPLC-NMR (¹³C, 125 MHz, obtained from the WET-2D HSQC NMR experiment, ppm); 134.0 (d, C-5), 133.2 (t, C-1), 63.5 (d, C-7), 48.0 (t, C-8), 27.9 (q, C-10), all other carbons not observed. *indicates signal was partially suppressed.

Isoplocamenone (5.24)

HPLC-NMR (WET-1D, 500 MHz, 70% CH₃CN/D₂O, δ): 6.78 (s, H-5), 5.93 (s, H-1b), 5.80 (s, H-1a), 4.85 (dd, $J = 2.0, 9.5$ Hz, H-7), 4.27 (dd, $J = 2.0, 12.5$ Hz, H-8b), 2.06 (s, H-10), 1.92 (s, H-9)*, H-8a suppressed. *indicates signal was partially suppressed.

7.5.2 Chapter 5 Off-line Characterisation

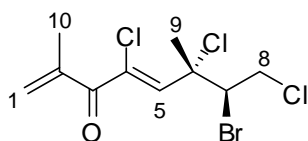
Plocamenone (5.21) also known as (*Z*)-7-Bromo-4,6,8-trichloro-2,6-dimethylocta-1,4-dien-3-one



Isolated as a stable colorless to light brown oil; $[\alpha]_D^{21} -21.5^\circ$ (c, 4.58 mg/mL in CHCl₃); IR (film) ν_{\max} cm⁻¹: 2960, 1670, 1450, 1349, 1092, 947; UV (MeOH) λ_{\max} 244 nm ($\epsilon = 17000$); UV profile extracted from HPLC using photodiode array detection (CH₃CN/H₂O) 236 nm; ¹H NMR (500 MHz), ¹³C (125 MHz), COSY, HSQCAD and HMBC assignments are detailed in **Table 5.2** (CDCl₃) and in **Table 5.4** (CD₃OD); ESI-MS (positive) m/z 335 [M+H]⁺, 299 [M-Cl]⁺, 219

[M–Cl–Br]⁺; GC-MS (EI); *m/z* 299 [M–Cl]⁺, 191 [M–C₂H₃BrCl]⁺, 169, 156 [M–C₂H₃BrCl₂]⁺, 127, 91, 77, 69, 51; HR-GC-MS (EI); *m/z* 298.9050 [M–Cl]⁺ (calculated for C₁₀H₁₂O³⁵Cl₂⁸¹Br: *m/z* 298.9403), 216.9908 [M–Cl–Br]⁺, 190.9774 [M–C₂H₃BrCl]⁺, 169.0190, 156.0127 [M–C₂H₃BrCl₂]⁺, 77.0285, 69.0248.

Isoplocamenone (**5.24**) also known as (*E*)-7-Bromo-4,6,8-trichloro-2,6-dimethylocta-1,4-dien-3-one

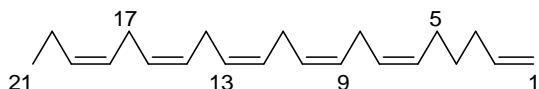


Isolated as an unstable colorless to light brown oil; UV profile extracted from HPLC using photodiode array detection (CH₃CN/H₂O) 240 nm; ¹H NMR (500 MHz), ¹³C (125 MHz), COSY, HSQCAD and HMBC assignments are detailed in **Table 5.3** (CDCl₃) and in **Table 5.4** (CD₃OD); ESI-MS (positive) *m/z* 335 [M+H]⁺, 299 [M–Cl]⁺, 219 [M–Cl–Br]⁺; GC-MS (EI); *m/z* 299 [M–Cl]⁺, 191 [M–C₂H₃BrCl]⁺, 169, 156 [M–C₂H₃BrCl₂]⁺, 127, 91, 77, 69, 51; HR-GC-MS (EI); *m/z* 298.9397 [M–Cl]⁺ (calculated for C₁₀H₁₂O³⁵Cl₂⁸¹Br: *m/z* 298.9403), 217.0148 [M–Cl–Br]⁺, 191.0016 [M–C₂H₃BrCl]⁺, 169.0419, 156.0326 [M–C₂H₃BrCl₂]⁺, 77.0365, 69.0311.

7.6 Chapter 6 Experimental

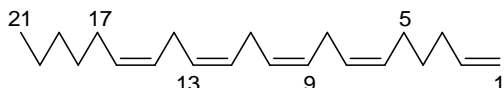
7.6.1 Chapter 6 HPLC-NMR Characterisation (from on-flow HPLC-NMR)

Compound (6.1)



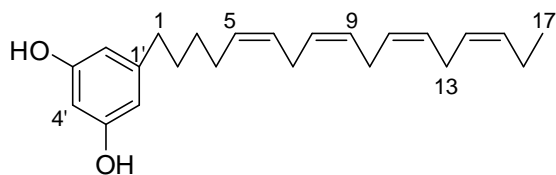
HPLC-NMR (WET-1D, 500 MHz, 90:10 CH₃CN:D₂O, δ) 5.77 (1H, tt, $J = 8.0, 7.0, 1.5$, H-2), 5.31 (10H, m, H-6, H-7, H-9, H-10, H-12, H-13, H-15, H-16, H-18, H-19), 4.95 (1H, d, $J = 17.5$ Hz, H-1a), 4.88 (1H, d, $J = 10.0$ Hz, H-1b), 1.38 (2H, tt, $J = 7.5, 7.0$ Hz, H-4), 0.89 (3H, t, $J = 7.5$ Hz, H-21), all other peaks suppressed; GC-MS (EI); m/z 284 (6) [M]⁺ 159 (17), 145 (34), 131 (52), 119 (54), 105 (100).

Compound (6.2)



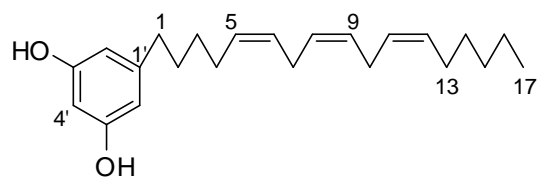
HPLC-NMR (WET-1D, 500 MHz, 90:10 CH₃CN:D₂O, δ) 5.77 (1H, m, H-2), 5.30 (8H, s, H-6, H-7, H-9, H-10, H-12, H-13, H-15, H-16), 4.95 (1H, dd, $J = 16.5, 1.0$ Hz, H-1a), 4.88 (1H, dd, $J = 11.0, 1.0$ Hz, H-1b), 1.38 (2H, tt, $J = 7.5, 7.0$ Hz, H-4), 2.36 (4H, t, $J = 7.5$ Hz), 1.48 (2H, tt, $J = 7.5, 7.0$ Hz, H-4), 1.29 (2H, m), 1.23 (6H, m), 0.82 (3H, t, $J = 7.0$ Hz, H-21), all other signals suppressed; GC-MS (EI); m/z 286 (2) [M]⁺, 215 (32), 201 (30), 175 (48), 161 (53), 147 (100).

Compound (6.14)



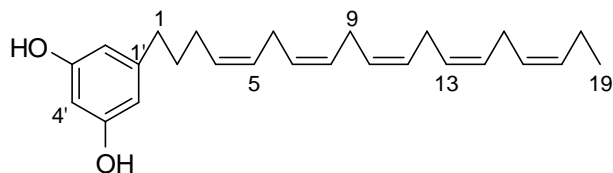
HPLC-NMR (WET-1D, 500 MHz, 80:20 CH₃CN:D₂O, δ) 6.08 (2H, d, $J = 2.0$ Hz, H-2', H-6'), 6.02 (1H, d, $J = 2.0$ Hz, H-4'), 5.29 (8H, m, H-5, H-6, H-8, H-9, H-11, H-12, H-14, H-15), 2.76 (6H, m, H-7, H-10, H-13), 2.37 (2H, t, $J = 7.5$ Hz, H-1), 1.48 (2H, tt, $J = 7.5, 7.5$ Hz, H-2), 1.28 (2H, tt, $J = 7.5, 7.5$ Hz, H-3), 0.87 (3H, t, $J = 7.5$ Hz, H-17); ESI-MS (negative): m/z 339 [M-H]⁻.

Compound (6.15)



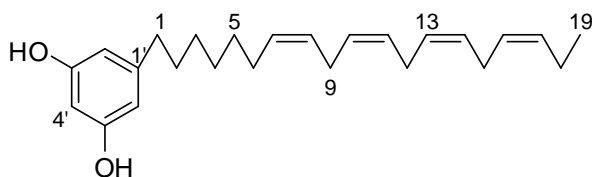
HPLC-NMR (WET-1D, 500 MHz, 80:20 CH₃CN:D₂O, δ) 6.08 (2H, d, $J = 1.5$ Hz, H-2', H-6'), 6.02 (1H, d, $J = 1.0$ Hz, H-4'), 5.28 (6H, m, H-5, H-6, H-8, H-9, H-11, H-12), 2.74 (4H, m, H-7, H-10), 2.37 (2H, t, $J = 7.5$ Hz, H-1), 1.48 (2H, tt, $J = 7.5, 7.5$ Hz, H-2), 1.28 (2H, tt, $J = 7.5, 7.5$ Hz, H-3), 0.87 (3H, t, $J = 7.0$ Hz, H-17); ESI-MS (negative): m/z 341 [M-H]⁻.

Compound (6.16)



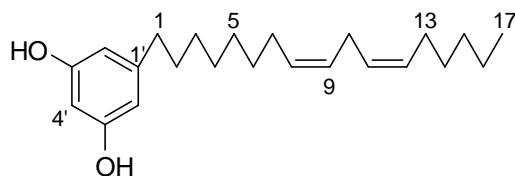
HPLC-NMR (WET-1D, 500 MHz, 80:20 CH₃CN:D₂O, δ) 6.08 (2H, d, $J = 2.0$ Hz, H-2', H-6'), 6.02 (1H, d, $J = 2.0$ Hz, H-4'), 5.30 (10H, m, H-4, H-5, H-7, H-8, H-10, H-11, H-13, H-14), 2.76 (8H, m, H-6, H-9, H-12, H-15), 2.38 (2H, t, $J = 8.0$ Hz, H-2), 1.53 (2H, t, $J = 7.5$ Hz, H-2), 0.87 (3H, t, $J = 7.5$ Hz, H-19); ESI-MS (negative): m/z 365 [M-H]⁻.

Compound (6.17)



HPLC-NMR (WET-1D, 500 MHz, 80:20 CH₃CN:D₂O, δ) 6.08 (2H, d, $J = 1.0$ Hz, H-2', H-6'), 6.02 (1H, d, $J = 1.5$ Hz, H-4'), 5.29 (8H, m, H-7, H-8, H-10, H-11, H-13, H-14, H-16, H-17), 2.74 (6H, m, H-9, H-12, H-15), 2.36 (q, $J = 8.0$ Hz), 1.53 (t, $J = 7.5$ Hz), 0.80 (3H, t, $J = 7.0$ Hz, H-19); ESI-MS (negative): m/z 367 [M-H]⁻.

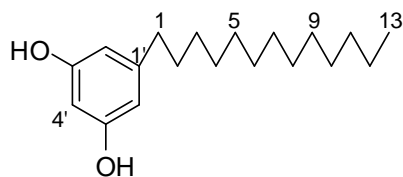
HPLC-NMR assignment of compound (6.18)



HPLC-NMR (WET-1D, 500 MHz, 80:20 CH₃CN:D₂O, δ) 6.08 (2H, d, J = 2.0 Hz, H-2', H-6'), 6.01 (1H, d, J = 2.0 Hz, H-4'), 5.28 (m), 2.70 (t, J = 6.5 Hz), 2.36 (t, J = 8.0 Hz), 0.80 (3H, t, J = 7.0 Hz, H-17); ESI-MS (negative): m/z 343 [M-H]⁻.

7.6.2 Chapter 6 Off-line Characterisation

Compound (6.12)



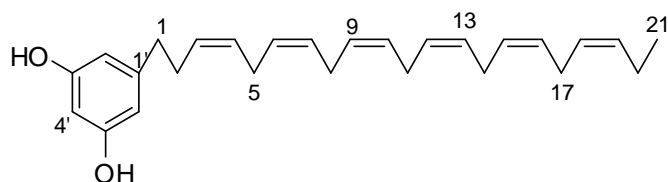
ESI-MS (negative): m/z 291 [M-H]⁻

Compound (6.14)



¹H NMR (500 MHz, CDCl₃) and ¹³C (125 MHz, CDCl₃) details as well as the 2D NMR COSY and HMBC NMR correlations are detailed in **Table 6.2**.

Compound (6.19)



ESI-MS (negative): m/z 391 [M-H]⁻

References

- [1] Sarker, S. D., Latif, Z., Gray, A. I., Editors, *Natural Products Isolation, Second Edition*. [In: *Methods Biotechnol.*; 2005, 20], Humana Press Inc. 2005.
- [2] Ng, R., *Drugs: From Discovery to Approval*, 2004.
- [3] Fowler, M. W., *Journal of the Science of Food and Agriculture*, 2006, 86, 1797-1804.
- [4] Newman, D. J., Cragg, G. M., Snader, K. M., *Journal of Natural Products*, 2003, 66, 1022-1037.
- [5] Newman, D. J., Cragg, G. M., *Journal of Natural Products*, 2012, 75, 311-335.
- [6] Chemical Abstract Service, 2012, American Chemical Society, <http://www.cas.org/> (Accessed 29/11/12)
- [7] Dictionary of Natural Products Online™, 2012, A subset of the Chapman & Hall/CRC Chemical Database™, <http://dnp.chemnetbase.com/dictionary-search.do?method=view&id=6930629&si=> (Accessed 29/11/12)
- [8] MarinLit Database™, 2012, University of Canterbury, Christchurch, New Zealand, (Accessed 29/11/12)
- [9] Colegate, S. M., Molyneux, R. J., Editors, *Bioactive Natural Products: Detection, Isolation, and Structural Determination, Second Edition*, CRC Press 2008.
- [10] Cragg, G. M., Newman, D. J., *Pure and Applied Chemistry*, 2005, 77, 7-24.
- [11] Newman, D. J., Cragg, G. M., *Journal of Natural Products*, 2004, 67, 1216-1238.
- [12] Bhatnagar, I., Kim, S.-K., *Marine Drugs*, 2010, 8, 2702-2720.
- [13] Blunt, J. W., Copp, B. R., Munro, M. H. G., Northcote, P. T., Prinsep, M. R., *Natural Product Reports*, 2005, 22, 15-61.
- [14] Hill, R. A., *Annual Reports on the Progress of Chemistry, Section B*, 2012, 108, 131-146.
- [15] Murti, Y., Agrawal, T., *International Journal of ChemTech Research*, 2010, 2, 2198-2217.
- [16] Agosta, W. C., *Journal of Chemical Education*, 1997, 74, 857-860.
- [17] Jager, A. K., Saaby, L., *Molecules*, 2011, 16, 1471-1485.
- [18] Cazarolli, L. H., Zanatta, L., Alberton, E. H., Figueiredo, M. S. R. B., Folador, P., Damazio, R. G., Pizzolatti, M. G., Silva, F. R. M. B., *Mini-Reviews in Medicinal Chemistry*, 2008, 8, 1429-1440.
- [19] Corradini, E., Foglia, P., Giansanti, P., Gubbionti, R., Samperi, R., Lagana, A., *Natural Product Research*, 2011, 25, 469-495.
- [20] Calderon-Montano, J. M., Burgos-Moron, E., Perez-Guerrero, C., Lopez-Lazaro, M., *Mini-Reviews in Medicinal Chemistry*, 2011, 11, 298-344.
- [21] Tsao, R., McCallum, J., *Fruit and Vegetable Phytochemicals*, Wiley-Blackwell 2010, pp. 131-153.
- [22] SciFinder®, 2012, American Chemical Society, <http://www.cas.org/products/scifinder> (Accessed 29/11/12)
- [23] Chahar, M. K., Sharma, N., Dobhal, M. P., Joshi, Y. C., *Pharmacognosy Reviews*, 2011, 5, 1-12.
- [24] Androutsopoulos, V. P., Papakyriakou, A., Vourloumis, D., Tsatsakis, A. M., Spandidos, D. A., *Pharmacology and Therapeutics*, 2010, 126, 9-20.
- [25] Colabufo, N. A., Berardi, F., Contino, M., Inglese, C., Perrone, R., *Research Signpost* 2008, pp. 171-201.
- [26] Mojzic, J., Varinska, L., Mojzicova, G., Kostova, I., Mirossay, L., *Pharmacological Research*, 2008, 57, 259-265.
- [27] Tan, W., Lu, J., Huang, M., Li, Y., Chen, M., Wu, G., Gong, J., Zhong, Z., Xu, Z., Dang, Y., Guo, J., Chen, X., Wang, Y., *Chinese Medicine*, 2011, 6, 27.
- [28] Shukla, S., Gupta, S., *Pharmaceutical Research*, 2010, 27, 962-978.
- [29] Anita, S., Manjul, P. S., Roshan, P., Neelam, D., Gulzar, A., *Journal of Pharmacy Research*, 2010, 3, 2834-2835.
- [30] Jan, A. T., Kamli, M. R., Murtaza, I., Singh, J. B., Ali, A., Haq, Q. M. R., *Food Reviews International*, 2010, 26, 302-317.
- [31] Veitch, N. C., Grayer, R. J., *Natural Product Reports*, 2008, 25, 555-611.
- [32] Bourjot, M., Apel, C., Martin, M.-T., Grellier, P., Nguyen, V. H., Gueritte, F., Litaudon, M., *Planta Medica*, 2010, 76, 1600-1604.
- [33] Tripathi, R., Samadder, T., Gupta, S., Surolia, A., Shaha, C., *Molecular Cancer Therapeutics*, 2011, 10, 255-268.
- [34] Haggag, E. G., Kamal, A. M., Abdelhady, M. I. S., El-Sayed, M. M., El-Wakil, E. A., Abd-Elhamed, S. S., *Pharmaceutical Biology*, 2011, 49, 1103-1113.
- [35] Liu, H., Xiao, Y., Xiong, C., Wei, A., Ruan, J., *European Journal of Pharmacology*, 2011, 654, 209-216.

- [36] Huang, X. H., Xiong, P. C., Xiong, C. M., Cai, Y. L., Wei, A. H., Wang, J. P., Liang, X. F., Ruan, J. L., *Phytomedicine*, 2010, 17, 930-934.
- [37] Khoo, B. Y., Chua, S. L., Balaram, P., *International Journal of Molecular Sciences*, 2010, 11, 2188-2199.
- [38] Androutsopoulos, V. P., Ruparelia, K., Arroo, R. R. J., Tsatsakis, A. M., Spandidos, D. A., *Toxicology*, 2009, 264, 162-170.
- [39] Xie, Y.-Y., Yuan, D., Yang, J.-Y., Wang, L.-H., Wu, C.-F., *Journal of Asian Natural Products Research*, 2009, 11, 771-778.
- [40] Fawzy, G. A., Al-Taweel, A. M., Abdel, B. N. A., Marzouk, M. S., *African Journal of Pharmacy and Pharmacology*, 2012, 6, 1166-1175.
- [41] Geethangili, M., Rao, Y. K., Fang, S.-H., Tzeng, Y.-M., *Phytotherapy Research*, 2008, 22, 1336-1341.
- [42] Li, F., Awale, S., Tezuka, Y., Kadota, S., *Bioorganic and Medicinal Chemistry*, 2008, 16, 5434-5440.
- [43] Hsu, C.-L., Shyu, M.-H., Lin, J.-A., Yen, G.-C., Fang, S.-C., *Food Chemistry*, 2011, 127, 127-134.
- [44] Lee, J.-Y., Kim, J.-K., Cho, M.-C., Shin, S., Yoon, D.-Y., Heo, Y. S., Kim, Y., *Journal of Natural Products*, 2010, 73, 1261-1265.
- [45] Mohammed, M. M. D., El-Sharkawy, E. R., Matloub, A. A., *Journal of Medicinal Plants Research*, 2011, 5, 5099-5103.
- [46] Wu, L.-S., Wang, X.-J., Wang, H., Yang, H.-W., Jia, A.-Q., Ding, Q., *Journal of Ethnopharmacology*, 2010, 130, 460-464.
- [47] Chidambara, M. K. N., Kim, J., Vikram, A., Patil, B. S., *Food Chemistry*, 2012, 132, 27-34.
- [48] Zarebczan, B., Pinchot, S. N., Kunnimalaiyaan, M., Chen, H., *The American Journal of Surgery*, 2011, 201, 329-333.
- [49] Bai, N., He, K., Zhou, Z., Lai, C.-S., Zhang, L., Quan, Z., Shao, X., Pan, M.-H., Ho, C.-T., *Food Chemistry*, 2010, 122, 831-835.
- [50] Tumbas, V. T., Canadanovic-Brunet, J. M., Cetojevic-Simin, D. D., Cetkovic, G. S., Djilas, S. M., Gille, L., *Journal of the Science of Food and Agriculture*, 2012, 92, 1273-1281.
- [51] Bai, N., He, K., Roller, M., Lai, C.-S., Shao, X., Pan, M.-H., Ho, C.-T., *Journal of Agricultural and Food Chemistry*, 2010, 58, 5363-5367.
- [52] Mamadalieva, N. Z., Herrmann, F., El-Readi, M. Z., Tahrani, A., Hamoud, R., Egamberdieva, D. R., Azimova, S. S., Wink, M., *Journal of Pharmacy and Pharmacology*, 2011, 63, 1346-1357.
- [53] Yang, S. F., Yang, W. E., Chang, H. R., Chu, S. C., Hsieh, Y. S., *Journal of Dental Research*, 2008, 87, 401-406.
- [54] Zakaria, I., Ahmat, N., Jaafar, F. M., Widyawaruyanti, A., *Fitoterapia*, 2012, 83, 968-972.
- [55] Phillips, P. A., Sangwan, V., Borja-Cacho, D., Dudeja, V., Vickers, S. M., Saluja, A. K., *Cancer Letters (New York, NY, United States)*, 2011, 308, 181-188.
- [56] ClinicalTrials.gov, U.S. National Institutes of Health, Department of Health and Human Services, <http://www.clinicaltrials.gov/> (Accessed 11/12/12)
- [57] Yao, N., Chen, C.-Y., Wu, C.-Y., Motonishi, K., Kung, H.-J., Lam, K. S., *Journal of Medicinal Chemistry*, 2011, 54, 4339-4349.
- [58] Choi, Y.-J., Kim, H. M., Kim, H.-D., *Archives of Pharmacal Research*, 2009, 32, 59-63.
- [59] Pradhan, D., Panda, P. K., Tripathy, G., Nayak, J. R., Pattanayak, A., *Journal of Pharmacy Research*, 2009, 2, 983-985.
- [60] Kang, Y.-J., Min, H.-Y., Hong, J.-Y., Kim, Y. S., Kang, S. S., Lee, S. K., *Biomolecules and Therapeutics*, 2009, 17, 282-287.
- [61] Centers for Disease Control and Prevention, 2012, CDC, <http://www.cdc.gov/>, (Accessed 30/12/2012)
- [62] World Health Organisation, 2012, WHO, <http://www.who.int/en/>, (Accessed 30/12/2012)
- [63] Batista, R., Silva, A. d. J., Jr., Braga, d. O. A., *Molecules*, 2009, 14, 3037-3072.
- [64] Willcox, M., *Journal of Alternative and Complementary Medicine*, 2009, 15, 101-109.
- [65] Yenesew, A., Akala, H. M., Twinomuhwezi, H., Chepkirui, C., Irungu, B. N., Eyase, F. L., Kamatenesi-Mugisha, M., Kiremire, B. T., Johnson, J. D., Waters, N. C., *Acta Tropica*, 2012, 123, 123-127.
- [66] Nour, A. M. M., Khalid, S. A., Kaiser, M., Brun, R., Abdalla, W. I. E., Schmidt, T. J., *Journal of Ethnopharmacology*, 2010, 129, 127-130.
- [67] Kunert, O., Swamy, R. C., Kaiser, M., Presser, A., Buzzi, S., Rao, A. V. N. A., Schuehly, W., *Phytochemistry Letters*, 2008, 1, 171-174.
- [68] Muhammad, A., Anis, I., Ali, Z., Awadelkarim, S., Khan, A., Khalid, A., Shah, M. R., Galal, M., Khan, I. A., Iqbal, C. M., *Bioorganic and Medicinal Chemistry Letters*, 2012, 22, 610-612.

- [69] Ramirez-Macias, I., Marin, C., Diaz, J. G., Rosales, M. J., Gutierrez-Sanchez, R., Sanchez-Moreno, M., *The Scientific World Journal*, 2012, 203646, 203610 pp.
- [70] Marin, C., Boutaleb-Charki, S., Diaz, J. G., Huertas, O., Rosales, M. J., Perez-Cordon, G., Gutierrez-Sanchez, R., Sanchez-Moreno, M., *Journal of Natural Products*, 2009, 72, 1069-1074.
- [71] Marin, C., Ramirez-Macias, I., Lopez-Cespedes, A., Olmo, F., Villegas, N., Diaz, J. G., Rosales, M. J., Gutierrez-Sanchez, R., Sanchez-Moreno, M., *Journal of Natural Products*, 2011, 74, 744-750.
- [72] Arioka, S., Sakagami, M., Uematsu, R., Yamaguchi, H., Togame, H., Takemoto, H., Hinou, H., Nishimura, S.-I., *Bioorganic and Medicinal Chemistry*, 2010, 18, 1633-1640.
- [73] Dixon, R. A., Pasinetti, G. M., *Plant Physiology*, 2010, 154, 453-457.
- [74] Salas, C. O., Faundez, M., Morello, A., Maya, J. D., Tapia, R. A., *Current Medicinal Chemistry*, 2011, 18, 144-161.
- [75] Babula, P., Adam, V., Havel, L., Kizek, R., *Current Pharmaceutical Analysis*, 2009, 5, 47-68.
- [76] Verma, R. P., *Anti-Cancer Agents in Medicinal Chemistry*, 2006, 6, 489-499.
- [77] Rodrigues de Almeida, E., *The Open Natural Products Journal*, 2009, 2, 42-47.
- [78] Kuete, V., Wabo, H. K., Eyong, K. O., Feussi, M. T., Wiench, B., Krusche, B., Tane, P., Folefoc, G. N., Efferth, T., *PLoS One*, 2011, 6, e21762.
- [79] Benites, J., Valderrama, J. A., Taper, H., Buc, C. P., *Investigational New Drugs*, 2011, 29, 760-767.
- [80] Bonifazi, E. L., Rios-Luci, C., Leon, L. G., Burton, G., Padron, J. M., Misico, R. I., *Bioorganic and Medicinal Chemistry*, 2010, 18, 2621-2630.
- [81] Kitagawa, R. R., Vilegas, W., Carlos, I. Z., Raddi, M. S. G., *Revista Brasileira de Farmacognosia*, 2011, 21, 1084-1088.
- [82] Esteves-Souza, A., Lucio, K. A., Sousa, d. C. A., Pinto, A. d. C., Lima, E. L. d. S., Camara, C. A., Vargas, M. D., Gattass, C. R., *Oncology Reports*, 2008, 20, 225-231.
- [83] Tapia, R. A., Cantuarias, L., Cuellar, M., Villena, J., *Journal of the Brazilian Chemical Society*, 2009, 20, 999-1002.
- [84] Im, Y.-S., Chung, Y., Won, D. Y., Kwon, S. H., Kim, H.-R., Lee, D. G., Kim, S.-R., Park, K. D., Lee, H.-K., Choi, J.-K., *Genes Genomics*, 2010, 32, 592-598.
- [85] Zhou, J., Duan, L., Chen, H., Ren, X., Zhang, Z., Zhou, F., Liu, J., Pei, D., Ding, K., *Bioorganic and Medicinal Chemistry Letters*, 2009, 19, 5091-5094.
- [86] Cao, S., Murphy, B. T., Foster, C., Lazo, J. S., Kingston, D. G. I., *Bioorganic and Medicinal Chemistry*, 2009, 17, 2276-2281.
- [87] Cui, X.-R., Tsukada, M., Suzuki, N., Shimamura, T., Gao, L., Koyanagi, J., Komada, F., Saito, S., *European Journal of Medicinal Chemistry*, 2008, 43, 1206-1215.
- [88] Montenegro, R. C., Araujo, A. J., Molina, M. T., Marinho, F. J. D. B., Rocha, D. D., Lopez-Montero, E., Goulart, M. O. F., Bento, E. S., Alves, A. P. N. N., Pessoa, C., Odorico, d. M. M., Costa-Lotufo, L. V., *Chemico-Biological Interactions*, 2010, 184, 439-448.
- [89] Kanaan, Y. M., White, D. F., Das, J. R., Berhe, S., Bakare, O., Kenguele, H., Beyene, D., Zhou, Y., Day, A. A., Copeland, R. L., Jr., *Anticancer Research*, 2010, 30, 519-528.
- [90] Xu, K., Xiao, Z., Tang, Y. B., Huang, L., Chen, C.-H., Ohkoshi, E., Lee, K.-H., *Bioorganic and Medicinal Chemistry Letters*, 2012, 22, 2772-2774.
- [91] Zakharova, O. g. D., Ovchinnikova, L. P., Goryunov, L. I., Troshkova, N. M., Shteingarts, V. D., Nevinsky, G. A., *European Journal of Medicinal Chemistry*, 2010, 45, 2321-2326.
- [92] Zakharova, O. g. D., Ovchinnikova, L. P., Goryunov, L. I., Troshkova, N. M., Shteingarts, V. D., Nevinsky, G. A., *Bioorganic and Medicinal Chemistry*, 2011, 19, 256-260.
- [93] Pradidphol, N., Kongkathip, N., Sittikul, P., Boonyalai, N., Kongkathip, B., *European Journal of Medicinal Chemistry*, 2012, 49, 253-270.
- [94] Ding, Z.-S., Jiang, F.-S., Chen, N.-P., Lv, G.-Y., Zhu, C.-G., *Molecules*, 2008, 13, 220-229.
- [95] Hafeez, B. B., Zhong, W., Mustafa, A., Fischer, J. W., Witkowsky, O., Verma, A. K., *Carcinogenesis*, 2012, 33, 2586-2592.
- [96] Sagar, S., Green, I. R., *Cancer Letters (Shannon, Ireland)*, 2009, 285, 23-27.
- [97] Yang, H., Zhou, P., Huang, H., Chen, D., Ma, N., Cui, Q. C., Shen, S., Dong, W., Zhang, X., Lian, W., Wang, X., Dou, Q. P., Liu, J., *International Journal of Cancer*, 2009, 124, 2450-2459.
- [98] Gong, K., Li, W., *Free Radical Biology and Medicine*, 2011, 51, 2259-2271.
- [99] Valderrama, J. A., Leiva, H., Rodriguez, J. A., Theoduloz, C., Schmeda-Hirshmann, G., *Bioorganic and Medicinal Chemistry*, 2008, 16, 3687-3693.
- [100] Phutdhawong, W., Eksinitkun, G., Ruensumran, W., Taechowisan, T., Phutdhawong, W. S., *Archives of Pharmacal Research*, 2012, 35, 769-777.
- [101] Zhao, L. M., Xie, T. P., He, Y. Q., Xu, D. F., Li, S. S., *Chinese Chemical Letters*, 2008, 19, 1206-1208.

- [102] Kongkathip, N., Pradidphol, N., Hasitapan, K., Kongkathip, B., *Bioscience, Biotechnology and Biochemistry*, 2010, *74*, 1205-1214.
- [103] Ross, A. E., Emadi, A., Marchionni, L., Hurley, P. J., Simons, B. W., Schaeffer, E. M., Vuica-Ross, M., *BJU International*, 2011, *108*, 447-454.
- [104] Hughes, L. M., Lanteri, C. A., O'Neil, M. T., Johnson, J. D., Gribble, G. W., Trumpower, B. L., *Molecular and Biochemical Parasitology*, 2011, *177*, 12-19.
- [105] Lu, X., Altharawi, A., Gut, J., Rosenthal, P. J., Long, T. E., *ACS Medicinal Chemistry Letters*, 2012, *3*, 1029-1033.
- [106] Lanfranchi, D. A., Belorgey, D., Muller, T., Vezin, H., Lanzer, M., Davioud-Charvet, E., *Organic and Biomolecular Chemistry*, 2012, *10*, 4795-4806.
- [107] Muller, T., Johann, L., Jannack, B., Bruckner, M., Lanfranchi, D. A., Bauer, H., Sanchez, C., Yardley, V., Deregnacourt, C., Schrevel, J., Lanzer, M., Schirmer, R. H., Davioud-Charvet, E., *Journal of the American Chemical Society*, 2011, *133*, 11557-11571.
- [108] Kongkathip, N., Pradidphol, N., Hasitapan, K., Grigg, R., Kao, W.-C., Hunte, C., Fisher, N., Warman, A. J., Biagini, G. A., Kongsaree, P., Chuawong, P., Kongkathip, B., *Journal of Medicinal Chemistry*, 2010, *53*, 1211-1221.
- [109] Bolognesi, M. L., Lizzi, F., Perozzo, R., Brun, R., Cavalli, A., *Bioorganic and Medicinal Chemistry Letters*, 2008, *18*, 2272-2276.
- [110] Lezama-Davila, C. M., Isaac-Marquez, A. P., Kapadia, G., Owens, K., Oghumu, S., Beverley, S., Satoskar, A. R., *Biological and Pharmaceutical Bulletin*, 2012, *35*, 1761-1764.
- [111] Khraiwesh, M. H., Lee, C. M., Brandy, Y., Akinboye, E. S., Berhe, S., Gittens, G., Abbas, M. M., Ampy, F. R., Ashraf, M., Bakare, O., *Archives of Pharmacal Research*, 2012, *35*, 27-33.
- [112] Carneiro, P. F., do, N. S. B., Pinto, A. V., Pinto, M. d. C. F. R., Lechuga, G. C., Santos, D. O., dos, S. J. H. M., Resende, J. A. L. C., Bourguignon, S. C., Ferreira, V. F., *Bioorganic and Medicinal Chemistry*, 2012, *20*, 4995-5000.
- [113] da Silva, E. N. J., de Melo, I. M. M., Diogo, E. B. T., Costa, V. A., de Souza, F. J. D., Valenca, W. O., Camara, C. A., de Oliveira, R. N., de Araujo, A. S., Emery, F. S., dos Santos, M. R., de Simone, C. A., Menna-Barreto, R. F. S., de Castro, S. L., *European Journal of Medicinal Chemistry*, 2012, *52*, 304-312.
- [114] da Silva, E. N. J., Guimaraes, T. T., Menna-Barreto, R. F. S., Pinto, M. d. C. F. R., de Simone, C. A., Pessoa, C., Cavalcanti, B. C., Sabino, J. R., Andrade, C. K. Z., Goulart, M. O. F., de Castro, S. L., Pinto, A. V., *Bioorganic and Medicinal Chemistry*, 2010, *18*, 3224-3230.
- [115] Ramos, E. I., Garza, K. M., Krauth-Siegel, R. L., Bader, J., Martinez, L. E., Maldonado, R. A., *The Journal of Parasitology*, 2009, *95*, 461-466.
- [116] Stevens, P. F., 2001-, *Angiosperm Phylogeny Website*, <http://www.mobot.org/MOBOT/research/APweb/>, (Accessed 03/09/2010)
- [117] Judd, W., Manchester, S., *Brittonia*, 1997, *49*, p384-405.
- [118] Vasudeva, N., Sharma, S. K., *Pharmaceutical Biology*, 2008, *46*, 145-153.
- [119] Parmar, N. S., Ghosh, M. N., *Indian Journal of Pharmacology*, 1978, *10*, 277-293.
- [120] Veshkurova, O., Golubenko, Z., Pshenichnov, E., Arzanova, I., Uzbekov, V., Sultanova, E., Salikhov, S., Williams, H. J., Reibenspies, J. H., Puckhaber, L. S., Stipanovic, R. D., *Phytochemistry*, 2006, *67*, 2376-2379.
- [121] Ghosal, S., Chauhan, R. B. P. S., Mehta, R., *Phytochemistry*, 1975, *14*, 830-832.
- [122] Khan, M. S. Y., Bano, S., Javed, K., Mueed, M. A., *Journal of Scientific and Industrial Research*, 2006, *65*, 283-298.
- [123] Hadj Salem, J., Chevalot, I., Harscoat-Schiavo, C., Paris, C., Fick, M., Humeau, C., *Food Chemistry*, 2010, *124*, 486-494.
- [124] Waage, S. K., Hedin, P. A., *Phytochemistry*, 1984, *23*, 2509-2511.
- [125] Morales-Escobar, L., Braca, A., Pizza, C., De Tommasi, N., *Archive for Organic Chemistry*, 2007, 349-358.
- [126] Matlawska, I., Sikorska, M., *Acta Poloniae Pharmaceutica*, 1999, *56*, 69-71.
- [127] Vickery, J. R., *Journal of the American Oil Chemists Society*, 1980, *57*, 87-91.
- [128] Rao, K. S., Jones, G. P., Rivett, D. E., Tucker, D. J., *Fett Wissenschaft Technologie*, 1992, *94*, 37-38.
- [129] McCann, I. R., *The Grampians In Flower*, Victorian National Parks Association Inc. 2000.
- [130] Harborne, J., *Phytochemistry*, 1964, *3*, 151-160.
- [131] da Costa, D., Silva, D., Cavalcanti, A., de Medeiros, M., de Lima, J., Cavalcanti, J., da Silva, B., de Agra, M., de Souza, M., *Quimica Nova*, 2007, *30*, 901-903.
- [132] Maheswara, M., Koteswara, Y., Madhava Rao, V., Venkata Rao, C., *Asian Journal of Chemistry*, 2006, *18*, 2761-2765.

- [133] Horhammer, L., Stich, L., Wagner, H., *Naturwissenschaften*, 1959, 46, 358.
- [134] Bhutani, S., Chibber, S., Seshadri, T., *Phytochemistry*, 1969, 8, 299-303.
- [135] Kuroyanagi, M., Fukuoka, M., Yoshihira, K., Natori, S., Yamasaki, K., *Chemical and Pharmaceutical Bulletin*, 1978, 26, 3594-3596.
- [136] Dembinska-Migas, W., Gill, S., *Polish Journal of Pharmacology & Pharmacy*, 1973, 25, 599-606.
- [137] Dembinska-Migas, W., Gill, S., Symonowicz, E., Worobiec, S., *Herba Polonica*, 1985, 31, 5-11.
- [138] Matlawska, I., *Herba Polonica*, 1992, 38, 163-172.
- [139] Nguyen, X. C., Trinh, T. d. I., Phan, V. k., Tran, T. h., Chau, V. m., Braca, A., *Tap Chi Hoa Hoc*, 2007, 45, 348-352.
- [140] Ribereau-Gayon, P., *Annales de Physiologie Vegetale*, 1964, 6, 119-139.
- [141] Wu, T., Lin, J., Yang, Y., Abdulla, R., Chen, J., Aisa, H. A., *Separation and Purification Technology*, 2009, 66, 295-298.
- [142] Tsukamoto, S., Tomise, K., Aburanti, M., Onuki, H., Hirota, H., Ishiharajima, E., Ohta, T., *Journal of Natural Products*, 2004, 67, 1839-1841.
- [143] Nikaido, T., Ohmoto, T., Sankawa, U., *Chemical and Pharmaceutical Bulletin*, 1987, 35, 675-681.
- [144] Lin, J., Lin, Y., Chen, F., *Journal of the Chinese Chemistry Society*, 1976, 23, 57-59.
- [145] da Costa, D., Matias, W., Lima, I., Xavier, A., Costa, V., Diniz, M., Agra, M., Batista, L., de Souza, M., *Quimica Nova*, 2009, 32, 48-50.
- [146] Matlawska, I., Sikorska, M., *Acta Poloniae Pharmaceutica - Drug Research*, 2004, 61, 65-68.
- [147] Falcao-Silva, V. S., Silva, D. A., Souza, M. d. F. V., Siqueira-Junior, J. P., *Phytotherapy Research*, 2009, 23, 1367-1370.
- [148] Budzianowski, J., Skrzypczak, L., *Phytochemistry*, 1995, 38, 997-1001.
- [149] Curir, P., Dolci, M., Lanzotti, V., Tagliatela-Scafati, O., *Phytochemistry*, 2001, 56, 717-721.
- [150] Lee, E., Moon, B.-H., Park, Y., Hong, S., Lee, Y., Lim, Y., *Bulletin of the Korean Chemical Society*, 2008, 29, 507-510.
- [151] Choudhary, M. I., Naheed, N., Abbaskhan, A., Ali, S., Atta ur, R., *Phytochemistry*, 2009, 70, 1467-1473.
- [152] Barron, D., El Aidi, C., Mariotte, A.-M., *Phytochemical Analysis*, 1994, 5, 309-314.
- [153] Liu, H., Orjala, J., Sticher, O., Rali, T., *Journal of Natural Products*, 1999, 62, 70-75.
- [154] Saracoglu, I., Varel, M., Calis, I., Donmez, A., *Turkish Journal of Chemistry*, 2003, 27, 739-747.
- [155] Akdemir, Z., Tatli, I., Bedir, E., Khan, I., *FABAD Journal of Pharmaceutical Sciences*, 2003, 28, 71-75.
- [156] Noor, A., Fatima, I., Ahmad, I., Malik, A., Afza, N., Iqbal, L., Latif, M., Khan, S., *Molecules*, 2007, 12, 1447-1454.
- [157] Demetzos, C., Magiatis, P., Typas, M., Dimas, K., Sotiriadou, R., Perez, S., Kokkinopoulos, D., *Cellular and Molecular Life Sciences*, 1997, 53, 587-592.
- [158] Ferreira, J. F. S., Luthria, D. L., Sasaki, T., Heyerick, A., *Molecules*, 2010, 15, 3135-3170.
- [159] Kumarasamy, Y., Cox, P. J., Jaspars, M., Rashid, M. A., Sarker, S. D., *Pharmaceutical Biology*, 2003, 41, 237-242.
- [160] Opitz, S., Schneider, B., *Phytochemistry*, 2002, 61, 819-825.
- [161] Mpalantinos, M. A., De, M. R. S., Parente, J. P., Kuster, R. M., *Phytotherapy Research*, 1998, 12, 442-444.
- [162] Opitz, S., Otalvaro, F., Echeverri, F., Quinones, W., Schneider, B., *Nat. Prod. Lett.*, 2002, 16, 335-338.
- [163] Weiss, U., Edwards, J. M., *Tetrahedron Lett.*, 1969, 49, 4325-4328.
- [164] Opitz, S., Holscher, D., Oldham, N. J., Bartram, S., Schneider, B., *J. Nat. Prod.*, 2002, 65, 1122-1130.
- [165] Cooke, R. G., Dagley, I. J., *Aust. J. Chem.*, 1979, 32, 1841-1847.
- [166] Fang, J.-J., Paetz, C., Hoelscher, D., Munde, T., Schneider, B., *Phytochemistry Letters*, 2011, 4, 203-208.
- [167] Opitz, S., Schnitzler, J. P., Hause, B., Schneider, B., *Planta*, 2003, 216, 881-889.
- [168] Otalvaro, F., Gorls, H., Holscher, D., Schmitt, B., Echeverri, F., Quinones, W., Schneider, B., *Phytochemistry*, 2002, 60, 61-66.
- [169] Thomas, R., *Pure and Applied Chemistry*, 1973, 34, 515-528.
- [170] Thomas, R., *Journal of the Chemical Society D: Chemical Communications*, 1971, 739-740.
- [171] Edwards, J. M., Schmitt, R. C., Weiss, U., *Phytochemistry*, 1972, 11, 1717-1720.
- [172] Beecher, C. W. W., Sarg, T. M., Edwards, J. M., *Journal of Natural Products*, 1983, 46, 932-933.
- [173] Hoelscher, D., Schneider, B., *Journal of the Chemical Society D: Chemical Communications*, 1995, 525-526.

- [174] Hoelscher, D., Schneider, B., *Natural Product Letters*, 1995, 7, 177-182.
- [175] Schmitt, B., Schneider, B., *Phytochemistry*, 1999, 52, 45-53.
- [176] Opitz, S., Schneider, B., *Phytochemistry*, 2003, 62, 307-312.
- [177] Hoelscher, D., Schneider, B., *Phytochemistry*, 2005, 66, 59-64.
- [178] Munde, T., Maddula, R. K., Svatos, A., Schneider, B., *Phytochemistry*, 2011, 72, 49-58.
- [179] Schmitt, B., Holscher, D., Schneider, B., *Phytochemistry*, 2000, 53, 331-337.
- [180] Brand, S., Hoelscher, D., Schierhorn, A., Svatos, A., Schroeder, J., Schneider, B., *Planta*, 2006, 224, 413-428.
- [181] Ishikawa, Y., Morimoto, K., Iseki, S., *Journal of the American Oil Chemists' Society*, 1991, 68, 666-668.
- [182] Rosquete, L. I., Cabrera-Serra, M. G., Pinero, J. E., Martin-Rodriguez, P., Fernandez-Perez, L., Luis, J. G., McNaughton-Smith, G., Abad-Grillo, T., *Bioorganic and Medicinal Chemistry*, 2010, 18, 4530-4534.
- [183] Perpelescu, M., Kobayashi, J. i., Furuta, M., Ito, Y., Izuta, S., Takemura, M., Suzuki, M., Yoshida, S., *Biochemistry*, 2002, 41, 7610-7616.
- [184] Shiomi, K., Matsui, R., Isozaki, M., Chiba, H., Sugai, T., Yamaguchi, Y., Masuma, R., Tomoda, H., Chiba, T., Yan, H., Kitamura, Y., Sugiura, W., Omura, S., Tanaka, H., *The Journal of Antibiotics*, 2005, 58, 65-68.
- [185] Luis, J. G., Fletcher, W. Q., Echeverri, F., Grillo, T. A., *Tetrahedron*, 1994, 50, 10963-10970.
- [186] Luis, J. G., Fletcher, W. Q., Echeverri, F., Abad, T., Kishi, M. P., Perales, A., *Natural Product Letters*, 1995, 6, 23-30.
- [187] Luis, J. G., Quinones, W., Echeverri, F., Grillo, T. A., Kishi, M. P., Garcia-Garcia, F., Torres, F., Cardona, G., *Phytochemistry*, 1996, 41, 753-757.
- [188] Lazzaro, A., Corominas, M., Marti, C., Flors, C., Izquierdo, L. R., Grillo, T. A., Luis, J. G., Nonell, S., *Photochemical & Photobiological Sciences*, 2004, 3, 706-710.
- [189] Quinones, W., Escobar, G., Echeverri, F., Torres, F., Rosero, Y., Arango, V., Cardona, G., Gallego, A., *Molecules*, 2000, 5, 974-980.
- [190] Otalvaro, F., Nanclares, J., Vasquez, L. E., Quinones, W., Echeverri, F., Arango, R., Schneider, B., *Journal of Natural Products*, 2007, 70, 887-890.
- [191] Luque-Ortega, J. R., Martinez, S., Saugar, J. M., Izquierdo, L. R., Abad, T., Luis, J. G., Pinero, J., Valladares, B., Rivas, L., *Antimicrobial Agents and Chemotherapy*, 2004, 48, 1534-1540.
- [192] Zhang, Q., Kang, W., *Zhongguo Zhongyao Zazhi*, 2010, 35, 2424-2427.
- [193] Yang, W., Tian, J., Bai, B., Guan, J., Ding, L., *Zhongcaoyao*, 2001, 32, 681-683.
- [194] Dias, D. A., Goble, D. J., Silva, C. A., Urban, S., *J. Nat. Prod.*, 2009, 72, 1075-1080.
- [195] Sheldrick, G. M., *Acta Crystallogr., Sect. A: Found. Crystallogr.*, 2008, A64, 112-122.
- [196] Farrugia, L. J., *J. Appl. Crystallogr.*, 1997, 30, 565.
- [197] Farrugia, L. J., *J. Appl. Crystallogr.*, 1999, 32, 837-838.
- [198] Timmers, M. A., Brkljača, R., White, J. M., Urban, S., manuscript submitted to *Phytochemistry*.
- [199] Cremona, T. L., Edwards, J. M., *Lloydia*, 1974, 37, 112-113.
- [200] Edwards, J. M., Weiss, U., *Phytochemistry*, 1974, 13, 1597-1602.
- [201] Dora, G., Xie, X. Q., Edwards, J. M., *Journal of Natural Products*, 1993, 56, 2029-2033.
- [202] Cooke, R. G., Dagley, I. J., *Tetrahedron Letters*, 1978, 7, 637-638.
- [203] Australian Tropical Rainforest Plants, 2010, CSIRO, <http://keys.trin.org.au:8080/key-server/data/0e0f0504-0103-430d-8004-060d07080d04/media/Html/taxon/Droseraceae.htm> (Accessed 07/06/2012)
- [204] Culham, A., Gornall, J., *Biochemical Systematics and Ecology*, 1994, 22, 507-515.
- [205] Krolicka, A., Szpitter, A., Gilgenast, E., Romanik, G., Kaminski, M., Lojkowska, E., *Enzyme and Microbial Technology*, 2008, 42, 216-221.
- [206] Michelitsch, A., Wurglics, M., Schubert-Zsilavec, M., Likussar, W., *Phytochemical Analysis*, 1999, 10, 64-68.
- [207] Kreher, B., Neszmelyi, A., Wagner, H., *Phytochemistry*, 1990, 29, 605-606.
- [208] Harden, G. J., The Plant Information Network System of The Royal Botanic Gardens and Domain Trust, 1999, *Family Droseraceae*, <http://plantnet.rbgsyd.nsw.gov.au/cgi-bin/NSWfl.pl?page=nswfl&lvl=fm&name=DROSERACEAE>, (Accessed 20/05/2011)
- [209] Biswas, A., Bari, M., Roy, M., Bhadra, S., *Indian Journal of Traditional Knowledge*, 2010, 9, 77-89.
- [210] Ziaratnia, S. M., Kunert, K. J., Lall, N., *South African Journal of Botany*, 2009, 75, 97-103.
- [211] Hook, I., Walsh, J., Kavanagh, P., Reininger, R., *Pharmaceutical and Pharmacological Letters*, 1997, 7, 93-95.

- [212] FloraBase - the Western Australian Flora, 1998-, Western Australian Herbarium, <http://florabase.dec.wa.gov.au/potm/?y=2009&m=5> (Accessed 07/06/2012)
- [213] Caniato, R., Filippini, R., Cappelletti, M., *International Journal of Crude Drug Research*, 1989, 27, 129-136.
- [214] Didry, N., Dubreuil, L., Troitin, F., Pinkas, M., *Journal of Ethnopharmacology*, 1998, 60, 91-96.
- [215] Melzig, M. F., Pertz, H. H., Krenn, L., *Phytomedicine*, 2001, 8, 225-229.
- [216] Madhavan, V., Kumar, B. H. P., Murali, A., Yoganarasimhan, S. N., *Pharmaceutical Biology*, 2009, 47, 128-131.
- [217] Paper, D. H., Karall, E., Kremser, M., Krenn, L., *Phytotherapy Research*, 2005, 19, 323-326.
- [218] Marczak, L., Kawiak, A., Lojkowska, E., Stobiecki, M., *Phytochemical Analysis*, 2005, 16, 143-149.
- [219] Budzianowski, J., *Planta Medica*, 2000, 66, 667-669.
- [220] Tokunaga, T., Takada, N., Ueda, M., *Tetrahedron Letters*, 2004, 45, 7115-7119.
- [221] Budzianowski, J., *Phytochemistry*, 1996, 44, 75-77.
- [222] Keifer, P. A., *Journal of Magnetic Resonance*, 2009, 199, 75-87.
- [223] Sankaram, A. V. B., Narayana Reddy, V. V., Marthandamurthi, M., *Phytochemistry*, 1986, 25, 2867-2871.
- [224] Nair, A. G. R., Shanmugasundaram, P., Madhusudhanan, K. P., *Fitoterapia*, 1990, 61, 85-86.
- [225] Gunaherath, G. M. K. B., Gunatilaka, A. A. L., Sultanbawa, M. U. S., Balasubramaniam, S., *Phytochemistry*, 1983, 22, 1245-1247.
- [226] Thomson, R. H., *Journal of the Chemical Society*, 1949, 1277-1278.
- [227] Schoelly, T., Kapetanidis, I., *Pharmaceutica Acta Helveticae*, 1989, 64, 66-67.
- [228] McDonald, I. A., Simpson, T. J., Sierakowski, A. F., *Australian Journal of Chemistry*, 1977, 30, 1727-1734.
- [229] Kubo, I., Taniguchi, M., Chapya, A., Tsujimoto, K., *Planta Medica*, 1980, 40, 185-187.
- [230] Chen, Z.-F., Tan, M.-X., Liu, L.-M., Liu, Y.-C., Wang, H.-S., Yang, B., Peng, Y., Liu, H.-G., Liang, H., Orvig, C., *Dalton Transactions*, 2009, 10824-10833.
- [231] Likhitwitayawuid, K., Kaewamatawong, R., Ruangrunsi, N., Krungkrai, J., *Planta Medica*, 1998, 64, 237-241.
- [232] Higa, M., Ogihara, K., Yogi, S., *Chemical and Pharmaceutical Bulletin*, 1998, 46, 1189-1193.
- [233] Luo, P., Wong, Y. F., Ge, L., Zhang, Z. F., Liu, Y., Liu, L., Zhou, H., *Journal of Pharmacology and Experimental Therapeutics*, 2010, 335, 735-742.
- [234] Blunt, J. W., Copp, B. R., Hu, W.-P., Munro, M. H. G., Northcote, P. T., Prinsep, M. R., *Natural Product Reports*, 2009, 26, 170-244.
- [235] Blunt, J. W., Copp, B. R., Munro, M. H. G., Northcote, P. T., Prinsep, M. R., *Natural Product Reports*, 2010, 27, 165-237.
- [236] Hill, R. A., *Annual Reports on the Progress in Chemistry, Section B*, 2009, 105, 150-166.
- [237] Cragg, G. M., Newman, D. J., in: Colegate, S. M., Molyneux, R. J. (Eds.), *Bioactive Natural Products 2008*, pp. 323-370.
- [238] Dias, D., Urban, S., *Phytochemical Analysis*, 2008, 19, 453-470.
- [239] Dias, D. A., Urban, S., *J. Sep. Sci.*, 2009, 32, 542-548.
- [240] Dias, D., White, J., Urban, S., *Nat. Prod. Commun.*, 2009, 4, 157-172.
- [241] Timmers, M., Urban, S., *Natural Product Communications*, 2011, 6, 1605-1616.
- [242] Urban, S., Separovic, F., *Frontiers in Drug Design and Discovery*, 2005, 1, 113-166.
- [243] Saunders, G. W., Lehmkuhl, K. V., *European Journal of Phycology*, 2005, 40, 293-312.
- [244] Markus, N., Marla, R., Christopher, L., 1999, *World Distribution of Plocamium sp.*, <http://www.nilauro.com/plocamium/biogeog.htm> and <http://www.nilauro.com/plocamium/taxnomen.htm>, (Accessed 18/08/2011)
- [245] Faulkner, D. J., Stallard, M. O., *Tetrahedron Letters*, 1973, 1171-1174.
- [246] Stallard, M. O., Faulkner, D. J., *Comparative Biochemistry and Physiology - Part B*, 1974, 49, 25-35.
- [247] Crews, P., Kho, E., *Journal of Organic Chemistry*, 1974, 39, 3303-3304.
- [248] Mynderse, J. S., Faulkner, D. J., *Tetrahedron*, 1975, 31, 1963-1967.
- [249] Blunt, J. W., Hartshorn, M. P., Munro, M. H. G., Yorke, S. C., *Tetrahedron Letters*, 1978, 4417-4418.
- [250] Crews, P., Kho-Wiseman, E., *Journal of Organic Chemistry*, 1977, 42, 2812-2815.
- [251] Higgs, M. D., Vanderah, D. J., Faulkner, D. J., *Tetrahedron*, 1977, 33, 2775-2780.
- [252] Crews, P., Kho-Wiseman, E., Montana, P., *Journal of Organic Chemistry*, 1978, 43, 116-120.
- [253] Norton, R. S., Warren, R. G., Wells, R. J., *Tetrahedron Letters*, 1977, 3905-3908.

- [254] Dunlop, R. W., Murphy, P. T., Wells, R. J., *Australian Journal of Chemistry*, 1979, 32, 2735-2739.
- [255] Leary, J. V., Kfir, R., Sims, J. J., Fulbright, D. W., *Mutation Research*, 1979, 68, 301-305.
- [256] Brownlee, R. T. C., Hall, J. G., Reiss, J. A., *Organic Magnetic Resonance*, 1983, 21, 544-547.
- [257] Kazlauskas, R., Murphy, P. T., Quinn, R. J., Wells, R. J., Schoenholzer, P., *Tetrahedron Letters*, 1976, 4451-4454.
- [258] Konig, G. M., Wright, A. D., Sticher, O., *Journal of Natural Products*, 1990, 53, 1615-1618.
- [259] Jongaramruong, J., Blackman, A. J., *Journal of Natural Products*, 2000, 63, 272-275.
- [260] Mann, M. G. A., Mkwanzani, H. B., Antunes, E. M., Whibley, C. E., Hendricks, D. T., Bolton, J. J., Beukes, D. R., *Journal of Natural Products*, 2007, 70, 596-599.
- [261] Konig, G. M., Wright, A. D., De, N. R., *Journal of Natural Products*, 1999, 62, 383-385.
- [262] Konig, G. M., Wright, A. D., Linden, A., *Phytochemistry*, 1999, 52, 1047-1053.
- [263] Ankisetty, S., Nandiraju, S., Win, H., Park, Y. C., Amsler, C. D., McClintock, J. B., Baker, J. A., Diyabalanage, T. K., Pasaribu, A., Singh, M. P., Maiese, W. M., Walsh, R. D., Zaworotko, M. J., Baker, B. J., *Journal of Natural Products*, 2004, 67, 1295-1302.
- [264] Knott, M. G., Mkwanzani, H., Arendse, C. E., Hendricks, D. T., Bolton, J. J., Beukes, D. R., *Phytochemistry*, 2005, 66, 1108-1112.
- [265] Argandona, V. H., Roviroso, J., San-Martin, A., Riquelme, A., Diaz-Marrero, A. R., Cueto, M., Darias, J., Santana, O., Guadano, A., Gonzalez-Coloma, A., *Journal of Agriculture and Food Chemistry*, 2002, 50, 7029-7033.
- [266] Afolayan, A. F., Mann, M. G. A., Lategan, C. A., Smith, P. J., Bolton, J. J., Beukes, D. R., *Phytochemistry*, 2009, 70, 597-600.
- [267] Kim, J.-Y., Yoon, M.-Y., Cha, M.-R., Hwang, J.-H., Park, E., Choi, S.-U., Park, H.-R., Hwang, Y.-I., *Journal of Medicinal Food*, 2007, 10, 587-593.
- [268] Stierle, D. B., Sims, J. J., *Tetrahedron*, 1979, 35, 1261-1265.
- [269] Naylor, S., Manes, L. V., Crews, P., *Journal of Natural Products*, 1985, 48, 72-75.
- [270] Stierle, D. B., Sims, J. J., *Tetrahedron Letters*, 1984, 25, 153-156.
- [271] Kesternich, V., Martinez, R., Gutierrez, E., Ballesteros, K., Mansilla, H., *Boletin de la Sociedad Chilena de Quimica*, 1997, 42, 105-108.
- [272] Gribble, G. W., *Fortschritte der Chemie Organischer Naturstoffe* 2010, 91, 9-348.
- [273] Rezanka, T., Dembitsky, V. M., *Phytochemistry*, 2001, 57, 607-611.
- [274] Crews, P., Naylor, S., Hanke, F. J., Hogue, E. R., Kho, E., Braslau, R., *Journal of Organic Chemistry*, 1984, 49, 1371-1377.
- [275] Crews, P., *Journal of Organic Chemistry*, 1977, 42, 2634-2636.
- [276] Abreu, P. M., Galindro, J. M., *Journal of Natural Products*, 1996, 59, 1159-1162.
- [277] Hevesi, L., Nagy, J. B., Krief, A., Derouane, E. G., *Organic Magnetic Resonance*, 1977, 10, 14-19.
- [278] Chukovskaya, E. C., Dostovalova, V. I., Vasileva, T. T., Freidlina, R. K., *Organic Magnetic Resonance*, 1976, 8, 229-232.
- [279] Kimpenhaus, W., Auf, d. H. W., *Liebigs Annalen der Chemie*, 1983, 378-392.
- [280] Darias, J., Roviroso, J., San, M. A., Diaz, A. R., Dorta, E., Cueto, M., *Journal of Natural Products*, 2001, 64, 1383-1387.
- [281] Advanced Chemistry Development, Inc., *ACD/labs*, 2012, www.acdlabs.com.
- [282] PerkinElmer Inc., *ChemDraw Ultra*, 2012, http://www.cambridgesoft.com.
- [283] Tobey, S. W., *Journal of Organic Chemistry*, 1969, 34, 1281-1298.
- [284] Pascual, C., Meier, J., Simon, W., *Helvetica Chimica Acta*, 1965, 49, 164-168.
- [285] Crews, P., Kho-Wiseman, E., *Tetrahedron Letters*, 1978, 2483-2486.
- [286] Lopez, A., Gerwick, W. H., *Lipids*, 1987, 22, 190-194.
- [287] Itokawa, H., Morris-Natschke, S. L., Akiyama, T., Lee, K.-H., *Journal of Natural Medicines*, 2008, 62, 263-280.
- [288] 2012, <http://www.algaebase.org> (Accessed 20/07/2012)
- [289] Amico, V., *Phytochemistry*, 1995, 39, 1257-1279.
- [290] Valls, R., Piovetti, L., *Biochemical Systematics and Ecology*, 1995, 23, 723-745.
- [291] Bian, B., Van, A. I. A., *Australian Journal of Chemistry*, 1998, 51, 1157-1165.
- [292] Laird, D. W., Van, A. I. A., *Phytochemistry* 2006, 67, 944-955.
- [293] Gregson, R. P., Kazlauskas, R., Murphy, P. T., Wells, R. J., *Australian Journal of Chemistry*, 1977, 30, 2527-2532.
- [294] Kato, T., Kumanireng, A. S., Ichinose, I., Kitahara, Y., Kakinuma, Y., Nishihira, M., Kato, M., *Experientia*, 1975, 31, 433-434.
- [295] Spence, I., Jamieson, D. D., Taylor, K. M., *Experientia*, 1979, 35, 238-239.

- [296] Jamieson, D. D., De, R. P. J., Taylor, K. M., *Journal of Pharmaceutical Sciences*, 1980, 69, 462-465.
- [297] Kazlauskas, R., King, L., Murphy, P. T., Warren, R. G., Wells, R. J., *Australian Journal of Chemistry*, 1981, 34, 439-447.
- [298] Capon, R. J., Ghisalberti, E. L., Jefferies, P. R., *Phytochemistry*, 1981, 20, 2598-2600.
- [299] Ravi, B. N., Murphy, P. T., Lidgard, R. O., Warren, R. G., Wells, R. J., *Australian Journal of Chemistry*, 1982, 35, 171-182.
- [300] Gregson, R. P., Daly, J. J., *Australian Journal of Chemistry*, 1982, 35, 649-657.
- [301] Koch, M., Gregson, R. P., *Phytochemistry*, 1984, 23, 2633-2637.
- [302] Mueller, D. G., Clayton, M. N., Gassmann, G., Boland, W., Marner, F. J., Schotten, T., Jaenicke, L., *Naturwissenschaften*, 1985, 72, 97-99.
- [303] Czeuczuga, B., Taylor, F. J., *Biochemical Systematics and Ecology*, 1986, 15, 5-8.
- [304] Van, A. I. A., *Australian Journal of Chemistry*, 1988, 41, 49-56.
- [305] Glombitza, K.-W., Hauperich, S., *Phytochemistry*, 1997, 46, 735-740.
- [306] Glombitza, K.-W., Keusgen, M., Hauperich, S., *Phytochemistry*, 1997, 46, 1417-1422.
- [307] Sailler, B., Glombitza, K.-W., *Phytochemistry*, 1999, 50, 869-881.
- [308] Sailler, B., Glombitza, K.-W., *Natural Toxins*, 1999, 7, 57-62.
- [309] Laird, D. W., Poole, R., Wikstroem, M., Van, A. I. A., *Journal of Natural Products*, 2007, 70, 671-674.
- [310] Fort, D. M., Ubillas, R. P., Mendez, C. D., Jolad, S. D., Inman, W. D., Carney, J. R., Chen, J. L., Ianiro, T. T., Hasbun, C., Bruening, R. C., Luo, J., Reed, M. J., Iwu, M., Carlson, T. J., King, S. R., Bierer, D. E., Cooper, R., *Journal of Organic Chemistry*, 2000, 65, 6534-6539.
- [311] Reddy, P., Urban, S., *J. Nat. Prod.*, 2008, 71, 1441-1446.
- [312] Laird, D. W., Bennett, S., Bian, B.-H., Sauer, B., Wright, K., Hughes, V., van, A. I. A., *Biochemical Systematics and Ecology*, 2010, 38, 187-194.
- [313] Barrow, R. A., Capon, R. J., *Australian Journal of Chemistry*, 1991, 44, 1393-1405.
- [314] Halsall, T. G., Hills, I. R., *Journal of the Chemical Society D: Chemical Communications*, 1971, 448-449.
- [315] Smallcombe, S. H., Patt, S. L., Keifer, P. A., *Journal of Magnetic Resonance, Series A*, 1995, 117, 295-303.